ANUL XLII 1997

STUDIA

UNIVERSITATIS BABEȘ-BOLYAI

CHEMIA

1-2

Editorial Office: 3400 CLUJ-NAPOCA, Gh. Bilașcu no.24, ♦ Tel. 194315; int. 167

SUMAR - CONTENTS - SOMMAIRE - INHALT

ACADEMICIAN IONEL HAIDUC AT HIS 60th ANNIVERSARY

A gifted, dedicated scientist, born to be a creator in his field, will almost always manifest himself as an outstanding intellect while still in school, marking his way to accomplishment with original work at a time when others struggle with routine drills. The life and work of ***Professos dr. Ionel Haiduc*** *is a peremptory demonstration of his statement: now, when the scientific community is saluting his 60th anniversary, he can look back to 41 years of valuable contributions to the chemistry of inorganic and organometallic compounds, as he published his first paper in 1956, while not yet 19 years old, and being a student in his second year of study.*

Born in Cluj, the historical and intellectual capital of Transylvania, on May 9th, 1937, in a family of kind, industrious people, whose credo was honest work, Ionel Haiduc distinguished himself already during his years in the lyceum as an exceptional personality, deeply impressing both his teacher and his colleagues by the dedication for study, the insatiable scientific curiosity, the wide field of interests, and the uncanny capacity of memorising and interrelating a huge amount of knowledge, although his compass was already firmly set on the direction of chemistry. These remarkable results, reflected in a flawless collection of maximum marks, enabled him to be admitted in 1954 to the Faculty of Chemistry of the University of Cluj without admission examination - a privilege reserved only to a handful of exceptional applicants. Fully confirming this brilliant start, he repeated the performance of obtaining only the best marks at all the 41 exams he had to pass until graduation in 1959.

This was the official beginning of a quite outstanding scientific and teaching career. Intense studies at the "M.V. Lomonosov" Institute of Fine Chemical Technology in Moscow, under the guidance of such a celebrity as Academician K.A. Andrianov brought him the equivalent of a PhD in chemistry with a dissertation entitled "Investigations on the chemistry of silicon-containing inorganic rings" This was in 1964, and the young Roumanian scientist was on leave from his Alma Mater, which remained also his only permanent employer, from 1959 until present time; he serves faithfully and well the greatest academic institution of Transylvania, as he has done all his life, and his work was deservedly rewarded by a continuous ascension up the university ladder, reaching the step of full professor in 1973, at the age of 36. He completed his formation as a research chemist during three postdoctoral stages in the United States, as a Fulbright scholar, between 1966 and 1972, working with Prof. Henry Gilman and Prof R.B. King, in Ames, Iowa, and Athens, Georgia, respectively.

An attempt to summarize the monumental contribution of Academician Ionel Haiduc to the literature of inorganic and organometallic chemistry is an arduous task, because no matter how faithfully carried out, such an endeavour will inevitably make injustice to many facets of a creative work embodied in nine books, published in Roumanian, English, Polish and Greek, 23 chapters in the most famous collective volumes, encyclopaedias etc., and 236 papers which appeard in practically all journals that really matter in his field of research, as shown in the list of publication.

Using as a guiding line Professor Haiduc's own statement concerning the main directions of his scientific interests, one can distinguish six fields of chemical science which benefited from his creative activity. The first, historically, and not only so, is the chemistry of ***inorganic rings****. The* ***chemistry of co-ordination***

and organometallic compounds *has to be mentioned next. Starting with the field of heteropolyacids, a traditional theme of the Cluj school of complex inorganic compounds, and continuing with several other types of substances, he concentrated in recent years on the co-ordination chemistry of organothiophosphorus and organoarsenic ligands. The* ***inorganic and organometallic compounds with biological activity*** *(including antitumor agents) became one of his favourite preoccupation followed by the interest in the explosively developing field of* ***organometallic supramolecular chemistry.***

Although an independent thinker, like all born leaders and really creative minds, Professor Haiduc was always connected in many ways to the pulse of the chemists community life. He devoted much attention to the problems of communication, of chemical language, and his work on the ***nomenclature in chemistry*** *was interspersed with other scientific interests all the time. He vigorously fought for quality in the academic life - very often attracting enmities for being outspoken against mediocrity - and is an active propagator of the principles of ethics in science. As a member or leader of many academic bodies, he participated with all the force of his strong moral convictions and creative thought to the elaboration and implementation of* ***policies and managerial decisions*** *in science, with special, but not exclusive, reference to chemistry.*

The brilliant career brought him well-deserved satisfactions and recognition. He received the "Gheorghe Spacu" award of the Roumanian Academy in 1974, was elected corresponding member in 1990 and titular member of the Roumanian Academy in 1991. Professor Haiduc was Rector of the "Babeș-Bolyai" University, Cluj-Napoca, between 1990 and 1993, being elected, in this capacity, vice-president of National Conference of Rectors in our country, is now president of the Cluj-branch of the Roumanian Academy, member of the Presidium of the same institution, and also a member in a long series of councils involved in the management of research and of university life.

Academician Ionel Haiduc is a personality of internationally recognised value. Seven journals, four of them published in the United States and the United Kingdom, have elected him as a member of the editorial scientific board. He is a member of the International Council for Main Group Chemistry, of IUPAC, and of the Alliance of the Universities for Democracy. Many universities invited him as a visiting professor: University of Georgia, USA, Universidad Nacional Autonoma de Mexico, Universidad de Santiago de Compostella, Spain, and Universidad Federal de Sao Carlos, Brazil. Everywhere, and in all these capacities, he was a credit to the Roumanian school of chemical research, to the Roumanian Academy. His quick wits, good natured humor, his kindness and the capacity of creating a friendly atmosphere around him while not making concessions in matters related to quality, are among the reasons of his immense popularity with young researchers and students. This is also an explanation of his succes in creating a high-level research school of inorganic and organometallic chemistry at the University of Cluj, and for the large audience always present at his lectures for the students.

The 60th anniversary of the birthday of Professor Ionel Haiduc is an excellent opportunity for the whole community of Roumanian chemists to express their appreciation for this outstanding representative of science in our country, and to present him with the very best wishes of long, fruitful life, and many successes in the years to come.

THE EDITORIAL BOARD

LIST OF PUBLICATIONS

A. BOOKS

1. Ionel Haiduc, ***Introducere în chimia ciclurilor anorganice***, Editura Academiei, Bucuresti, 1960, 338 pages.
2. Ionel Haiduc, ***Wstep do chemii nieorganicznych zwiazkow pierscieniowych***. PWN Warszawa, 1964, 369 pages (revised and updated translation of # 1).
3. Ionel Haiduc, ***The Chemistry of Inorganic Ring Systems***, Wiley-Interscience, London, New York, 1970, Vol.1, 622 pages; vol. 2, 575 pages.
4. Ionel Haiduc, ***Chimia compușilor metalorganici***, Editura Științifică, București, 1974, 492 pages.
5. Ionel Haiduc (coordonator), ***Chimia anorganica – pentru perfecționarea profesorilor***, Editura Didactica si Pedagogica, Bucuresti, 1983.
6. I. Haiduc and J. J. Zuckerman, ***Basic Organometallic Chemistry***, Walter de Gruyter Publ. Co., Berlin, New York, 1985; Hardcover (Professor's) Edition 488 pages, Paperback (Student) Edition 376 pages.
7. Ionel Haiduc and D. B. Sowerby (editors), ***The Chemistry of Inorganic Homo- and Heterocycles***, Academic Press, London, New York, 1987, Vol. 1, 415 pages, vol. 2, 417 pages.
8. Ionel Haiduc and Cristian Silvestru, ***Organometallics in Cancer Chemotherapy. Volume 1. Main Group Metal Compounds***, CRC Press, Inc., Boca Raton, Florida, 1989, 254 pages.
9. Ionel Haiduc and Cristian Silvestru, ***Organometallics in Cancer Chemotherapy. Volume 2. Transition Metal Compounds***, CRC Press, Inc., Boca Raton, Florida, 1990, 355 pages.

B. CHAPTERS IN BOOKS

1. K. J. Wynne und I. Haiduc, Kohlenstoff-Schwefel(IV) Verbindungen, in vol. ***Methodicum Chimicum, Band 7. Hauptgruppenelemente und deren Verbindungen***. Herausgegeben von, H. Zimmer und K. Niedenzu, G. Thieme Verlag, Stuttgart, 1976, p. 683-698.
2. I. Haiduc und K. J. Wynne, Kohlenstoff-Schwefel(VI) Verbindungen, ***ibidem***, p. 699-756.
3. I. Haiduc, Cyclische Schwefel-Stickstoff Verbindungen, ***ibidem***, p. 811-829.
4. L. Marta and I. Haiduc, The platinum metals. Part I. Ruthenium, osmium, rhodium and iridium, in. vol. ***Annual Reports in Inorganic and General Synthesis-1976***, Edited by H. Zimmer, Academic Press, New York, 1977, p. 241-263.

5. I. Haiduc, Recent advances in sulfur-nitrogen inorganic heterocycles, ***ibidem***, p. 350-372.
6. I. Haiduc and V. Popa, Metal complexes of π-ligands containing organosilicon groups, in vol. ***Advances in Organometallic Chemistry***, Edited by F.G.A. Stone and R. West, Academic Press, New York, 1977, Vol. 15, p. 113-146.
7. K. J. Wynne and I. Haiduc, Carbon-sulfur(IV) compounds, in vol. ***Methodicum Chimicum, Vol 7B, Main Group Elements and their Compounds***, Edited by H. Zimmer and K. Niedenzu, Academic Press, New York, 1979, p. 652-669.
8. I. Haiduc and K. J. Wynne, Carbon-sulfur(VI) compounds, ***ibidem***, p. 670-734.
9. I. Haiduc, Cyclic sulfur-nitrogen compounds, ***ibidem***, p. 789-809.
10. I. Haiduc and D. B. Sowerby, Introduction, in. vol. ***The Chemistry of Inorganic Homo- and Heterocycles***, Edited by I. Haiduc and D. B. Sowerby, Academic Press, London, 1987, p. 1-14.
11. I. Haiduc, Boron homocycles (cyclopolyboranes), ***ibidem***, p. 15-17.
12. I. Haiduc, Boron-oxygen heterocycles, ***ibidem***, p. 109-142.
13. I. Haiduc, Silicon-sulphur heterocycles, ***ibidem***, p. 349-360.
14. I. Haiduc and M. Drager, Germanium homocycles (cyclopolygermanes) and related heterocycles, ***ibidem***, p. 361-366.
15. I. Haiduc, Germanium-containing heterocycles, ***ibidem***, p. 367-376.
16. I. Haiduc, Nitrogen homocycles, ***ibidem***, p. 417-422.
17. I. Haiduc and D. B. Sowerby, Cycloarsanes, ***ibidem***, p. 701-712.
18. I. Haiduc, Sulphur-oxygen, selenium-oxygen and selenium-nitrogen heterocycles, ***ibidem***, p. 871-877.
19. I. Haiduc, Comments on the nomenclature of inorganic ring systems, in. vol. ***The Chemistry of Inorganic Ring Systems***, Edited by R. Steudel, Elsevier Science Publishers, Amsterdam, 1992, p. 451-477.
20. I. Haiduc, Inorganic (carbon-free) chelate rings: a dithioimidodiphosphinato ligand and some of its metal complexes, in vol. ***Inorganic Experiments***, Edited by J. Derek Woollins, VCH Weinheim, New York, Basel, Cambridge, Tokyo, 1994, p. 145-149.
21. I. Haiduc and C. Silvestru, Supramolecular associations in organotin, organoantimony and other main group organometallic compounds, in vol. ***Main Group Elements and their Compounds***, V. G. Kumar Das, Editor, Narosa Publishing House, New Delhi, London, 1996, p. 355-369.
22. C. Silvestru and I. Haiduc, Organoantimony(III) compounds. A new class of organometallic antitumor agents, ***ibidem***, p. 453-462.
23. I. Haiduc and R. B. King, Large Inorganic Ring Molecules, in vol. ***Large Ring Molecules***, Edited by J. Semlyen, John Wiley & Sons, Chichester, New York, 1996, pag. 525-598.

C. ARTICLES IN SCIENTIFIC JURNALS AND PERIODICALS

1. I. Haiduc, Compuşi macromoleculari şi ciclici anorganici, ***Rev. Chim. (Bucureşti)*** 1956, 7, 721-726.
2. I. Haiduc, Despre structura heteropoliacizilor, ***Rev. Chim. (Bucuresti)*** 1959, 10, 168-170.
3. I. Haiduc, Sur la structure probable de la silicodiimide SiN_2H_2 ***Bull. Soc. Chim. France***, 1960, 489-490.
4. I. Haiduc, Electronegativity of elements and the formation of inorganic rings and chains, ***Zhur. Obshch. Khim.*** 1960, 30, 1395-1396; ***J. Gen. Chem.*** USRR (Engl. Transl.) 1960, 30, 1426.
5. I. Haiduc, Despre relaţia dintre chimia organică şi anorganică, ***Studia Univ. Babes-Bolyai, Chemia***, Ser. I, 1960, Fasc. 2, p. 23-38.
6. R. Ripan, G. Marcu şi I. Haiduc, Schimbul izotopic dintre cobaltimolibdaţi şi ionul Co^{2+} marcat cu cobalt radioactiv-60, ***Studia Univ. Babes-Bolyai, Chemia***, Ser. I, 1960, Fasc. 1, p. 71-76.
7. I. Haiduc si G. Marcu, Cercetări asupra cobaltowolframaţilor cu ajutorul cobaltului radioactiv Co^{60}. Reacţii de interconversiune. Schimb izotopic, ***Studia Univ. Babes-Bolyai, Chemia***, 1960, Ser. I, Fasc. 2. p. 77-84.
8. I. Haiduc, A systematization of inorganic cyclic compounds, ***J. Chem. Educ.*** 1961, 38, 134-137.
9. I. Haiduc, About the systematization of inorganic cyclic compounds (in Russian), ***Zhur. Strukt. Khim.*** 1961, 2, 374-382.
10. I. Haiduc, Polymeric coordination compounds, ***Uspekhi Khim***. 1961, 30, 1124-1166, ***Russ. Chem. Revs. (Engl. transl.)*** 1961, 30, 243-248.
11. I. Haiduc, Despre caracterul aromatic al ciclurilor anorganice, ***Studia Univ. Babes-Bolyai, Chemia***, Ser.I, 1961, Fasc. 2, p. 9-17.
12. K. A. Andrianov, I. Haiduc, L. M. Khananashvili and I. Nekhaeva, Synthesis of dimethylcyclosilthioxanes, ***Zhur. Obshch. Khim.*** 1962, 32, 3447-3448; ***J. Gen. Chem. USSR (Engl. transl.)*** 1962, 32, 3380.
13. K. A. Andrianov, I. Haiduc, L. M. Khananashvili and M. B. Lotarev, Synthesis of cyclosilazane vinyl derivatives, ***Izvest. Akad. Nauk SSR, Ser. Khim***, 1963, 948-950; ***Bul. Acad. Sci. USSR, Ser. Khim. (Engl. transl.)*** 1963, 860.
14. K. A. Andrianov, I. Haiduc, and L. M. Khananashvili, Inorganic silicon-containing cyclic compounds and their organic derivatives, ***Uspekhi Khim***. 1963, 32, 539-589; ***Russian Chem. Revs. (Engl. transl.)*** 1963, 32, 243-.
15. K. A. Andrianov, I. Haiduc, and L. M. Khananashvili, Unsaturated derivatives of cyclotrisilazane and their structure, ***Doklady Akad. Nauk SSSR***, 1963, 150, 93-95; ***Doklady-Chemistry, Proc. Acad. Sci. USSR, Engl. transl.*** 1963, 150, 385.
16. K. A. Andrianov, I. Haiduc, and L. M. Khananashvili, A new inorganic ring – trisildiazoxane ***Zhur. Obshch. Khim.*** 1963, 33, 2790-2791; ***J. Gen. Chem. USSR (Engl. transl.)*** 1963, 33. 2717-.
17. I. Haiduc and K. A. Andrianov, Nomenclature of inorganic silicon heterocycles, ***Izvest. Akad. Nauk SSR, Ser. Khim***. 1963, 1537-1544; ***Bull. Acad. Sci. USSR, Ser. Khim. (Engl. transl.)*** 1963, 1403-6.

18. K. A. Andrianov, I. Haiduc, and L. M. Khananashvili, New eight-membered cyclosilazoxanes ***Izvest. Akad. Nauk SSR, Ser. Khim.*** 1963, 1701-1702; ***Bull. Acad. Sci. USSR, Ser. Khim. (Engl. transl.)*** 1963, 1565.
19. K. A. Andrianov, I. Haiduc, and L. M. Khananashvili, Formation of polycyclic silazanes in the ammonolysis of dimethyldichorosilane, ***Zhur. Obshch. Khim.*** 1964, 34, 912-914; ***J. Gen. Chem. USSR (Engl. transl.)*** 1964, 34, 905.
20. I. Haiduc, Carboranii $B_nC_2H_{n+2}$ o noua clasa de compusi cvasiaromatici, ***Studii Cercet. Chimie (Bucuresti)*** 1964, 13, 783-803.
21. K. A. Andrianov, I. Haiduc, and L. M. Khananashvili, The ability of elements to form polymers with inorganic molecular chains (in Russian), ***Uspekhi Khim.*** 1965, 34, 27-43; ***Russ. Chem. Revs. (Engl. transl.)*** 1965, 34, 13-. Reprinted in the volume "***Progress of Polymer Chemistry***" (in Russian), Edited by V. V. Korshak, Izdatel'stvo Akademii Nauk SSSR, Moskva, 1969, p. 32-46.
22. I. Haiduc und H. Mantsch, Das Infrarotspektrum einiger neuer Methylsilazoxanringe, ***Spectrochim. Acta***, 1965, 21, 981-985.
23. I. Haiduc, Contributions to the chemistry of polysilazanes. Polysilazoxanes, ***International Symposium on Organosilicon Chemistry. Scientific Communications***, Prague, 1965, 301-305.
24. I. Haiduc, Combinatiile organice ale siliciului. I. Monomeri silicoorganici, ***Studii Cercet. Chimie (Bucuresti)*** 1965, 13, 789-811.
25. I. Haiduc, Combinatiile organice ale siliciului. II. Polimeri silicoorganici, ***Studii Cercet. Chimie (Bucuresti)*** 1965, 13, 813-833.
26. I. Haiduc, A convenient method for preparing short-chain α,ω-dichloromethysiloxanes, ***Rev. Roum. Chim.*** 1966, 11, 897-899.
27. I. Haiduc, Despre sinteza organociclosilazanilor si a unor compusi inruditi, ***Studia Univ. Babes-Bolyai, Chemia***, 1966, Nr. 2, p. 43-46.
28. I. Haiduc, Chemia heterociclurilor cu siliciu si azot. ***Studii Cercet. Chimie (Bucuresti)*** 1967, 15, 71-127.
29. I. Haiduc and H. Gilman, Some organosilicon derivatives of 1,2,3,4-tetrafluorobenzene, ***J. Organomet. Chem.*** 1968, 11, 55-61.
30. I. Haiduc, Iov. Haiduc and H. Gilman, Ultraviolet spectra of some polyhaloaromatic organosilicon derivatives, ***J. Organomet. Chem.*** 1968, 11, 459-462.
31. I. Haiduc and H. Gilman, Some organosilicon derivatives prepared via metalation of 1,3,5-trichlorobenzene, ***J. Organomet. Chem.*** 1968, 12, 394-396.
32. I. Haiduc and H. Gilman, Pentachloro- and pentafluorophenyl-dimethylchlorosilane, ***J. Organomet. Chem.*** 1968, 13, 257-260.
33. I. Haiduc and H. Gilman, Lithiation of 1,2,3-trichloro- and 1,2,3,4-tetrachlorobenzenes. Organosilicon derivatives, ***J. Organomet. Chem.*** 1968, 13, 4P-6P.
34. I. Haiduc and H. Gilman, Perhaloaromatic organosiloxanes, ***J. Organomet. Chem.*** 1968, 14, 73-78.
35. I. Haiduc and H. Gilman, The metalation of some pentachlorophenyl-substituted organosilicon compounds, ***J. Organomet. Chem.*** 1968, 14, 79-85.

36. I. Haiduc and H. Gilman, Selective reactions of organolithium reagents with some polychlorobenzenes, ***Chemistry & Industry (London)*** 1968, 1278-1279.
37. H. Gilman and I. Haiduc, Comment on the thermal decomposition of triphenylthallium, ***J. Am. Chem. Soc.*** 1968, 90, 5912.
38. C. Ungurenasu and I. Haiduc, Die Reaktion von Polydimethylsiloxanchloriden mit Bis-cyclopentadienyl-titan(IV)- dihydrogensulfid, ***Rev. Roum. Chim.*** 1968, 13, 957-962.
39. T. H. Kinstle, I. Haiduc and H. Gilman, Mass spectrometry of cyclopolysilanes, ***Inorg. Chim. Acta*** 1969, 3, 373-377.
40. I. Haiduc and H. Gilman, N-Dilithiopentafluoroaniline and some silicon and germanium organoderivatives, ***J. Organomet. Chem.*** 1969, 18, 5P-7P.
41. D. Ballard, T. Brennan, F. W. G. Fearon, K. Shiina, I. Haiduc and H. Gilman, Silylation of some polyhalogenated compounds, ***Pure & Applied Chemistry*** 1969, 19, 449-472.
42. F. Denes, C. Ungurenasu and I. Haiduc, Plasma polymerization in electrical discharges. Condensation of octamethylcyclotetrasiloxane in a silent discharge, ***European Polymer J.*** 1970, 6, 1155-1160.
43. L. Vancea and I. Haiduc, The ammonolysis of organotrichlorosilanes, ***Studia Univ. Babes-Bolyai, Chemia***, 1970(2), 45-52.
44. I. Haiduc and H. Gilman, N-Pentafluorophenyl substituted cyclosilazoxanes, ***Syn. Inorg. Metal-org. Chem.*** 1971, 1, 69-74.
45. I. Haiduc and H. Gilman, N-Pentafluorophenyl silazanes and a cyclodigermazane, ***Syn. Inorg. Metal-org. Chem.*** 1971, 1, 75-81.
46. I. Haiduc and H. Gilman, The reaction of tetrachlorothiophene with some organolithium compounds, ***Rev. Roum. Chim.*** 1971, 16, 305-310.
47. I. Haiduc and H. Gilman, The reaction of pentachloropyridine with some organolithium compounds, ***Rev. Roum. Chim.*** 1971, 16, 597-600.
48. I. Haiduc and H. Gilman, Reactions of polychlorobenzenes with organolithium reagents. Polychloroaromatic organosilicon compounds, ***Rev. Roum. Chim.*** 1971, 16, 907-918.
49. R. B. King and I. Haiduc, Some ring size effects in the intramolecular transannular cyclizations of macrocyclic alkadiynes with iron carbonyls, ***J. Am. Chem. Soc.*** 1972, 94, 4044-4046.
50. I. Haiduc, Some tendencies in the literature of organometallic chemistry, ***J. Chem. Documentation*** 1972, 12, 175-178.
51. R. B. King, I. Haiduc and A. Efraty, Reactions of transition metal compounds with macrocyclic alkadiynes. II. Cyclopentadienylnickel and dicobalthexacarbonyl complexes retaining the macrocyclic alkadiyne structure unit, ***J. Organomet. Chem***. 1973, 47, 145-151.
52. R. B. King, I. Haiduc and C. W. Eavenson, Reactions of transition metal compounds with macrocyclic alkadines. III. Intramolecular transannular cyclizations and related processes with iron carbonyls, ***J. Am. Chem. Soc.*** 1973, 95, 2508-2516.

53. I. Haiduc, R. B. King and H. Gilman, Reactions of some pentafluorophenyl-silicon derivatives with the π-cyclopentadienyliron dicarbonyl anion, ***Rev. Roum. Chim***. 1974, 19, 1709-1715.
54. I. Haiduc and M. Curtui, Thin layer chromatography of some transition metal diethyldithiophosphates, ***Studia Univ. Babes-Bolyai, Chemia***, 1974, 19(2), 71-75.
55. A. Ziegler, V. P. Botha and I. Haiduc, Transition metal complexes of organothiophosphorus ligands. I. Nicke(II) chelates of some new diphenylthiophosphinyl thioreas, ***Inorg. Chim. Acta***, 1975, 12, 123-128.
56. I. Haiduc, F. Martinas, D. Ruse and M. Curtui, Metal-organic derivatives of organothiophosphorus acids. I. Tri- and diphenyllead phosphorodithioates, ***Syn. React. Inorg. Metal-org. Chem.*** 1975, 5, 103-114.
57. I. Haiduc and E. Veres, Metal-organic derivatives of organo-thiophsphorus acids. II. Arylmercury dialkylphosphorodithioates, ***Syn. React. Inorg. Metal-org. Chem***. 1975, 5, 115-122.
58. I. Haiduc, A. Ziegler and R. Kuchel, Methyl-phenyl substituted cyclotrisilazanes. Preparation and isomerism, ***1er Symoposium International de Chimie Heterocyclique Minerale***. Besancon, 16-19 Juin 1975, p. 317-329.
59. I. Haiduc and V. P. Botha, Carbon-free chelate rings: inorganic metallocycles containing imidodiphosphinato groups, ***1er Symoposium International de Chimie Heterocyclique Minerale***. Besancon, 16-19 Juin 1975, p. 437-449.
60. O. Cozar, V. Znamirovschi and I. Haiduc, On the metal-ligand bonding in copper(II)-bis(8-hydroxyquinolinate), ***Studia Univ. Babes-Bolyai, Physica***, 1975, 20, 29-36.
61. V. P. Botha, A. Ziegler and I. Haiduc, Transition metal complexes of organothiophosphorus ligands. II. Cobalt(II) chelates of some diphenylthiohosphoryl thioreas, ***Inorg. Chim. Acta.*** 1976, 17, 13-16.
62. R. Micu-Semeniuc, L. Dumitrescu-Silaghi and I. Haiduc, Transition metal complexes of organo-thiophosphorus ligands. III. Six-coordinate adducts of nickel(II) bis(diphenylphosphorodithioate) with aromatic and heterocyclic diamines, ***Inorg. Chim. Acta***, 1976, 17, 5-11.
63. R. Constantinescu, F. Martinas and I. Haiduc, Transition metal complexes of organothiophosphorus ligands. IV. Six-coordinate adducts of nickel(II) bis(diphenylphosphorodithioates) with symmetrically substituted ethylenediamines, ***Inorg. Chim. Acta***, 1976, 19, 105-108.
64. O. Cozar, V. Znamirovschi and I. Haiduc, ESR investigation of the effect of ethanol upon the structure of [Cu(trien)SCN]SCN in mixed water-ethanol solutions, ***J. Molec. Struct***. 1976, 31, 153-159.
65. I. Haiduc and M. Curtui, Preparation of bis(dialkylphosphorodithioato)dioxo (triphenylphosphine oxide) uranium(VI) complexes, ***Syn. React. Inorg. Metal-org. Chem***. 1976, 6, 125-132.
66. D. B. Sowerby and I. Haiduc, The crystal and molecular structure of a mixed ligand complex: tetramethylethylenediamine-bis-(O,O'-diethylphosphorodithioato)nickel(II), ***Inorg. Chim. Acta***, 1976, 17, L15-L16.

67. D. B. Sowerby and I. Haiduc, The crystal structure of N,N'-diphenylethlenediamine-bis-(O,O'-diethylphosphorodithioato)nickel(II), ***Inorg. Nucl. Chem. Letters*** 1976, 12, 791-793.
68. M. Curtui, G. Marcu, D. Diaconeasa and I. Haiduc, Solvent extraction of uranium(VI) with dialkyphosphrodithioic acids.II. The extraction of uranium with di-isopropyl- and bis(2-ethylhexyl)-phosphorodithionic acids in butanol, ***Studia Univ. Babes-Bolyai, Chemia*** 1976, 21, 63-67.
69. M. Curtui, G. Marcu and I. Haiduc, Solvent extraction of uranium(VI) with dialkyphosphorodithioic acids.III. Dialkylphosphorodithioic acids in nonmiscible water-n-butanol and water-benzene solvent extraction systems, ***Studia Univ. Babes-Bolyai, Chemia*** 1976, 21, 74-79.
70. G. Marcu, M. Curtui and I. Haiduc, Solvent extraction of dioxouranium(VI) with dialkylphosphorodithioic acids. I. The mechanism of extraction in n-butanol, ***J. Inorg. Nucl. Chem***. 1977, 39, 1415-1418.
71. I. Gergen, R. Micu-Semeniuc and I. Haiduc, Mixed ligand nickel(II) complexes containing tetrathiomolybdato and tetrathioarsenato groups and diamines, ***Syn. React. Inorg. Metal-org. Chem***. 1977, 7, 183-193.
72. K. A. Andrianov, M. Curtui, P. L. Prohodko, I. Haiduc, V. M. Kopylov, Zh. Syrtsova and M. I. Shkolnik, Reactions of organosilazanes with alcohols (original in Russian), ***Zhur. Obshch. Khim.*** 1977, 47, 600-603.
73. I. Balazs, V. Farcasan and I. Haiduc, Synthesis od di- and triphenyllead polychloroacetates, ***Rev. Roum. Chim.*** 1977, 22, 379-383.
74. I. Haiduc, G. Marcu and M. Curtui, Solvent extraction of uranium(VI) with dialkylphosphorodithioic acids. V. Synergistic effect of tributylphosphate, ***Rev. Roum. Chim***. 1977, 22, 626-632.
75. G. Marcu, I. Haiduc and M. Curtui, Solvent extraction of uranium(VI) with dialkylphosphorodithioic acids. VII. The synergistic effect of n-butanol in the extraction with benzene, ***Studia Univ. Babes-Bolyai, Chemia***, 1977, 22, 49-54.
76. M. Curtui, I. Haiduc and G. Marcu, Solvent extraction of dixouranium(VI) with dialkylphosphorodithioic acids. IV. Partition in the benzene-water solvent system, ***J. Radioanal. Chem.*** 1978, 44, 109-117.
77. I. Haiduc, Inorganic fragments in graft and block copolymers: a review of solved and unsolved problems, ***J. Polym. Sci., Polym. Symp.*** 1978, 64, 43-55.
78. O. Cozar, V. Znamirovschi and I. Haiduc, Solvent dependent EPR spectra of copper(II) monoethanolamine complexes in water-ethaol mixtures, ***Studia Univ. Babes-Bolyai, Physica***, 1978, 23, 6-9.
79. R. Micu-Semeniuc, L. Dumitrescu-Silaghi and I. Haiduc, Transition metal complexes of organothiophosphorus ligands. V. Some arly esters and amides of dithiophosphoric acid and their nickel(II) and cobalt(II and III) complexes, ***Inorg. Chim. Acta*** 1979, 33, 281-285.
80. S. P. Bone, D. B. Sowerby, R. Constantinescu and I. Haiduc, The preparation and crystal structure of bis(O-isopropyl-ethyldithiophosphonato)nickel(II), ***J. Chem. Res.*** 1979, (S) 69; (M) 0933-0963.

81. K. C. Molloy, M. B. Hossain, D. Van der Helm, J. J. Zuckerman and I. Haiduc, Crystal and molecular structure of (O.O'-diethyldithiophosphato)triphenyltin(IV) at 138K. A unique monodentate dithiophosphate derivative, ***Inorg. Chem.*** 1979, 18, 3507-3511.
82. M. J. Begley, D. B. Sowerby and I.Haiduc, Pentagonal pyramidal co-ordination; X-ray crystal structure of antimony(III) tris(diphenyldithiophosphinate), ***J. Chem. Soc. Chem. Commun.*** 1980, 64-65.
83. J. L. Lefferts, K. C. Molloy, J. J. Zuckerman, I. Haiduc, C. Guta and D. Ruse, Triorganotin(IV) dithiophosphate esters, ***Inorg. Chem***. 1980, 19, 1662-1670.
84. K. C. Molloy, M. B. Hossain, D. Van der Helm, J. J. Zuckerman and I. Haiduc, X-Ray crystal and molecular structure of bis(O,O'-diisopropyl dithiophosphato) diphenyltin(IV), a monomeric, molecular, virtual polymer, ***Inorg. Chem.*** 1980, 19, 2041-2045.
85. J. L. Lefferts, K. C. Molloy, J. J. Zuckerman, I. Haiduc, M. Curtui, C. Guta and D. Ruse, Diorganotin(IV) bis(dithiophosphate) esters, ***Inorg. Chem.*** 1980, 19, 2861-2868.
86. I. Haiduc, A survey of the nomenclature of inorganic ring systems. Proposals for a unified nomenclature, ***Rev. Inorg. Chem.*** 1980, 2, 219-249.
87. V. Coldea and I. Haiduc, Preparation and spectral properties of some organotin mono- and dithiocarboxyates, ***Syn. React. Inorg. Metal-org. Chem***. 1980, 10, 417-424.
88. V. Coldea and I. Haiduc, Determinarea staniului din compusi organostanici, ***Rev. Chim. (Bucuresti)*** 1980, 31, 86-87.
89. R. Micu-Semeniuc, L. Silaghi-Dumitrescu, N. Chirila and I. Haiduc, Transition metal complexes of organothiophosphorus ligands. VI. Six-coordinate adducts of nickel(II) bis(dialkyldithiophosphorodithiate) with aromatic amines, ***Rev. Roum. Chim***. 1980, 25, 1025-1031.
90. R. Micu-Semeniuc, C. Opris and I. Haiduc, Transition metal complexes of organothiophosphorus ligands. VII. Amine adducts of di(α- and β-naphtyl)phosphorodithioato nickel(II), ***Rev. Roum. Chim***. 1980, 25, 1489-1498.
91. I. Silaghi-Dumitrescu and I. Haiduc, The infrared spectrum of dimethyldithiophosphinato anion $(CH_3)_2PS_2^-$ Normal coordinate analysis and Urey-Bradley force field calculations, ***Rev. Roum. Chim.*** 1980, 25, 815-821.
92. I. Silaghi-Dumitrescu and I. Haiduc, Vibrational characteristics of Ni(II) dithiophosphinato chelates. Normal coordinate analysis and Urey-Bradley force field calculations of $Ni[S_2P(CH_3)_2]_2$, ***Rev. Roum. Chim.*** 1980, 25, 823-830.
93. R. Micu-Semeniuc, F. Vesa and I. Haiduc, Transition metal complexes of organothiophosphorus ligands. VII. Amine adducts of nickel(II) and cobalt(II) bis(diphenyl- and phenoxyethyl-phosphorodithioates), ***Studia Univ. Babes-Bolyai, Chemia*** 1980, 25(2), 44-48.
94. M. Curtui and I. Haiduc, Solvent extraction of dioxouranium(VI) with dialkylphosphorodithioic acids. VI. Synergic effect of triphenylphosphine oxide, ***J. Inorg. Nucl. Chem.*** 1981, 43, 1076-1078.

95. M. Curtui and I. Haiduc, Solvent extraction of thorium(IV) with diethyldithiophosphoroic acid, ***Radiochem. Radioanal. Letters***, 1981, 50(1), 55-66.
96. I. Haiduc, Inorganic heterocycles as ligands, ***Chem. Britain*** 1981, 17, 330-333.
97. I. Haiduc, Coordination patterns of dithiophosphorus ligands, ***Rev. Inorg. Chem.*** 1981, 3, 353-370.
98. V. Coldea, M. Coldea and I. Haiduc, Proton magnetic resonance spectra of some di- and triorganotin mono- and dithiocarboxylates, ***Rev. Roum. Chim.*** 1981, 26, 71-79.
99. I. Haiduc and L. Silaghi-Dumitrescu, Organotin and tin(IV) derivatives of dimethyldithioarsinic acid, ***J. Organomet. Chem.*** 1982, 225, 225-232.
100. I. Haiduc, Interconversion reactions of inorganic heterocycles, ***Rev. Inorg. Chem.*** 1982, 4, 179-210.
101. I. Silaghi-Dumitrescu and I. Haiduc, Bonding in organophosphorus compounds. A CNDO/2 calculation of electronic structure, ***Phosphorus & Sulfur***, 1982, 12, 205-212.
102. P. Clare, D. B. Sowerby and I. Haiduc, The crystal structure of a cyclo-silazoxane $[Me_2Si)_2ONC_6F_5]_2$, ***J. Organomet. Chem.*** 1982, 236, 293-299.
103. C. Silvestru and I. Haiduc, Combinatiile coordinative si organometalice in chimioterapia cancerului, ***Rev. Chim. (Bucuresti)*** 1982, 33, 81-88.
104. I. Haiduc, Contributii la chimia coordinativa a liganzilor ditiofosforici, ***Rev. Chim. (Bucuresti)*** 1982, 33, 234-238.
105. I. Silaghi-Dumitrescu, L. Silaghi-Dumitrescu and I. Haiduc, Normal coordinate analysis of the vibrational spectrum of dimethyldithioarsinato anion, $(CH_3)_2AsS_2^-$, ***Rev. Roum. Chim.*** 1982, 27, 911-916.
106. I. Haiduc, Inorganic cyclic compounds: Annual review covering year 1980, ***Revs. Inorg. Chem.*** 1983, 5, 7-121.
107. I. Haiduc, The coverage of inorganic heterocycles in Chemical Abstracts, ***J. Chem. Inf. Computer Sci.*** 1983, 23, 74-79.
108. I. Haiduc, C. Silvestru and M. Gielen, Organotin compounds: new organometallic derivatives exhibiting antitumor activity, ***Bull. Soc. Chim. Belge*** 1983, 92, 187-189.
109. D. B. Sowerby, I. Haiduc, A. Barbul-Rusu and M. Salajan, Antimony(III) diorganophosphoro- and diorganophosphinodithioates. Crystal structure of $Sb[S_2P(OR)_2]_3$ (R = Me or i-Pr), ***Inorg. Chim. Acta*** 1983, 68, 87-96.
110. L. Silaghi-Dumitrescu and I. Haiduc, Convenient preparation of phenylarsenic(III) chlorides from tetraphenyltin and arsenic(III) chloride, ***Synth. React. Inorg. Metal-org. Chem.*** 1983, 13, 475-480.
111. L. Silaghi-Dumitrescu and I. Haiduc, A sulfotropic molecular rearrangement of diphenylphosphinyl diorganodithioarsinates. Formation of diorganoarsenic(III) diphenyldithiophosphinates, ***J. Organomet. Chem.*** 1983, 252, 295-299.
112. R. Micu-Semeniuc, S. Popse and I. Haiduc, Some novel salts and ligand properties of the cyclic $P_2S_8^{2-}$ anion, ***Rev. Roumaine Chim.*** 1983, 28, 605-614.

113. L. Silaghi-Dumitrescu and I. Haiduc, Organo-silicon, -germanium and -lead derivatives of dimethyl- and diphenyl-dithioarsinic acids, ***J. Organomet. Chem***. 1983, 259, 65-69.
114. I. Haiduc, An inorganic chemist's view on polymer chemistry, in vol. ***IUPAC Macromolecular Division, 29th International Symposium on Macromolecules. Plenary and Invited Lectures***, Bucharest, Romania, September 5-9, 1983, Part 1, p. 449-476.
115. M. Curtui and I. Haiduc, Extraction of uranium(VI) with di-2-ethylhexyldithiophosphoric acid in different organic solvents, ***J. Radioanal. Nucl. Chem. Letters*** 1984, 86(5), 281-290.
116. T. Braun, P. Bull, J. Fardy, I. Haiduc, F. Makasek, W. J. McDowell, N. Z. Misak, J. D. Navratil and T. Sato, Solvent extraction of uranium, thorium and rare earths with dialkyldithiophosphoric acids, ***J. Radioanal. Nucl. Chem***. 1984, 84, 461-468.
117. I. Haiduc, I.Silaghi-Dumitrescu, R.Grecu, R.Constantinescu and L.Silaghi-Dumitrescu, Vibrational spectra of phosphorodithioic metal complexes. Normal coordinate treatment of bis(O isopropylethyldithiophoshonato) nickel(II), ***J. Mol. Struct.*** 1984, 114, 467-470.
118. I. Silaghi-Dumitrescu and I. Haiduc, Electronic structure and force constants of the dithionitronium cation NS_2^+, ***J. Mol. Struct.*** 1984, 106, 217-223.
119. L. Silaghi-Dumitrescu, I. Haiduc and J. Weiss, Preparation and properties of some organotin dimethyl- and diphenyl-dithioarsinates. The crystal structure of $(CH_3)_2Sn[S_2As(CH_3)_2]_2$, ***J. Organomet. Chem.*** 1984, 263, 159-165.
120. I. Silaghi-Dumitrescu and I. Haiduc, The electronic structure and bonding in the thiophosphoryl cation PS^+, ***Phosphorus & Sulfur*** 1985, 22, 85-91.
121. P. B. Hitchcock, J. F. Nixon, I. Silaghi-Dumitrescu and I. Haiduc, The crystal and molecular structure of a versatile ligand: tetraphenyldithioimidodiphosphinate, $Ph_2(S)P\text{-}NH\text{-}P(S)Ph_2$, ***Inorg. Chim. Acta*** 1985, 96, 77-80.
122. I. Haiduc and C. Silvestru, Trichlorodiphenylantimony(V), ***Inorg. Syntheses*** 1985, 23, 194-195.
123. I. Haiduc, M. Curtui, Iov. Haiduc and I. Silaghi-Dumitrescu, Solvent extraction of uranium, thorium and rare earths with dialkyldithiophopshoric acids, in vol. ***Chemical Aspects of Nuclear Methods of Analysis, IAEA-TECDOC-350***, A Technical Document Issued by the International Atomic Energy Agency, Vienna, 1985, p. 101-172.
124. I. Haiduc and I. Silaghi-Dumitrescu, Inorganic (carbon-free) chelate rings, ***Coord. Chem. Revs.*** 1986, 74, 127-270.
125. I. Silaghi-Dumitrescu and I. Haiduc, Why are cyclodisilazane rings more stable than cyclodisiloxanes? A qulitative molecular orbital approach to the bonding in cyclodisilazanes and cyclodisiloxanes, ***Inorg. Chim. Acta*** 1986, 112, 159-165.
126. I. Haiduc, M. Curtui and Iov. Haiduc, Solvent extraction of uranium(VI) with di-2-ethylhexyldithiophosphoric acid from aqueous nitrate, chloride, sulfate and phosphate media, ***J. Radioanal. Nucl. Chem. Articles*** 1986, 99, 257-263.

127. C. Silvestru, L. Silaghi-Dumitrescu, I. Haiduc, M. J. Begley, M. Nunn and D. B. Sowerby, Synthesis of diphenylantimony(III) dialkldithio- and diaryldithiophosphinates and -arsinates. Crystal structures of $Ph_2SbS_2MPh_2$ (M = P or As), ***J. Chem. Soc. Dalton Trans.*** 1986, 1031-1034.
128. F. Dogar, L. Silaghi-Dumitrescu, R. Grecu and I. Haiduc, Amine adducts of nickel(II) diphenyldithiophosphinate with substituted ethylenediamines, ***Rev. Roumaine Chim.*** 1986, 31, 79-83.
129. P. Clare, D. B. Sowerby and I. Haiduc, The crystal structure of bis(N-pentafluorophenyl)tetraphenyl-cyclodisilazane-tetrabenzene, $(Ph_2SiNC_6F_5)_2$ $4C_6H_6$, J. ***Organomet. Chem.*** 1986, 310, 161-167.
130. M. J. Begley, D. B. Sowerby, D. M. Wesolek, C. Silvestru and I. Haiduc, Diphenylantimony(III) diphenylphosphinate and diphenylmonothiophosphinate: synthesis, spectra and crystal structure, ***J. Organomet. Chem.*** 1986, 316, 281-289.
131. F. Dogar, L. Silaghi-Dumitrescu, R. Grecu and I. Haiduc, Amine adducts of nickel(II) diphenyldithiophosphinate with substituted ethylenediamines, ***Rev. Roum. Chim.*** 1986, 31, 79-83.
132. L. Silaghi-Dumitrescu, L. A. Avila-Diaz and I. Haiduc, Dimethyl- and diphenyldithioarsinates of some main group metals, ***Rev. Roum. Chim.*** 1986, 31, 335-340.
133. I. Silaghi-Dumitrescu and I. Haiduc, The bonding in dialkyldithiophosphinato metal complexes. A molecular orbital study of bis(dimethyldithiophosphinato) nickel(II), ***Rev. Roum. Chim.*** 1986, 31, 955-962.
134. M. J. Begley, D. B. Sowerby and I. Haiduc, The crystal structures of the diphenyldithiophosphinates of antimony(III) and bismuth(III): $M(S_2PPh_2)_3$ (M = Sb or Bi) ***J. Chem. Soc. Dalton Trans.*** 1987, 145-150.
135. D. B. Sowerby and I. Haiduc, The crystal structure of bismuth diethyldithiophosphinate-benzene(1/1), $Bi(S_2PEt_2)_3C_6H_6$, ***J. Chem. Soc. Dalton Trans.*** 1987, 1257-1259.
136. C. Silvestru, I. Haiduc, S. Klima, U. Thewalt, M. Gielen and J. J. Zuckerman, Synthesis and characterization of di- and triorganotin(IV) diethyldithiophosphinates. The crystal and molecular structure of bis(diethyldithiophosphinato)dimethyltin(IV), $Me_2Sn(S_2PEt_2)_2$, ***J. Organomet. Chem.*** 1987, 327, 181-191.
137. C. Silvestru, F. Ilies, I. Haiduc, M. Gielen and J. J. Zuckerman, Di- and triorganotin(IV) diphenyldithiophosphinates, ***J. Organomet. Chem.*** 1987, 330, 3115-3124.
138. I. Silaghi-Dumitrescù and I. Haiduc, Linear versus bent bis (diphenylphosphine)iminium cations. A molecular orbital discussion of the bonding in $[H_3PNPH_3]$ and related species, ***Rev. Roum. Chim.*** 1988, 33, 133-142.
139. I. Silaghi-Dumitrescu and I. Haiduc, Electronic structure and bonding in diamidoboron cations. A molecular orbital study of $[H_2NBNH_2]^+$, ***Rev. Roumaine Chim.*** 1988, 33, 851-856.
140. M. Curtui and I. Haiduc, Extractia toriului si a pamanturilor rare cu acizi dialchilditiofosforici, ***Rev. Chim. (Bucuresti)*** 1988, 39, 1099-1102.

141. O. Cozar, R. Semeniuc, V. Znamirovschi and I. Haiduc. ESR and IR studies of some oxovanadium dithiophosphonates, ***Rev. Roumaine Phys.*** 1988, 33, 1131-1135.
142. L. Silaghi-Dumitrescu. I. Silaghi-Dumitrescu and I. Haiduc, The sulfotropic rearrangement of tetraorganodiarsine disulfides, ***Rev. Roumaine Chim.*** 1989, 34, 305-315.
143. C. Silvestru and I. Haiduc, Synthesis and characterization of di- and triorganotin(IV) dimethyldithiophosphinates, ***J. Organomet. Chem.*** 1989, 365, 83-90.
144. I. Haiduc and C. Silvestru, Rhodium, iridium, cooper and gold antitumor organometallic compounds (review), ***In Vivo*** 1989, 3, 285-293.
145. M. Curtui and I. Haiduc, Solvent extraction of praseodium(III) and samarium(III) with di(2-ethylhexy)dithiophosphoric acid, ***Studia Univ. Babes-Bolyai, Chemia***, 1989, 34(1), 89-92.
146. C. Silvestru, F. Ilies and I. Haiduc, Organotin diphenylphosphinates, R4-nSn(O2PPh2)n ***Studia Univ. Babes-Bolyai, Chemia***, 1989, 34(1), 93-96.
147. I. Silaghi-Dumitrescu, R. Grecu, L. Silaghi-Dumitrescu and I. Haiduc, Vibrational spectra and coordination behavior of organodithiohosphorus ligands, ***Studia Univ. Babes-Bolyai, Chemia***, 1989, 34(1), 97-101.
148. I. Haiduc and C. Silvestru, Metal compounds in cancer chemotherapy, ***Coord. Chem. Revs.*** 1990, 99, 253-296.
149. C. Silvestru, C.Socaciu, A.Bara and I. Haiduc, The first organoantimony(III) compounds possessing antitumor properties: diphenylantimony(III) derivatives of dithiophosphorus ligands ***Anticancer Research*** 1990, 10, 803-804.
150. R. Grecu, R. Constantinescu, I. Silaghi-Dumitrescu and I. Haiduc, The infrared spectra of methyl(O-methyl)dithiophosphonic acid. Multiplicity of some bands due to different conformers, ***J. Mol. Struct.*** 1990, 218, 111-116.
151. I. Silaghi-Dumitrescu and I. Haiduc, The electronic structure of $[H_3SiNSiH_3]^-$ anion. A simple molecular orbital treatment, ***Rev. Roumaine Chim***. 1990, 35, 480-484.
152. I. Haiduc and I. Silaghi-Dumitrescu, The richness of structures available to P_2N_2 inorganic heterocycles. A topological and molecular orbital (EHMO) analysis; ***Rev. Roum. Chim***., 1991, 36, 527-544; ***Phosphorus, Sulfur & Silicon*** 1992, 65, 53-56 (short version).
153. A. Bara, C. Socaciu, C. Silvestru and I. Haiduc, Antitumor organometallics. I. Activity of some diphenyltin(IV) and diphenylantimony(III) derivatives on in vitro and in vivo Ehrlich ascites tumor, ***Anticancer Res***. 1991, 11, 1651-1656.
154. C. Socaciu, A. Bara, C. Silvestru and I. Haiduc, Antitumor organometallics. II. Inhibitory effects of two diphenylantimony(III) dithiophosphprus derivatives on in vitro and in vivo Ehrlich ascites tumor, ***In Vivo*** 1991, 5, 425-428.
155. C. Silvestru, I. Haiduc, M. Mahieu and M. Gielen, Di- and triorganotin(IV) diphenylphosphinates, $R_{4-n}S_n(O_2PPh_2)_n$. Structural considerations based upon ^{119m}Sn Mossbauer spectra, ***Main Group Metal Chem.*** 1991, 14, 257-262.
156. M. Curtui and I. Haiduc, Solvent extraction of lanthanum(III) and cerium(IV) with dialkyldithiophosphoric acids. Separation from thorium(IV), ***J. Radioanal. Nucl. Chem., Letters***, 1992, 164(2), 91-101.

157. I. Haiduc, A graph-based classification and enumeration of inorganic homo- and heterocycles, ***Phosphorus, Sulfur and Silicon***, 1992, 64, 169-178.
158. C. Silvestru, M. Curtui, I. Haiduc, M. J. Begley and D. B. Sowerby, Phenylantimony(III) diorganophosphorodithioates: the crystal structure of diphenylantimony(III) di isopropylphosphorodithioate, $Ph_2SbS_2P(OPr^i)_2$; unusual polymerization through semibonding, ***J. Organomet. Chem.*** 1992, 426, 49-58.
159. M. Curtui, I. Haiduc and Iov. Haiduc, Solvent extraction of thorium(IV) with dialkyldithiophosphoric acids, ***J. Radioanal. Nucl. Chem., Letters***, 1992, 165(2) 95-105.
160. I. Haiduc, C. Silvestru, H. W. Roesky, H. G. Schmidt and M. Noltemeyer. A new inorganic metallacycle containing tin, sulfur, phosphorus and nitrogen. Crystal and molecular structure of spirobicyclic $Me_2Sn(SPPh_2NPPh_2S_2)_2$ ***Polyhedron*** 1993, 12, 69-75.
161. F. T. Edelmann, M. Riekhoff, I. Haiduc and I. Silaghi-Dumitrescu, ansa-Metallocenderivate des Samariums und Ytterbiums mit "weichen" Donorliganden, ***J. Organomet. Chem.*** 1993, 447, 203-208.
162. M. Curtui and I. Haiduc, Synergic extraction of dioxouranium(VI) with di(2-ethylhexyl)dithiophosphoric acid and triphenylphosphine oxide in benzene, ***J. Radioanal. Nucl. Chem. Letters*** 1993 (3) 233-243.
163. C. Silvestru, I. Haiduc, F. Caruso, M. Rossi, B. Mahieu and M. Gielen, Organotin diphenylmonothiophosphinates. Crystal structure of bis(diphenylmonothiophosphinato)dimethyltin(IV), $Me_2Sn(OSPPh_2)_2$, ***J. Organomet. Chem***. 1993, 448, 75-82.
164. I. Silaghi-Dumitrescu, I. Haiduc and D. B. Sowerby, Fully inorganic (carbon-free) fullerenes? The boron-nitrogen case, ***Inorg. Chem***. 1993, 32, 3755-3758.
165. M. G. Newton, I. Haiduc, R. B. King and C. Silvestru, A unique macrocyclic structure of tetrameric trimethyltin(IV) diphenylphoshinate, $[Me_3SnO_2PPh_2]_4$, contaning a sixteen-membered $Sn_4O_8P_4$ inorganic ring, ***J. Chem. Soc. Chem. Commun***. 1993, 129-130.
166. M. G. Newton, R. B. King, I. Haiduc and A. Silvestru, A unique supramolecular structure of catena-poly[bis(μ-diphenylphosphinodithioato)-ditellurium(I)(Te-Te)], $[Te_2(S_2PPh_2)_2]_n$, containing Te-Te...Te-Te... chains, ***Inorg. Chem.*** 1993, 32, 3795-3796.
167. I. Haiduc, R. Micu-Semeniuc and L. Silaghi-Dumitrescu, Transition metal complexes of organothiophosphorus ligands. IX. Adducts of nickel alkoxy- and phenoxyethyl phosphorodithioates with primary and tertiary mono- and diamines, ***Syn. React. Inorg. Metal-org. Chem***. 1993, 23, 1629-1643.
168 C. Silvestru, I. Haiduc, R. Kaller, K. H. Ebert and H. J. Breunig, Synthesis, spectroscopic characterization and molecular structure of dimeric (diethyldithio-phosphinato)di(para-tolyl)antimony(III), $[(p\text{-}CH_3C_6H_4)_2SbS_2P(C_2H_5)_2]_2$, containing a novel monocyclic $P_2S_4Sb_2$ inorganic ring system, formed through Sb...S semibonding interactions, ***Polyhedron*** 1993, 12, 2611-2617.

169. R. Rosler, C. Silvestru, I. Haiduc, F. Kayser, M. Gielen and B. Mahieu, Synthesis and characterization of some new organotin(IV) tetraphenyldithiomidodiphosphinates, ***Main Group Metal Chem.*** 1993, 16, 435-443.
170. I. Silaghi-Dumitrescu and I. Haiduc, On the ring angles in the four-membered cyclodiphosphazanes, ***Studia Univ. Babes-Bolyai, Chemia***, 1993, 38, 183-186.
171. I. Haiduc, R. B. King and M. G. Newton, Stereochemical aspects of tellurium complexes with sulfur ligands. Molecular compounds and supramolecular associations, ***Chem. Revs***. 1994, 94, 301-326.
172. C. Silvestru, I. Haiduc, K. H. Ebert, H. J. Breunig and D. B. Sowerby, Trimethylantimony(V) diorganomonophosphinates. The crystal structure of bis(diphenylmonothiophosphinato)trimethylantimony(V), $Me_3Sb(OSPPh_2)_2$, containing a monodentate monothiophosphinato ligand, ***J. Organomet. Chem***. 1994, 468, 113-119.
173. F. T. Edelmann, M. Noltemeyer, I. Haiduc, C. Silvestru and Raymundo Cea-Olivares, Bismuth(III) dimethyldithiophosphinate, $Bi(S_2PMe_2)_3$ another dimer formed through secondary bonding. The stereochemically active lane pair revisited, ***Polyhedron*** 1994, 13, 547-552.
174. D. B. Sowerby, M. J. Begley, L. Silaghi-Dumitrescu, I. Silaghi-Dumitrescu and I. Haiduc, Antimony(III) and phenylantimony(III) dimethyldithioarsinates. Synthesis and mass spectral study. Crystal structure of $Ph_2SbS_2AsMe_2$, the first coordination polymer associated via bridging dimethyldithioarsinate ligands, ***J. Organomet. Chem***. 1994, 469, 45-53.
175. M. Curtui and I. Haiduc, Solvent extraction of thorium(IV) with dialkyldithiophosphoric acid in various organic solvents, ***J. Radioanal. Nucl. Chem.*** 1994, 186, 273-280.
176. M. Rieckhoff, M. Noltemeyer, F. T. Edelmann, I. Haiduc and I. Silaghi-Dumitrescu, Ein alter Ligand in neuer Umgebung: Dreifach verbruckendes O,O'-Dimethyldithiophosphat im Organosamarium-Komplex $[(C_5Me_5)Sm\{S_2P(OMe)_2\}_2]_2$, ***J. Organomet. Chem***. 1994, 469, C19-C21.
177. A. Silvestru, I. Haiduc, K. H. Ebert and H. J. Breunig, Novel coordination pattern of dithiophosphorus ligands. Crystal and molecular structure of (diphenylphosphinodithioato)phenyltellurium(II), $PhTeS_2PPh_2$ Supramolecular association through monodentate biconnective dithiophosphorus ligands, ***Inorg. Chem***. 1994, 33, 1253-54.
178. K. H. Ebert, H. J. Breunig, C. Silvestru, I. Stefan and I. Haiduc, Crystal and molecular structure of bis(diphenyldithiophosphinato)lead(II) $^1[Pb(S_2PPh_2)_2]$, a new type of polymer associated through Pb...S secondary interactions, ***Inorg. Chem***. 1994, 33, 1695-1699.
179. K. H. Ebert, R. E. Schulz, H. J. Breunig, C. Silvestru and I. Haiduc, Syntheses and structures of dimesitylbismuth(III) bromide, Mes_2BiBr, and bis(diphenyl-dithiophosphinato)mesitylbismuth(III), $MesBi(S_2PPh_2)_2$, ***J. Organomet. Chem.*** 1994, 470, 93-98.

180. B. K. Keppler, C. Silvestru and I. Haiduc, Antitumor organometallics. III. In vivo activity of diphenylantimony(III) and diorganotin(IV) dithiophosphorus derivatives against P388 leukemia, ***Metal-Based Drugs***, 1994, 1, 75-80.
181. I. Haiduc, C. Silvestru, F. Caruso, M. Rossi and M. Gielen Organotin(IV) diethylmonothiophosphinates. The structure of molecular, monomeric $Me_2Sn(OSPEt_2)_2$ versus polymeric $Me_2Sn(OSPPh_2)_2$, ***Rev. Roumaine Chim***. 1994, 39, 53-64.
182. J. S. Casas, A. Castineiras, I. Haiduc, A. Sanchez, J. Sordo and E. M. Vazquez-Lopez, Supramolecular self-organization in catena-poly [(dimethylphosphinothioato)thallium(III)]. $[TlMe_2\{S(O)PPh_2\}]_n$, a polymer with secondary interactions between the chain segments, ***Polyhedron***, 1994, 13, 1805-1809.
183. C. Silvestru, D. B. Sowerby, I Haiduc, K. H. Ebert and H. J. Breunig. Organoantimony(V) and –antimony(III) derivatives of diorganodithio-phosphinato ligands. Synthesis, spectroscopic characterization and X-ray molecular structure of $Me_3Sb(S_2PPh_2)_2$, ***Main Group Matal Chem***. 1994, 17, 505-518.
184. R. Cea-Olivares, J. G. Alvarado, G. Espinosa-Perez, C. Silvestru and I. Haiduc, Synthesis and characterization of phenoxarsin-10-yl diorganodithiophosphinates. A folded phenoxarsine system in the first dimeric organoarsenic(III) 1,1-dithiolate associated through As...S secondary bonding, ***J. Chem. Soc. Dalton Trans***. 1994, 2191-2195.
185. K. H. Ebert, H J. Breunig, C. Silvestru and I. Haiduc, Crystal and molecular structure of (dimethydithiophosphinato)dimethylantimony(III), $^1[Me_2SbS_2PMe_2]$, a chain polymer built through secondary, intermolecular Sb...S interactions, ***Polyhedron*** 1994, 13, 2531-2535.
186. C. Socaciu, I. Pasca, C. Silvestru, A. Bara and I. Haiduc, Antitumor organometallics. IV. The mutagenic potential of some diphenylantimony(III) dithiophosphorus derivatives, ***Metal-Based Drugs*** 1994, 1, 291-297.
187. J. S. Casas, A. Castineiras, I. Haiduc, A. Sanchez, J. Sordo and E. M. Vazquez-Lopez, Crystal and molecular structure of spirobicyclic bis(tetraphenyldithioimidodiphosphinato)-lead(II), $[Pb\{(SPPh_2)_2N\}_2]$, containing a new inorganic (carbon-free) PbS_2P_2N chelate ring and $Pb(h^6\text{-}C_6H_5)$ interactions, ***Polyhedron*** 1994, 13, 2873-2879.
188. A. Silvestru, I. Haiduc, K. H. Ebert, H. J. Breunig and D. B. Sowerby, New aryltellurium(II)diorganophosphinodithioates. Crystal structure of red (294 K) and yellow (173 K) $^1[PhTeS(S)PPh_2]$, a supramolecular polymer displaying an unusual coordination pattern of the phosphinodithioato ligand. ***J. Organomet. Chem***. 1994, 284, 253-259.
189. C. Silvestru, I. Haiduc, R. Cea-Olivares and A. Zimbron, Diorganotin(IV) derivatives of tetraphenylimidodiphosphinic acid. Crystal and molecular structure of $n\text{-}Bu_2Sn[(OPPh_2)_2N]_2$, a trans-octahedral spiro-bicyclic compound, ***Polyhedron*** 1994, 13, 3159-3165.
190. C. Silvestru, A. Silvestru, I. Haiduc, R. G. Ramirez and R. Cea-Olivares, Phenyllead(IV) diorganophosphinodithioates $Ph_nPb(S_2PR_2)_{4-n}$. Synthesis, spectroscopic characterization and NMR study of the redistribution/decomposition of diphenyllead(IV) derivatives, ***Heteroatom Chem.*** 1994, 15, 327-336.

191. I. Haiduc, Formation of inorganic quasi-cyclic structures through secondary interactions. A few cases of heterogeometrism, ***Phosphorus, Sulfur and Silicon,*** 1994, 93/94, 345-348.
192. O. Jimenez-Sandoval, R. Cea-Olivares, I. Haiduc, C. Silvestru and G. Espinosa-Perez, New organotin(IV) derivatives of 1-phenyl-1H-tetrazole-5-thiol, a five-membered nitrogen heterocycle, ***Phosphorus, Sulfur and Silicon***, 1994, 93/94, 387-388.
193. I. Silaghi-Dumitrescu, L. Serban, L. Silaghi-Dumitrescu and I. Haiduc, Chelating versus bridging coordination of dithiophosphates in copper complexes. An EHMO study, ***Rev. Roumaine Chim.***, 1994, 39, 1397-1405.
194. I. Silaghi-Dumitrescu and I. Haiduc, On the geometry of 1,3-diazadiphosphetidines. The cis-trans isomerism, ***Phosphorus, Sulfur and Silicon***, 1994, 91, 21-36.
195. R. Cea-Olivares, V. Lomeli, S. Hemandez-Ortega and I. Haiduc, Crystal and molecular structures of spiro-bis(trihiastannocane), $Sn(SCH_2CH_2SCH_2CH_2S)_2$, and spiro-bis(oxadithiastannocane), $Sn(SCH_2CH_2OCH_2CH_2S)_2$. Distortion of the SnS_4 tetrahedral coordination produced by transannular Sn...X (X = S, O) interactions, ***Polyhedron*** 1995, 14, 747-755.
196. J. S. Casas, A. Castineiras, I. Haiduc, A. Sanchez, J. Soedo and E. M. Vazquez-Lopez, Crystal and molecular structure of diphenylthallium (II) tetraphenyldithioimidodiphosphinate, $[TlPh_2\{(SPPh_2)_2N\}]$, containing a new inorganic (carbon-free) TlS_2P_2N metallocycle, ***Polyhedron*** 1995, 14, 805-809.
197. I. Haiduc, R. Cea-Olivares, R. A. Toscano and C. Silvestru, X-ray crystal structure of (tetraphenyldithioimidodiphosphinato)(triphenylphosphine) copper(I), $(Ph_3P)Cu(SPPh_2)_2N$, a monocyclic inorganic (carbon-free) chelate ring compound, ***Polyhedron*** 1995, 14, 1067-1071.
198. K. C. Molloy, M. Mahon, I. Haiduc and C. Silvestru, Solid state supramolecular structure of (tetraphenyldithioimidodiphosphinato)-trimethyltin(IV).benzene, $^1[Me_3Sn(SPPh_2)_2N.C_6H_6]$, a unique polymer containing a bridging SPR_2NPR_2S ligand, ***Polyhedron*** 1995, 14, 1169-1174.
199. A. Silvestru, I. Haiduc, H. J. Breunig and K. H. Ebert, Diphenyltellurium(IV) bis(diorganophosphinodithioates). X-ray crystal structure of $Ph_2Te(S_2PPh_2)_2.O.5CHCl_3$ and a multinuclear NMR study of the decomposition process of $Ph_2Te(S_2PR_2)_2$ to Ph_2Te^{II} and $[R_2P(S)S]_2$, ***Polyhedron*** 1995, 14, 1175-1183.
200. C. Silvestru, I. Haiduc, R. Cea-Olivares and S. Hemandez-Ortega, A. new eight-membered $Pb_2S_4S_2$ inorganic ring. Crystal and molecular structure of dimeric $[Pb(S_2PMe_2)_2]_2$, associated into polymeric chains through intermolecular Pb...S interactions, ***Inorg. Chim. Acta*** 1995, 233, 151-154.
201. L. Silaghi-Dumitrescu, I. Haiduc, J. Escudie, C. Couret and J. Satge, Investigations in the field of Group 14 difluorenyl compounds, ***Synth. React. Inorg. Met.-org. Chem.*** 1995, 25, 575-590.
202. R. Cea-Olivares, O. Jimenes-Sandoval, S. Hemandez-Ortega, M. Sanchez, R. A. Toscano and I. Haiduc, Electron distribution in 1-organo-1H-tetrazole-5-thiols. Crystal and molecular structure of 1-methyl-1H-tetrazole-5-thiol and its potassium(18-crown-6) salt, ***Heteroatom Chem.*** 1995, 16, 89-97.

203. C. Silvestru, R. Rosler, I. Haiduc, R. Cea-Olivares and G. Espinoza-Perez, Crystal and molecular structure of tetramethyldithioimidodiphosphinic, acid, $(SPMe_2)2NH$, and its cobalt(II) complex, $Co[SPMe_2)_2N]_2$, containing a tetrahedral CoS4 core, ***Inorg. Chem.*** 1995, 34, 3352-3354.
204. I. Haiduc, R. Cea-Olivares, S. Hernandez-Ortega and C. Silvestru, Unexpected linear P-N-P fragment in the anion $[SPh_2PNPPh_2S]^-$: Crystal structure of bis(triphenylphosphine)iminium dithiotetraphenylimido-diphosphinate, $[Ph_3PNPPh_3]^+[SPh_2PNPPh_2S]^-$, ***Polyhedron*** 1995, 14, 2041-2046.
205. A. Silvestru, I. Haiduc, R. A. Toscano and H. J. Breunig, Triphenyltelluronium derivatives of dithiophosphorus ligands: Crystal and molecular structure of $[Ph_3Te][S_2PPh_2]$ and $[Ph_3Te][(SPPh_2)_2N]$, displaying weak cation-anion Te...S secondary interactions, ***Polyhedron*** 1995, 14, 2047-2053.
206. C. Silvestru, R. A. Toscano, J. Cardenas, R. Cea-Olivares, A. Silvestru and I. Haiduc, Synthesis and characterization of triphenylgermanium(IV) diorganophosphinodithioates: Crystal and molecular structures of $Ph_3GeS(S)PR_2$ (R = Me, Ph), ***Polyhedron*** 1995, 14, 2231-2237.
207. J. Zukerman-Schpector, I. Haiduc, C. Silvestru and R. Cea-Olivares, Crystal structures of antimony and indium phosphinodithioates, $M(S_2PR_2)_3$ (M = Sb, R = Et; M = In, R = Me and Ph). Is the lone pair responsible for the structural differences? ***Polyhedron*** 1995, 14, 3087-3094.
208. I. Haiduc, D. B. Sowerby and Shao-Fang Lu, Stereochemical aspects of phosphor-1,1-dithiolato metal complexes (dithiophosphates, dithiophosphinates): coordination patterns, molecular structures and supramolecular associations. I (Polyhedron Report Number 57), ***Polyhedron*** 1995, 14, 3389-3472.
209. R. Cea-Olivares, M. R. Estrada, G. Espinoza-Perez, I. Haiduc, P. Garcia y Garcia, M. Lopez-Cardoso, M. Lopez-Vaca and A. M. Cotero-Villegas, 1-Oxa-4,6-dithia-5-arsocane and 1,3,6-trithia-2-arsocane dithiocarbamates. Competition between transannular and exocyclic secondary bonding to arsenic, ***Main Group Chem.*** 1995, 1, 159-164.
210. C. Silvestru, I. Haiduc, E. R. T. Tiekink, D. de Vos, M. Biesemans, R. Willem and M. Gielen, Synthesis, structural characterization and in vitro antitumour properties of triorganoantimony(V) disalicylates: Crystal and molecular structures of $[5\text{-}Y\text{-}2\text{-}(HO)\text{-}C_6H_3COO]_2SbMe_3$ (Y = H, Me, MeO), ***Appl. Organomet. Chem.*** 1995, 9, 597-607.
211. R. Landtiser, J. T. Mague, M. J. Fink, C. Silvestru and I. Haiduc, Cleavage of bis(thiophosphinyl)disulfanes, $R_2P(S)\text{-}S\text{-}S\text{-}P(S)R_2$ (R = Et, Ph), by a low-valent palladium dimer, ***Inorg. Chem.*** 1995, 34, 6141-6144.
212. C. C. Landry, A. Hynes, A. R. Barron, I. Haiduc and C. Silvestru, Gallium and indium compounds of sulphur donor ligands: pyridine-2-thiolates and diphenylthiophosphinates, ***Polyhedron*** 1996, 15, 391-402.
213. R. Rosler, C. Silvestru, G. Espinoza-Perez, I. Haiduc and R. Cea-Olivares, Tetrahedral vs. square planar NiS4 core in solid-state nickel(II) bis(dithioimidodiphosphinato) chelates. Crystal structures of $Ni[(SPPh_2)(SPR_2)N]_2$ (R = Me, Ph), ***Inorg. Chim. Acta*** 1996, 241, 47-54.

214. R. Rosler, J. E. Drake, C. Silvestru, J. Yang and I. Haiduc, The first X-ray structure of mixed chalcogen derivatives $SnR_2[(OPPh_2)(SPPh_2)_2N]_2$ (R = Me, Ph), ***J. Chem. Soc., Dalton Trans.*** 1996, 391-399.
215. C. Silvestru and I. Haiduc, Structural patterns in inorganic and organoantimony derivatives of oxo- and thiodiorgano-phosphorus ligands, ***Coord. Chem. Rev.*** 1996, 147, 117-146.
216. I. Haiduc and D. B. Sowerby, Stereochemical aspects of phosphor-1,1-dithiolato metal complexes (dithiophosphates, dithiophosphinates): coordination patterns, molecular structures and supramolecular associations of dithiophosphinates and related compounds (Polyhedron Report Number 60), ***Polyhedron*** 1996, 15, 2469-2521.
217. C. Socaciu, I. Pasca, C. Silvestru and I. Haiduc, Genotoxicity of some metal-based antineoplastics, evaluated by SOS Chromotest and cytogenetic analysis, ***Metal-Based Drugs*** 1996, 3, 91-99.
218. A. T. Balaban, I. Haiduc, H. Hopfl, N. Farfan and R. Santillan, Spiroborates revisited. X-ray crystal and molecular structures of boron chelate compounds with tropolone and 1,3-diketones, ***Main Group Metal Chem***. 1996, 19, 385-395.
219. M. Nunn, M. J. Begley, D. B. Sowerby and I. Haiduc, Complexes of organoantimony(III) and (V) halides with nitrogen donors, ***Polyhedron*** 1996, 15, 3167-3174.
220. C. Silvestru, R. Rosler, I. Haiduc, R. A. Toscano and D. B. Sowerby, Dichlorodiphenylantimony(V) derivatives of oxo- and thioimidodiphosphinic acids, containing novel inorganic SbO_2P_2N and $SbOSP_2N$ rings: crystal and molecular structures of $Ph_2SbCl_2[(OPPh_2)(XPPh_2)N]$ (X = O, S), ***J. Organomet. Chem.*** 1996, 515, 131-138.
221. L. Silaghi-Dumitrescu, M. N. Gibbons, I. Silaghi-Dumitrescu, J. Zukerman-Schpector, I. Haiduc and D. B. Sowerby, Oxidation of $(AsPh_2)_2E$ (E = O or S); supramolecular hydrogenbonded self-assembly of an unusual tetranuclear adduct and X-ray crystal structure of $[AsPh_2(O)(OH).AsPh_2(S)OH]_2$, ***J. Organomet. Chem.*** 1996, 517, 101-106.
222. R. Gavino-Ramirez, R. A. Toscano, C. Silvestru and I. Haiduc, Studies on inorganic tin diphenyldithiophosphinates. Crystal and molecular structure of cis-dichlorobis(diphenyldithiophosphinato)tin(IV), ***Polyhedron***, 1996, 15, 3857-3867.
223. M. N. Gibbons, C. Silvestru, I. Haiduc and D. B. Sowerby, Reduction of antimony(V) by dithiophosphinates and the crystal structure of dimeric diphenylantimony(III) dimethyldithiophosphinate, $[Ph_2SbS_2PMe_2]_2$, ***Polyhedron*** 1996, 15, 4573-4578.
224. I. Silaghi-Dumitrescu, F. Lara-Ochoa, P. Bishof and I. Haiduc, More about boron-nitrogen $B_{12+3n}N_{12+3n}$ fullerene-like cages. An ab initio and AM1 investigation of some 4/6 isomers, ***J. Mol. Struct. (Theochem)*** 1996, 367, 47-54.

225. I. Silaghi-Dumitrescu, F. Lara-Ochoa, and I. Haiduc, $A_{12}B_{12}$ (A = B, Al; B = N, P) 4/6 fullerene-like cages and their hydrogenated forms stabilized by exohedral bonds. An AM1 molecular orbital study, ***J. Mol. Struct. (Theochem)*** 1996, 370, 17-23.
226. I. Haiduc, Supramolecular associations, secondary bonds, quasi-cyclic structures and heterogeometrism in metal derivatives of phosphorus- and arsenic-based thioacids and oxo analogues, ***Coord. Chem. Revs.*** 1997, 158, 325-358.
227. J. S. Casas, A. Castineiras, I. Haiduc, A. Sanchez, J. Sordo and E. Vazquez-Lopez, Supramolecular self-organization in methyl(dyphenylphosphinothioato) mercury(II), $[HgMe\{S(O)PPh_2\}]_n$, a ladder polymer containing eight-membered rings $Hg_2O_2P_2S_2$ interconnected through secondary Hg...O bonds, ***Polyhedron*** 1997, 16, 781-787.
228. A. Silvestru, C. Silvestru, I. Haiduc, J. E. Drake, J. Yang and F. Caruso, Metal-oxygen versus metal-sulfur bonding of the ambident monothiophosphinato ligand in some triphenyl metal(IV) derivatives, $Ph_3M[OSPR_2]$ (M = Ge, Sn, Pb). Crystal structures of $Ph_3Ge[O(S)PPh_2]$ and $[Ph_2Sn\{O(S)PPh_2\}(u\text{-}OH)]_2$, ***Polyhedron*** 1997, 16, 949-961.
229. Ioan Silaghi-Dumitrescu, Francisco Lara-Ochoa and Ionel Haiduc, On the formation of cyclodisilazanes via the coordination of bis(dialkylaminosilanes) to halogenosilanes. An *ab initio* and AM1 molecular orbital study of the 4644 $R_2Si(NR')_2{:}SiX_4$ ring systems, ***J. Mol. Struct. (TEOCHEM)*** 1997, 397, 213-222.
230. C. Silvestru, A. Silvestru, I. Haiduc, D. B. Sowerby, K. H. Ebert and H. J. Breunig, Triorganoantimony(V) diorganophosphinates, Crystal and molecular structure of (diphenylphosphinato)(hydroxo)trimethylantimony(V) exhibiting a polymeric chain. Supramolecular self-assembly through hydrogen bonds, ***Polyhedron*** 1997, 16(15) 2643-2649.
231. Raymundo Cea-Olivares, Klaus H. Ebert, Luminita Silaghi-Dumitrescu and Ionel Haiduc, Bismuth(III(dimethyldithioarsinate, $Bi(S_2AsMe_2)_3$: A new dimer formed through Bi-S secondary bonding, ***Heteroatom Chem***. 1997, 8, 317-321.
232. M. Venter, I. Haiduc, L. David and O. Cozar, IR and ESR studies on new-bis-triazenido cobalt(II) and copper(II) complexes, ***J. Mol. Struct.*** 1997, 408-409, 483-486.
233 Ionel Haiduc, Metals in medicine: past, present, future in vol. ***"Metal Elements in Environment, Chemistry and Biology"***, Edited by Z. Garban and D. Dragan, Proceedinds of the 2nd International Symposium on Metal elements in environment, Medicine and Biology, Timisoara, October 27-29, 1996, Publishing House "Eurobit" Timisoara, 1997, pag. 35-42.

234. Luminita Silaghi-Dumitrescu, Sofia Pascu, Alexander J. Blake, Ionel Haiduc and D. Bryan Sowerby, The first oxyge-bridged diorganoarsenic(V) compound: the crystal structure of $AsMe_2(S)OAs(S)Me_2$, ***J. Organomet. Chem.,*** 1997, 549, 187-192.
235. Francisco Cervantes-Lee, Hemant K. Sharma, Ionel Haiduc and Keith Pannell, A unique self-assembled tricyclic stannasiloxane containing a planar Sn_3SiO_5 fused 6.4.4. tricyclic ring system., ***J. Chem. Soc. Dalton Trans.*** 1998(1) 1-2.
236. Cristian Silvestru, Roland Rosler, John E. Drake, Jincai Yang, Georgina Espinosa-Perez and Ionel Haiduc, Bis(thiophosphinoy)amines and their neutral cobalt(II) complexes, containing stable tetrahedral CoS_4 cores. Crystal structures of $NH(SPMe_2)(SPPh_2)$ and $[Co\{[(SPMe_2)(SPPh_2)N\}_2]$, ***J. Chem. Soc. Dalton Trans.*** 1998 (1) 73-78.

STUDIA UNIVERSITATIS BABEȘ-BOLYAI, CHEMIA, XLII, 1-2, 1997

THE EFFECT OF PRECURSOR SOLUTION ON THE STRUCTURE OF CeO_2/Al_2O_3 CATALYSTS

RADU CRÀCIUN[1], LILIANA CRĂCIUN[2]

ABSTRACT. A cerium (IV) methoxyethoxide (Ce-Alk) 18-20% precursor solution was used to prepare cerium promoted γ-Al_2O_3 catalysts by grafting impregnation. Modified precursor were obtained by mixing Ce-Alk with 2,4-pentanediol (diol) at various diol: Ce-Alk molar ratios (q = 0, 1, 2, 3) and utilized for CeO_2/γ-Al_2O_3 (DqCe) catalysts preparation, as well. Fourier transform infrared spectroscopy (FTIR) data on the precursor solutions show peaks characteristic of formation of a *weak* complex between cerium alkoxide and diol. NMR results are consistent with the IR observations, indicating a shift in the protons corresponding to the diol coordinated to cerium metal. X-ray diffraction (XRD) and X-ray photoelectron spectroscopy (XPS) were used for bulk and surface characterization of the CeO_2/γ-Al_2O_3 catalysts, designated as DqCe. The chemical nature of the precursor solution plays an important role in the surface configuration of the impregnated CeO_2. After thermal treatment at 500^0C and 800^0C, XRD analysis indicates that the particle sizes of the CeO_2 formed on the support surface are comparable for the different catalysts prepared using diol modified precursors. However, semiquantitative XRD data show that the intensity of the XRD pattern corresponding to CeO_2 <111> and <200>, characteristic of CeO_2 crystalline phase formed on the alumina support, increases with calcination temperature and the decrease in the q value from 3 to 0. Results from X-ray photoreduction studies using XPS analysis show data consistent with those obtained from semiquantitative XRD calculations. Information derived from XRD and XPS analysis for the dried and calcined catalysts, indicate an increase in the CeO_2 despersion (small CeO_2 crystallites and high Ce_{3d}/Al_{2p} XPS intensity ratio) for catalysts prepared from modified cerium alkoxide precursors (pDqCe, where $q \geq 1$).

INTRODUCTION

Anchoring cerium alkoxide species in an organic medium, followed by calcination, have proven to be a reliable preparation technique for CeO_2/g-Al_2O_3 catalysts [1]. This impregnation method is based on the chemical interaction

[1] Department of Chemistry, Michigan State University, East-Lansing, Michigan 48824-1322, USA, on leave of absence from Facultatea de Chimie și Inginerie Chimică, Universitatea Babeș-Bolyai RO-3400 Cluj-Napoca, Romania.

[2] Facultatea de Chimie și Inginerie Chimică, Universitatea Babeș-Bolyai RO-3400 Cluj-Napoca, Romania.

between the cerium alkoxide compound and the hydroxyl groups from the support surface [2], interaction enhanced by high temperature and reflux conditions [3]. Simple grafting at room temperature leads after calcination to a poorly dispersed CeO_2 phase on alumina. This was attributed partly to the polymerization of cerium alkoxide molecules on the support surface during impregnation, drying, and calcination. A significant amount of the cerium phase deposited on the alumina surface was found to be in an amorphous state. The increase of calcination temperature to 800^0C leads to a growth in the CeO_2 crystallite size deposited on the g-Al_2O_3 support surface.

Many previous studies emphasized the strong correlation between the cerium surface structure and its promoter and/or catalytic properties [4-10]. Sanchez *et al.* [11] have studied the cerium sol-gel chemistry using 2,4-pentanedione (*acac*) as a ligand for the gelation process. Using extended X-ray absorption fine structure (EXAFS) analysis combined with Fourier-transform infrared (FTIR) and Raman spectroscopy, they found that cerium isopropoxide is present in the gel as monomer or as alkoxide dimers. Cerium can coordinate one, two or three *acac* molecules forming complexes with well defined structure. Based on this idea, it should be possible to design a new alkoxide precursor, more stable but reactive enough to be used for grafting impregnation of a high surface area support, like Al_2O_3 TiO_2 or SiO_2. Diols are organic compounds containing two hydroxyl groups in their molecule which can be used as moderate bidentate ligands in complexation reactions due to the unpaired electrons from the oxygens of the hydroxyl groups [12].

This work is part of a study that investigates new synthetic methods suitable for catalysts preparation. In this paper the effect of 2,4-pentanediol complexation in the precursor solution used for grafting impregnation, on the surface structure of CeO_2 deposited on g-Al_2O_3 support, will be presented. Nuclear magnetic resonance (NMR) and Fourier-transform infrared (FTIR) spectroscopy analysis will be used to characterize the molecular structure of the diol-modified precursors. X-ray diffraction (XRD) and X-ray photoelectron spectroscopy (XPS) will give us information about the bulk and surface structure of the CeO_x/g-Al_2O_3 catalysts prepared from the modified precursors.

EXPERIMENTAL

Catalyst Preparation. Catalysts were prepared by grafting impregnation of g-alumina (Cyanamid, g-Al_2O_3, surface area = 200 m^2/g, pore = 0.6 mL/g) using solutions of modified cerium alkoxide with a diol (DqCe, q = diol:alkoxide molar ratio) as precursors. The alumina support was finely ground (< 230 mesh) and calcined in air at 500^0C for 24 h prior to impregnation. Catalysts were derived from pure alkoxide using Ce^{4+}-methoxyethoxide (18-20% alkoxide in methoxyethanol) obtained from Gelest Inc. The modified cerium methoxyethoxide precursors were prepared using 2,4-pentanediol purchased from Aldrich Chemical Company. The cerium content chosen for our catalysts was Ce/Al = 6.0 x 10^{-2} atomic ratio (or 16.5% CeO_2 by weight), a value close to the monolayer coverage for a g-Al_2O_3 support. Different diol: cerium alkoxide molar ratios in the precursor solutions were used to prepare the DqCe catalysts, where q = 0:1, 1:1, 2:1 and 3:1. The catalysts

were prepared by wet impregnation of the g-Al_2O_3 support with the alkoxide and the modified precursor solutions, at room temperature, under inert atmosphere and continuous mixing for 24 hours. After impregnation, the catalysts were dried at 120°C for 12 h and calcined 24 hours in air 500°C and 800°C, respectively.

FTIR Spectroscopy. An FTIR Mattson Inst. Galaxy-3000 was used for infrared analysis. Thin precursor films were prepared on KBr pellets and were acquired with resolution of 2.0 cm^{-1}, 50 scans, on a 400-4000 cm^{-1} wavenumber range.

NMR analysis. ^{1}H-NMR spectra of the modified cerium precursors were collected with a Gemini 300 MHz spectrometer in $CDCl_3$, at room temperature. The ^{1}H-NMR spectrum of pure 2,4-pentanedion in $CDCl_3$, was acquired as reference for the chemical shifts of the modified precursors.

X-Ray Diffraction. X-ray powder diffraction patterns were obtained with a Rigaku XRD diffractometer employing Cu K_a radiation (l = 1.54184Å). The X-ray was operated at 45 kV and 100 mA. Diffraction patterns were obtained using a scan rate of 0.5 degrees/min with slits = 1 mm. Powdered samples were mounted on glass slides by pressing the powder into an indentation on one side of the slide. The mean crystallite size (d) of the CeO_2 particles was determined from XRD line broadening measurements using the Scherrer equation [13]:

$$\bar{d} = K\lambda / \beta \chi o\sigma \theta \qquad (1)$$

where l is the X-ray wavelength, K is the particle shape factor, taken as 0.9, and b is the full width at half maximum (fwhm), in radians, of the CeO_2 <111> line. Semiquantitative X-ray diffraction data were obtained by comparing CeO_2 <111> / Al_2O_3 <440> intensity ratios measured for catalyst samples with peak ratios determined for physical mixtures of CeO_2 and g-Al_2O_3.

XPS Analysis. XPS data were obtained using a Perkin-Elmer Surface Science instrument equipped with a magnesium anode (1253.6 eV) operated at 300 W (15 kV, 20 mA), and a 10-360 hemispherical analyzer operated with a pass energy of 50 eV. Spectra were collected using a PC137 board interfaced to a Zeos 386SX computer. The instrument typically operates at pressures below 6.67 x 10^{-6} N/m^2 (1 x 10^{-8} torr) in the analysis chamber. Samples were analyzed as powders dusted onto double-sided sticky tape. Binding energies for the catalyst samples were referenced to the Al_{2p} peak (74.5 eV). XPS binding energies were measured with a precision of ±0.2 eV or better. The model proposed by Kerkhof and Moulijn [14] has been used for quantitative XPS analysis. The photoelectron cross sections and the mean escape depths of the photoelectrons, used in these calculations, were taken from Scofield [15] and Penn [16], respectively. For a phase (p) present as discrete particles, the experimental intensity ratio (I_p/I_s) is given by the following expression:

$$I_p/I_s = I^0p/I^0_s[1-\exp(-d/I_p)] / d/I_p \qquad (2)$$

where (I^0p/I^0_s) is the theoretical monolayer intensity ratio, (d) is the length of the edge of the cubic crystallites of the deposited phase, and (I_p) is the mean escape

depth of the photoelectrons in the deposited phase. Pure CeO_2 (Aldrich) for Ce^{4+} XPS spectrum and $CeAlO_3$ (just prepared) for Ce^{3+} XPS spectrum were used as standards. $CeAlO_3$ was prepared and analysed *in-situ,* by reduction of CeO_2 under continuous H_2 flow at 900^0C for 16 hours.

RESULTS AND DISCUSSION

Modified precursors. In solution, cerium with a coordination number of six may form different complexes with bidentate organic ligands. Different discrete structures will be obtained by using different cerium-ligand molar ratios [2]. Previous studies on cerium alkoxide coordination chemistry used 2,4-pentanedione *acac* as ligand, at different metal to ligand molar ratios, for metal stabilization by complexation [17]. In this case, cerium methoxyethoxide formed a precipitate when *acac* was added. In order to perform a grafting impregnation, it is necessary to have a homogeneous cerium solution. This was provided by the modified cerium alkoxide solution with 2,4-pentanediol (a weaker ligand than *acac*). Mass spectrometry analysis have indicated that cerium methoxyethoxide is present in solution as a monomer. Adding the diol at different diol: cerium alkoxide molar ratios, homogeneous cerium solutions have been obtained. However, after aging, the solutions changed their color and formed gels. In general, aging is an important factor for gels preparation. To avoid the gelation process, the fresh modified solution must be used immediately in the impregnation process. The strongest gelation effect was observed in the case of the diol modified cerium alkoxide with a molar ratio of 3:1. ^{1}H-NMR and FTIR analysis were used to explain the changes in the solutions aspect.

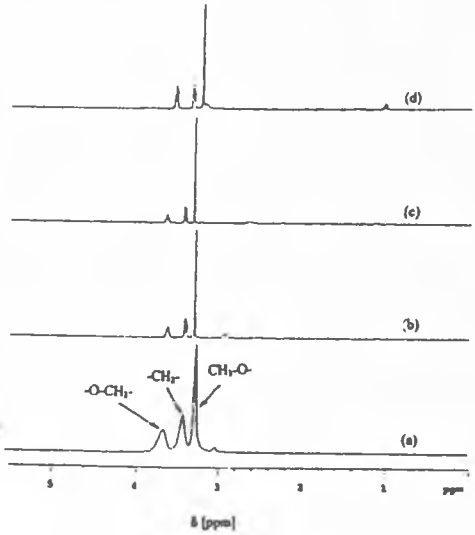

Fig. 1. ^{1}H NMR spectra of precursor solutions: a) pD0Ce; b) pD1Ce; c) pD2Ce; d) pD3Ce

Figure 1 shows the ^{1}H-NMR spectrum of the cerium methoxyethoxide (pD0Ce) solution (a), in comparison with the diol modified alkoxide (pDqCe, with q ≥ 1) solutions (b-d). From spectrum (a) one can observe that the resonance peaks corresponding to - O-CH_3 (d = 3.279 ppm), -CH_2- (d = 3.425 ppm) and -O-CH_2- (d = 3.664 ppm) protons are broad instead of narrow siglets for -CH_3, and multiplet resonance peaks for -CH_2- groups. This is attributed in the literature [11] to an average resonance obtained from fast (on the NMR time scale) chemical exchange of the ligand and different ligand groups (terminal or solvated molecules), with the solvent. The ligand, which in this case is methoxyethoxide, will be in a dynamic equilibrium with methoxyethanol solvent molecules.

Figure 1 (b-d) shows the ^{1}H-NMR for the diol modified cerium alkoxide solutions at different molar ratios [(a) 1:1, (b) 2:1, (c) 3:1]. In these cases, the spectra show characteristic resonances for the protons corresponding to the methoxyethoxide ligand from solution: singlet for -CH_3 and multiplet for CH_2- and -O-CH_2- groups.

By adding the diol to the cerium alkoxide solution at variable diol: cerium alkoxide molar ratios, different complexes are obtained. Table 1 shows the chemical shifts observed for the 2.4-pentanediol protons in the modified solution (pDqCe) as compared with the pure diol solution.

Table 1. ^{1}H-NMR data of the 2,4-pentanediol from the modified cerium alkoxide precursors

	Diol d [ppm]	pD1Ce d [ppm]	pD2Ce d [ppm]	pD3Ce d [ppm]
CH_3	1.107	1.085	1.118	1.033
	1.125	1.107	1.139	1.055
	1.134	1.114	1.149	1.080
	1.155	1.135	1.170	----
CH_2	1.445	1.429	1.458	1.350
	1.458	1.434	1.468	1.379
	1.471	1.453	1.484	1.398
	1.496	1.475	1.512	1.414
CH	3.918	3.396	3.424	3.348
	3.939	3.411	3.439	3.361
	3.959	3.422	3.444	3.378
	3.981	3.427	3.456	----
	4.020	3.612	3.635	3.562
	4.041	3.622	3.652	3.577
	4.059	3.636	3.666	3.592
	4.079	3.651	3.684	----

Due to the presence of asymmetric carbons in 2,4-pentanediol (at positions 2 and 4; 2,4- pentanediol was purchased from Aldrich as a mixture of stereoisomers), the two protons at carbon 3 are diastereotopic [18], and accordingly they induce additional splittings at the adjacent protons (the -CH- signal is a doublet of quartets, while the -CH_2- one is a doublet of doublets). The data in Table 1 reveals that the NMR spectra of the diol in the modified precursors exhibit new resonances located at different chemical shifts as compared with pure

diol. These new resonance values for the chemical shifts of the diol protons were assiigned to diol molecules coordinated to cerium atoms. The presence of diol in the system may have as well a moderator effect, changing the viscosity of the solution and interfering in the dynamic equilibrium established between the ligands attached to the cerium atom and solvent molecules.

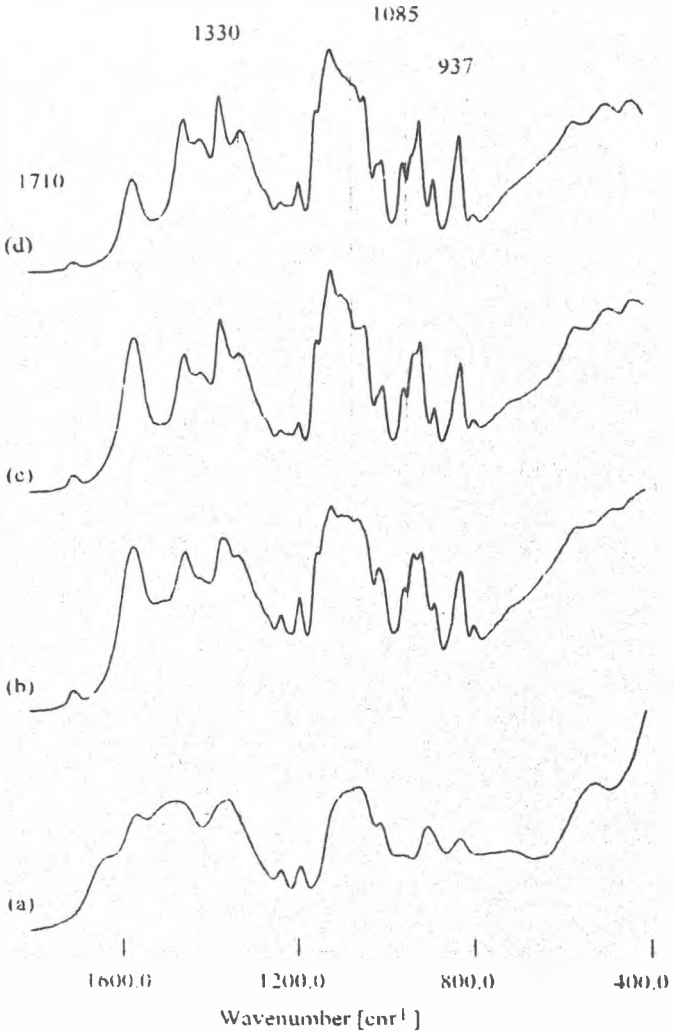

Fig. 2. The infrared spectra of the title compounds

Additional information about the complexation and gelation process can be obtained from FTIR analysis. Figure 2 shows the IR spectra of cerium alkoxide (pD0Ce) solution (a) in comparison with the modified solution, and (b-d) at various diol: cerium alkoxide molar ratios (pDqCe, with $q \geq 1$). Metal alkoxides exhibit characteristic bands for -C-O- vibration at ca. 1000 cm^{-1} and for M-O- vibration at

600-300 cm^{-1} [9]. For example, cerium isopropoxide exhibits a strong and characteristic absorption band corresponding to the -C-O-Ce vibration at 980 cm^{-1} [20]. The IR spectrum of pure cerium methoxyethoxide indicates a specific band at 910 cm^{-1}, attributed to the alkoxide -C-O-Ce bond vibration [19]. As the diol is added to the alkoxide, a new band appears at 937 cm^{-1} which can be attributed to the -C-O-Ce bond of a diol -C-O-. Other new bands appear in the IR spectra of the diol modified solution at 1085 cm^{-1}, 1330 cm^{-1} and 1710 cm^{-1}. The IR absorption band at 1710 cm^{-1} usually is attributed to a carboxylate group in the system. It is conceivable that during the complexation and gelation process, a small amount of carboxylate was formed in the system from the free ligand by cerium alkoxide decomposition.

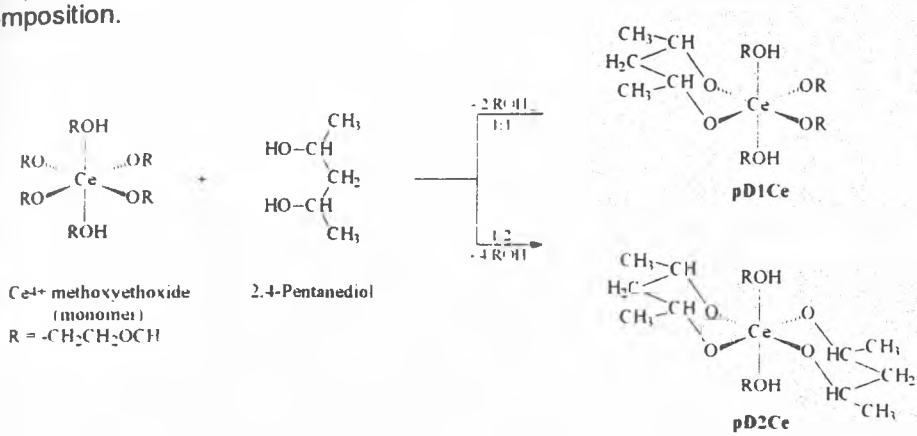

Fig. 3. Complex formation by reaction of cerium alkoxide with 2,4-pentandiol in various molar ratios

Leaustic et al. [21] explained the chemical modification of metal alkoxides [$(Ti\text{-}OR)_4$] with *acac* in a similar manner, using FTIR and ^{1}H-NMR, respectively. The structural differences are related to the ability of the alkoxide groups to behave as exchange ligand. Another factor which might be considered is the humidity during the preparation of the diol modified cerium alkoxide. It is well known that atmospheric water vapors play an important role in the gelation process. To avoid the gelation before and during impregnation, a dry atmosphere is needed. As a conclusion, 2,4-pentanediol forms with Ce^{4+} from cerium methoxyethoxide molecules a weak complex which avoids polymerization of the alkoxide, initially present as a monomer. Below are presented the reactions and possible structures of such complexes for diol: cerium alkoxide molar ratios of q = 1 and 2.

Extreme conditions like high vacuum or high temperature will easily decompose the complexes. Nevertheless these diol modified precursors were used for grafting impregnation of the g-Al_2O_3 support. The impregnation process is similar with that described in our previous paper [1]. The interaction between the precursor and support implies reaction of the cerium alkoxide with the surface hydroxyl groups from the support. Finally, the diol itself and the coordination complexes ultimately formed, will play the role of moderators, changing the

viscosity of solution, inhibiting the polymerization of cerium alkoxide, and as a result, allowing time for the grafting interaction to occur.

Bulk Characterization. After preparation of the diol modified precursors and the impregnation of the g-Al_2O_3 support, the DqCe catalysts were calcined at 500^{0}C and 800^{0}C in air. XRD analysis gave us information about the bulk structure (particles > 30 Å) of the catalysts.

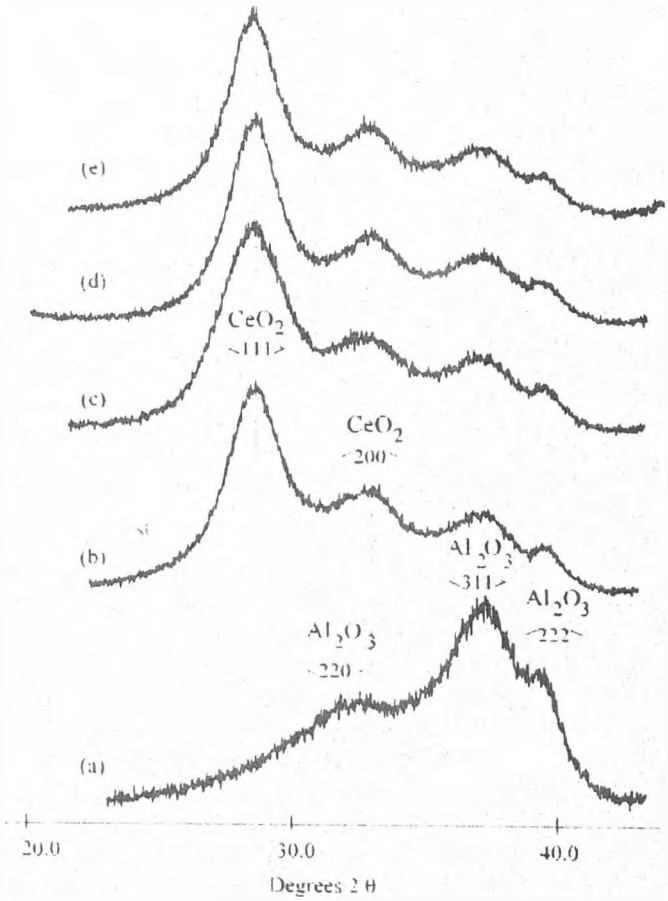

Fig. 4. XRD patterns of the DqCe catalysts calcinated at 500^{0}C: a) Al_2O_3, b) D0Ce, c) D1Ce, d) D2Ce, e) D3Ce catalysts

Figure 4 (b-2) shows the XRD patterns of the DqCe catalysts calcined at 500^{0}C under air, in comparison with the pure g-Al_2O_3 support. The presence of CeO_2 crystalline phase was noticed for all catalyst samples. The particle size for the crystallites formed on the catalysts surface can be evaluated from line broadening

calculations. The results for the DqCe catalysts are presented in Table 2. The CeO_2 particle sizes are around 4.0 nm with the exception of the catalyst with y = 1, where the particle size is about 3.2 nm. Smaller cerium oxide particles usually correspond to a better dispersion on the high surface area support. This observation can be correlated with a good interaction of the cerium promoters with the support during grafting impregnation.

Table 2. CeO_2 article size and crystallinity for DqCe catalysts calcined at 500^0C determined from XRD line broadening and XPS I_{Ce3d}/I_{Al2p} intensity ratios

Catalyst	CeO_2 Crystalline Phase		Particle Size (d) [nm]			
	500°C	800°C	500°C		800°C	
DqCeA	[%]		XRD	XPS	XRD	XPS
D0CeA	8.5	19.1	4.0	8.7	9.0	2.2
D1CeA	10.6	16.5	3.2	3.8	7.1	3.5
D2CeA	10.4	12.7	4.1	2.2[a]	11.9	0.5[a]
D3CeA	10.0	15.8	4.2	1.9[a]	15.9	a

a - due to the inhomogeneity of the CeO_2 on the alumina support Kerkhof-Moulijn model cannot be applied to correctly evaluate the particle size.

In order to have a unequivocal and complete characterization of the catalysts structure, semiquantitative XRD must be consistent with data obtained from XPS analysis. The CeO_2 crystalline phase present in the DqCe catalyst is around 50% from the total amount of cerium loading added to the catalyst. The presence of CeO_2 will determine an increase in the thermal resistance of the catalysts, being often used in exothermic catalytic processes [22, 23]. In order to reveal the structural transformation of cerium, the DqCe catalysts were calcined at high temperature and their structural changes after the thermal treatment were examined.

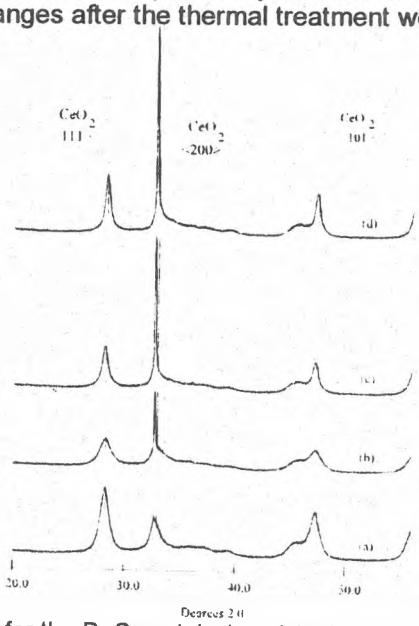

Fig. 5. XRD patterns for the DqCe catalysts calcinated at 800^0C: a) D0Ce, b) D1Ce, c) D2Ce, d) D3Ce catalysts

Figure 5 (a-d) shows the XRD pattern of the DqCe catalysts calcined at 800^0C. The observed XRD pattern from the figure corresponding to a 2q = 28^0 was assignet to CeO_2 <111> phase. Crystalline $CeAlO_3$ phase will indicate a major XRD pattern at 2q = 32.4^0 corresponding to the <110> peak [24]. Previous studies have indicated that a $CeAlO_3$-like phase can be obtained by calcination of $Ce(OH)_4$ at high temperature (> 800^0C) but only under a hydrogen atmosphere treatment [25]. At high temperature, the small CeO_2 crystallites may penetrate into the alumina lattice (a porous defect-spinel structure), and favored by the presence of reducing atmosphere in the system, the dispersed cerium/alumina mixture will lead to formation of the cerium-aluminate ($CeAlO_3$) phase. Consequently, the observed XRD pattern at 2q = 32.5^0, represents a sample holder artifact. Figure 4 (a-d) represents the XRD pattern for the DqCe catalysts. The intense pattern corresponding to the CeO_2 <111> suggests that cerium in these catalysts is present mostly as CeO_2 crystalline phase. However, semiquantitative XRD data presented in Table 2 indicate a significant amount of amorphous or small crystallites in the case of D1Ce and D2Ce catalysts (16.5% and 12.7% CeO_2 crystalline compared with the theoretical calculated CeO_2 concentration of 20.7%), even after calcination at 800^0C, in comparison with the D0Ce and D3Ce catalysts where cerium is present only as CeO_2 crystalline phase. The higher CeO_2 crystallinity observed in the case of these catalysts can be attributed to the high temperature calcination effect when crystalline phase formation is favored.

Surface Characterization. The XPS spectra for the standard $Ce^{3+}AlO_3$ (a) and $Ce^{4+}O_2$ (b) compounds are presented in Figure 6.

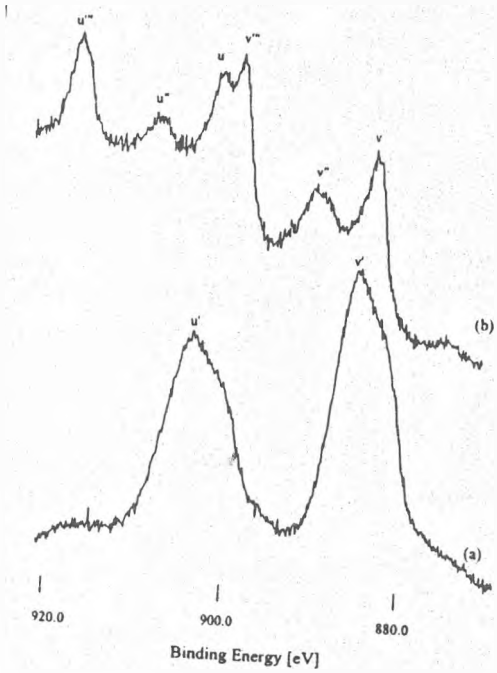

Fig. 6. XPS spectra of standard cerium compounds: a) $Ce^{3+}AlO_3$, $Ce^{4+}AlO_2$

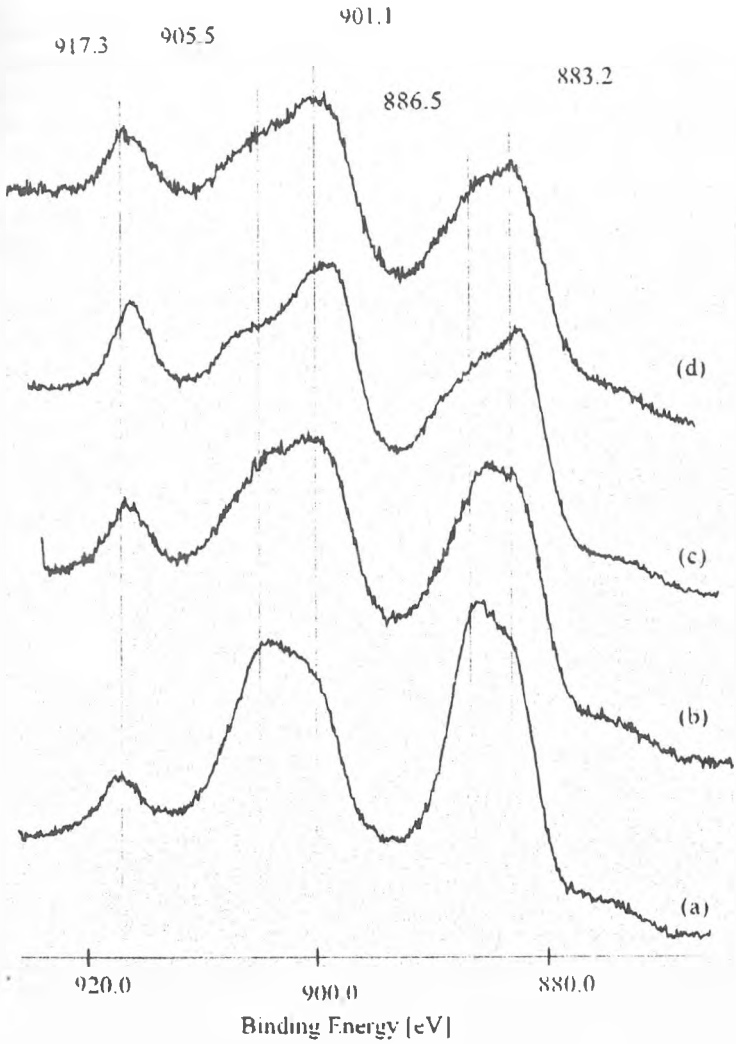

Fig. 7. XPS spectra of the DqCe catalysts calcinated at 500^0C, a) D0Ce, b) D1Ce, c) D2Ce, d) D3Ce catalysts

The XPS Ce3d spectra observed for cerium standard compounds are complicated due to the covalent mixing of the Ce 4f orbitals with the ligand valence band. The Ce3d spectrum measured for $CeAlO_3$ (Figure 6a) is relatively a simple one, containing two major $3d_{5/2}$ peaks at 883.1 eV (v) and 886.5 eV (v'), and the main $Ce3d_{3/2}$ features which appear at 900.1 eV (u) and 905.5 eV (u'). These doublets have been assigned to cerium atoms with $4f^1$ and $4f^2$ orbitals strongly mixed. The Ce3d spectrum measured for CeO_2 (Figure 6b) contains three main

$3d_{5/2}$ features at 883.2 eV (v), 889.2 eV (v"') and three main $Ce3d_{3/2}$ features which appear at 901.1 eV (u), 907.7 eV (u"), and 917.3 eV (u"'). The high binding energy doublet v"' (u"') has been assigned to a final state with primarily $4f^0$ configuration. The v and v (u " and u) doublets are generally assigned to final states with strong mixing of $4f^1$ and $4f^2$ orbital configurations. These states arise from the core hole potential in the final state and the 4f hybridization of cerium atoms in the initial state [26-30]. It should be noted that cerium compounds which contain only Ce^{3+} do not have u"' (v"') peaks characteristic of the $4f^0$ final state. This suggests that the u"' peak may be used to indicate the presence of Ce^{4+} in the catalysts. However, it must be considered that the relative intensity of the u"' feature cannot be used to determine the amount of Ce^{4+} present in the catalysts unless the dispersion of the Ce^{4+} and Ce^{3+} -phases is known, and it is assured that cerium photoreduction does not occur [31].

In our previous work we have shown that cerium is photoreduced by X-rays during XPS analysis, even in the case of samples previously calcined at very high temperature [1]. This fact precludes the quantitative analysis of Ce^{3+} and Ce^{4+} for our catalysts using XPS measurements. Park *et al.* [32] have shown that the cerium photoreduced fraction will decrease with the increase in the CeO_2 crystalline phase, whereas the amorphous cerium phase is strongly reduced.

Figure 7 (a-d) shows the XPS spectra for the DqCe catalysts calcined at 500^0C in air, acquired with identical scanning numbers. This implies that all the catalysts were exposed to X-rays for the same period of time.

From Figure 7 (a) one can be observe that the intensity of the Ce v' (u') feature, characteristic to Ce^{3+}, is dominant in the Ce3d XPS spectrum, even if initially cerium was present as Ce^{4+} -phase. The intensity of the Ce v' (u') feature is annihilated in the case of the D2Ce and D3Ce. In these cases, the Ce^{4+} -feature (u", u and v", v) dominates the Ce3d XPS spectrum.

The XPS spectrum observed for the D1Ce catalyst is a mixed Ce^{4+} -Ce^{3+} -like shape. Previous studies have indicated that cerium is present as amorphous phase when simple grafting method was used for alumina impregnation [1]. Under these conditions, long X-ray exposure will determine cerium to appear strongly reduced in the XPS spectrum. The less photoreduction effect observed in the case of the DqCe catalysts with $q \leq 1$, obtained by impregnation with the diol modified precursors, can be related to the amount of CeO_2 crystalline phase formed. The cerium will be present more as a crystalline CeO_2 phase, crystallinity which is increased in the order: D0Ce < D1Ce < D2Ce < D3Ce. These data provided us additional information about the crystallinity of the cerium phase deposited on the alumina support for the studied DqCe series of catalysts. Despite of this inconvenience, XPS analysis can be used for particle size evaluation. Table 2 presents the cerium oxide particle sizes evaluated from XPS Ce/Al intensity ratio. The data show a decrease in the CeO_2 particle size from 8.7 nm for the D0Ce catalysts to 2.2 or 1.9 nm in the case of D2Ce and D3Ce catalysts. This decrease in the particle size can be related with the nature of the impregnation process. The diol modification will determine a stabilization of the cerium alkoxide in the solution. Consequently, cerium alkoxide will be stronger anchored and stabilized on the alumina suport. In this way the agglomeration and formation of big particles during

calcination will be significantly reduced. The difference in the particle size observed in the case of XPS analysis as compared with the particle size evaluation from XRD line broadening, can be explained by the difference in the information provided by each type of analysis. XRD gives us information about the bulk and crystalline catalysts structure, whereas XPS analysis gives us information about the first ten molecular layers (10-50 Å) of the catalysts surface.

Table 3 shows the XPS intensity ratio I_{ce3d}/I_{Al2p} for the DqCe catalysts. It can be observed that the Ce/Al intensity area ratio increases from 1.7 to 6.3, when the alkoxide: diol molar ratio in the precursor solution (q) varies from 0 to 3. This result indicates a significant improvement in cerium dispersion. The theoretical monolayer dispersion calculated for a Ce/Al = 6.0 x 10^{-2} atomic ratio gives a value of 15.3 for the I_{Ce3d}/I_{Al2p} XPS intensyti ratio.

Table 3. XPS intensity area ratio $I_{(Ce3d)}/I_{(Al2p)}$ for DqCe catalysts

Temperature [°C]	D0Ce	D1Ce	D2Ce	D3Ce
120	3.8	5.6	12.2	6.6
500	1.7	3.8	6.1	6.8
800	0.9	1.6	3.0	3.5

The difference in the experimental value for I_{Ce3d}/I_{Al2p} *versus* the theoretical calculation was attributed to crystalline growth and sampe inhomogeneity [14]. In the case of catalysts dried at 120°C, the value for the I_{Ce3d}/I_{Al2p} XPS intensity ration varies from 3.8, for the D0Ce catalyst, to 12.2, for the D2Ce one. For D1Ce and D3Ce catalysts these values are comparable and close to the value of 3.

This fact be considered an indication that the modified precursor used for DqCe catalysts preparation, where $q \geq 1$, have significantly influenced the surface interaction of the cerium promoter with the alumina support. As a consequence, the cerium surface configuration for DqCe calcined catalysts ($q \geq 1$) will be completely different from the D0Ce catalyst. The grafting process will occur similarly for each type of cerium modified precursor solutions, but will be more efficient for pDqCe, where q = 1 or 2. The deviation from the theoretical value can be interpreted as poor cerium dispersion or sample inhomogeneity.

The high values for the I_{Ce3d}/I_{Al2p} XPS intensity rations in the case of the D1Ce, D2Ce, and D3Ce catalysts indicate that the impregnated cerium phase remains well dispersed, being strongly anchored on the support surface even after calcination at 500°C. This fact can be considered as an indication that the modified precursor used for DqCe catalysts ($q \leq 1$) has significantly altered the surface structure of cerium deposited on the alumina support. In this case, the deviation of the XPS I_{Ce3d}/I_{Al2p} experimental value can be related to the growth of the CeO_2 crystal during calcination. The large deviation in the experimental value of I_{Ce3d}/I_{Al2p} XPS intensity ratio for the D0Ce catalyst calcined at 500°C, as compared with the theoretically calculated one, is attributed to sampe inhomogeneity. Furthermore, due to the increase in the precursor solution viscosity as diol is added to cerium

alkoxide, the deviation from the theoretical value for I_{Ce3d}/I_{Al2p} in the case of DqCe catalysts ($q \geq 1$) can be party attributed to sample inhomogeneity, as well. For inhomogeneous catalysts, the validity of Kerkhof - Moulijn model is limited.

Table 3 shows the values for experimental XPS I_{Ce3d}/I_{Al2p} for DqCe catalysts calcined at 800^0C. As it can be observed, calcination at very high temperature, will lead to a decrease in the cerium dispersion which can be attributed to the increase in the CeO_2 crystallies size. XPS spectra of the DqCe catalysts ($q \geq 1$) calcined at 800^0C (not shown) and very similar with those calcined at 500^0C, indicate after 3-5 minutes of scanning the presence of Ce^{4+} -like species with a very small fraction of Ce^{3+} -like species present on the catalyst surface, due to the X-ray photoreduction effect.

CONCLUSIONS

Cerium alkoxide is present in solution as monomer and forms with 2,4-pantanediol, after aging, a weak complex with gel aspect. Before gelation, the modified cerium alkoxide solution was used for grafting impregnation of a g-Al_2O_3 support. The diol and the complex formation will play the role of a moderator, changing the viscosity of precursor solutions, inhibiting polymerization of cerium alkoxide and in this way, allowing time for the grafting interaction to take place. As a consequence, the surface configuration of the cerium promoter (CeO_2 crystallinity and dispersion) vary with the amount of diol present in the precursor solution. XRD data have indicated the presence of small CeO_2 crystallites ($\overline{d}$ = 4 nm) on the alumina surface, after calcination at 500^0C. The amount of CeO_2 crystalline phase vary with the calcination temperature and with the diol: cerium alkoxide molar ratio (q) in the precursor solution. XPS data indicate that cerium is present on the alumina surface as Ce^{4+}, unless reduction due to X-ray occurs. The amorphous CeO_2 from the alumina surface is more sensitive to X-ray reduction during XPS analysis. The combined information from XPS and XRD analysis for the DqCe catalysts calcined at 800^0C in air, indicate that cerium is present mostly as large CeO_2 crystallites ($\overline{d} \leq 7$nm).

ACKNOWLEDGEMENT

Financial support from an All-University Research Initiation Grand administered by Michigan State University is gratefully acknowledged.

REFERENCES

1. Ledford, J. S., Craciun, R. *FACSS-Symposia*, Detroit, USA, October 17 1993.
2. Kifenski, J., Baiker, A., Glinski, M., Dollenmeier, P., Wokaun, A. *J. Catal.* 1986, 101, 1.
3. Smith, P. D., Klendworth, D. D., McDaniel, M.P. *J. Catal.* 1987, 105, 187.
4. Schaper, H., Doesburg, E.B.M., Van Reijen, L. L. *Appl. Catal.* 1983, 7, 211.

5. Yang, J. K., Swartz, W. E. *Spectrosc. Lett.*1984, 17(6&7), 331.
6. Yu - Yao, Y. F., Kummer, J. T. *J. Catal.* 1987, 106, 307.
7. Oudet, F., Courtine, P., Vejux, A. J.*J. Catal.*1988, 114, 112.
8. Pembo, J. M., Lenzi, M., Lenzi, J., Lebugle, A. *Surf. Inter. Anal.* 1990, 15(11), 663.
9. Koberstein, E.*Unst. St. Proc. Catal.*, Matros, Y.S., Ed., 1990, 643.
10. Chojnacki, T., Krause, K., Schmidt, L. D. *J. Catal.* 1991, 128(1), 161.
11. Sanchez, C., Toledano, P., Ribot, F. *Mat. Res. Soc. Symp. Proc.* 1990, 180, 47.
12. Solomons, G. T. W.in *Organic Chemistry,* 5th ed., 1992, Wiley: New York, p 125, p 694.
13. Klug, H. P., Alexander, L. E. *X-ray Diffraction Procedures for Polycrystalline and Amorphous Materials,* 1 st ed., 1954, Wiley: New York.
14. Kerkhof, F. P. J. M., Moulijn, J. A.*J. Phys. Chem.* 1979, 83, 1612.
15. Scofield, J. H. *J. Electron Spectrosc. Relat. Phenom.*1976, 8. 129
16. Penn. D. R. *J. Electron Spectrosc. Relat. Phenom.* 1979, 9, 29.
17. Ribot, F., Sanchez, C., Livage, J. in *Chemical Processing of Advanced Materials,* 1992, Wiley: New York, p 267-275.
18. Drago, R. S. in *Physical Methods for Chemists,* 2nd ed., 1992, Saunders C. P.: Orlando, p 211-273.
19. Nakamoto, K. *Infrared and Raman Spectra of Inorganic and Coordinative Compounds,* 3rd ed., 1976, Wiley: New York, p 230-231.
20. Brown, L. M. Mazdiyasni, K. S.*Inorg. Chem.* 1970, 12(9), 2783.
21. Leaustic, A., Babonneau, F., Livage, J. *Chem. Mat.*1989, 1(2), 240.
22. Haneda, M., Mizushima, T., Kakuta, N., Ueno, A., Sato, Y., Matsuura, S., Kasahara, K., Sato, M. *Bull. Chem. Soc. Jpn.*1993, 66, 1279-1288.
23. Graham, G. W., Schmitz, P. J., Usmen, R. K., McCabe, R. W. *Cat. Lett.* 1993, 17, 175.
24. Shyu, J. Z., Weber, W. H., Gandhi, H. S. J. *Phys. Chem.* 1988, 92, 4964.
25. *Powder Diffraction File Search Manual,* I. C. D. D, Swarthmore, 1987, 57, 534.
26. Fujimori, A.*Phys. Rev. B.*1983, 28, 2281.
27. Wuilloud, E., Delley, B., Schneider, W. D., Baer, Y. *Phys. Rev. Lett.*1984, 202.
28. Fujimori, A.*Phys. Rev. Lett.*1984, 53, 2518.
29. Wuilloud, E., Delley, B., Schnieder, W. D., Baer, Y. *Phys. Rev. Lett.* 1984, 53, 2519.
30. Jo, J., Kotani, A. *Phys. Scrp.* 1987, 35, 570.
31. Stranick, M. A., Houalla, M., Hercules, D. M. J. *Catal,* 1987, 103, 151-159.
32. Park, W.P.; Ledford, J. S. *Langmuir*, 1996, 12, 1794.

STUDIA UNIVERSITATIS BABEŞ-BOLYAI, CHEMIA, XLII, 1-2, 1997

ENVIRONMENTAL FIELD ANALYSIS[1]

IOVANCA HAIDUC[2]

ABSTRACT. Field Analytical Chemistry (FAC) and Environmental Field Analysis (EFA) have emerged in recent years as self-consistent areas of chemical analysis and analytical chemistry. Only in the period of 1994-1996 more than 450 papers on EFA have been published. This paper attempts a systematization and review of EFA methods and some comments based upon a selection of ca. 100 papers.

INTRODUCTION

The Field Analytical Chemistry (FAC) is a rapidly growing area of chemical analysis in which the analytical measurements are carried out entirely at the site where the analyte is located. Because of their major field of application, they are known as "environmental field analyses" (EFA).

A first review about EFA appeared in Analytical Chemistry Application Reviews in 1997 [1]. In 1995, the first symposium on "Field Screening Methods for Hazardous Wastes and Toxic Chemicals" was organized in Las Vegas [2] and in 1996 the first issue of a new journal "Field Analytical Chemistry Technology" appeared [3]. Traditionally, an analysis is performed by collecting a sample from a remote site, then the sample is transported to an analytical laboratory, where it is stored until the laboratory is prepared for the analysis. Collection, transportation and storage of samples require time and money, and the results are obtained with some delay. This is undesirable, since some decisions, such as those concerning human safety and product reliability, are required in real time.

EFA can reduce the time and cost of analysis because the transportation and storage of the samples are eliminated from the analytical protocol.

It is true that laboratory-based instrumentation provides more precise and accurate data than most field methods, but in the past few years the reduced cost and potential real time decision of the EFA, compensated for this drawback and stimlated the rapid expansion of these methods.

ENVIRONMENTAL FIELD ANALYTICAL METHODS

The Environmental Field Analytical Methods (EFAM) developed in the past years can be summarized in Table 1-6.

Table 1 summarizes GC, MS and IMS in environmental field analysis.

The development of a field-portable tandem GC/GC and Photovac Snapshot GC/GC were reported. For portable GC various types of detectors were

---

[1] Dedicated to Professor Ionel Haiduc on the occasion of his 60-th anniversary

[2] Facultatea de Chimie, Universitatea "Babeş-Bolyai", Cluj-Napoca, Romania

used, such as an argon ionization detector [17], surface acoustic wave detector (SAW), FT-IR [18], pulsed discharged detector in the electron capture and photoionization mode [19] and surface ionization detector [20].

The use of mass spectrometry in on site/in site environmental analysis has been reviewed [21]. Sample introduction methods that have enjoyed much interest in recent years are membrane introduction mass spectrometry (MIMS) and solid-pha e microextraction (SPME). Using SPME/GC/MS analytes can be detected at ppt levels using ion trap mass spectrometry (ITMS) [22]. The performances of the Brucker-Franzen portable GC/MS were described [23, 24] and a Viking Spectra Trak GC/MS system and the Fisions MD 800 system were reported [25].

Table 1. Environmental Field Analytical GC, MS and IMS Methods

Method	Analyte/comments	References
HSGC	carbamate pesticides/thermally labile	4, 5
HSGC/MS	carbamate pesticide/thermally labile	4, 5
MS	toluene and dichlorethane/MIMS;ld=1ppq	6
MS	THMs/drinking water, ld=ppb	7
DSITMS	VOC/groundwater	8
GC/MS	substituted phenols/thermal desorption	9
GC/MS	VOC/field-mobile GC/MS	10
SPME/GC/MS	soil samples/analytes preconcentrated by headspace technique	11
UV/GC/MS	unleaded gasoline	12
IMS	explosives, space exploration	13
	PAC	14
	organic polutants, drugs	15, 16

A portable GC/MS system was patented recently by Inficon, Inc. [26, 27], and other equipment introduced iclude a quadrupole GC/MS system [28], mass spectrometer for plasma discharge ion analysis [28], portable ststic mass spectrometer with a static magnetic mass analyzer [29] (applicable in space mission to identify chemical compounds in planetary atmospheres).

Portable monitors based on recent developments in chemical sensors, biosensors, gas sensors and disposable test strip sensors have been reviewed [30]. Table 2 summarizes chemical and biosensors applied in field analysis.

Flow injection coupled with potentiometric striping analysis (PSA), can be applied to the determination of Lewisite in air samples at the levels 0,5-50 g/m^3 [41] or As (III) in aqueous solutions [42].

Several QCMs (Quartz Crystal Microbalances) that can measure a minimum mass change of 1 ng/cm^2 [43] are commercially available.

Sensors that combine the sensitivity of the QCM device and the specificity of immunochemical reactions, immunosensors have been reported [44, 45]. An application of SAW sensor coated with various polymeric films to analysis of organic vapor mixtures (chloroform, hexane, benzene, trichorethylene, isooctane, xylene) using patern recognition and Monte Carlo simulation was reported [45]. An

electrically conductive polymer, poly (3-hexylhiofene) is a thin film sensor for detection of ppb levels of hydrazine and monohydrazine in the presence of ammonia, amines and ambient water [46].

Table 2. Chemical and biosensors in EFA

Sensor	Analyte/comments	References
Chemical sensors		
QCMs	monitoring of air/in bildings, cars	31
SAW	soil gas/ld=1-10 ppm	32, 33
Electrochemical sensors		
iridium microelectrode	Pb(II)+Cd(II)/water	34
polymeric ruthenium oxide film	N-nitroso compound/water	35
FOCS	PAH	36
	NO_x	37
	pH+CO_2 +O_2	38
Biosensors		
potentiometric and amperometric	organophosphorus pesticide	39
amperometric	CN^-, chlorophenols, atrazine, carbamate pesticides	40

Since the early 1970's, when fiber-optic gyros and acoustic sensors (FOCS) were first demonstrated the fiber-optic technology has been developed intensively. The main advantages of FOCS and examples of sensors used in field measurements were described [47]. With FOCS were determined methanol [48], organic acids [49], PAH, petroleum products [50, 51], chlorinated solvents [52, 53], benzene, toluene and xylene [54], other volatile solvents such as acetone, chloform, toluene, cyclohexane [55] and nitric oxide [56].

Immunochemical techniques are used successfully in FEA. Field evaluation of two of the immunoassay methods was approved by EPA [57, 58]. Applications are widespread, covering many fields including human and ecological exposure, foods and pharmaceuticals, groundwater and soil monitoring, agricultural runoff etc. Enzyme immunoassay test kits are available commercially for analysis of pesticides in drinking water [59].

Table 3 summarizes immunochemical techniques in environmental fields studies.

Table 3. Immunochemical techniques for environmental field studies

Technique	Analyte/comments	Reference
ELISA	chlorpyrifos/in saliva ld=6ppb	60
	3,5,6-trichloro-2pyridinol, 0.034ppb	61
	PCB/fish	61
ELISA kits	PCB/on site (concrete floor,walls)	62
	Hg/environmental samples	63
	cyclodiene insecticide/ground water, 0,15 mg/L endrin; 17 mg/L aldrin	64
MAE/ELISA	PCB/soil/sediments	65
immunomagnetic assay	typhimurium/biological sample	66
IMAS/SFE	extraction with nonhazardous solvents	67
ELISA/SFE	environmental samples	68

Analysis of diesel fuel in soils is usually performed by EPA methods requiring Soxhlet or ultrasonic extraction. These methods are not suitable for EFA. Field analytical methods involve Freon extraction followed by IR methods to measure the aliphatic C-H stretch or a Friedel-Crafts alkylation to measure the aromatic component of the fuel mixture. For drinking water p-nitrofenol and 2-nitroaniline were monitored by using a portable absorption fluorometer [69]. Advantages and disadvantages of the fluorescence, phosphorescence, bioluminisence and chemiluminiscence for analytical determination of environmental pollutants were reviewed [70].

Table 4 summarizes optical spectrometry in environmental field analysis.

Table 4. Optical spectrometry in EFA

Technique	Analyte/comments	Reference
LIF	PAH/water	71
SERS	Cu, Pb, Cd, aromatics/aqueous solution	72, 73
FT-IR	air/monitoring	74, 75
XRF	metal monitoring in soil	76
LIBS	metal/soil and surface contamination	77
	Pb in plant, in concrete, Fe in water	77

Laser-induced breakdown spectroscopy (LIBS) is the newest of the analytical techniques used for field analysis and is used for screening of soil and surfaces for metal contamination. A portable instrument weighs 14.6 kg. The concentration range in which LIBS is most effective is from 0.01-1%. Remote sensing with LIBS has been investigated from distances up to 100 m from laser source and spectrometry via fiberoptic cable.

Radionuclear species have sufficient energies to promote measurable physico-chemical processes. The most common method for the field detection of radionuclear species is the detection of α, β and γ particles produced from naturally occuring nuclear reactions.

Table 5 summarizes radionuclear methods in EFA.

Table 5. Radionuclear methods in EFA

Analysis	Analyte/comments	Reference
Victoreen Alpha activity monitor	α particles/contaminated soils	78
Direct large-area α spectrometer	α particles/airborne dust	79
α track detectors	α particles /soil	80
Passive α detectors	U/contamination in fields	81
FDTAS	β particles/tritium in water	82
TSEE	weak β-emitting radionuclides	82
EIC	weak β-emitting radionuclides	83
Portable γ-ray spectrometer	without cryogenic cooling	84
γ detectors	underground water	85

Hot α particles were determined by image analysis and the energy of α particles have been used to screen uranium contamination in field [81]. For the monitoring of tritium in the field a robust sample handling and liquid scintillation counting procedure has been developed [86].

Recently, a field-portable instrument based on a new micronomad multichannel analyzer was described [87]. A CsI (Tl) scintillation detector with two sidemounted photodiodes [88], and a combination of portable γ-ray detectors with an artificial neural network to automatically identify radioactive isotopes in real time [89] have been reported.

Over the past years, field monitoring of radioactivity has been applied to a number of sites [90, 91].

Field analysis is often carried out by *remote sensing methods,* that can acquire and transport chemical information without the presence of an analyst at the samping site. Remote sensing methods have found a variety of applications such as making chemical measurements in stack and exhaust gases, waste streams, process streams, atmosphere, oceans and space.

Table 6 summarizes remote sensing methods in EFA.

Table 6. Remote sensing methods in EFA

Methods	Analyte/comments	References
Passive ORS Methods		
MAS	O_2,O_3,ClO.water vapor	92
microwave remote sensing	atmospheric analysis	93
ATMOS	NO and NO_2	94
DICOSPEC	SO_2 and NO_2	94
PYRAMHYD	OH	96
TES	O_3	97
FT-IR	molecular species in earth's atmosphere	98
IR-detection based on neural network techniques	CO	99
Active ORS Methods		
DIAL	monitoring stratosferic O_3 depletion	100
FAL	multiple vapor detection	100
liquid nitrogen-cooled diode lasers	atmospheric trace gas minitoring	101
FT-IR	CFCs	102, 103
	combustion products from airplanes	104, 105
CDIRS	organic pollutants	106
SPRS	gas monitoring	107

REFERENCES

1. Avila Lopez V., Hill H. H., *Anal. Chem.*, 1997, 69, 289R.
2. Overton E. B., Dharmasena H. P., Ehrmann U., Carney K. R., *Field Anal. Chem. Technol.* 1996, 1, 87.
3. Proceedings of the Field Screening Methods for Hazardous Wastes and Toxic Chemicals Symposium, Las Vegas, NV, 1995.
4. Sacks R., Klemp M., Akard M., *Field Anal. Chem. Tehnol.*, 1996, 1, 61.
5. Dagan S., Amirav A., *J. Am. Soc. Mass Spectrom*, 1996, 7, 737.

6. Soni M., Bauer S., Amy J. W., Wong P., Cooks R. G.,*Anal. Chem.*, 1995, 67, 1409.
7. Bauer S., Griffin T., Bauer J.,*Pittsburgh Conf. Chicago*, II, 1996.
8. Wise M. B., Merriwheather F., Guerin M., Thompson C. V., *Proceedings of the Field Screening Methods for Hazardous Wastes and Toxic Chemicals Symposium*, Las Vegas, NV, 1995, 920.
9. Jiao F., Robbat A., Jr., *J. AOAC Int.* 1996, 79, 131.
10. Ardito C. P., Duval T. A., Reaber D. W., *In Volatile Organic Compounds in the Environment* 1996; ASTM STP 1261.
11. James K. J., Stack M. A., *J High Resolut. Chromatogr.* 1996, 19, 515.
12. Hackett M., Wang H., Miller G. C., Bornhop D. J., *J. Chromatogr.* A 1995, 695, 243.
13. Mercado A., Marsden P.,*Proceeding International Workshop on Ion Mobility Spectrometry*, Galveston, TX, 1995, 168.
14. Ritchie R. K., Rudolph A., *Proceedings of the Third International Workshop on Ion Mobility Spectrometry, Cambridge, U. K.*, 1996, 193.
15. Giam C.S., Reed G.E., Holliday T.L., Chang L., Rhodes B.J., *Proceedings International Workshop on Ion Mobility Spectrometry, Galveston, TX*, 1995, 209.
16. Simpson G.,Klasmeier M., Hill H. H., Atkinson D., Padolovich G., Lopez-Avila V., Jones T. L., *J. High Resolut. Chromatogr.* 1996, 19, 301.
17. Linenberg A., *Proceedings of the Field Screening Methods for Hazardous Wastes and Toxic Chemicals Symposium, Las Vegas, NV* 1995, 236.
18. Soderstrom M. T., Bjork H., Hakkinen V. M. A., Kostiainen O., Kuitunen M. L., Ruatio M.,*J. Chromatogr.* 1996, 742, 191.
19. Wentworth W. E., Huang J., Chen E. C. M., Stearns S. D., *Chromatogr.* 1996, 43, 353.
20. Kishi H., Fuju T., Sato G., *J. Chromatogr.* 1996, 750, 335.
21. Kotiaho T.J., *Mass Spectrom.* 1996, 31, 1.
22. Khai M. Pawliszyn J., *Environ. Sci. Technol.* 1995, 29, 693.
23. Baykut G., Nolke B., Vetters H. P., Weiss G., *At-Onsite* 1995, 1, 34.
24. Baykut G., *Trends. Anal. Chem.*, 1995, 14, 10.
25. Virkki V. T., Ketola R. A., Djala M., Kotiaho T., Komppa V., Grove A., Facchetti S., *Anal. Chem.* 1995, 67, 1421
26. Voss G., Deluca S. J., Adams G., *Patent EP* 644576 A2, 1996.
27. Andersen B. D., Eckels J. D., Kimmons J. F., Myers D. W., *Patent U.S.* 5525799 A, 1996.
28. Tuszewski M., *Rev. Sci. Instrum.* 1996, 67, 2215.
29. Kogan V. T., Kazanskii A. D., Tubol'tsev Y. V., Chichagov Y. V., Gladkov G. Y., Illyasov E. I., *Prib. Tekh. Eksp.* 1995, 1, 159.
30. Alexander P., *Chem. Aust.* 1995, 14.
31. Craven M. A., Gardner J. W., Bartlett P. N., *Trends Anal. Chem.* 1996, 15, 486.
32. Frye G. C., Gilbert D. W., Colburn C., Cenosek R. W., Steinfort T. D., *Proceedings of the Field Screening Methods for Hazardous Wastes and Toxic Chemicals Symposium, Las Vegas, NV* 1995, 715.
33. Frye G. C., Pepper S. H., *At-Onsite* 1995, 1, 62.
34. Tercier M.L., Buffle J., *Anal. Chem.*, 1996, 68, 3670.
35. Cox J. A., Alber K. S., Brockway C. A., Tess M. E., Gorski W., *Anal. Chem.* 1995, 67, 993.
36. Campiglia A. D., Vo-Dinh T., *Talanta* 1996, 43, 1805.

37. Ge Z. F., Brown C. W., Alberts J., *J. Environ. Sci. Technol.* 1995, 29, 878.
38. Pantano P., Walt D. R., *Anal. Chem.* 1995, 481A.
39. Trojanowitcz M., Hichman M. L., *Trends Anal. Chem.*, 1996, 15, 38.
40. Besombes J. L., Cosnier S., Labbe P., Reverdy G., *Anal. Chim. Acta* 1995, 311, 255.
41. Alstadt J. H., Martin A. F., *Analyst* 1996, 121, 1387.
42. Alstadt J. H., Olson D. C., Martin A. F., *Anal. Chim. Acta* 1996, 317, 1.
43. Henry C., *Anal. Chem.* 1996, 68, 625A.
44. Welsch W., Klein C., von Schickfus M., Hunklinger S., *Anal. Chem.* 1996, 68, 2000.
45. Zellers e.t., Batterman S. A., Han M., Patrash S. J., *Anal. Chem.* 1995, 67, 1092.
46. Ellis D. L., Zankin M. R., Bernstein L. S., Rubner M. F., *Anal. Chem.* 1996, *Anal. Chem.* 1996, 68, 817.
47. Camara C., Perez-Conde C., Moreno-Bondi M. C., Rivas C., *Qual. Assur. Environ. Anal.* 1995, 165.
48. Zeng H. H., Wang K. M., Yang X. H., Yu R. Q., *Acta Chim. Sin.* 1995, 53, 78.
49. Kurauchi Y., Ogata T., Egashira N., Ohga K., *Anal. Sci.* 1996, 12, 55.
50. Ge Z. F., Brown C. W., Alberts J. J., *Environ. Sci. Technol.* 1995, 29, 878.
51. Shade W., Bubkitz J., *Environ. Sci. Technol.* 1996, 30, 1451.
52. Hoffman F., Ronen D., Rosin H., Milanovich F., *Talanta* 1996, 43, 681.
53. Milanovich F., Brown S. B., Colston B. W., Daley P. F., Langry K. C. *Talanta* 1994, 41, 2189.
54. Eving K. J., Nau G., Bucholtz F., Aggarwal I. D., Robitaille G.,*Proceeding of the Field Screening Methods for Hazardous Wastes and Toxic Chemicals Symposium, Las Vegas, NV*, 1995, 144.
55. Leonard K. M., *Sens. Actuators* 1995, B24-25, 458.
56. Zhou Z. J., Arnold M. A., *Anal. Chem.* 1996, 68, 1748.
57. EPA PCP Immunoassay Technologies, EPA/540/R-95/514, U.S. EPA Washington DC, 1995.
58. EPA Envirogard PCB Test Kit, Millipore, Inc-Innovative, EPA/540/R-95/517, U.S. EPA Washington DC, 1995.
59. Watt C. D., Hegarty B., *Pure Appl. Chem.*, 1995, 67, 1533.
60. Ferguson B. S., Nigg H. N., *BCPC Symp. Proc.* 1996, 65, 179.
61. Zajicek J. L., Tillitt D. E., Huckins J. N., Petty J. D., Potts M. E., Nardone D. A., In *Environmental Immunochemical Methods: ACS Symposium Series 646, American Chemical Society: Washington DC*, 1996, 307.
62. Harrison R.O., *At-Onsite* 1995, 1, 56.
63. Schweitzer C., Carlson L., Holmguist B., Riddle M., Wylie D., In *Environmental Immunochemical Methods: ACS Symposium Series 646, American Chemical Society: Washington DC*, 1996, 23.
64. Dombrowski T. R., Thurman E. M., Mohrman G. B., In *Environmental Immunochemical Methods: ACS Symposium Series 646, American Chemical Society: Washington DC*, 1996, 148.
65. Lopez-Avila V., Benedicto J., Charan C., Young R., Beckert W. F., *Environ. Sci. Technol.* 1995, 29, 2709.
66. Yu. H., Stopa P. J. In *Environmental Immunochemical Methods: ACS Symposium Series 646, American Chemical Society: Washington DC*, 1996, 297.
67. King J. W., Nam K. S., In *Immunoassays for Residue Analysis, ACS Symposium 621, ACS, Washington DC* 1996, 422.

68. Stearman G. K., Wells M.J.M., Adkisson S. M., Ridgill T. E., In *Environmental Immunochemical Methods: ACS Symposium Series 646, American Chemical Society: Washington DC,* 1996, 56.
69. Mittenzwey K. H., Sinn G., Hiersigk R., Krause M., Lenz P., Pfeil L., Rauchfuss J., Streich G., *Fresenius J. Anal. Chem.* 1996, 355, 724.
70. Steinberg S. M., Poziomek E. J., Engelmann W. H., Rogers K. R., *Proceedings of the Field Soreening Methods for Hazardous Wastes and Toxic Chemicals Symposium,* Las Vegas, NV 1995, 48.
71. Uebel U., Kubitz J., Anders A., *J. Plant Physiol.* 1996, 148, 586.
72. Crane L. G., Wang D. X., Sears L. M., Heyns B., Carron K., *Anal. Chem.* 1995, 67, 360.
73. Hill W., Wehling B., Gibbs C. G., Gutsche C. D., Klockow D., *Anal. Chem.* 1995, 67, 3187.
74. Engel J. R., Dorval R., Carlson D., Quinn T. G., *At-Onsite* 1995, 1, 71.
75. Bernick M. B., Kalnicky D. J., Prince G., Singhui R., *J. Hazard. Mater.* 1995, 43, 101.
76. Yamamoto K. Y., Cremers D. A., Ferris M. J., Foster L. E., *Appl. Spectrosc.* 1996, 50, 222.
77. Bescos B , Castano J., Urena A. G. *Laser Chem.* 1995, 16, 75.
78. Davises C. M., Telle H. H., Montgomery D. J., Corbett R. E., *Specrochim. Acta* 1995, B50, 1059.
79. Meyer K. E., *Proceedings of the Field Screening Methods for Hazardous Wastes and Toxic Chemicals Symposium,* Las Vegas, NV, 1995, 1081.
80. Sill C. W., *Health Phys.* 1995, 69, 21.
81. Meyer K. E., *Proceedings of the Field Screening Methods for Hazardous Wastes and Toxic Chemicals Symposium,* Las Vegas, NV, 1995, 1182.
82. Duney C. S., Meyer K. E., Gammage R. B., Wheeler R. V., Salaskey M., Kotrappa P., *Proceedings of the Field Screening Methods for Hazardous Wastes and Toxic Chemicals Symposium,* Las Vegas, NV, 1995, 1190.
83. Noakes J. E., Spauding J. D., Neary M. P., Hofstetter K. J., *Proceedings of the Field Screening Methods for Hazardous Wastes and Toxic Chemicals Symposium,* Las Vegas, NV, 1995, 1048.
84. Gammage R. B., *Proceedings of the Field Screening Methods for Hazardous Wastes and Toxic Chemicals Symposium,* Las Vegas, NV, 1995, 1197.
85. Xu C. X., Williams R. R., *Rev. Sci. Instrum.* 1995, 66, 2677.
86. Winn W. G , *J. Radioanal. Nucl. Chem.* 1995, 194, 345.
87. Rego J. H., Smith D. K., *J. Radioanal. Nucl. Chem.,* 1995, 194, 289
88. Lavietes A. D., McQuaid J. H., Ruhter W. D., Paulus J., *IEEE Trans. Nucl. Sci.* 1995, 42, 634.
89. Meisner J. E., Nicaise W. F., Stromswold D. C., *IEEE Trans. Nucl. Sci.* 1995, 42, 288.
90. Keller P. E., Kangas L. J., Troyer G. L., Hashem S., Kouzes T., *IEEE Trans. Nucl. Sci.* 1995, 42, 709.
91. Tykva R., *Proc SPIE-Int. Soc. Opt. Eng.* 1995, 2504, 386
92. Husain A., Breckenridge C. E., Storey D., *Nucl. Technol.* 1995, 109, 265.
93. Olivero J. J., Pauls T. A., Beviacqua R. M., Kriebel D., Daehler M., Richards M. L., Kampfer N., Berg A., Stodden C., *Geophys. Res. Lett.* 1996, 23, 2309.
94. Kampfer N., *Opt. Eng.* 1995, 34, 2413.
95. Newchurch M. J., *Geophys. Res. Lett.* 1996, 23, 2373.

96. Pujadas M., Alberdi J., Gamero E., Teres J., *Proc. SPIE-Int. Soc. Opt. Eng.* 1995, 2506, 236.
97. de Nivelle M. J. M. E., Bruijn M. P., Frericks M., de Vries R., Wijnbergen J. J., de Korte P. A. J., Sanchez S., Elwenspoek M., Heidenblut T., Schwierzi B., Michalke W., Steinbeiss E., *J. Phys. IV* 1996, 3, 423.
98. Puckrin E., Evans W. F. J., Adamson T. A. B., *Atmos. Environ.* 1996, 30, 563.
99. Camy-Peret C., *Spectrochim. Acta* 1995, 51A, 1143.
100. Clerbaux C., Chazette P., Megie G., *Proc. SPIE-Int. Soc. Opt. Eng.* 1995, 2578, 148.
101. Gelbwachs. J. A., *Appl. Opt.* 1996, 35, 2630.
102. Nelson D. D., Zahniser M. S., McManus J. B., Shorter J. H., Wornhoudt J. C., Kolb C. E., *Proc. SPIE-Int. Soc. Opt. Eng.* 1996, 2834, 148.
103. Theriault J. M., Bradette C., Gibert J., *Proc. SPIE-Int. Soc. Opt. Eng.* 1996, 2744, 664.
104. Wang J., Kang J., Chen Z., Huang M., Zhang J., Wang T., *J. Environ. Sci. Health* 1995, A30, 2111.
105. Gawnther P. L., Stedman D. H., Bishop G. A., Beaton S. P., Bean J. H., Quine R. W., *Rev. Sci. Instrum.* 1995, 66, 3024.
106. Bishop G. A., Stedman D. H., *Acc. Chem. Res.* 1996, 29, 489.
107. Stevens C. G., Kuzmenko P. J., Conaway W. E., Magnotta F., Thomas N. L., Galkowski J., Lewis I. T., Alger T. W., *Proc. SPIE-Int. Soc. Opt. Eng.* 1995, 2552, 284.
108. Niggermann M., Katerkamp A., Pellmann M., Boismann P., Reinhold J., Cammann K., *Proc. SPIE-Int. Soc. Opt. Eng.* 1995, 2508, 303.

STUDIA UNIVERSITATIS BABEŞ-BOLYAI, CHEMIA, XLII, 1-2, 1997

HETEROCYCLEN, 74. MITT.: QUARTÄRE AMMONIUMVERBINDUNGEN UND NITRONE DES THIAZOLS MIT ANTIMIKROBIELLER WIRKUNG

MARIANA PALAGE[1], DOINA MATINCA[1], M. HORN[1], I. SIMITI[1]

ABSTRACT. Quaternary ammonium compounds and nitrones of thiazole with antimicrobial action. The alkylation of some N - heterocyclic bases (Pyridine, Picoline, Quinoline, Urotropine) with 2 Aryl - 4 -halomethyl-thiazole leads to quaternary ammonium compounds; the coresponding nitrone have also been prepared. The antimicrobial effect of both classes of substances have been tested on gram-positive and gram-negative germes and also on Candida albicans.

EINLEITUNG

Die antimikrobielle Wirkung von quartären Ammoniumverbindungen ist wohlbekannt. Diese Verbindungen sind aktiv gegenüber grampositiven Keimen, weniger aktiv gegenüber gramnegativen Keimen und inaktiv gegenüber Pseudomonas aeruginosas. [1].

In der Fachliteratur der letzten Jahre werden neue heterocyclische Verbindungen mit quartärem Stickstoff [2-11], sowie Nitrone [12-14] mit antimikrobiellen Eigenschaften beschrieben.

Vorliegende Arbeit beschreibt die Darsteellung einer Reihe von Verbindungen in denen ein quartäres Stickstoffatom über eine CH_2-Gruppe an den -potentiell antimikrobiellen- Thiazolkern gernüpft ist; die entsprechenden Nitrone wurden ebenfalls beschrieben.

Aufgrund der getesteten antimikrobielle Wirkung der beschrieben Verbindungen, wunschen wir den Einfluss der Ionel- bzw. der semipolaren Bindung auf antimikrobielle Wirkung dieser Substanzen zu untersuchen, sowie einen Zusammenhang zwischen den verschiedenen Substituenten und der antibakteriellen oder fungiziden Wirkung festzustellen.

ERGEBNISSE UND DISKUSSION

Zur Darstellung der quartären Ammoniumverbindungen 3-42 wurden 2-Aryl- 4-halomethyl-thiazole 1 [15-17] mit verschiedenen Basen 2 behandelt (Schema 1).

[1] Universitatea de Medicină şi Farmacie "Iuliu Haţieganu", Laboratorul de Chimie Organică, Cluj-Napoca.

Schema 1

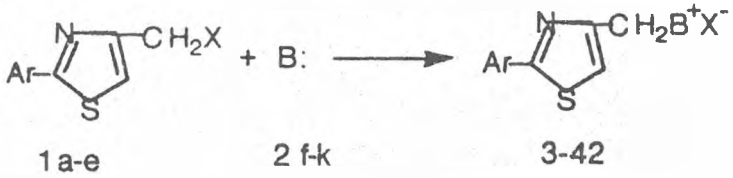

X=Cl ,I

1	1a	1b	1c	1d	1e
Ar	C_6H_5	$C_6H_4CH_3$ (4)	$C_6H_4OCH_3$ (4)	C_6H_4Cl (4)	$C_6H_4CF_3$(4)

2	2f	2g	2h	2i	2j	2k
B	Piridin	α-Picolin	β-Picolin	γ-Picolin	Chinolin	Urotropin

Diese N-Alkylierungsreaktionen lassen sich in absolutem Alkohol oder Chloroform ausführen, wobei die Ausbeuten sowohl vom Lösungsmittel als auch von der verwendeten Base bzw. vom Halogenatom beeinflusst werden. Die auf diese Weise dargestellten Verbindungen sind im allgemeinen in Wasser löslich und besitzen einen hohen Schmelzpunkt. Die zwischen 2200 - 2400 cm^{-1} liegenden IR-Banden der quartären Ammoniumverbindungen werden nur unwesentlich durch den Substituenten beeinflusst. Die UV-Spektren weisen Absorbtionsbanden zwischen 283,5 und 301 nm auf, deren Lage vor allem vom Substituenten am Phenylring und weniger von der Natur der heterocyclische Base beeinflusst wird.

Die Synthese der Nitrone 43-46 erfolgt durch Behandeln der Pyridinium-Salze 3,5,6,8 mit p-Nitroso-dimethylanilin in Gegenwart einer katalytischen Menge von Piperidin und Pyidin. (Schema 2).

Schema 2

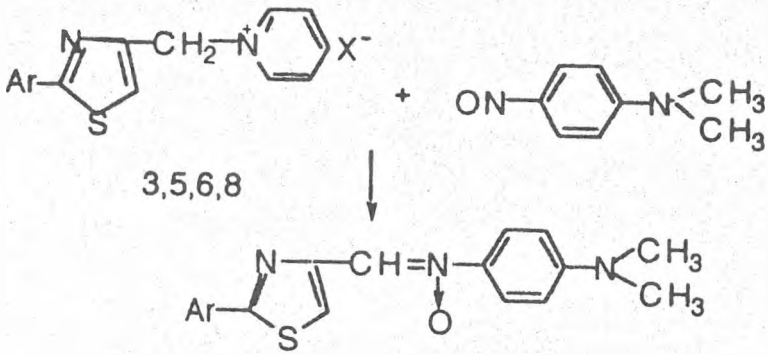

43-46

Durch saurer Hydrolyse, bei gelindem Erwärmen, gehen die erhaltenen Nitrone in die entsprechenden Carbonylverbindungen über, die identisch sind mit jenen, die man durch die Sommelet-Methode erhält [15, 18] (Schema 3).

Schema 3

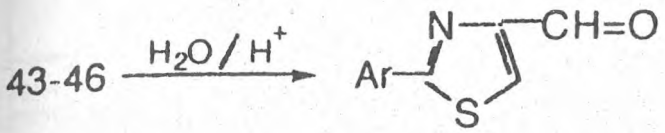

Die angeführten Reaktionsschritte entsprechen eigentlich der mit der Sommelet-Reaktion verwandten Kröhnke-Reaktion [19]. Sonst beide diese Reaktionen sind Darstellungsmethoden für Carbonylverbindungen. DieIR-Spektren der Nitrone weisen die für die exocyclische C = N Gruppe charakteristischen Banden auf.

Bemerkenswert ist die leichte Überführbarkeit der Nitrone in die entsprechenden Hydrazone unter Einwirken einer kalten.

2,4-Dinitrophenylhydrazin-Lösung.

Die antimikrobielle Wirkung der Verbindungen wurde getestet, indem man mittels der Diffusionsmethode die Hemmwirkung auf die Vermehrung von Mikroorganismen untersuchte.

Zum Einsatz kamen acht Keimstämme im Betracht: Grampositive Kokken (Staphylococcus aureus, Staphylococcus epidermidis, Sarcina lutea), gramnegative Kokken (Bacillus subtilis), gramnegative Bazillen (Escherichis col, i Klebsiella pneumoniae, Proteus vulgaris) und Pilze (Candida albicans). Anhand der erhaltenen Daten wurden die Verbindungen in drei Wirkungsklassen eingeteilt:

1. Klasse, Verbindungen die eine Hemmungszone mit einem Durchmesser grösser als 15 mm verursachen;

2. Klasse, Verbindungen bei denen der Durchmesser der Hemmungszone zwischen 11 mm und 15 mm lag;

3. Klasse, Verbindungen mit einem Durchmesser der Hemmungszone unter 10 mm.

Die Ergebnisse dieser Untersuchung sind in Tabelle 1 zu finden.

Tab. 1: Daten zur antimikrobiellen Wirkung

Verbindung	Wirkungsklasse/ Keimstamm							
	Coccaceae			Bacteriaceae			Fungi	Baciloccae
	Staphylococcus aureus	Staphylococcus epidermidis	Sarcina lutea	Proteus vulgaris	Escherichia coli	Klebsiella pneumoniae	Candida albicans	Bacillus subtilis
3	3	3	3	3	3	3	3	3
4	1	2	1	3	2	3	3	3
5	2	1	1	3	1	3	3	3
6	3	3	3	3	3	3	3	3
7	1	1	1	3	3	3	2	3
8	1	1	1	3	1	3	3	1
9	1	1	1	3	3	3	2	1
10	3	3	3	1	3	3	3	3
11	3	3	3	1	2	3	1	3
12	1	1	1	3	2	3	3	1
13	3	3	3	1	3	3	3	1
14	1	1	1	3	2	3	2	1
15	1	1	1	3	3	3	2	3
16	3	1	2	1	1	1	2	3
17	2	1	1	3	1	3	3	1
18	2	3	1	3	1	3	3	3
19	1	1	1	3	1	3	3	1
20	1	1	1	3	1	3	3	1
21	1	1	1	3	1	3	3	1
22	1	1	1	3	1	3	3	1
23	1	1	1	3	1	3	3	2
24	2	1	1	3	1	3	3	3
25	1	1	1	3	1	3	3	1
26	1	1	1	3	1	3	3	1
27	1	1	1	3	1	3	3	1
28	1	1	1	3	1	3	3	1
29	2	1	1	3	1	3	3	1
30	1	1	1	3	1	3	3	1
31	1	1	1	3	1	3	3	1
32	1	1	1	3	1	1	1	1
33	1	1	1	3	1	3	1	1
34	1	1	1	3	3	3	1	1
35	1	3	3	1	2	1	3	3
36	1	1	3	1	2	1	3	1
37	1	1	1	1	2	1	2	1
38	1	1	1	1	2	1	3	3
39	1	2	2	1	3	1	3	3
40	2	1	1	1	1	1	3	3
41	2	1	1	1	2	1	3	2
42	1	1	1	1	1	1	3	1
43	3	3	3	2	3	2	2	3
44	2	2	2	3	3	3	2	3
45	2	3	3	2	3	2	2	2
46	3	3	3	3	3	3	2	3

Diese Daten werden durch die Grob- Mengen- Theorie bearbeitet und werden Thema einer anderer wissenschaftlicher Arbeit sein.

EXPERIMENTELLER TEIL

Die Schmp, wurden mit dem Boetius Apparat bestimmt. IR-Spektren: FT-IR NICOLET 205, UV-Spektren: UV-NIS ULTROSPEC III. Die Elementaranalysen entsprachen den berechneten Werten.

2-Aryl-thiazol-4-yl-methyi-pyridinium-Halogenide 3-9

Ein mmol 2-Aryl-4-halomethyl-thiazol 1 a-e und ein mmol Pyridin werden in 3 ml Cnloroform gelöst und eine Stunde gekocht. Die sich beim Abkühlen abgeschiedenen Kristalle werden filtriert und aus absolutem Alkohol umkristallisiert.

3: Ar = C_6H_5; X=I; Schmp. 121^{0}C (C_2H_5OH), Ausb. 63,5%, IR(KBr) 2400 cm^{-1}, UV(CH_3OH): λ max (lg ε) = 284,4 nm (4,35), $C_{15}H_{13}IN_2S$ (380,25), Gerechnet: N, 7,37. Gefundet: N, 7,55.

4: Ar = $C_6H_4CH_3$ (4); X=Cl, Schmp. 195-196^{0}C (C_2H_5OH), Ausb. 66,2%, IR(KBr) 2400 cm^{-1}, UV(CH_3OH): λ max (lg ε) = 289 nm (4,34), $C_{16}H_{15}ClN_2S$ (302, 82). Gerechnet: N, 9,25. Gefundet: N, 9,23.

5: Ar = $C_6H_4CH_3$ (4); X=I, Schmp. = 177,2-178,5^{0}C (C_2H_5OH), Ausb. 40,0%, IR(KBr) 2400 cm^{-1}, UV(CH_3OH): λ max (lg ε) = 289,5 nm (4,29), $C_{16}H_{15}IN_2S$ (394,27). Gerechnet: N, 7,10. Gefundet: N, 6,86.

6: Ar = $C_6H_4CH_3$ (4); X=Cl, Schmp. 180-182^{0}C (C_2H_5OH), Ausb. 74,6%, IR(KBr) 2350 cm^{-1}, UV(CH_3OH): λ max (lg ε) = 301 nm (4,64), $C_{16}H_{15}ClN_2OS$ (318,82). Gerechnet: N, 8,80. Gefundet: N, 8,40.

7: Ar = C_6H_4Cl (4); X=Cl, Schmp. 178-180^{0}C (C_2H_5OH), Ausb. 75,7%, IR(KBr) 2400 cm^{-1}, UV(CH_3OH): λ max (lg ε) = 290 nm (4,63), $C_{15}H_{12}Cl_2N_2S$ (323,24). Gerechnet: N, 8,66. Gefundet: N, 8,56.

8: Ar = C_6H_4Cl (4); X=I, Schmp. 187-189^{0}C (C_2H_5OH), Ausb. 35,4%, IR(KBr) 2350 cm^{-1}, UV(CH_3OH): λ max (lg ε) = 289,5 nm (4,73), $C_{15}H_{12}ClIN_2S$ (414,69). Gerechnet: N, 6,75. Gefundet: N, 6,95.

9: Ar = $C_6H_4CF_3$ (4); X=Cl, Schmp. 215-217^{0}C (C_2H_5OH), Ausb. 59,70%, IR(KBr) 2400 cm^{-1}, UV(CH_3OH): λ max (lg ε) = 288,5 nm (4,49), $C_{16}H_{12}ClF_3N_2S$ (356,80). Gerechnet: N, 7.85. Gefundet: N, 8,25.

2-Aryl-thiazol-4-yl-methyl-α -picolinium-Halogenide 10-16

Darstellung analog zu den Pyridinium-Halogenide.

10: Ar = C_6H_5, X=I, Schmp. 183-185^{0}C (C_2H_5OH), Ausb. 60,0%, IR(KBr) 2350 cm^{-1}, UV(CH_3OH): λ max (lg ε) = 284 nm (4,48), $C_{16}H_{15}IN_2S$ (394,28). Gerechnet: N, 7,10. Gefundet: N, 7,45.

11: Ar = $C_6H_4CH_3$ (4); X=Cl, Schmp. 192-194^{0}C (C_2H_5OH), Ausb. 65,3%, IR(KBr) 2200 cm^{-1}, UV(CH_3OH): λ max (lg ε) = 289 nm (4,53), $C_{17}H_{17}ClN_2S$ (316,85). Gerechnet: N, 8,84. Gefundet: N, 9,24.

12: Ar = $C_6H_4CH_3$ (4); X=I, Schmp. 217-219^{0}C (C_2H_5OH), Ausb. 59,6%, IR(KBr) 2350 cm^{-1}, UV(CH_3OH): λ max (lg ε) = 291 nm (4,35), $C_{17}H_{17}IN_2S$ (408,30). Gerechnet: N, 6,86. Gefundet: N, 7,05.

13: Ar = $C_6H_4OCH_3$ (4); X=Cl, Schmp. 168-170^{0}C (C_2H_5OH), Ausb. 50,0%, IR(KBr) 2350 cm^{-1}, UV(CH_3OH): λ max (lg ε) = 300,5 nm (4,61), $C_{17}H_{17}ClN_2OS$ (332,85). Gerechnet: N, 8,42. Gefundet: N, 8,75.

14: Ar = C_6H_4Cl (4); X=Cl, Schmp. 163-165^{0}C (C_2H_5OH), Ausb. 85,0%, IR(KBr) 2350 cm^{-1}, $C_{16}H_{14}Cl_2N_2S$ (337,26). Gerechnet: N, 8,31. Gefundet: N, 8,50.

15: Ar = C_6H_4Cl (4); X=I, Schmp. 235-237^{0}C (C_2H_5OH), Ausb. 90,0%, IR(KBr) 2400 cm^{-1}, UV(CH_3OH): λ max (lg ε) = 290,5 nm (4,31), $C_{16}H_{14}ClIN_2S$ (428,71). Gerechnet: N, 6,53. Gefundet: N, 6,95.

16: Ar = $C_6H_4CF_3$ (4); X=Cl, Schmp. 200-202^{0}C (C_2H_5OH), Ausb. 65,0%, IR(KBr) 2350 cm^{-1}, $C_{17}H_{14}ClF_3N_2S$ (370,82). Gerechnet: N, 7,56. Gefundet: N, 7,68.

2-Aryl-thiazol-4-yl-methyl-β-picolinium-Halogenide 17-23.

Darstellung analog zu den Pyridinium-Halogenide.

17: Ar = C_6H_5; X=Cl, Schmp. 169-171^{0}C (C_2H_5OH), Ausb. 78,0%, IR(KBr) 2350 cm^{-1}, UV(CH_3OH): λ max (lg ε) = 283,5 nm (4,66), $C_{16}H_{15}ClN_2S$ (302, 82). Gerechnet: N, 9,25. Gefundet: N, 9,05.

18: Ar = C_6H_5; X=I, Schmp. 121-123^{0}C (C_2H_5OH), Ausb. 82,3%, IR(KBr) 2350 cm^{-1}, UV(CH_3OH): λ max (lg ε) = 283,5 nm (4,66), $C_{16}H_{15}IN_2S$ (394,28). Gerechnet: N, 7,10. Gefundet: N, 7,15.

19: Ar = C_6H_4CH (4); X=Cl, Schmp. 221-223^{0}C (C_2H_5OH), Ausb. 65,7%, IR(KBr) 2350 cm^{-1}, UV(CH_3OH): λ max (lg ε) = 289 nm (4,29), $C_{17}H_{17}ClN_2S$ (316,85). Gerechnet: N, 8,84. Gefundet: N, 8,55.

20: Ar = $C_6H_4CH_3$ (4); X=I, Schmp. 173-174^{0}C (C_2H_5OH), Ausb. 73,7%, IR(KBr) 2350 cm^{-1}, UV(CH_3OH): λ max (lg ε) = 289 nm (4,41), $C_{17}H_{17}IN_2S$ (408,30). Gerechnet: N, 6,86. Gefundet: N, 7,02.

21: Ar = $C_6H_4OCH_3$ (4); X=Cl, Schmp. 217-218^{0}C (C_2H_5OH), Ausb. 52,85%, IR(KBr) 2350 cm^{-1}, UV(CH_3OH): λ max (lg ε) = 301 nm (4,72), $C_{17}H_{17}ClN_2OS$ (332,85). Gerechnet: N, 8,41. Gefundet: N, 8,55.

22: Ar = C_6H_4Cl (4); X=Cl, Schmp. 203-250^{0}C (C_2H_5OH), Ausb. 72,5%, IR(KBr) 2375 cm^{-1}, UV(CH_3OH): λ max (lg ε) = 290 nm (4,69), $C_{16}H_{14}Cl_2N_2S$ (337,26). Gerechnet: N, 8,31. Gefundet: N, 8,45.

23: Ar = C_6H_4Cl (4); X=I, Schmp. 183-185^{0}C (C_2H_5OH), Ausb. 81,3%, IR(KBr) 2350 cm^{-1}, UV(CH_3OH): λ max (lg ε) = 289,5 nm (4,64), $C_{16}H_{14}ClIN_2S$ (428,71). Gerechnet: C, 44,83; H, 3,29; N, 6,53; S, 7, 48. Gefundet: C, 45,11; H, 3,22; N, 6,23; S, 7,42.

2-Aryl-thiazol-4-yl-methyl-γ -picolinium-Halogenide 24-29.

Darstellung analog zu den Pyridinium-Halogenide.

24: Ar = C_6H_5; X=I, Schmp. 199-200^{0}C (C_2H_5OH), Ausb. 75,0%, IR(KBr) 2350 cm^{-1}, UV(CH_3OH): λ max (lg ε) = 285 nm (4,27), $C_{16}H_{15}IN_2S$ (394,28). Gerechnet: N, 7,10. Gefundet: N, 7,15.

25: Ar = $C_6H_4CH_3$ (4); X=Cl, Schmp. 233-235^{0}C (C_2H_5OH), Ausb. 40,0%, IR(KBr) 2350 cm^{-1}, UV(CH_3OH): λ max (lg ε) = 289 nm (4,75), $C_{17}H_{17}ClN_2S$ (316,85). Gerechnet: N, 8,84. Gefundet: N, 8,65.

26: Ar = $C_6H_4CH_3$ (4); X=I, Schmp. 247-248^{0}C (C_2H_5OH), Ausb. 57,0%, IR(KBr) 2350 cm^{-1}, UV(CH_3OH): λ max (lg ε) = 289 nm (4,35), $C_{17}H_{17}IN_2S$ (408,30).

Gerechnet: C, 50,00; H, 4,20; N, 6,86; S, 7,85. Gefundet: C, 50,11; H, 4,23; N, 6,83; S, 7,76.

27: Ar = $C_6H_4OCH_3$ (4); X=Cl, Schmp. 203-205^{0}C (C_2H_5OH), Ausb. 70,0%, IR(KBr) 2350 cm^{-1}, UV(CH_3OH): λ max (lg ε) = 301 nm (4,54), $C_{17}H_{17}ClN_2OS$ (332,85). Gerechnet: N, 8,41. Gefundet: N, 8,55.

28: Ar = C_6H_4Cl (4); X=Cl, Schmp. 218-220^{0}C (C_2H_5OH), Ausb. 50,0%, IR(KBr) 2375 cm^{-1}, UV(CH_3OH): λ max (lg ε) = 290 nm (4,45), $C_{16}H_{14}Cl_2N_2S$ (337,26). Gerechnet: N, 8,31. Gefundet: N, 8,55.

29: Ar = C_6H_4Cl (4); X=I, Schmp. 252-253^{0}C (C_2H_5OH), Ausb. 50,0%, IR(KBr) 2350 cm^{-1}, UV(CH_3OH): λ max (lg ε) = 289,5 nm (4,47), $C_{16}H_{14}ClIN_2S$ (428,71). Gerechnet: C, 44,83; H, 3,29; N, 6,53; S, 7,48. Gefundet: C, 45,23; H, 3,30; N, 6,50; S, 7,46.

2-Aryl-thiazol-4-yl-methyl-chinolinium-Halogenide 30-34.

Darstellung analog zu den Pyridinium-Halogenide.

30: Ar = C_6H_5; X=I, Schmp. 200-202^{0}C (C_2H_5OH), Ausb. 36,0%, IR(KBr) 2375 cm^{-1}, UV(CH_3OH): λ max (lg ε) = 292 nm (4,35), $C_{19}H_{15}IN_2S$ (430,31). Gerechnet: N, 6,51. Gefundet: N, 6,50.

31: Ar = $C_6H_4CH_3$ (4); X=I, Schmp. 198-200^{0}C (C_2H_5OH), Ausb. 35,0%, IR(KBr) 2350 cm^{-1}, UV(CH_3OH): λ max (lg ε) = 296 nm (4,32), $C_{20}H_{17}IN_2S$ (444,34). Gerechnet: N, 6,30. Gefundet: N, 6,35.

32: Ar = C_6H_4Cl (4); X=Cl, Schmp. 210-212^{0}C (C_2H_5OH), Ausb. 35,0%, IR(KBr) 2350 cm^{-1}, $C_{19}H_{14}Cl_2N_2S$ (373,30). Gerechnet: N, 7,50. Gefundet: N, 7,35.

33: Ar = C_6H_4Cl (4); X=I, Schmp. 205-206^{0}C (C_2H_5OH), Ausb. 35,0%, IR(KBr) 2350 cm^{-1}, UV(CH_3OH): λ max (lg ε) = 297 nm (4,55), $C_{19}H_{14}ClIN_2S$ (464,75). Gerechnet: N, 6,02. Gefundet: N, 6,15.

34: Ar = $C_6H_4CF_3$ (4); X=Cl, Schmp. 105-106^{0}C (C_2H_5OH), Ausb. 33,0%, IR(KBr) 2350 cm^{-1}, $C_{20}H_{14}ClF_3N_2S$ (406,86). Gerechnet: N, 6,88. Gefundet: N, 7,11.

2-Aryl-thiazol-4-yl-methyl-urotropi[illegible]n-Halogenide 35-42.

Darstellung analog zu den Pyridinium-Halogenide.

35: Ar = C_6H_5; X=Cl, Schmp. 195-198^{0}C (C_2H_5OH), Ausb. 32,0%, IR(KBr) 2350 cm^{-1}, UV(CH_3OH): λ max (lg ε) = 283,5 nm (4,39), $C_{16}H_{20}ClN_5S$ (349,99). Gerechnet: N, 20,02. Gefundet: N, 20,42.

36: Ar = C_6H_5; X=I, Schmp. 186-188^{0}C (C_2H_5OH), Ausb. 33,0%, IR(KBr) 2350 cm^{-1}, UV(CH_3OH): λ max (lg ε) = [illegible]84 nm (4,30), $C_{16}H_{20}IN_5S$ (441,34). Gerechnet: N, 15,87. Gefundet: N, 15,65.

37: Ar = $C_6H_4CH_3$ (4); X=Cl, Schmp. 205-207^{0}C (C_2H_5OH), Ausb. 66,0%, IR(KBr) 2350 cm^{-1}, $C_{17}H_{22}ClN_5S$ (363,90). Gerechnet: N, 19,25. Gefundet: N, 19,55.

38: Ar = $C_6H_4CH_3$ (4); X=I, Schmp. 204-205^{0}C (C_2H_5-OH), Ausb. 66,0%, IR(KBr) 2375 cm^{-1}, UV(CH_3OH): λ max (lg ε) = 288 nm (4,38), $C_{17}H_{22}IN_5S$ (455,37). Gerechnet: N, 15,38. Gefundet: N, 15,57.

39: Ar = $C_6H_4OCH_3$ (4); X=Cl, Schmp. 213-215^{0}C (C_2H_5OH), Ausb. 60,0%, IR(KBr) 2350 cm^{-1}, $C_{17}H_{22}ClN_5OS$ (379,91). Gerechnet: N, 18,44. Gefundet: N, 18,53.

40: Ar = C_6H_4Cl (4); X=Cl, Schmp. 215-217^{0}C (C_2H_5OH), Ausb. 60,0%, IR(KBr) 2350 cm^{-1}, $C_{16}H_{19}Cl_2N_5S$ (384,33). Gerechnet: N, 18,22. Gefundet: N, 18,37.

41: Ar = C_6H_4Cl (4); X=I, Schmp. 205-207^{0}C (C_2H_5OH), Ausb. 60,0%, IR(KBr) 2350 cm^{-1}, UV(CH_3OH): λ max (lg ε) = 288,5 nm (4,57), $C_{16}H_{19}ClIN_5S$ (475,78). Gerechnet: N, 14,72. Gefundet: N, 14,36.

42: Ar = $C_6H_4CF_3$ (4); X=Cl, Schmp. 205-207^{0}C (C_2H_5OH), Ausb. 65,0%, IR(KBr) 2350 cm^{-1}, $C_{17}H_{19}ClF_3N_5S$ (417,88). Gerechnet: N, 16,76. Gefundet: N, 16,60.

2-Aryl-4-[(N-p-dimethyl-anilino)-N-oxo-iminomethylen] thiazol 43-46.

Ein mmol Pyridinium-Salz 3,5,6,8 wird in der kleinstmöglichen Menge absolutem Alkohol gelöst; zur Lösung werden ein mmol p-Nitroso-dimethylanilin, 0,1 ml Pyridin und o,1 ml Piperidin hinzugefügt und das Gemisch wird eine Stunde gekocht. Beim Abkühlen scheiden sich Kristalle ab, die aus absolutem Alkohol umkristallisiert werden.

43: Ar = C_6H_5, Schmp. 131-131,5^{0}C, Ausb. 30,0%, IR(KBr) 2630 cm^{-1} (HC=N), $C_{18}H_{17}N_3OS$ (323,42). Gerechnet: N, 12,99. Gefundet: N, 12,83.

44: Ar = $C_6H_4CH_3$ (4); Schmp. 133-134^{0}C, Ausb. 30,0%, IR(KBr) 1630 cm^{-1}, (HC =N), $C_{19}H_{19}N_3OS$ (337,45). Gerechnet: N, 12,45. Gefundet: N, 12,47.

45: Ar = $C_6H_4OCH_3$ (4), Schmp. 136-138^{0}C, Ausb. 30,0%, IR(KBr) 1630 cm^{-1}, (HC=N), $C_{19}H_{19}N_3O_2S$ (353,45). Gerechnet: N, 11,88. Gefundet: N, 11,85.

46: Ar = C_6H_4Cl (4), Schmp. 158-159^{0}C, Ausb. 30,0%, IR(KBr) 1630 cm^{-1}, (HC=N), $C_{18}H_{16}ClN_3OS$ (357,86). Gerechnet: C, 60,41; H, 4,51; N, 11,74;.S, 8,96. Gefundet: C, 60,37; H, 4,51; N, 11,97; S, 8,96.

LITERATUR

1. M. Schorderet, *Pharmacologie,* 2 Ed., Slatkine, Geneve, 1992, 784.
2. S. Kucharski, J. Krysinski, J. Pernak, *Pharmazie,* 1983, 38, 350.
3. J. Pernak, S. Kucharski, J. Krysinski, *Pharmazie,* 1983, 38, 752.
4. J. Pernak, L. Michalak, S. Kucharski, J. Krysinski, *Arch. Pharm.,* 1984, 317, 152.
5. J. Pernak, A. Skrzypczak, S. Kucharski, J. Krysinski, *Arch. Pharm.,* 1984, 317, 430.
6. J. Pernak, J. Krysinski, A. Skrypczak, *Pharmazie,* 1985, 40, 570.
7. J. Pernak, J. Krysinski, A. Skrypczak, *Arch. Pharm.,* 1988, 321, 193.
8. J. Pernak, J. Krysinski, A. Skrypczak, L. Michalak, *Arch. Pharm.,* 1990, 323, 307.
9. J. Pernak, A. Skrzypczak, L. Michalak, J. Krysinski, *Arch. Pharm.,* 1992, 325, 455.

10. J. Pernak, A. Skrzypczak, L. Michalak, J. Jedraszczyk, J. Krysinski, M. Kazmierczak, B. Mrowczynski, *Arch. Pharm.*, 1993, 326, 237.
11. J. Pernak, A. Skrzypczak, J. Krysinski, M. Kazmierczak, J. Jedraszczyk, L. Michalak, *Arch. Pharm.*, 1994, 327, 115.
12. H. Kim, K. Mitarb, *J. med. Chem.*, 1977, 20, 557.
13. W. Kliegel, *Pharmazie*, 1977, 32, 643.
14. W. Kliegel, *Pharmazie*, 1978, 33, 331.
15. A. Silberg, I. Simiti, H. Mantsch, *Chem. Ber.*, 1961, 94, 2887.
16. I. Simiti, M. Farkas, *Chem. Ber.*, 1965, 98, 3446.
17. I. Simiti, M. Farkas, *Acta. Chim. Sci. Hung.*, 1974, 83, 381.
18. I. Simiti, M. Farkas, *Bull. Soc. Chim. France.*, 1968, 9, 3862; F. Krohnke, E. Borner, *Chem. Ber.*, 1936, 69, 2006.

STUDIA UNIVERSITATIS BABEŞ-BOLYAI, CHEMIA, XLII, 1-2, 1997

HETEROCYCLES, 75: THIAZOLIC QUATERNARY AMMONIUM SALTS AND THIAZOLIC NITRONES. CHEMICAL STRUCTURE - ANTIMICROBIAL ACTIVITY (SAR).

MARIANA PALAGE, R. OPREAN, M. HORN, I. SIMITI[1]

ABSTRACT. The relation between chemical structure and antimicrobial activity of some thiazolic quaternary ammonium salts and thiazolic nitrones were analysed using the theory of rough sets. The smallest set of attributes significant for a high precision of classification, respectively the essential structure for the antimicrobial activity were established.

INTRODUCTION

In a previous paper we have dealt with the preparation and evaluation of antimicrobial potential of some thiazolic ammonium quaternary compounds (I) and of thiazolic nitrones (II) having in their molecule an ionic linkage and a semipolar one, respectively [1].

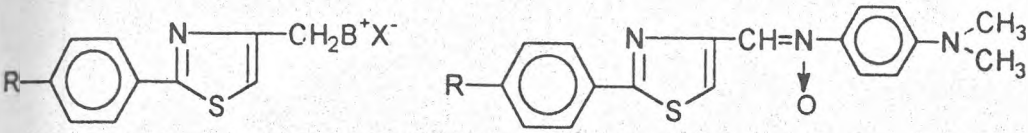

I II

In order to determine to what extent the antimicrobial activity is influenced by the various modifications made within the synthesized compounds structure, we have used the method of rough sets theory, introduced by Pawlak [2,3] and applied by Kryjinski [4,5,6] and [7,8].

METHOD

The obtained substances were divided into three classes of activity [1].

On the basis of the results we defined separately each class of activity from the viewpoint of the corresponding compounds. To achieve this object we applied a suitable encoding system of synthesized compounds. Thus, some clearly defined functions were introduced on the set, able to render evident through their values some structural features of the considered compounds. The functions were denominated as "attributes" according to the usual terminology. Table 1 presents the functions definition, showing both their field of definition and the

[1] Universitatea de Medicină şi Farmacie "Iuliu Haţieganu", Laboratorul de Chimie Organică Cluj-Napoca, Romania.

correspondance laws between compounds and the numeric values, as well as the occurred subordinations. Thus, the a_1 attribute is defined on the whole set of compounds receiving only the values zero and 1. However, a_2 attribute is defined only on the set of compounds for which a_1 receives the value 1. Thus, a_2 attribute was explained as a subordinate to a_1 attribute being registered as $a_2 \subset a_1$. In this way each synthesized compound was characterized by a multitude of attribute values significant to the compound and explained as codes.

Table 1. Attributes, their significance and the corresponding values

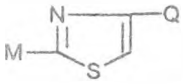

ATTRIBUTE	SIGNIFICANCE	ATTRIBUTES VALUES				
a_1	M presence	Absent M = H 0	Present M = R-C_6H_4 1			
a_2	R presence in M	0	1			
a_3	R nature	0	-CH_3 1	-OCH_3 2	-Cl 3	-CF_3 4
a_4	Q nature	0	-$CH_2B^+X^-$ 1	-CH=NO-$C_6H_4N(CH_3)_2$ (p) 2		
a_5	B nature in Q	0	Pyridine 1	Quinoline 2	Urotropine 3	
a_6	Substituent nature	0	-CH_3 1			
a_7	Substitute position on ring	0	α 1	β 2	γ 3	
a_8	X presence in Q	0	1			
a_9	X nature	0	-Cl 1	-Br 2	-I 3	

Subordination laws: $a_3 \subset a_2 \subset a_1$

$a_7 \subset a_6 \subset a_5 \subset a_4$

$a_9 \subset a_8 \subset a_4$

Table 2 illustrates the encoding system. In order to make evident the chemical structure specific to the compounds belonging to the same class of activity, a close analysis of each attribute contribution to outline the respective class was performed. The analysis consisted of a successive, one by one elimination of single or associated attributes examining the decrease related to class accuracy and considering only the remaining attributes. The eliminated attributes which did not induce a significant decrease of class accuracy (values exceeding 0,75) were interpreted as irrelevant to the respective class characterisation. The remaining essential attributes represent the most restricted set being the basis of obtaining a classification identical with the one required by the results of antimicrobial action test.

Table 2. Substances codes

Nr	CODES								
	a_1	a_2	a_3	a_4	a_5	a_6	a_7	a_8	a_9
3	1	0	0	1	1	0	0	1	3
4	1	1	1	1	1	0	0	1	1
5	1	1	1	1	1	0	0	1	3
6	1	1	2	1	1	0	0	1	1
7	1	1	3	1	1	0	0	1	1
8	1	1	3	1	1	0	0	1	3
9	1	1	4	1	1	0	0	1	1
10	1	0	0	1	1	1	1	1	3
11	1	1	1	1	1	1	1	1	1
12	1	1	1	1	1	1	1	1	3
13	1	1	2	1	1	1	1	1	1
14	1	1	3	1	1	1	1	1	1
15	1	1	3	1	1	1	1	1	3
16	1	1	4	1	1	1	1	1	1
17	1	0	0	1	1	1	2	1	1
18	1	0	0	1	1	1	2	1	3
19	1	1	1	1	1	1	2	1	1
20	1	1	1	1	1	1	2	1	3
21	1	1	2	1	1	1	2	1	1
22	1	1	3	1	1	1	2	1	1
23	1	1	3	1	1	1	2	1	3
24	1	0	0	1	1	1	3	1	3
25	1	1	1	1	1	1	3	1	1
26	1	1	1	1	1	1	3	1	3
27	1	1	3	1	1	1	3	1	1
28	1	1	3	1	1	1	3	1	3
29	1	1	2	1	1	1	3	1	1
30	1	0	0	1	2	0	0	1	3
31	1	1	1	1	2	0	0	1	3
32	1	1	3	1	2	0	0	1	1
33	1	1	3	1	2	0	0	1	3
34	1	1	4	1	2	0	0	1	1
35	1	0	0	1	3	0	0	1	1
36	1	0	0	1	3	0	0	1	3
37	1	1	1	1	3	0	0	1	1
38	1	1	1	1	3	0	0	1	3
39	1	1	2	1	3	0	0	1	1
40	1	1	3	1	3	0	0	1	1
41	1	1	3	1	3	0	0	1	3
42	1	1	4	1	3	0	0	1	1
43	1	0	0	2	0	0	0	0	0
44	1	1	1	2	0	0	0	0	0
45	1	1	2	2	0	0	0	0	0
46	1	1	3	2	0	0	0	0	0

RESULTS AND DISCUSSION

Figures 1 and 2 illustrate the decrease associated with the classification precision, by a successive elimination of attributes.

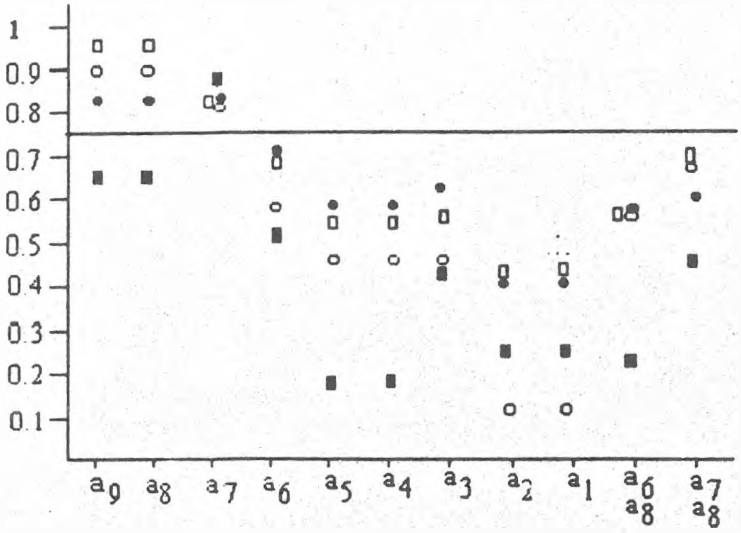

Fig. 1. The decrease of the classification precision by succesive elimination of attributes
o Staphylococcus aureus; • Staphylococcus epidermidis; ❑ Sarcina lutea; ■ Bacillus subtilis

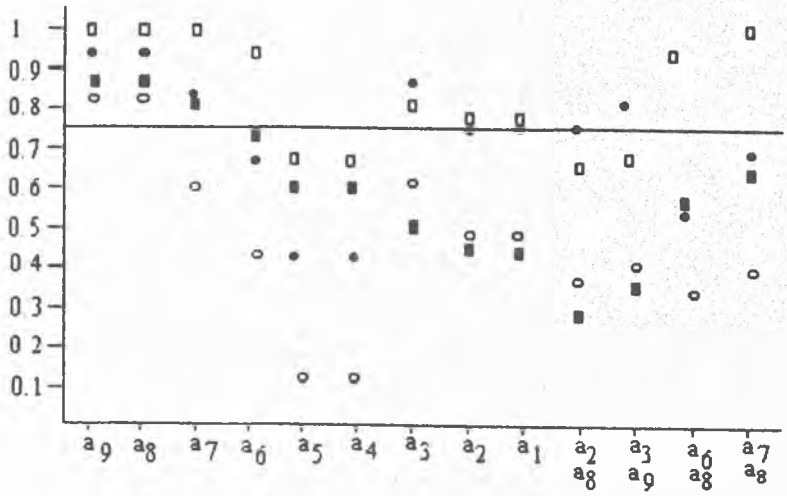

Fig. 2. The decrease of the classification precision by succesive by succesive elimination of attributes
o Escherichia coli; • Proteus vulgaris; ❑ Klebsiella pneumoniae; ■ Candida albicans

On the basis of the obtained results one can conclude that the presence of ionic link that can be considered a pharmacophore group, is favorable to compounds having an average or good antimicrobial effect. Depending on germ type, other attributes seem to be essential, too. Thus, concerning gram-positive microorganisms, gram-negative Escherichia coli and Candida albicans, all attributes are essential, excepting the anion nature from the ionic link corresponding, probably to the need for a hydrophil - lipofil balance, favourable to a good antimicrobial activity. However, the compounds having a semipolar linkage in the position 4 of thiazolic ring (CH = N → O) exert only a moderate effect upon Candida albicans.

Regarding the antimicrobial activity on gram-negative microorganisms, the aspects are differentiated depending on germ type, as follows: for the activity exerted on Klebsiella pneumoniae, both the attributes corresponding to the substitutes in the position 2 of thiazol and those in the position 4 are essential. On the other hand the substitute on the pyridinic ring and the anion nature are not essential to antimicrobial activity.

The activity exerted on Proteus vulgaris is dependent only on substitute nature in position 4 on thiazolic nucleus. The essential substitutions for class 1 of activity (compounds with a good antimicrobial effect) are presented in Table 3.

Table 3. Essential attributes for antimicrobial activity

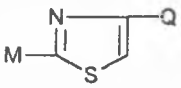

STRAIN TYPE	ESSENTIAL ATTTRIBUTE	ATTRIBUTES SIGNIFICANCE	ACTIVITY CLASS
For all germs	a_4	-CH=-B$^+$X$^-$	1
Gram positive cocci	a_1, a_2, a_3 a_5, a_6, a_7	M presence, R=H; -OCH_3, -CH_3,-Cl, CF_3 B=Py, Qui, Uro, β, γ -CH_3	1
Gram positive bacillus	a_1, a_2, a_3 a_5, a_6, a_7 a_8, a_9	M presence, R=H; -OCH_3, -CH_3,-Cl, CF_3 B=Py, Qui, α, β, γ -CH_3	1
		X= -Cl, -I	
Gram negative bacillus Escherichia coli	a_1, a_2, a_3 a_5, a_6, a_7	M presence, R=H; -OCH_3, -CH_3,-Cl, CF_3 B=Py, Qui, β, γ -CH_3	1
Klebsiella pneumoniae	a_1, a_2, a_3 a_5,	M presence, R=H; -OCH_3, -CH_3,-Cl, CF_3 B=Uro	1
Proteus vulgaris	a_5, a_6, a_7	B= Uro, Py γ -CH_3	1
Candida albicans	a_1, a_2, a_3 a_5, a_6, a_7	M presence, R= CH_3,-Cl, -CF_3 B=Qui	1

In conclusion, according to our anticipation, the presence of ionic linkage is important to a good antimicrobial activity. The compounds exerting the highest activity upon gram-positive microorganisms have a pyridinium rest, a pyridinium substitute or quinolinium in the thiazol 4 position. For a good activity upon gram-negative microorganisms, the urothropinic rest is essential.

REFERENCES

1. M. Palage, D. Matinca, M. Horn, I. Simiti, under publishing
2. Z. Pawlak, *Intern. J. Man - Machine Stud.*, 1984, 20, 469.
3. Z. Pawlak, *Lect. Notes Comput. Sci.*, 1986, 208, 186.
4. J. Krysinski, *Arch. Pharm. (Weinheim)*, 1991, 324, 827.
5. J. Krysinski, *Arch. Pharm. (Weinheim)*, 1994, 327, 247.
6. J. Krysinski, *Die Pharmazie*, 1995, 50, 593.
7. B. Briycki, A Skrzypczak, I. Mirska, J. Pernak, *Arch. Pharm. Med. Chem. (Weinheim)*, 1996, 329, 279.
8. D. Zaharia, V. Zaharia, O. Aramă, I. Simiti, *Farmacia*, 1996, 3-4, 65.

STUDIA UNIVERSITATIS BABEŞ-BOLYAI, CHEMIA, XLII, 1-2, 1997

CRITICAL MICELLE CONCENTRATION OF SODIUM CHOLATE SOLUTIONS

JÁNOS ZSAKÓ[1], AURORA MOCANU[1], CSABA RÁCZ[1], KATALIN RÁCZ[1], EMIL CHIFU[1]

ABSTRACT. Critical micelle concentration is determined in aqueous sodium cholate solutions by using 4 different methods. Results are compared with literature data. Molecular area of sodium cholate is calculated from the maximum adsorption at both CCl_4/water and benzene/water interfaces.

INTRODUCTION

The bile acids are amphiphilic compounds with surface active properties, and they answer for the transport of some water insoluble substances in the animal organism.

These compounds are synthesized in the liver and are final products of the cholesterol metabolism. Owing to their surface active properties in aqueous solutions they may form micelles, by reaching the average concentration of 3-5 mg/ml.

The concentration at which the association of the molecules begins is called CRITICAL MICELLE CONCENTRATION (CMC). Owing to their role in the animal organism, the stydy of micellization of these compounds is both of theoretical and practical importance [1].

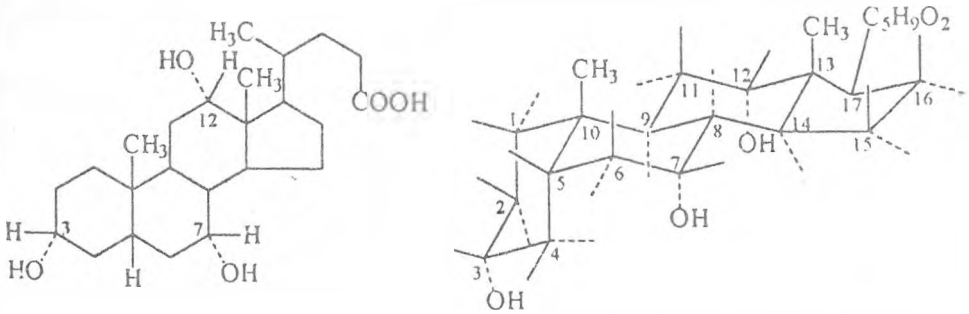

Fig. 1. The molecular structure of the cholic acid (3, 7, 12-trioxicolanic) [4]

[1] Faculatatea de Chimie şi Inginerie Chimică, Universitatea "Babeş-Bolyai", RO - 3400, Cluj-Napoca, România.

In the present paper the CMC of sodium cholate (NaC) is determined by means of different methods. The structure of the cholic acid molecule is presented in fig. 1. As seen, the molecule contains three hydroxi groups in the same part of the molecule and they form a triangle in the hydrophilic part of the steroid nucleus. The distance between these three OH groups is of 5Å [4].

The surface active properties of the sodium cholate have been studied by different methods [2-15].

RESULTS AND DISCUSSIONS

Carbon tetrachloride/water interfacial tension (γ) values, determined by using the drop volume method are presented in fig. 2, as function of logarithm concentration of NaC. The intersection of the two linear portions allows us to derive CMC.

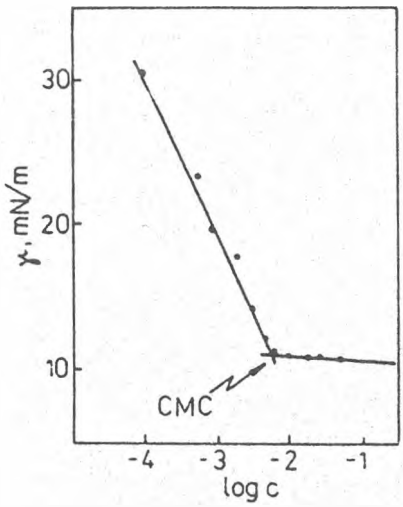

Fig. 2. Interfacial tension (γ) determined by drop volume method as function of logarithm concentration of NaC

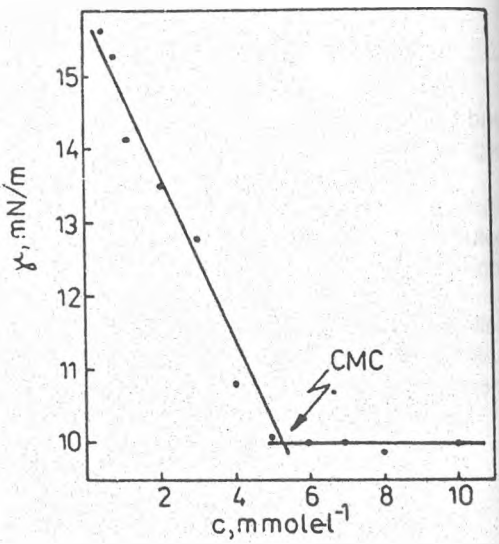

Fig. 3. Interfacial tension (γ) measured by means of Wilhelmy method, vs. molar concentration (c) of NaC

In fig. 3 the benzene/water interfacial tension values measured by means of the Wilhelmy method are plotted vs. molar concentration of NaC (c). The CMC also corresponds to the intersection of the two straight lines.

A plot of the equivalent conductivity (Λ) vs. $\sqrt{c}$, the square root of the NaC concentration is given in fig. 4. As seen, at CMC a sudden slope change is observed. The turbidity (τ) as function of the analytical NaC concentration is shown in fig. 5. Two linear portions appear and their intersection occurs at CMC.

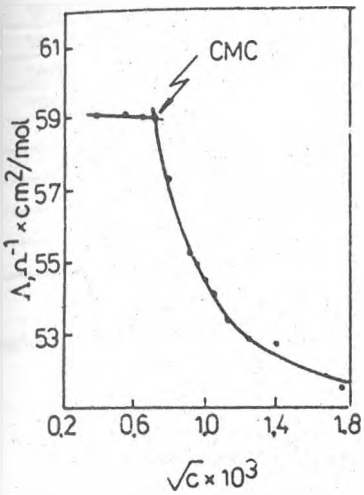

Fig. 4. Equivalent conductivity (Λ), vs. $\sqrt{c}$ of NaC

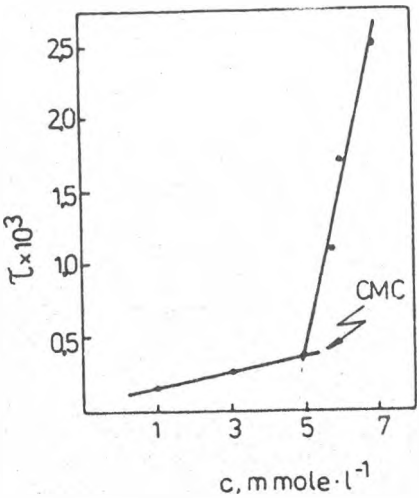

Fig. 5. Turbidity (τ) as function of molar concentration of NaC solutions

In the case of both tensiometric methods and with the turbidimetric one, CMC values have been derived by performing a linear regression in order to obtain the parameters of the straight lines approximating the linear portions and the concentration value corresponding to the intesection of the straight lines has been derived by calculation.

The concentration corresponding to the sudden slope change of the equivalent conductivity vs. $\sqrt{c}$ curve has been derived graphically.

The CMC values derived from our experimental data are presented in Tab. 1. The same table also contains some literature data.

As seen, the values reported by different authors are rather different and our results are in good agreement with some of them.

Gibbs'equation [21]:

$$\Gamma = -(RT)^{-1}\frac{d\gamma}{d\ln c} = -(2{,}3RT)^{-1}\frac{d\gamma}{d\lg c} \qquad (1)$$

allows us to derive the adsorption Γ at the liquid/liquid interface from the concentration dependence of the interfacial tension.

Table 1. CMC values for aqueous NaC solutions

metnod	temperature (°C)	CMC (mM / l)	reference
Drop volume	22	5.55	this paper
Plate	20	5.31	this paper
Conductometric	23	5.18	this paper
Turbidimetric	22	4.91	this paper
Light scattering	20	20	[8]
Solubilization	20	13	[6]
Surface tension	20	5	[10]
Surface tension	22	4.9	[4]
Surface tension	22	3.25	[4]

Since up to the CMC the carbon tetrachloride/water and the benzene/water interfacial tensions obey the linear relations:

$$\gamma = -10.823 \lg c - 12.818$$

and (2)

$$\gamma = -5.892 \lg c - 3.405$$

respectively, both with a correlation coefficient of r = 0.992, one may consider that in the concentration range investigated already the maximum adsorption Γ_m occurs. Thus, the molecular area in interface, A_0 will be given by the relation:

$$A_0 = (\Gamma_m N_A)^{-1} \quad (3)$$

where N_A stands for Avogadro's constant.

By using equations (1) and (3), from the coefficients of lg c in equation (2), the maximum adsorption and molecular area values given in Tab. 2 have been derived.

Table 2. Maximum adsorption and molecular area of NaC at liquid/liquid interfaces

interface	$\Gamma_m \times 10^{10}$, mol·cm^{-2}	A_0, Å^2
CCl_4/water	1.92	86.8
benzene/water	1.05	158.4

For the molecular area of NaC at the air/water interfaces Å^2 has been reported [4, 14]. Since at oil/water interfaces higher molecular area values may be expected [22] our results obtained for the benzene/water interface are very resonable. The quite low value derived for the Ccl_4/water interface might be due to the much higher solubility of cholic acid in CCl_4 as compared to benzene.

EXPERIMENTAL

Commercial sodium cholae "E. Merck" was used for determinations. Aqueous solutions in the concentration range between 10^{-4} and $3 \cdot 10^{-2}$ M have been prepared by using twice distilled water (pH = 6-7). Two tensiometric methods have been used [16]:

1. The drop-volume method has been used for measuring the CCl_4/water interfacial tension. For this purpose the volume is determined for the carbon tetrachloride drop which is formed in the aqueous solution of sodium cholate.
Measurements have been performed at room temperature (22^{0}C) by using CCl_4 of analytical quality "Reactivul București".

2. The plate method (Wilhelmy) has been used to measure benzene/water interfacial tensions. In the oil phase benzene of analytical quality "Reactivul București" was used and the water phase consisted of aqueous solutions of NaC.
Measurements have been made in thermostated samples at 20 ± 0,5^{0}C.

3. Conductometric method [16]. Measurements have been performed by means of a Gt 12 type conductometer at 23^{0}C.

4. Turbidimetric method [20].
Investigations have been made by means of a Specol-10 Spectrophotometer equipped with a device of TK type turbidimeter.
Measurements have been performed at 483 nm, where a maximum of sensitivity had been observed. Working temperature: 22^{0}C.

ACKNOWLEDGEMENT
Authors thank Merch for the sodium cholate offered us free of charge.

REFERENCES

1. J. Prieto, J. Rodés, D. A. Shafritz, "Hepatobiliary Diseases", Springer-Verlag, New York, 1992, pp. 201-270.
2. A. I. Hofman, *Biochem J.*, 1963, 89, p. 57.
3. M. C. Carey, D. M. Small, *Am. J. Med.*, 1970, 45, 590.
4. D. M. Small, *Physical Chemistry of Cholanic Acids* in "The Bile Acids - Chemistry, Physiology and Metabolism", Eds., P. P. Nair, D. Kritchevsky, Plenum Press, New York, 1971, p. 255.
5. J. P. Kratohvil, H. T. Dellicolli, *Can. J. Biochem.*, 1967, 46, 945.
6. P. Ekwall, K. Fontell, A. Sten, *Proc. Intem. Congr. Surface Activity*, London, Butterworths, London, 1957, p. 357.
7. A. Norman, *Acta Chem. Scand.*, 1996, 14, 1295.
8. De Moerloose, R. Ruyssen, *J. Pharm. Belg.*, 1959, 14, 95.
9. T. Furusawa, Fukuoka, *Acta Med.*, 1962, 53, 124.

10. H. Miyake, T. Murakoshi, T. Hisatsugu, *Fukuoka Igaku Zassi,* 1962, 53, 659.
11. T. Bates, *Doctoral Thesis,* Columbia Univ., New York, 1966.
12. T. Bates, M. Gibaldi, J. L. Konig, *Nature,* 1966, 120, 1331.
13. S. A. Johnston, J. W. McBrain, *Proc. Roy. Soc. London, Scr. A,* 1943, 181, 119.
14. A. Roda, A. F. Hofmann, K. J. Mysels, *J. Biol. Chem,* 1983, 258, 6362
15. F. P. Woodford, *J. Lipid. Res.,* 1969, 10, 539.
16. I. Mândru, D. M. Ceacăreanu, "Chimia Coloizilor şi Suprafeţelor - Metode experimentale", Ed. Tehn. Bucureşti, 1976, pp. 395-404.
17. K. B. Serebrovskaya, G. A. Korneeva, *Kolloid. Zh.,* 1972, 34, 954.
18. R. E. Howard, R. M. Burton, Biochim., *Biophys. Acta,* 1964, 84, 435.
19. E. Vikingstad, O. Kvammen, *J. Colloid Interface Sci.,* 1980, 74, 16.
20. C. Y. Chang, S. J. Wang, I. J. Lin, Y. C. Chin, *J. Chin. Chem Soc,* 1987, 34, 243.
21. J. T. Davies, E. K. Rideal, "Interfacial Phenomena", Acad. Press., New York, Cap. 4, 1963.
22. M. C. Carey, Phisical-chemical properties of bile acids and their salts in "Sterols and Bile Acids" Eds., J. Sjövall, H. Danielson, Elsevier, 1985, pp. 345-403.

STUDIA UNIVERSITATIS BABEŞ-BOLYAI, CHEMIA, XLII, 1-2, 1997

THE ALKYLATION REACTION OF SOME SUBSTITUTED PYRIMIDINONES[1]

DALILA KOVACS[2], LUMINIŢA MUNTEAN[2], LILIANA CRĂCIUN[2], S. MAGER[2]

ABSTRACT. The S-, O- and N-alkylation reactions of some substituted pyrimidinones have been studied, including the influence of the alkylating agent, the temperature, the time of the reaction and the nature of the solvent on the selectivity of the reaction. The ratios of the alkylated mixtures were determinated by means of NMR spectroscopy.

INTRODUCTION

The synthesis, the structure and the reactivity of some pyrimidinonic compounds are of major importance from both the practical and theoretical points of view. Many of these compounds show an important biological activity [1-5] and an interesting reactivity especially in connection with the possible existence of different tautomeric structures [6-13]. The tautomerism of the 4-pyrimidinone is represented (Scheme 1) by two lactam toutomers, 4(1H)-pyrimidinone [N(1)-H] and 4(3H)- pyrimidinone [N(3)-H] and an enol (phenoı) one, the 4-hydroxypyrimidine (4-OH):

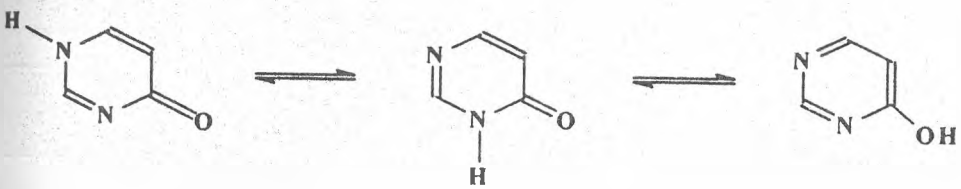

N(1) – H N(3) – H 4 –O H

Scheme 1

Many papers on the subject have been published, leading to the general conclusion that the equilibrium in solutions is largely shifted towards the N(3)-H isomer [6, 7, 10, 11, 14, 15]. That, in spite of the contradictory conclusion found as

---

[1] Author to whom correspondance should be adressed.

[2] Universitatea "Babeş-Bolyai", Catedra de Chimie Organică, Str. Arany Janos nr. 11, RO-3400, Cluj-Napoca, Romania.

a result of some determinations of ionisation constants in dilute aqueous solutions [8,9]. An exception is also furnished by infrared spectra recorder in gas phase and low-temperature inert matrices giving comparable populations of both keto and enol (phenol) forms [12, 13]. The tautomerism of the pyrimidinone (pyrimidinol) unit is strongly dependent on the substituents liked especially in positions 2 and 5, determined by starting compounds of the synthes: the synthon introducing in the molecule the two nitrogen atoms and the substituted or unsubstituted acetoacetic ester (Scheme 2 and 3).

The usual way of the synthesis [16] starts from thiourea [17, 18] or guanidine [19-24] with acetoacetic ester. In order to diminish the number of tautomeric structures, the N,N-dialkylguanidine and substituted acetoacetic esters were used:

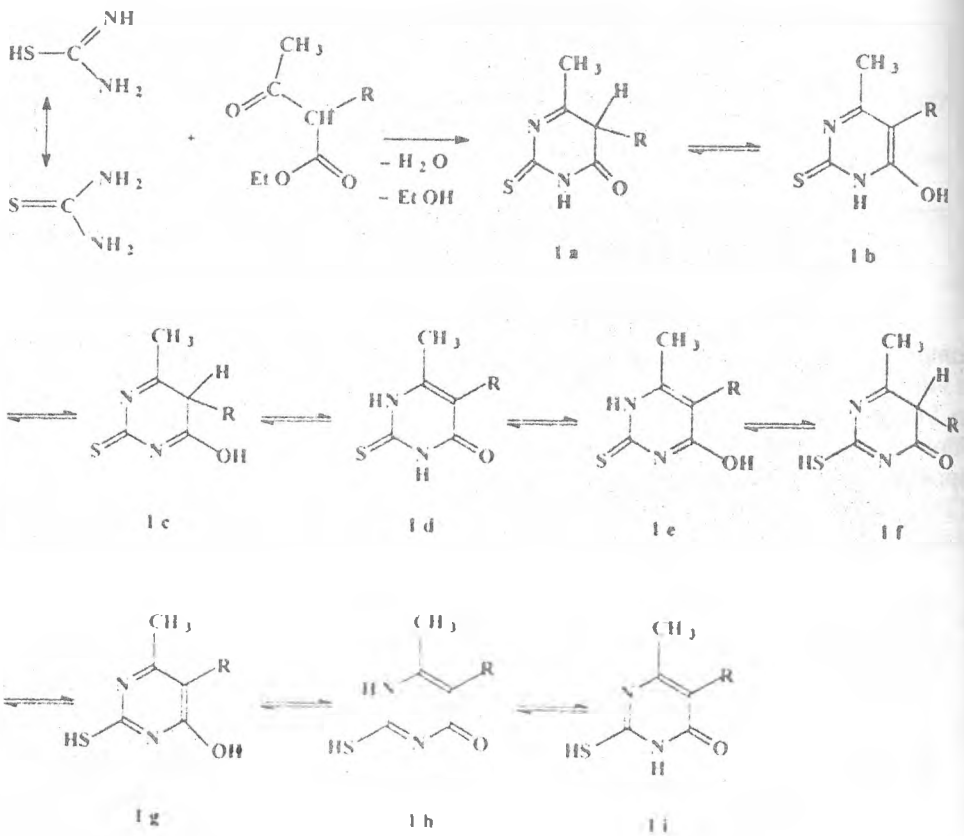

Scheme 2

Not all the theoretically possible tautomers have been really detected. If a dimethylated (alkyated) acetoacetic ester was used, the obtained 2-diethylamino-5.5.6-trimethyl-4(5H)- pyrimidinone *3* was the unic possible isomer [25].

The real existing tautomers may be chemically identified by means of the alkylation reaction, as in the case of compounds *2*, when the fixed O- and N-methylated isomers ***4a,b*** have been identified [2]:

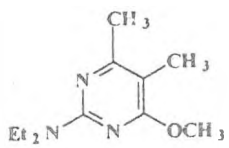

4a

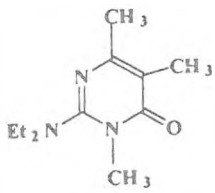

4b

Such an attempt has also made in the case of pyrimidinone compounds *1* obtained from thiourea. The tautomeric structures offer the possibility to study the S-, O- and N-alkylation reactions.

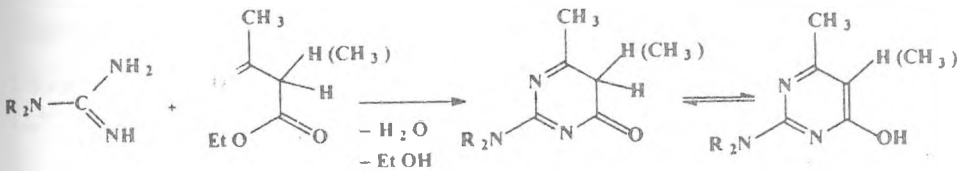

2 a

2 b

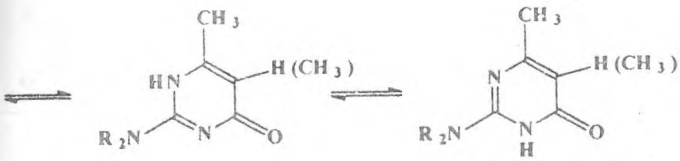

2 c

2 d

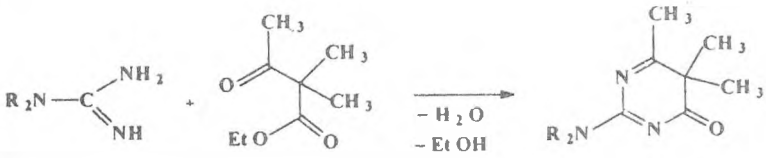

3

Scheme 3

RESULTS AND DISCUSSION

The alkylation reaction was studied on the 5-alkyl-6-methyl-2-thio-4(3H)-pyrimidinone obtained from thiourea and 5-methyl- respectivelly 5-butyl-ethykacetoacetate (Scheme 2), in order to try to establish also the possible involvement of the steric factor. As alkylating agents, methyl and ethyl iodide as well as ethyl sulfates were used.

The temperature, the time of the reaction and influence of the solvent were also taken into account.

The selectivity of the reaction (based on the different reactivities of the SH, NH and OH groups of the tautomers) run in appropriate conditions, makes possible the isolation of the S-alkylpyrimidinones ***5*** and ***5'*** with partial fixes structures (Scheme 4). These were further alkylated offering the possibility to observe the competition between the remaining NH and OH functions of the isomers in the alkylation reaction.

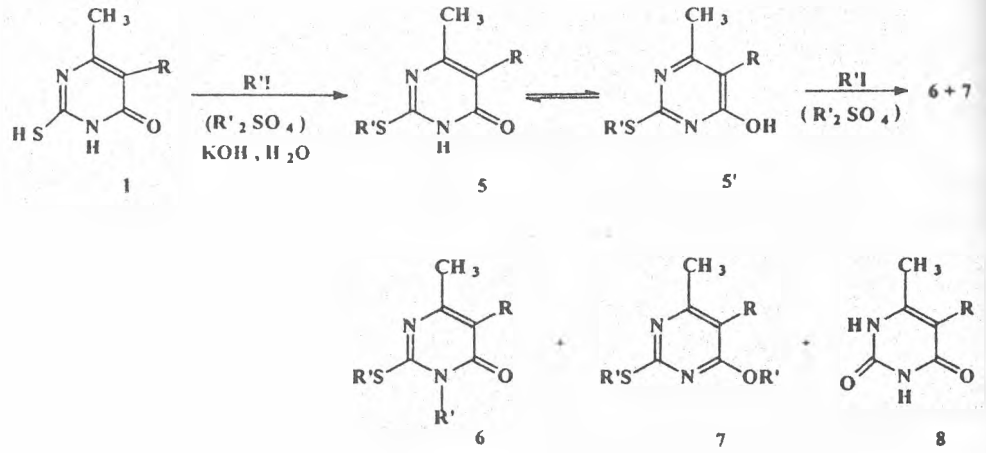

R = – CH 3 , – (CH 2) 3 CH 3

R' = – CH 3 , – CH 2 CH 3

Scheme 4

The results of the alkylations are presented in Table 1. It must be mentioned that in our experiments no alkylation product at N(1) was separated nor identified in the reaction mixtures. In most alkylation reactions a part of the starting pyrimidinone was recovered at the end of the reaction and only the S-alkylated compounds ***5*** and ***5'*** were obtained as pure, crystalline products. Therefor the results are given not in yields for individual compounds but as conversion percentages of the starting compound.

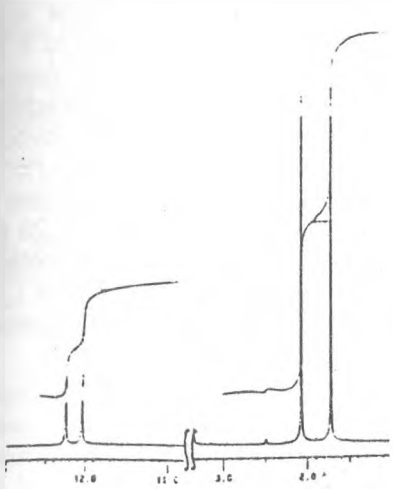

Fig. 1a

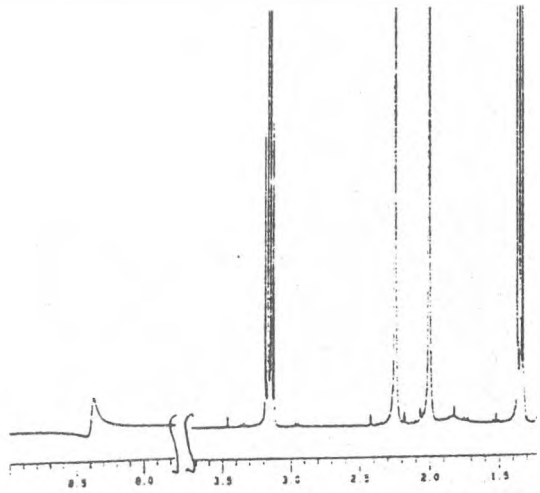

Fig. 1b

Table 1

Starting comp.	R	R'	Alkylation agent	Reaction conditions Temp ^{0}C	Time (h)	Products	Conv. % (total)	Obs.
1	Me	Me	MeI	20	1	**5**	86.6	
				20	24	**5+6**	81.3	**6** 5%
	Bu		Me_2SO_4	20	24	**5+6**	58.6	**6** 13.4%
	Me			60	1	**5+6**	71.3	**6** 4.4%
				100	1	**5+6+8**	55.3	**6** 6% **8** 7.7%
	Bu	Et	EtI	20	24	**5**	61	
	Me			100	1	**5+6+7**	70.4	**6+7** mixture
	Me		Et_2SO_4	20	24	**5+6+7**	89.6	**6+7** mixture
				60	1.5	**5+6+7**	62.5	**6+7** mixture
				100	1	**5+6+7+8**	64	**6+7** mixture
5	Me	Me	MeI	20	24	**6**	9.7	
	Bu		Me_2SO_4	20	8	**6**	24.5	
				100	2	**6**	56.3	
	Me	Et	EtI	100	8	**6+7**	73.9	mixture
			Et_2SO_4	100	8	**6+7**	70	mixture

The composition of the S-ethyl, N-ethyll *(6)* and S-ethyl, O-ethyl *(7)* mixture was determined by means of the NMR spectroscopy, as well as the structure of the starting compound *(1)* and of the mono S-ethylated derivative *(5)*. The mass spectra also confirm the structure of compound ***5*** showing clear M - C_2H_5SCN, M - OCNH and M - CO peaks. The comparison of Fig. 1a and 1b

confirm demonstrates the disappearance of one of down field protons in the spectrum of ***1*** and the appearance of the S-ethyl signal in the spectrum of ***5***. The very well separated and clear signals of the two quartets at 4.04 and 4.37 ppm and of the singlets (between 2 and 2.3 ppm) belonging to the methyl groups attached to C(5) and C(6) (Fig. 2) permit the evaluation of an about 2:1 ratio in the favour of the O-ethyl, S-ethyl isomer ***7***. The small signals, the quartets at 4.04 ppm (for N - $\underline{CH_2}$ - CH_3) and 3.14 ppm (for S - $\underline{CH_2}$ - CH_3), the singlets of 1.48 and 2.2 ppm [for the methyl groups connected to C(5) respectively C(6)] and the triplet of 1.26 ppm (for S - $\underline{CH_3}$ - CH_3) belong to the S-ethyl, N-ethyl isomer ***7***. The multiplet between 1.3 and 1.4 ppm represents a superposition of three triples: two big ones for $\underline{CH_3}$ - CH_2 - S and $\underline{CH_3}$ - CH_2 - O of isomer ***7*** and a small one for $\underline{CH_3}$ - CH_2 - N of isomer ***6***.

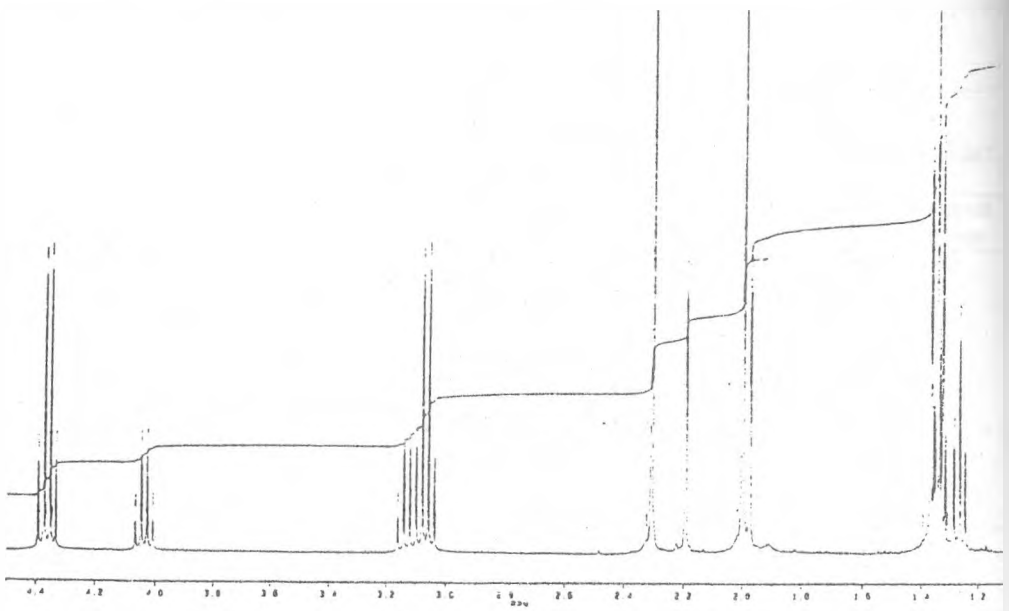

Fig. 2

It has to be mentioned the prefference of the O-ethylation as compared to the N-ehylation, if the alkylation agent is diethylsulfate (the iodide has a prefference for the N-alkylation). The O-alkylation is also favoured by temperature. The high temperature favours in the same time the nucleofilic substitution of the SH group with OH (experiments are run in aqueous solution) having as a result the formation of the substituted uracil ***8*** as a side product.

Concerning the influence of the solvent the yields are favoured in the case of protic solvents (water) as compared with the aprotic dipolar dimethylformamide.

The attempts to use diazomethane in order to try to render evident an OH tautomer failled, for sure because of the two low acidity of the enolic OH.

The alkylation in phase-transfer catalysis conditions leads to a mixture product of the S-methyl and N-methyl isomers in the case of methylation, with resonable yields, but to very poor results in the case of ethylation reaction.

EXPERIMENTAL

Proton NMR spectra were recorded at room temperature, using DMSO or $CDCl_3$ as solvent, in 5 mm tubes, on a Bruker AM 400 Fourier transform NMR spectrometer equiped with a dual ^{13}C-^{1}H head, operating at 400 MHz.

1. Alkylation of 2-thio-pyrimidin-4-one

a) with alkyl iodides

To a solution of 0.09 mol KOH and 0.045 mol 2-thio-pyrimidin-4-one (1) in 120 mL water, warmed at the desired temperature, 0.09 mol of alkyl iodide was dropwise added. After stirring for 1-24 hours, the mixture was cooled at room temperature and extracted with ether (3x20 mL). The organic layer was separated, dried and concentrated, to give the S,N-dimethylated (6) compound (when the reaction was carried out with methyl iodide) or the mixture of S,N-diethylated (6) and S.O-diethylated (7) compounds (when the alkylating agent was ethyl iodide).

The aqueous layer was treated with acetic acid (pH = 5) and the resulting white precipitate was filtered; after purification by recrystallization (methanol-water) the S-alkyl derivative (5) was obtained.

b) with alkyl sulfates

To a solution of 0.09 mol KOH and 0.045 mol 2-thio-pyrimidin-4-one (1) in 120 mL water, warmed at the desired temperature, 0.09 mol of alkyl sulfate was dropwise added. After stirring for 1-24 hours, the mixture was cooled at room temperature and the resulting white precipitate was filtered. After purification by recrystallization (methanol-water) the S-alkyl derivative (5) was obtained.

In some hours, the filtrate gave a new white precipitate; after filtration and recrystallization (water) the uracil derivative (8) was obtained.

The second aqueous filtrate was extracted with ether (3x20 mL). The organic layer was separated, dried and concentrated to give the S,N-dimethylated (6) product (when the alkylating agent was the dimethyl sulfate) or the mixture of S,N-diethylated (6) and S.O-diethylated (7) products (when the alkylation was carried out with diethyl sulfate).

2. Alkylation of 2-alkylthio-pyrimidin-4-one

a) with alkyl iodides

To a solution of 0.09 mol KOH and 0.045 mol 2-alkylthio-pyrimidin-4-one (5) in 120 mL water, 0.09 mol of alkyl iodide was dropwise added. After stirring for 8-24 hours, the mixture was extracted with ether (3x20 mL). The organic layer was separated, dried and concentrated to give the S,N-dimethylated (6) product (when the alkylating agent was methyl iodide) or the mixture of S,N-diethylated (6) and S,O-diethylated (7) products (when the alkylation was carried out with ethyl iodide). The aqueous layer was treated with acetic acid (pH = 12-13) and the white precipitate obtained was filtered; after recrystallization (methanol-water) the S-alkyl derivative (5) was recovered.

b) with alkyl sulfates

To a solution of 0.09 mol KOH and 0.045 mol 2-alkylthio-pyrimidin-4-one (5) in 120 mL water, 0.09 mol of alkyl sulfate was dropwise added. After stirring for 8-24 hours, the mixture was cooled at room temperature and the resulting white precipitate was filtered. The precipitate was treated with NaOH solution (pH = 12-13) and the insoluble part of it was filtered again; after the purification by recrystallization (methanol-water) the S,N-dimethylated (6) product was obtained.

The filtrate was treated with aqueous acetic acid (pH = 5) and the white precipitate obtained was filtered; after recrystallization (methanol-water) the S-alkyl derivative (5) was recovered.

If the alkylating agent was ethyl sulfate, after the filtration of the white precipitate obtained (the S-alkyl derivative (5) recovered) the filtrate was extracted with ether (3x20 mL). The organic layer was separated, dried and concentrated to give a mixture of S,N-diethylated (6) and S.O- diethylated (77) products.

REFERENCES

1. D. I. Brown, in *The Chemistry of Heterocyclic Compounds*, Vol. 52, The Pyrimidines, Wiley and Sons, New York, 1993.
2. W. Saenger, in *Principles of Nucleic Acids Structure*, Springer Verlag, New York, 1993.
3. S. Mager, I. Cristea, I. Hopârtean, V. Fărcăsan, F. Paiu, I. Panea and V. Popa, *Rom. Pat.* Nr. 77114, 1981.
4. I. Panea, S. Mager, V. Fărcăsan, F. Paiu, I. Hopârtean and I. Cristea, *Rom. Pat.* Nr. 79028, 1981.
5. S. Mager, M. Diudea, F. Jugrestan, I. Cristea and I. Panea, *Rom. Pat.* Nr. 103578, 1991.
6. D. Brown and L. Short, *J. Chem. Soc.*, 1953, 331.
7. D. Brown, E. Hoerger and S. Mason, *J. Chem. Soc.*, 1955, 211.
8. S. Mason, *J. Chem. Soc.*, 1958, 674.
9. T. Kitagawa, S. Mizukami and E. Hirai, *Chem. Pharm. Bull.*, 1974, 22, 1239.
10. A. Albert and E. Spinner, *J. Chem. Soc.*, 1960, 1221.
11. Y. Inone, N. Furutachi and K. Nakanishi, *J. Org. Chem.*, 1966, 31, 175.
12. R. Czerminski, K. Kucsera, H. Rostkowska, M. Noroak and K. Szczepaniak, *J. Mol. Struct.*, 1986, 140, 235.
13. D. Shugarand and K. Szczepaniak, *Int. J. Quantum Chem.*, 1981, 20, 573.
14. A. Katritzky and J. Lagowski, *Adv. Heteroccycl. Chem.*, 1963, 1, 331 and 339.

15. J. Elguero, C. Marzin, A. Katritzky and P. Linda, *Adv. Heteroccycl. Chem. Suppl.*, 1976, 1, 1 and 127.
16. H. Wamhoff and F. Korte, *Synthesis*, 1972, 151.
17. H. Wheeler and D. McFarland, *Am. Chem. J.*, 1907, 42, 101.
18. F. Fischer and J. Roch, *Liebigs Ann. Chem.*, 1951, 572, 217.
19. R. Hull, B. Lovell, H. Openshaw, L. Payman and A. Todd, *J. Chem. Soc.*, 1946, 357.
20. E. Falco, P. Russell and G. Hitchings, *J. Am. Chem. Soc.*, 1951, 73, 3753.
21. C. Overberger and I. Kogon, *J. Chem. Soc.*, 1954, 76, 1879.
22. F. Gomez-Contreras, T. Manzano and P. Navarro, *Heterocycles*, 1980, 14, 769.
23. S. Mager, I. Cristea, L. Crăciun, F. Irimie and M. Diudea, *Rev. Roum. Chim.*, 1991, 36, 665.
24. L. Crăciun, D. Kovacs, R. Crăciun and S. Mager, *Studia Univ. "Babeș-Bolyai" Chem., in press.*
25. L. Crăciun, A. Horvath and S. Mager, *Studia Univ. "Babeș-Bolyai" Chem., in press.*

STUDIA UNIVERSITATIS BABEȘ-BOLYAI, CHEMIA, XLII, 1-2, 1997

ELECTROCHEMICAL STUDY OF VANADIUM CONTAINING KEGGIN-TYPE HETEROPOLYTUNGSTATE AND HETEROPOLYMOLYBDATE ACIDS

ALEXANDRA FODOR[1], LIANA MUREȘAN[2], A. ȘUTEU[3], I.C.POPESCU[2]

ABSTRACT. Cyclic voltammetric measurements were performed in acidic media (0.5 M Na_2SO_4 + H_2SO_4) in the pH range 1-3 and at different voltage scan rates for $H_5[PW_{10}V_2O_{40}]$ $24H_2O$, $H_6[PMo_{10}V_2O_{40}]$ $30H_2O$ and $H_5[SiMo_{10}V_2O_{40}]$ $25H_2O$ on Pt electrodes. The features of the W/Mo oxo-cage electrochemical activity were found in accordance with the previously reported data, in spite of the deleterious effect of hydrogen evolution reaction on Pt electrode. An electrochemical reversible wave was observed for V. Its formal redox potential is shiffed towards more negative potentials as compared with the VO_2^+ / VO^{2+} couple and is more influenced by the nature of the central heteroatom (P, Si) as by the transition metal (W, Mo) from the peripheral octahedra. Thus, changing the identity of the central heteroatom, (P with Si), a slight shift of the formal potential of the $[PMo_{10}V_2{}^{V}O_{40}]^{n-}$ / $[XMo_{10}V_2{}^{IV}O_{40}]^{(n+1)-}$ redox couple. was observed, while the replacement of W from the host oxo-matrix with Mo, practically does not change the formal potential of the $[PM_{10}V_2{}^{V}O_{40}]^{5-}$ / $[PM_{10}V_2{}^{IV}O_{40}]^{6-}$ redox couple.

INTRODUCTION

Heteropolyacids and their salts have been studied extensively owing to their interesting catalytic properties [1]. Several metal-substituted heteropolyoxometalates have been the subject of electrochemical studies in order to investigate their electrochemical [2-7] or electrocatalytical [8-16] behavior.

A class of these compounds, presenting a Keggin structure with mixed addenda, is represented with the general formula $[XM_{10}[x1]V_2O_{40}]^{m-}$, where X is a tetrahedral coordinated heteroatom such as P or Si and M is a transition metal (W, Mo). Taking into account that vanadium could modify the redox activity of parent anions with single species addenda, $[XM_{12}O_{40}]^{y-}$, it might be expected that this class of polyoxometalates offer new possibilities to perform electrocatalytical processes.

The aim of this paper is study the electrochemical behavior of three vanadium substituted heteropolyacids: $H_5[PW_{10}V_2O_{40}]$. $24H_2O$ ***(I)***, $H_6[PMo_{10}V_2O_{40}]$.

[1] Facultatea de Medicină și Farmacie, Universitatea Oradea, 3700 Oradea, Romania
[2] Facultatea de Chimie și Inginerie Chimică, Universitatea Babeș-Bolyai, 3400 Cluj-Napoca, Romania.
[3] Facultatea de Energetică, Universiatatea Oradea, 3700 Oradea, Romania

$30H_2O$ ***(II)*** and $H_5[SiMo_{10}V_2O_{40}]$. $25H_2O$ ***(III)***. Cyclic voltammetric measurements, performed in different experimental conditions, allowed us to obtain information about the electrochemical reversibility of the involved redox processes and the pH dependence of the corresponding formal potentials.

EXPERIMENTAL

Reagents. $H_5[PW_{10}O_{40}]$. $24H_2O$, $H_6[PMo_{10}V_2O_{40}]$. $30H_2O$ and $H_5[SiMo_{10}V_2O_{40}]$. $25H_2O$ were synthesized by a modification of the Kokorin's method [17-21] using the following molar ratios between the reagents: for compound ***(I)*** $NaH_2PO_4/NaVo_3/Na_2WO_4$ = 1: 10: 5, for compound ***(II)*** $Na_3PO_4/NaVO_3/Na_2MoO_4$ = 1: 6: 10 and for compound ***(III)*** $Na_2SiO_3/NaVO_3/Na_2MoO_4$ 1: 1.5: 5. The three heteropoliacids were separated by double ether extraction and recrystalised at room temperature in darkness.

All chemicals were reagent grade and used as received. 0.5 M buffer solutions (pH = 1-3) were prepared from Na_2SO_4 (Reactivul Bucureşti) and H_2SO_4 (Merck). All solutions were prepared with distilled water. Their pH was measured with a combined glass electrode (Metrohm, Switzerland) and a digital pH-meter (WV-Präcitronic, GDR).

Electrochemical experiments. Electrochemical experiments were performed using a potentiostatic set-up consisting of a potentiostat (PS 3 Meinsberg, GDR), a signal generator (PV2 Meinsberg, GDR) and a XY- recorder (Endim 620.02, Meinsberg, GDR). A conventional three electrodes cell was used. The working electrode was a Pt disk (Φ=5 mm). The reference electrode was a saturated calomel electrode (SCE). The Pt counter electrode was separated from the test solution by a glass frit. All measurements were performed at room temperature.

RESULTS AND DISCUSSIONS

The voltammograms for the three vanadium containing heteropolyanions are presented in figures 1 and 2.

Irrespective of the compound identity, at least two reduction waves and the corresponding reoxidation waves are observed. Thus, for compound ***(I)***, due to the low overpotential for the hydrogen evolution reaction (HER) on Pt electrode, the more negative potential wave, clearly visible at pH = 2.5 (figure 1b), is not completely developed at pH 1.2 (figure 1a). The one electron wave ($\varepsilon^{0'}$ = - 0.17 V/SCE) was identified with the most positive wave of the three waves set characterizing, as previously reported in [2, 6, 16], the oxidation/reduction of the tungsten-oxo cage. The wave with $\varepsilon^{0'}$ = 0.37 V/SCE was attributed to $V^{V/N}$ couple from ***(I)***. The negative shift of about 300 mV existing between the formal redox potential corresponding to VO_2^+/VO^{2+} couple [22] and that for $[PW_{10}V_2O_{40}]^{5-}/[PW_{10}V_2O_{40}]^{6-}$ is due to its insertion in the tungsten-oxo cage [2].

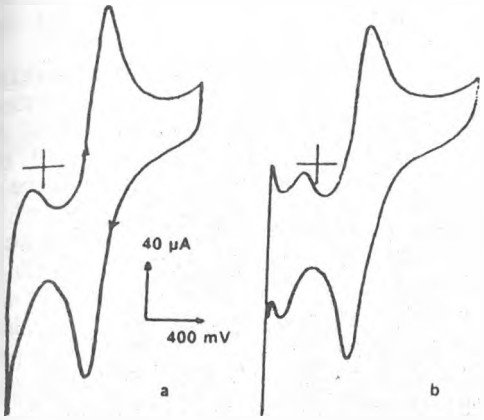

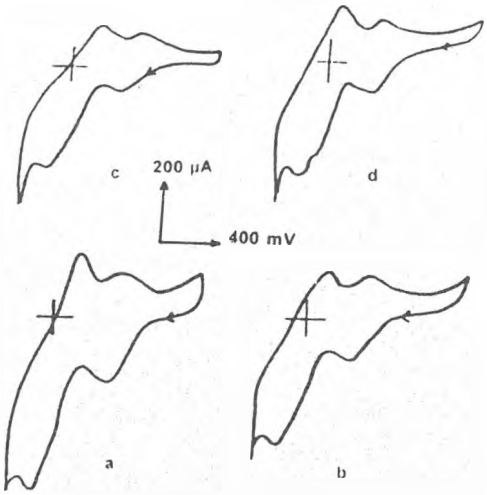

Fig. 1. Cyclic voltammograms of 0.5 mM $H_5[PW_{10}V_2O_{40}]$ a) pH=1.2; b) pH=2.5, Experimental conditions: supporting electrolyte, 0.5M Na_2SO_4; scan rate 100 mV/s.

Fig. 2. Cyclic voltammograms of 0.5 mM $H_5[PMo_{10}V_2O_{40}]$ (a,b) and of 0.5 mM $H_6[SiMo_{10}V_2O_{40}]$ (c,d); (a) and (c), pH=1.7; (b) and (d), pH=2.5. Experimental conditions as in figure 1.

The comparison of the redox behavior of compound ***(I)*** (fig. 1) and compound ***(II)*** (fig. 2a and b) shows that the replacement of W from the host oxo-matrix with Mo, does not change the formal potential of the $[PM_{10}V_2^{V}O_{40}]^{5-}$ /$[PM_{10}V_2^{IV}O_{40}]^{6-}$ redox couple (table 1), as was pointed out also for other Keggin-type anions [6]. In the same time, the reduction waves corresponding to molybden-oxo cage appear at more positive potentials than those corresponding to tungsten-oxo cage (figures 1 and 2a, b) [6].

Table 1. Formal redox potentials for $[XM_{10}V_2^{V}O_{40}]^{m-}$/$[XM_{10}V_2^{IV}O_{40}]^{(m+1)-}$ couple for the investigated compounds

Compound	$\varepsilon^{0'}$, V/SCE
$H_5[PW_{10}V_2O_{40}]$	0.35*
$H_5[PMo_{10}V_2O_{40}]$	0.41*
$H_6[SiMo_{10}V_2O_{40}]$	0.36*

*estimated from the recorded voltammograms (fig.1, 2) as an average, for pH 1.2-2.5

However, changing the identity of the central heteroatom (P with Si), a slight shift of the formal potential of the $[XMo_{10}V_2^{V}O_{40}]^{-n}/[XMoV_2^{IV}O_{40}]^{(n+1)-}$ redox couple was observed (figure 2c and d compared with 2a and b). This effect was attributed to the difference between the overall ionic charge of the two corresponding anions [6, 13].

Beside the $[XM_{10}V_2^{V}O_{40}]^{m-}/[XMV_2^{IV}O_{40}]^{(m+1)-}$ wave, the other waves existing in the voltammograms for compounds (II) and (III). were attributed to oxidation-reduction of molybdenum-oxo cage, more or less overlapped with HER [16]. As expected, the position of these waves is influenced by the nature of the heteroatom, being shifted towards more negative potentials with the increase of the overall ionic charge [6].

The cyclic voltammograms recorder for three compounds at different scan rates and constant pH, showed that the peak potentials (ε_p) for $[XM_{10}V_2^{V}O_{40}]^{m-}/[XM_{10}V_2^{IV}O_{40}]^{(m+1)-}$ were independent of the voltage scan rate in the range 0.01-0.1 $V.s^{-1}$, suggesting reversible or quasi-reversible electron transfer. Taking into account that, irrespective to the scan rate, $\Delta\varepsilon_p$ is slightly higher than 0.059/n V [18] and that $I_{p,a} / I_{p,c} \approx 1$, it is most probable that the redox process corresponding to vanadium couple involves one electron and is quasi-reversible.

On the other hand, for all compounds, the $V^{V/N}$ current peaks are proportional to the square root of the voltage scan rate in the range 0.01-0.1 Vs^{-1}, as can be seen in figure 3 for compound ***(I)***, indicating that the electrode process is diffusion controlled.

The compounds ***(I)-(III)*** are stable in aqueous media in the investigated pH range [4]. As previously reported [5-7, 24], protons are involved in $V^{V/N}$ redox process for all investigated compounds. The $\varepsilon^{0'}$ value for $V^{V/N}$ couple is linearly dependent on pH as can be seen in figure 4 for compound ***(III)***. The slopes of $\varepsilon^{0'}$ vs. pH plots (table 2) show a H^+/e^- ratio of about 1.5/1, in the investigated pH range. It is interesting to note that slopes of $\varepsilon^{0'}$ vs. pH plots are, in the limit of experimental errors, almost identical and are corresponding to parallel lines. This shows once again, that the oxo cage has an influence upon the ε^{0} for $V^{V/N}$ couple.

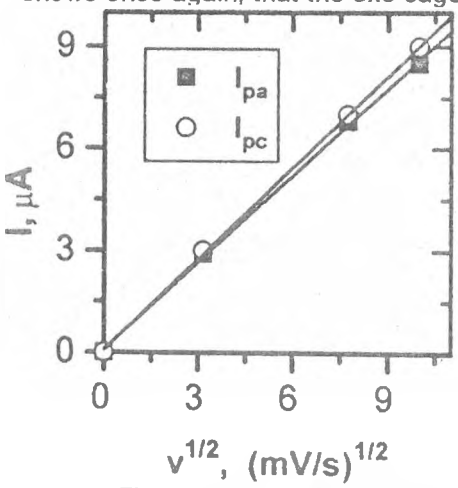

Fig. 3. Anodic ($I_{p,a}$) and cathodic ($I_{p,c}$) peak currents vs. square root of scan rate ($v^{1/2}$) corresponding to $V^{V/IV}$ redox couple in $H_5[PW_{10}V_2O_{40}]$.

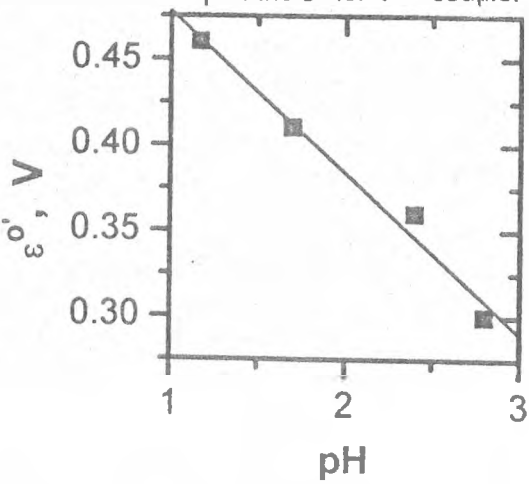

Fig. 4. pH dependence of formal redox potential for ($V^{V/IV}$) couple in $H_6[SiMo_{10}V_2O_{40}]$.

Table 2. Dependence on pH of the formal redox potentials for V/IV couple in the investigated compounds

Compound	$\Delta\varepsilon^0 / \Delta pH$ (V/pH)	Correlation coefficient / no. of points
$H_5[PW_{10}V_2O_{40}]$	0.074	0.940 / 4
$H_5[PMo_{10}V_2O_{40}]$	0.084	0.969 / 4
$H_6[SiMo_{10}V_2O_{40}]$	0.093	0.990 / 4

CONCLUSIONS

Cyclic voltammetric measurements were performed in acidic media (0.5 M Na_2SO_4 + H_2SO_4) in the pH range 1-3 and at different voltage scan rates for $H_5[PW_{10}V_2O_{40}]$ $24H_2O$, $H_6[PMo_{10}V_2O_{40}]$ $30H_2O$ and $H_5[SiMo_{10}V_2O_{40}]$ $25H_2O$, on Pt electrodes. The features of the W/Mo-oxo cage electrochemical behavior were found in accordance with the previously reported data, in spite of the deleterious effect of hydrogen evolution reaction on Pt electrode. An electrochemical reversible wave was observed for V. Its formal redox potential is shifted towards more negative potentials as compared with the VO_2^+ / VO^{2+} couple and is more influenced by the nature of the central heteroatom (P, Si) as by the transition metal (W, Mo) from the peripheral octahedra.

REFERENCES

1. M. T. Pope, "Heteropoly and Isopoly Oxometalates", Springer, Berlin, 1983.
2. C. Rong and M. T. Pope, *J. Am. Chem. Soc.*, 1992, 114, 2932.
3. J. C. Bart and F. C. Anson, *J. Electroanal. Chem.*, 1995, 390, 11.
4. H. Wang, Z. Yu and E. Wang, *J. Electroanal. Chem.*, 1995, 380, 69.
5. S. Himeno, K. Maeda, T. Osakai, A. Saito and T. Hori, *Bull. Chem. Soc. Jpn.*, 1993, 66, 109.
6. K. Maeda, H. Katano, T. Osakai, S. Himeno and A. Saito, *J. Electroanal. Chem.*, 1995, 389, 167.
7. A. M. Bond, J. B. Cooper, F. Marken and D. M. Way, *J. Electroanal. Chem.*, 1995, 396, 407.
8. O. Savadogo and D. L. Piron, *Int. J. Hydrogen Energy*, 1990, 15, 715.
9. B. Keita, L. Nadjo, G. Krier and J. F. Muller, *J. Electroanal. Chem.*, 1987, 223, 287.
10. O. Savadogo and S. Levesque, *J. Appl. Electrochem.*, 1991, 21, 457
11. B. Keita, L. Nadjo and J. M. Saveant, *J. Electroanal. Chem.*, 1988, 243, 105.

12. P. Wang, Y. Li, *Electroanal. Chem.*, 1996, 408, 77.
13. J. E. Toth and F. C. Anson, *J. Am. Chem. Soc.*, 1989, 111, 2444.
14. P. J. Kulesza, G. Rosnolek and L. R. Faulkner, *J. Electroanal. Chem.*, 1990, 280, 233.
15. S. Dong and M. Liu, *J. Electroanal. Chem.*, 1994, 372, 94.
16. C. Rong and F. Anson, *inorg. Chem. Acta*, 1996, 242, 11
17. A. I. Kokorin and N. A. Polotebnova, *Zhur. Obsehehei Khim.*, 1954, 24, 967.
18. A. I. Kokorin and N. A. Polotebnova, *Zhur. Obsehehei Khim.*, 1954, 24, 1573.
19. A. I. Kokorin and N. A. Polotebnova, *Zhur. Obsehehei Khim.*, 1954, 24, 1718.
20. A. I. Kokorin and N. A. Polotebnova, *Uchenye Zapiski Kishinev Univ.*, 1953, 6, 63.
21. A. I. Kokorin and P. L. Diamant, *Zhur. Obsehehei Khim.*, 1954, 24, 971.
22. M. S. Antelman, "The Encyclopedia of Chemical Electrode Potentials", Plenum Press, N. York, 1982.
23. R S. Nicholson, I. Shain, *Anal. Chem.*, 1964, 36, 706.
24. B. Keita, L. Nadjo, *J. Electroanal. Chem.*, 1987, 227, 7 and references cited therein.

STUDIA UNIVERSITATIS BABEŞ-BOLYAI, CHEMIA, XLII, 1-2, 1997

CRYSTAL GROWTH AND CRYSTALLINE STRUCTURE OF OCTACHLOROPHENOTHIAZINE

PETRU STETIU[1], IOAN SILBERG[2], GHEORGHE BORODI[3]
IULIA BOBAILA[1], LUCIAN ILES[2]

ABSTRACT. Using the zonal vapour-phase crystallization technique, big single crystals of octachlorophenothiazine (OCPT) of needle; or ribbon-like form were grown for the first time. Using X-ray techniques (diffractometry, Kulpe's and Weisemberg's methods) its crystalline structure was established; this is monocline with the lattice constants a = 12.26 Å, b = 3.71 Å, c = 17.11 Å, ß = 100^0. The unit cell contains two molecules. The preferential growth direction is along the b axis and crystals have their plater faces parallel to c axis.

INTRODUCTION

Our interest on OCPT is justified by its remarcable chemical and physical stability and by its promising physical properties.

OCPT was first synthetized by Rupprecht [1], using a method of photo-chlorination of phenothiazine (PT). Later, Bodea and Silberg [2] reported another method, the chlorination of PT up to undecachlorophenothiazine (UDCPT) followed by its reduction to OCPT. The second method leads to better results, OCPT synthetized this way being more pure.

Using a Debye-Scherrer technique, Silberg [3] established *d/n* values for OCPT but neither Bodea and Silberg [2], nor Silberg [3], did establish the crystalline structure of OCPT. Using a picnometric method and polycrystalline OCPT, Silberg [3] measured the density of this substance and found ρ = 1.92 g/cm^3. The melting point of OCPT, 340^0 C, was established by Silberg [3] using a capillary method. Silberg [3] reported also about some IR spectral analyses on OCPT. No other reports on OCPT's physical properties were found in the literature.

This paper reports about synthesis of the raw material, the crystal growt and the structure studies of prepared single crystals of OCPT.

[1] Faculty of Physics.
[2] Faculty of Chemistry, Babeş-Bolyai University, 1, Kogălniceanu St., 3400 Cluj-Napoca, Romania.
[3] Institute of Molecular and Isotopic Technologies, 65-103, Donath St., RO-3400 Cluj-Napoca, Romania.

SYNTHESIS AND PURIFICATION OF THE STARTING RAW MATERIAL

The OCTP raw material used in this work was prepared using the Bodea and Silberg's method [2]. The OCPT obtained this way was then purified by multiple recrystallizations from dichlorbenzene (DCB). The saturated solutions of OCPT in boiling DCB were cooled down to room temperature. In final account it was obtained the OCPT raw material used in this study, consisting of small needles with sizes of 0.01 x 0.02 x 1-2 mm, clear green -yellow color. These small crystals were used to perform X-ray diffractometry and crystal growth.

THE GROWTH OF OCPT SINGLE CRYSTALS

Several techniques were used to grow large single crystals of OCPT, such as the crystallization from solutions of DCB and dimethylformamide (DMF), the classical vapour phase crystallization technique and Bridgman method. None of these methods led to good results, the obtained crystals being either small or impurified with octachlorophenotiazinyl radical, which has a dark-green colour [3]. The best results were obtained using a method consisting of a combination between the zone-melting and vapour-phase method. We called this technique *vapour-phase zone technique* (VPZT). Thus far we do not know any report about such a technique in the literature, which this way could be an original one. The method was inspired by the fact that at a temperature near the melting point, OCPT has a high vapour pressure.

The VPZT equipment consisted of a classical one-zone melting equipment, which had the hot zone of 1-2 cm long, and a temperature in the proximity of the reported [3] melting point. The hot zone was pulled along an ampula, containing the raw OCPT material, with a speed of 10-20 mm/hour. The results were very promising.

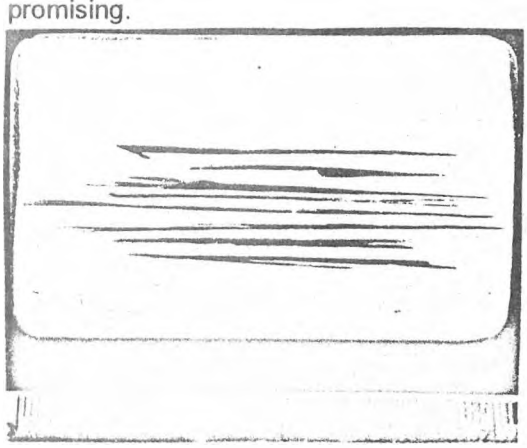

Fig. 1. OCPT single crystals grown with VPZM technique.

Fig. 2. Surface microstructure (350x) of a OCPT ribbon-like single crystal.

By refining this method we obtained very big clear-green single crystals of OCPT, some of which are presented in Fig. 1. They are of two kinds:

a) needle like crystals, with dimensions of 0.1-0.2 x 0.3-0.5 x 50-70 mm.

b) ribbon-like single crystals, with dimensions of 0.02-0.08 x 0.5-1.5 x 50-70 mm. The surface of these crystals showed, Fig. 2., regular steps of growth.

THE CRYSTAL STRUCTURE OF OCPT

To establish the crystalline structure of the OCPT it was first used the X-ray diffractometry method. For this purpose, was used the grounded OCPT raw material. A modified TUR-M62 X-ray equipment was used, able to measure diffraction peaks step by step, with steps of 0.05^0 on the 2θ scale. The results were stored in a computer and then used in combination with a PC-programm developed in CERN-Geneva. Neglecting some small peaks, this computational program found the crystal structure of OCPT as being rhombic. This result was not credible because in rhombic crystals the optical indicatrices have to be parallel to external growth faces. Our measurements showed that there is an angle of about 4^0 between the optical indicatrice and the growth faces. Therefore, we had to search further-on, using this time single crystal X-ray techniques as well.

We used first Kulpe's method (a variant of Laue's method for single crystals, with cylindrical camera), a *Cuk*α radiation, λ = 1.54178 Å. The oscillating axis was parallel to the single crystal preferential growing direction, *i.e.*, the lenght of needles. The obtained X-ray patterns allowed us to find the first unit-cell parameter, i.e. *b* = 3.71 Å, the preferential growth direction being this *b* axis. Because the spot-layers of the first order were symmetrically disposed relative to the spot layer of zero order, we could say that the unit cell had a plane of symmetry perpendicular on the *b* axis, which meant the structure is at least monoclinic.

The next step was to use Weissemberg's method. The translation of the single crystal was along the preferential growth direction, *i.e.* the *b* axis. For this experiment we used *Fek*α radiation with λ = 1.93728 Å. Using Weisemberg's patterns we determined other two parameters of the reciprocical lattice, c^* = 0.0594, and a^* = 0.0828, their directions forming angle β^* = 80^0. Therefore, the corresponding unit cell parameters in the direct space were:

$$a = \frac{1}{a^* \cdot \sin\beta^*} = 12.21\ \text{Å}\ ,\ c = \frac{1}{c^* \cdot \sin\beta^*} = 17.11\ \text{Å}\ ,\ \beta = 100^\circ$$

Kowing these parameters we could index the X-ray diffraction spectrum using the expression:

$$\frac{1}{d^2} = \frac{1}{\sin^2\beta}\left[\frac{h^2}{a^2} + \frac{k^2\sin^2\beta}{b^2} + \frac{l^2}{c^2} - \frac{2hl\cos\beta}{ac}\right] = \frac{4.\sin^2\beta}{\lambda^2}$$

In Fig. 3a, we present this indexed spectrum for a *ground* OCPT single crystal and in Fig. 3b, the same for the starting, *not ground,* raw material. One can see that reflections from planes 100, 200, 300, 400, 500 are much higher for the raw material than for grounded single crystal. This means that crystals grow preferentially along the *b* axis and have their larger face parallel to *c* axis.

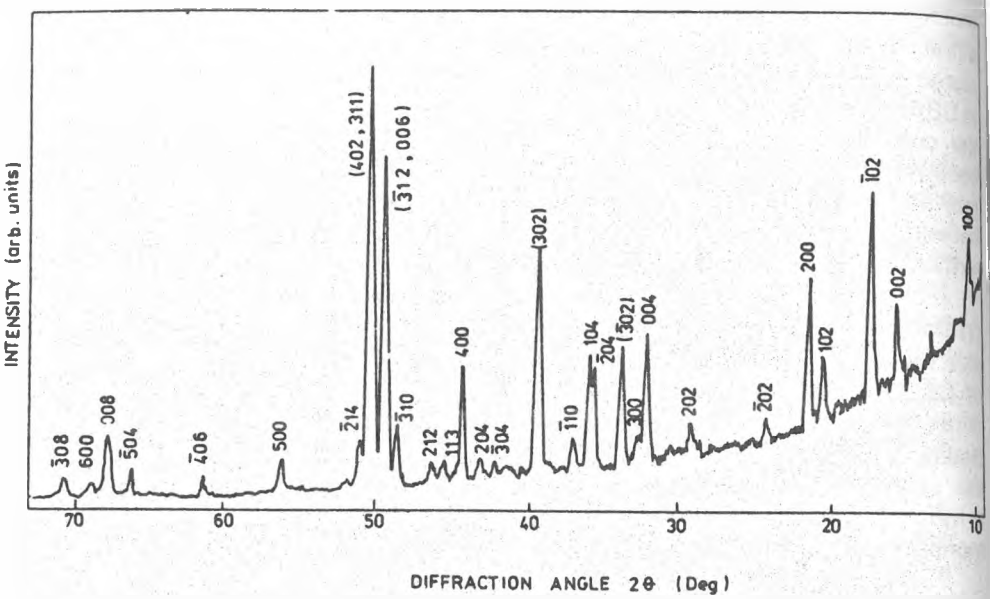

Fig. 3. a. Indexed X-ray diffractograms of OCPT, ground single-crystal.

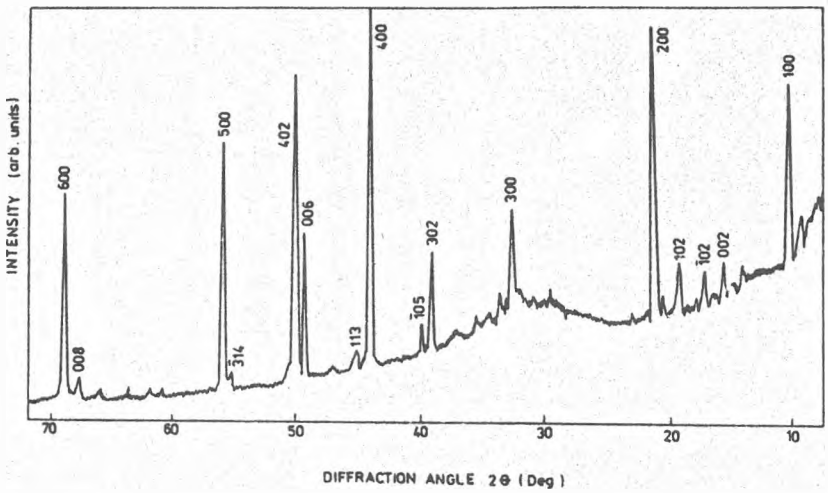

Fig. 3. b. Indexed X-ray diffractogram of OCPT, not ground raw material.

Using the found unit cell parameters and assuming there are two molecules per unit cell, we found the theoretical X-ray density of the OCPT as being.

$$\rho_{th} = \frac{NM}{V} = 2.06 g/cm^3$$

where N = 2, M = 478.8 g/mol is the molecular weight of OCPT and V is the unit cell volume. Comparing this result with the experimental density determined by Silberg, ρ_{exp} = 1.92g/cm^3, we found a relative error of only 6%. Taking into account that Silberg [3] used poweder OCPT, we could understand his results were lower than theoretical ones.

CONCLUSIONS

1. A crystal growth method was imagined, consisting of a combination between vapour-phase and zone melting methods. We called it "zonal vapour-phase method" (ZVPM).

2. Using ZVPM we succeded for the first time to grow large OCPT single crystals needles of 0.1-0.2 x 0.3-0.5 x 50-70 mm size or ribbon-like of 0.02-0.08 x 0.5-1.5 x 50-70 mm size. These crystals have grass-green or bright yellow color and present growth steps.

3. It was determined for the first time the crystalline structure of OCPT using three X-ray techniques, namely, diffractometry, Kulpe's and Weisemberg's. The OCPT lattice is found to be monoclinic, with the unit cell parameters:

$$a = 12.26 \text{ Å}, \quad b = 3.71 \text{ Å}, \quad c = 17.11 \text{ Å}, \quad \beta = 100^0.$$

4. From the X-ray analysis we could conclude that the preferential growth direction of OCPT is along to *b* axis and the crystals have a plate surface parallel to *c* axis.

5. Comparing the X-ray density and the picnometric-experimental density of OCPT it results that there are two molecules per unit cell.

ACKNOWLEDGEMENTS

We thank Mr. R. Bratfalean (at present at Clarendon College, Oxford, U.K.), Mr. I. Burda and Mr. M. Andrecut all from Babeș-Bolyai University of Cluj, Romania, for their help in the preliminary stages of this work.

REFERENCES

1. E. Rupprecht, Ph. D. Dissertation, Univ. Münich, 1955, cf. Houben-Weyl "Methoden der Organischer Chemie" (E. Müller - editor), Ed. IV, Vol. 5/3, 732.
2. C. Bodea and I. Silberg, Rev. Roum. Chimie, 1964, 9, 425.
3. I. Silberg, Ph. D. Dissertation, Inst. Chimie, Cluj, 1970.

STUDIA UNIVERSITATIS BABEŞ-BOLYAI, CHEMIA, XLII, 1-2, 1997

SEPARATION OF URANIUM(VI) BY EXTRACTION WITH DIETHYLDITHIOPHOSPHORIC ACID[1]

MARIA CURTUI[2]

ABSTRACT. The extraction of uranium(VI) from aqueous solutions with diethyldithiophosphoric acid in benzene and butanol was studied. The effect of various factors, such as the nature of solvent, neutral donor extractant, metal concentration and pH of the aqueous phase was investigated in order to find the optimum condition for separation of metal from nitrate aqueous solutions. The percent extraction (E%) is calculated and posibility of uranium(VI) separation is discussed.

INTRODUCTION

In our previous work we studied the extraction of uranium(VI) and thorium(IV) with dialkyldithiophosphoric acids from aqueous solutions [1-7]. The data obtained show that the dithioligands extract uranium(VI) through an ion exchange mechanism and the magnitude of the distribution ratios depends on different parameters of the extraction system. The knowledge accumulated during our investigations can be used to explore the posibility of uranium separation from aqueous solutions. It is obvious that the separation and purification of actinides, especially of uranium, is of particular interest in processing and reprocessing of nuclear fuel.

The aim of this paper is to investigate the extraction of uranium(VI) with diethyldithiophosphoric acid HEtdtp, and neutral extracting agents in order to find the right conditions for separation of the metal from nitrate aqueous solutions.

RESULTS AND DISCUSSIONS

The effect of diluting solvent, pH and neutral extracting agent as tributylphosphate (TBP) and triphenylphosphine oxide (TPPO) on the extraction of uranium(VI) with HEtdtp was investigated.

U(VI)-HETDTP SYSTEM

The extraction of uranium(VI) with HEtdtp in benzene and butanol from nitrate solution was studied at various pH values. The uranium(VI) concentration in the aqueous phase was 0.001M. The results presented in Table 1 show that the percent extraction, E% of U(VI) increase with increasing of pH. The highest value obtained is 15% in benzene and 68% in butanol. The higher values of percent extraction in butanol systems can be understood taking into account that in the extraction process $UO_2(Etdtp)_2$ species is involved [1]. In this case the anion $Etdtp^-$

---

[1] In honour of Professor Ionel Haiduc, the teacher who influenced so much the scientific careers of those who had the privilege to work with him and the outstanding scientist, at his 60-th anniversary.

[2] Facultatea de Chimie, Universitatea Babeş-Bolyai, Cluj-Napoca.

acts as a bidentate ligand and unsaturated coordination sites of uranium(VI) may be occupied by water molecules, making the complex species less soluble in the organic solvent. An oxygen containing polar solvent such as n-butanol may substitute water molecules increasing the extractability of the uranium complex in organic phase.

Table 1. Extraction of U(VI) with HEtdtp in benzen and butanol

C_{HEtdtp}=0.1M; C_U=0.001M

Benzene		n-Butanol	
pH	E%	pH	E%
0.7	4.76	0.5	16.50
1.0	9.09	1.0	34.90
1.2	11.90	1.4	47.50
1.4	13.00	1.8	59.00
1.7	12.95	2.3	65.00
2.0	10.71	2.9	68.00
2.2	9.09	3.4	67.00
3.0	9.02	3.8	61.00

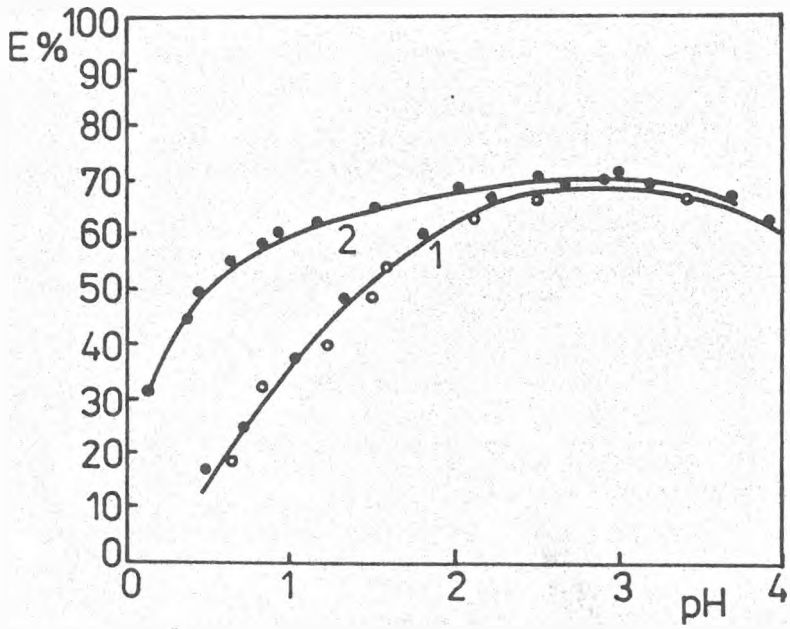

Fig. 1. Extraction of U(VI) with HEtdtp in butanol: C_U=0.001M(•); 0.005M(o)
curve 1 - without $NaNO_3$; curve 2 - in the presence of $NaNO_3$

The effect of uranium(VI) concentration in the extraction process has been investigated in the range of 10^{-4} - 5.10^{-2}M.

The results show that the extent of extraction is more or less constant suggesting that the extracting species do not change (Figure 1, curve 1).

Addition of sodium nitrate (1M) to the aqueous phase resulted in increased extraction of uranium at low pH values. Higher percentage extraction are obtained owing to the salting-out effect of nitrate (Fig. 1 curve 2).

The extraction of U(VI) was also investigated with solvent mixtures (benzene and butanol). The results, illustrated in Table 2 show that the addition of butanol in benzene increases the quantity of uranium(VI) in the organic phase. The highest extraction is achieved when 20-30% (volume) benzene is replaced by butanol (B).

The extraction of uranium with a mixture of 20% butanol and 80% benzene at different pH values of the aqueous phase was examinated. The concentration of HEtdtp in the organic phase was 0.1M. The results presented in Table 2 show that the percentage extraction is higher than 75% in the pH range 2-3.

It could be noticed that extraction systems with solvent mixtures show less emulsification tendencies.

Table 2. Extraction of U(VI) with mixtures of butanol and benzene

C_U=0.001M; C_{HEtdtp}=0.1M

pH=1.5		C_B=20% volume	
C_B(% volume)	E%	pH	E%
2	16.63	0.45	38.20
5	39.70	0.80	56.50
8	50.20	1.10	65.02
10	62.26	1.50	71.85
20	71.85	2.00	73.40
30	71.41	2.50	74.50
40	70.56	3.00	75.80
60	70.25	3.50	75.20

U(VI) - HETDTP - NEUTRAL ORGANOPHOSPHORUS LIGAND SYSTEM

The influence of tributylphosphate and triphenylphosphine oxide on the extraction of uranium(VI) with HEtdtp was investigated in benzene. The data illustrated in Table 3 afford some conclusions about the effect of these neutral ligands (S) on the separation of uranium from nitrate aqueous phase.

It can be seen that HEtdtp alone extracts only 5.5% of uranium(VI) initially present in aqueous phase (pH 0.7). Under the same conditions, TBP and TPPO respectively, alone in benzene extract very poorly uranium(VI) from nitrate solutions.

Table 3. Extraction of U(VI) with a mixture HEtdtp and neutral organophosphoric ligands

C_L=0.002M; pH=0.7

	HEtdtp+TPB=0.01M	HEtdtp+TPPO=0.03M
C_S (%)	E %	E %
—	5.5	0.26
10	56.76	54.85
20	75.00	77.50
30	83.89	86.90
40	85.48	87.80
50	83.89	86.10
60	80.05	83.92
70	77.2	80.40
80	64.28	61.30
90	42.85	0.30
100	0.90	0

When mixtures of 0.1M HEtdtp+TBP are used, a significant increase of the extraction is observed. Namely, a mixture containing 30-40% TBP affords a percentage extraction of about 85%. This represents a 90 times increase of the distribution ratio. It follows that TBP exhibits a significant synergic effect uppon the extraction of uranium(VI) with HEtdtp.

In the extraction system HEtdtp - TPPO, a percentage extraction of 87% is achieved when a mixture of 0.03M HEtdtp+TPPO containing 30-40% TPPO is used. This value represents a 2700 times increase of the distribution ratio. Therefore TPPO has a synergic effect even greater than TBP.

The dependence of uranium extraction on concentration of neutral organophosphorous ligands was also studied at constant pH of the aqueous phase (0.7) and constant HEtdtp concentration (0.1M). The data presented in Table 4 show that the percentage extraction of uranium(VI) increases with increasing the neutral ligand concentration.

The very strong synergic effects of neutral organophosphorous ligand are due to the formation of mixed compounds $UO_2(Etdtp)_2.S$ (S = TBP, TPPO), very soluble in organic phase [8]. The coordination of S through the oxygen atom is suported by infrared spectroscopic data, which indicated a shift of the P = O streching vibration towards lower wave numbers. The adduct with TPPO can be isolated in solid state [9].

The extraction of uranium(VI) with HEtdtp and neutral organophpsphorous ligands is pH dependent. The data are presented in Table 5. The concentration of HEtdtp and neutral ligand were maintained constant. It is noticed that using a mixture of 0.1M HEtdtp and 0.01M TBP in benzene, a percentage extraction higher than 90% can be obtained, in the pH range 2-3.

Table 4. Influence of neutral organophosphoric ligand concentration

C_{HEtdtp}=0.1M; C_U=0.002M; pH=0.7

TBP		TPPO	
C_{TBP}(M)	E %	C_{TPPO} (M)	E %
0.0001	7.32	0.0002	76.90
0.0005	20.00	0.0005	90.90
0.0010	28.46	0.0010	95.22
0.005	64.19	0.002	97.25
0.010	75.60	0.003	98.60
0.020	86.30	0.005	98.75
0.050	94.10	0.010	99.4
0.100	96.93	0.020	99.7

In extraction system containing TPPO, a percentage extraction of 90% is achieved under more advantageous conditions (lower concentrations of extractants and lower pH values).

Table 5. Influence of pH

C_U=0.002M

TBP		TPPO	
C_{HEtdtp}=0.1M; C_{TBP}=0.01M		C_{HEtdtp}=0.1M; C_{TBP}=0.01M	
pH	E %	pH	E %
0.50	70.50	0.55	68.15
0.92	81.40	0.70	81.68
1.20	84.90	1.00	93.39
1.50	89.50	1.20	95.80
2.00	91.00	1.50	97.05
2.80	90.50	2.10	97.40
3.00	90.90	3.00	97.50

EXPERIMENTAL

Reagents and equipment: The diethyldithiophosphoric acig was prepared by the reaction of phosphorus pentasulfide with ethanol [10]. Further purification is not necessary. Uranium salts, phosphorus pentasulfide, tributylphosphate and Arsenazo III were obtained from Aldrich and Ventron AG, Germany. Triphenyphosphine oxide was prepared by oxidation of triphenyphosphine with $KMnO_4$ [11] and recrystalised from acetone.

A Spekol C. Zeiss Jena (DDR) Spectrophtometer was used for the colorimetric determination of uranium(VI). The acidity of the aquoeus phase was determined with an Orion Model 611 pH-meter/milivoltmeter.

Preparation of the aqueous and organic phases. The aqueous phases were prepared from a solution of uranium nitrate 0.1M (standardized gravimetrically) by succesive dilutions. Various pH of the aqueous phase were attained by using HNO_3 and NaOH. In certain cases $NaNO_3$ was added to the aqueous phase.

From freshly synthesized diethyldithiophosphoric acid, 1M standard organic solution was prepared. From this solution organic phases of desired concentrations were obtained by succesive dilutions. To the solution of HEtdtp determined amounts of butanol, TBP and TPPO were added.

The determination of percentage extractions (E%) of uranium. Equal volumes (10 ml) of organic and aqueous phase were shaken together. Preliminary experiments have shown that 3 minutes were enough to attain the partition equilibrium. The phases were then allowed to separate. The uranium concentration in the aqueous phases, determined spectrophotometrically with Arsenazo III [12], was used for calculation of the percentage extractions (E%).

FINAL REMARKS

From the fore-cited data, some useful suggestions for the separation of uranium(VI) with diethyldithiophosphoric acid can be made

Diethyldithiophosphoric acid in benzene extracts poorly uranium from nitrate aqueous phase. When an oxygen containing solvent is used as diluting agent for HEtdtp the percentage extraction increases up to 68%, at pH 2. Higher values of percentage extraction are obtained in synergic reaction systems with mixtures of HEtdtp and oxygen containing neutral extractants such as n-butanol, TBP and TPPO. The increase of uranium extractability follows the order:

$$\text{n-butanol} < \text{TBP} < \text{TPPO}$$

From the obtained results, it is possible to select the optimal experimental conditions in order to achieve successful separations.

REFERENCES

1. G. Marcu, M. Curtui, I. Haiduc, *J. Inorg. Nucl. Chem.*, 1977, 39, 1415.
2. I. Haiduc, G. Marcu, M. Curtui, *Rev. Roumaine Chim.*, 1977, 22, 625.
3. M. Curtui, I. Haiduc, G. Marcu, *J. Radioanal. Chem.*, 1978, 44, 109.
4. G. Marcu, I. Haiduc, M. Curtui, *Studia Univ. Babeş-Bolyai, Chemia*, 1977, 22, 49.
5. M. Curtui, I. Haiduc, *J. Radioanal. Nucl. Chem., Letters*, 1992, 164, 91.
6. M. Curtui, I. Haiduc, *J. Radioanal. Nucl. Chem., Letters*, 1993, 176, 233.
7. M. Curtui, I. Haiduc, *J. Radioanal. Nucl. Chem., Letters*, 1994, 186, 273.
8. M. Curtui, I. Haiduc, *J. Inorg. Nucl. Chem.*, 1981, 43, 1078.
9. I. Haiduc, M. Curtui, *Synth. React. Inorg. Metalorg. Chem*, 6, 125, 1976.
10. K. Sasse, *Methoden der Organischen Chemie* (Huben-Weyl) Band XII, Teil 2, p. 684, G. Thieme Verlag, Stuttgart, 1964.
11. Ref. 7, p. 143.
12. S. B. Savin, *Talanta*, 1061, 8, 673.

STUDIA UNIVERSITATIS BABEȘ-BOLYAI, CHEMIA, XLII, 1-2, 1997

THEORETICAL STUDY OF THE DI- AND TETRAHALOGENO DERIVATIVES OF TETRAMETHYLDIARSINE OXIDE. A PM3 MOLECULAR ORBITAL CALCULATION OF THE HEATS OF FORMATION[1].

LUMINIȚA SILAGHI-DUMITRESCU[2], RADU SILAGHI-DUMITRESCU[2], IOAN SILAGHI-DUMITRESCU[2]

ABSTRACT. The heats of formation for $Me_2As(X_2)$ $OAsMe_2$, and $Me_2As(X_2)OAs(X_2)Me_2$ (where X = Cl, Br, I) and their relative stabilities were estimated using the semiempirical molecular orbitas PM3 method. Some of the possible decomposition pathways in anhydrous media and in the presence of water are discussed on the basis of the termodinamic data and molecular orbital patterns of there systems.

INTRODUCTION

The chemistry of organoarsenic R_2As-Y-AsR_2 derivatives containing two arsenic(III) atoms, where Y = O, S or NH and their transformation into arsenic(V) compounds is currently in our attention [1,2]. One of the possibilities to change the oxidation state of the arsenic(III) to arsenic(V) is the reaction with halogens. Excepting for a paper refering the reaction of tetraphenyldiarsineoxide with chlorine [3] there are no data in the literature on the oxidation of a diarsenic compound of the type R_2As-Y-AsR_2 where Y is a chalcogene atom with halogens. The oxidation of R_2As-Y-AsR_2 (Y = O,S) with oxygen containing reagents (t-BuOOH) or with sulfur does not always proceed with the preservation of the As-Y-As bridge [1]. In view of the lack of data on the basic chemistry of such compounds, we found worthwhile to investigate the relative stability and the properties of di- and tetrahalogeno derivatives of tetraalkyldiarsine oxides.

There are few reports in the literature concerning theoretical approaches on the polyatomic arsenic compounds. This is due mainly to two reasons: rigurous *ab initio* molecular orbital calculations are still time consuming and quite expensiv [4] (only some simple arsenic hydride derivatives have been investigated so far [5]) and the semiempirical methods on the other hand (more rapid and less expensive) could not be used because the arsenic atom has not been parametrized until recently.

---

[1] Dedicated to Professor Ionel Haiduc, Member of the Roumanian Academy, the outstanding scientist and inspiring teacher on the occasion of his 60-th anniversary.

[2] Facultatea de Chimie și Inginerie Chimică, Universitatea "Babeș-Bolyai" Cluj-Napoca, RO-3400 Cluj-Napoca, Roumania.

Both the MNDO (Modified Neglect of Diatomic Differential Overlap) and PM3 (Parametric Method 3) methods including arsenic [6,7] made possible molecular orbital calculations for larger organoarsenic compounds like those which we are interested in. In this paper we report the results of geometry optimizations and the heat of formation of R_2As-Y-AsR_2, R_2X_2As-Y-AsR_2 and R_2X_2As-Y-AsX_2R_2 (Y = O, X = Cl, Br, I, R = Me) systems calculated by the PM3 method [8].

RESULTS AND DISCUSSION

Depending on the molar ratio of the reactants, two types of compounds are expected to be formed during the oxidation of tetramethyldiarsineoxide with halogens: the 1:1 Me_2As-O-$AsMe_2$:X2 molar ratio might lead to As(III)/As(V) dihalides, $Me_2As(X_2)$-O-$AsMe_2$, white using an 1:2 Me_2As-O-$AsMe_2$:X2 ratio the As(V)/As(V) tetrahalides, $Me_2As(X_2)$-O-$As(X_2)Me_2$ should be formed as primary products (eq 1-2).

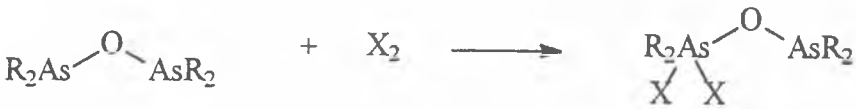

(1)

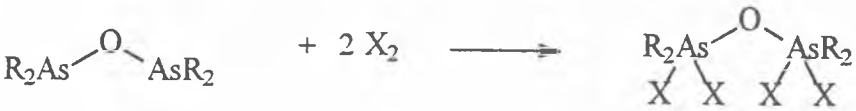

(2)

Table 1 lists the heats of formation of $(Me_2AsX_n)O(AsMe_2X_m)$ (n = 0, m = 2; n = 2, m = 2, X = Cl, Br, I) and the variation of enthalpy in reactions 1 and 2. These data show that there is a monothonous increase in the reaction enthaply as changing the halogene from chlorine to iodine.

The addition of two or four chlorine or bromine atoms is exothermal whereas that of iodine is slightly endothermal. A similar trend has been noticed for the reaction enthalpies of oxidation of cacodyl oxyde with oxygen and sulfur [9] and reflect the decreasing of the As-X bond energies on increasing the volume of X atom. Note also that the thermal effect on the addition of iodine is grossly equal to that calculated on the reaction of $Me_2AsOAsMe_2$ with sulfur [9].

As we mentioned above the As-O-As bridge is not always preserved during the oxidation of tetraorganodiarsineoxides [1-3]. Thus, the oxidation of Ph_2As-O-$AsPh_2$ with $SOCl_2$ leads to the break of the oxigen bridge and $Ph_2As(OH)_2Cl$ is formed [3]. Similarly, when Ph_2As-O-AsPh2 was reacted with iodine, Ph2AsI and diphenylarsenic acid, Ph2As(O)OH were obtained after the recrystallization of the reaction product from dichloromethane [10,11].

Table 1. The heat of formation of $(Me_2As)_2O$ and the corresponding di- and tetrahalides (kcal/mol)

	Compound	Heat of formation	ΔH for reactions 1 or 2
I	$Me_2AsOAsMe_2$	-64.53	-
IIa	$Me_2Cl_2AsOAsMe_2$	-98.46	-32.35
IIb	$Me_2Br_2AsOAsMe_2$	-77.46	-17.85
IIc	$Me_2I_2AsOAsMe_2$	-35.59	8.20
IIIa	$Me_2Cl_2AsOAsMe_2Cl_2$	-133.82	-46.13
IIIb	$Me_2Br_2AsOAsMe_2Br_2$	-88.09	-33.40
IIIc	$Me_2I_2AsOAsMe_2I_2$	-5.62	17.43

Several decomposition pathways of the oxidized species will be commented in the following. In anhydrous media the As-O-As bridge might be broken with the for-mation of dihalogenoarsine and arsineoxide (3) or trihalogenoarsorane and monohalogenoarsenoxide (4):

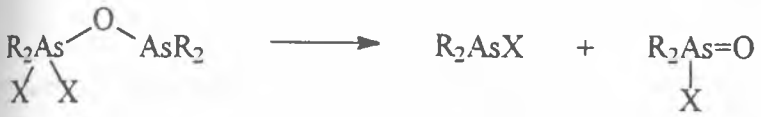

(3)

(4)

Table 2. The entalpy of reaction for the decomposition of di- and tetrahalo- diarsinearsineoxide (kcal/mol)

Compound	$\Delta H_{reaction}(3)$	Compound	$\Delta H_{reaction}(4)$
IIa	3.41	**IIIa**	13.14
IIb	12.97	**IIIb**	22.86
IIc	10.87	**IIIc**	16.45

The corresponding enthalpies of reactions listed in Table 2 suggest that the bromo derivatives ***(IIb, IIIb)*** are somewhat more stable toward the decomposition (3,4) than the chloro ***(IIa, IIIa)*** or iodo ***(IIc, IIIc)*** derivatives.

The addition of water to $R_2As(O)X$ lead to the formation of the very stable dihydroxy species (5):

$$R_2AsOX + H_2O \longrightarrow R_2As(OH)_2X \qquad (5)$$

as shown by the large changes in the enthalpies of these reactions: -26.24 kcal/mol (X = Cl); -32.74 kcal/mol (X = Br); and -37.66 kcal/mol (X = I).

Thus, traces of water add two other ways of decomposition (6,7) of ***II*** and ***III***:

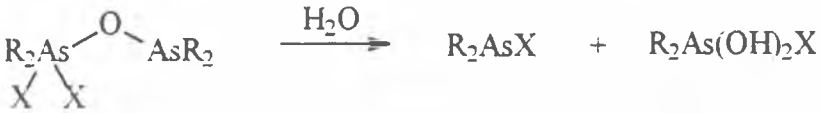

(6)

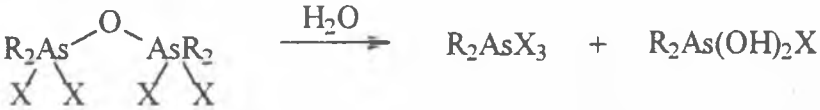

(7)

The ΔH values of Table 3 show again that both ***IIb*** and ***IIIb*** are solmewhat less prone to hydrolysis than ***(IIa,c)*** or ***(IIIa,c)***:

Table 3. The change of the enthalpy during the hydrolysis of ***IIa-b*** and ***IIIa-b***

Compound	$\Delta H_{reaction}(6)$	Compound	$\Delta H_{reaction}(7)$
IIa	-27.14	IIIa	-13.10
IIb	-23.45	IIIb	-9.88
IIc	-29.44	IIIc	-21.21

However, solvatation of HX makes these reactions more exothermal than appear in Table 3.

Based on experimental data mentioned above [10,11] the formation of the corresponding diorganoarsinic acid instead of the hydrated form of the halides (5) was also considered (8):

$$R_2AsOX + H_2O \longrightarrow R_2As(O)OH + HX \qquad (8)$$

The reaction entlapies for the global processes (9,10) are presented in Table 4.

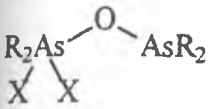

$$\xrightarrow{H_2O} R_2AsX + R_2As(O)OH + HX \qquad (9)$$

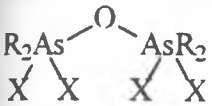

$$\xrightarrow{H_2O} R_2AsX_3 + R_2As(O)OH + HX \qquad (10)$$

These data show that the dichloride and tetrachoride might follow also route 9 and 10 but the bromo- and iodo- diarsineoxides are more resistive towards the elimination of hydracides through this pathway.

Table 4. The change of the enthalpy during the global reactions (9) and (10)

Compound	$\Delta H_{reaction}(9)$	Compound	$\Delta H_{reaction}(10)$
IIa	3.06	IIIa	12.79
IIb	23.03	IIIb	33.17
IIc	24.29	IIIc	59.11

The kinetic lability of the compounds investigated can be estimated on the basis of the HOMO-LUMO gap. The calculated values of HOMO and LUMO energies are listed in Table 5.

Table 5. The energy of the HOMO and LUMO orbitals

COMPOUND	LUMO	HOMO	HOMO-LUMO gap
$Me_2AsOAsMe_2$	-8.90	-0.08	8.81
$Me_2Cl_2AsOAsMe_2$	-9.46	-2.20	7.26
$Me_2Br_2AsOAsMe_2$	-9.58	-2.50	7.08
$Me_2I_2AsOAsMe_2$	-8.47	-3.69	4.78
$Me_2Cl_2AsOAsMe_2Cl_2$	-10.65	-2.79	7.86
$Me_2Br_2AsOAsMe_2Br_2$	-10.29	-3.49	6.80
$Me_2I_2AsOAsMe_2I_2$	-8.77	-4.35	4.42

The HOMO-LUMO gaps in the organoarsenic halides are, in all cases., smaller than in Me2As(O)-O-AsMe2 and Me2As(O)-O-As(O)Me2. The smalles gap was found for iodine derivatives, indicating the lowest kinetic stability for these representatives.

The charges on the atoms and the shape of the HOMO and LUMO orbitals offer additional information on the possible mechanism for the decomposition of these compounds. The relevant charges together with hologen-arsenic distances are summarised in Table 6.

In the As(III)/As(V) halogenides the HOMO is localized on the As(III) with a small contribution from the oxigen (*a*) and the LUMO has the shape sketched in (***b***) (it has mainly As-X antibonding character). In the totally oxidised species, the corresponding orbitals are shown in (*c*) (HOMO, weakly O...X bonding) and (***d***) (LUMO, As-X antibonding and As-O bonding)).

Significantly, the distance between one of the halogen atoms and the As(III) atom was found to be comparable with the sum of their van der Waals radii.

Table 6. Atomic charges on arsenic, oxygen and halogen and the halogen-arsenic distances (A)

COMPOUND	Charge on As*	Charge on O	Charge on halogen	X-As(V) Distance	X...As(III) Distance**
$Me_2AsOAsMe_2$	0.581* 0.581*	-0.640	—	—	
$Me_2Cl_2AsOAsMe_2$	1.745 0.711*	-0.860	-0.636 (ax) -0.396(eq)	2.25(ax) 2.18(eq)	3.83
$Me_2Br_2AsOAsMe_2$	1.720 0.722*	-0.818	-0.663(ax) -0.465(eq)	2.41(ax) 2.34(eq)	3.84
$Me_2I_2AsOAsMe_2$	1.436 0.730*	-0.787	0.593(ax) 0.411(eq)	2.76(ax) 2.58(eq)	4.24
$Me_2Cl_2AsOAsMe_2Cl_2$	1.795 1.794	-1.046	-0.605(ax) -0.605(ax) -0.364 (eq) -0.365(eq)	2.24(ax) 2.16(eq)	4.04
$Me_2Br_2AsOAsMe_2Br_2$	1.745 1.711	-0.990	-0.632 (ax) -0.632(ax) -0.424(eq) -0.424(eq)	2.38(ax) 2.33(eq)	4.00
$Me_2I_2AsOAsMe_2I_2$	1.468 1.468	-0.902	-0.580 (ax) -0.580(eq) -0.346(ax) -0.346(eq)	2.75(ax) 2.59(eq)	4.12

*Charge on As(III); ax(eq) refer the axial(equatorial) positions in the trigonal-bypiramidal coordination at of the oxidized arsenic

** The sum of the van der Waals radii of As and X(Cl, Br,I) is: 3.80, 3.95 and 4.15 Å respectively

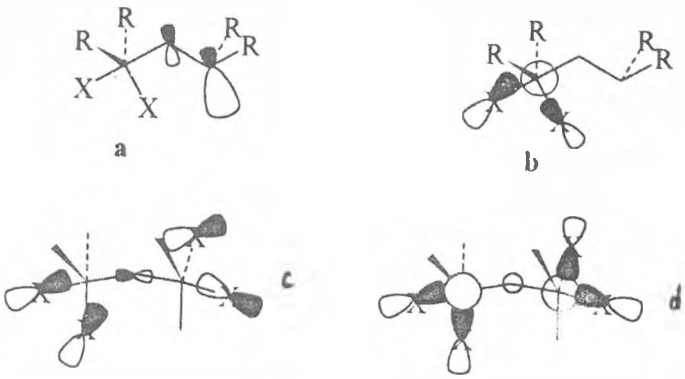

terms of intramolecular HOMO-LUMO interactions, the decomposition of II.a-c in anhydrous media could take the following way:

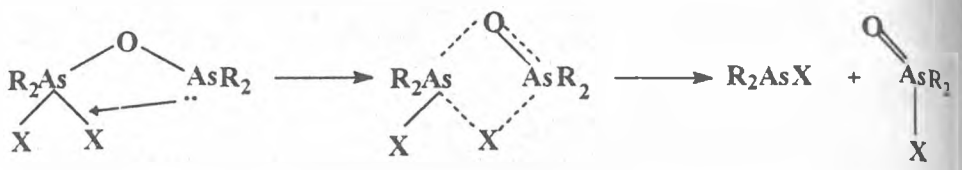

When water is present in the reaction mixture, a nucleophilic attack at the arsenic(V) is also possible, (large contribution to HOMO from the arsenic- ***b)*** with the formation of an unstable arsorane with subseqvent elimination of dioraganoarsenic halide and formation of diorganodihydroxihaloarsorane:

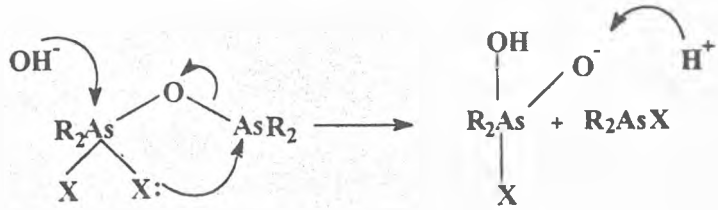

In view of the composition of ***c*** and ***d*** similar interactions might cause the decomposition of the As(V)/As(V) tetrahalogenides.

The large increase of the positive charges on the arsenic(V) atoms (from 0.58 to 1.44-1.80) (see Table 6) indicate also some charge control of these reactions.

CALCULATION DETAILS

The models of the investigated compounds were constructed by using the molecular mechanics facility of Spartan 4.0 (Sybil force field) [8]. The conformers generated by systematic search (rotations around the two As-X bonds were subjected to complete geometry optimisations by using the PM3 module of the same package). All PM3 optimisations were done with the following exit conditions: gradient norm less than 1.0×10^{-5}, difference of the energy less 1.0×10^{-4}.

ACKNOWLEGEMENTS

We thank dr. Francisco Lara-Ochoa from Instituto de Quimica, Universidad Nacional Autonoma de Mexico for the computer facilities made available.

REFERENCES

1. L. Silaghi-Dumitrescu, M. N. Gibbons, I. Silaghi-Dumitrescu, J. Zukerman-Schpector, I. Haiduc and D. B. Sowerby, *J. Organomet. Chem.*, 1996, 517, 101.

2. L. Silaghi-Dumitrescu, S. Pascu, I. Silaghi-Dumitrescu, I. Haiduc, M. N. Gibbons D. B. Sowerby, *J.Organometal. Chem.*, 1997, 549, 187.
3. G. J. Burrows, E. P. Santford and A. Lenca, *J. Proc. Roy. Soc. N. S. Wales*, 1937, 70, 300; C.A. 31, 4965 (1938).
4. W. J. Hehre, "Practical Strategies for Electronic Structure Calculations" Wavefunction, Inc. (Irvine, California, USA, 1995).
5. J. Moc and K. Morokuma, *J. Am. Chem. Soc.* 1995, 117, 11790. G. R. Willey, M. D. Rudd, C. J. Samuel and M. G. B. Drew, *J. Chem. Soc., Dalton Trans.*, 1995, 759.
6. S. K. Ignatov, A. G. Razuvaev, *Zh. Strukt. Khim.*, 1994, 35(2), 141.
7. J. J. P. Stewart, *J. Comput. Chem.*, 1991, 12, 320.
8. Spartan 4.0, Wavefunction Inc., 18401 Von Karman Ave., #370, Irvine CA 92715 U.S.A. ©1995 Wavefunction, Inc.
9. L. Silaghi-Dumitrescu, S. Pascu, I. Silaghi-Dumitrescu and I. Haiduc, Rev. Roumaine Chim., 1997, 42, 747.
10. M. J. Begley, D. B. Sowerby and L. Silaghi-Dumitrescu, *Acta Crystallogr.*, 1995, C51, 1623.
11. L. Silaghi-Dumitrescu, I. Haiduc, M. G. Gibbons and D. B. Sowerby, *Studia Univ. "Babeș-Bolyai", Ser. Chem.*, 1996, 41, 43.

STUDIA UNIVERSITATIS BABEȘ-BOLYAI, CHEMIA, XLII, 1-2, 1997

CATION RADICAL SALTS OF 1,4-BENZOTHIAZINO-[2,3-b]-PHENOTHIAZINE[1]

CASTELIA CRISTEA, IOAN A. SILBERG[2]

ABSTRACT. The paper presents the synthesis and spectral properties of the cation radical salts of the new electrono-donor phenothiazine derivative 1,4-benzothiazino-[2,3-b]-phenothiazine, **3**, and of its dibenzoderivative: 16H, 19H-dibenzo-[c,l]-7,9-dithia-16, 18-diazapentacene **4**.

INTRODUCTION

Phenothiazine has been known to form a number of cation radical salts since 1913 (Pummerer and Gassner [1]) long before the concept of cation radical salt had been established. These salts are now considered also as charge-transfer complexes. The phenothiazine component acts as a donor and the electronegative part acts as electron acceptor, but when phenothiazine is oxidized, the phenazathionium cation formed acts as an electron acceptor with respect to the halide ion. This implies a fundamental change in geometry, from a folded conformation, which allows the conjugation of the lone pair of nitrogen and sulfur with the π system of the ring, to a planar one, which presents such conjugation. The structures **1** and **2** presented in the Scheme 1 contribute considerably to the real state of the molecule.

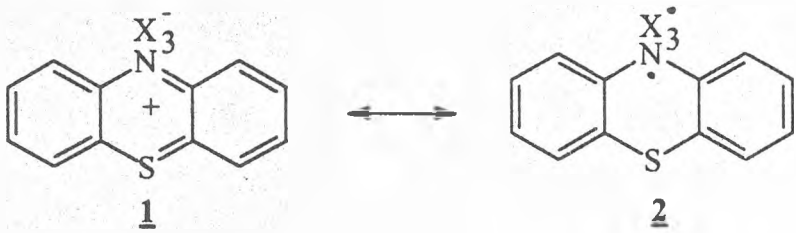

Scheme 1

[1] The paper is dedicated to Prof. Dr. IONEL HAIDUC, member of the Romanian Academy, "Babeș-Bolyai" University, Faculty of Chemistry and Chemical Engineering, for his 60th anniversary.

[2] Facultatea de Chimie și Inginerie Chimică, Universitatea "Babeș-Bolyai", str. Arany Janos nr. 11, RO-3400 Cluj-Napoca Romania.

RESULTS AND DISCUSSION

1,4-Benzothiazino-[2,3-b]-phenothiazine **3** is a strong electron donating molecule [2]. The chemical method of generating the phenothiazine cation radical by solving phenothiazine in concentrated sulfuric acid [3, 4, 5] leads to a solution which exhibits a golden yellow colour. The same method applied to **3** generates a green solution with the UV-VIS absorption maxima at: 293, 330, 410, 430 and 725 nm (fig. 1a). The same pattern with a bathochromic shift of about 20 nm has been obtained for the concentrated sulphuric acid solutions of 16H, 18H-dibenzo-[c,l]-7,9-dithia-16,18-diazapentacene **4** (fig. 1b).

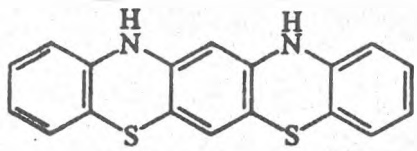

3

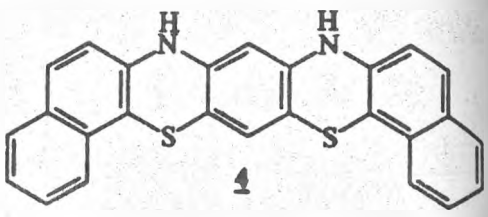

4

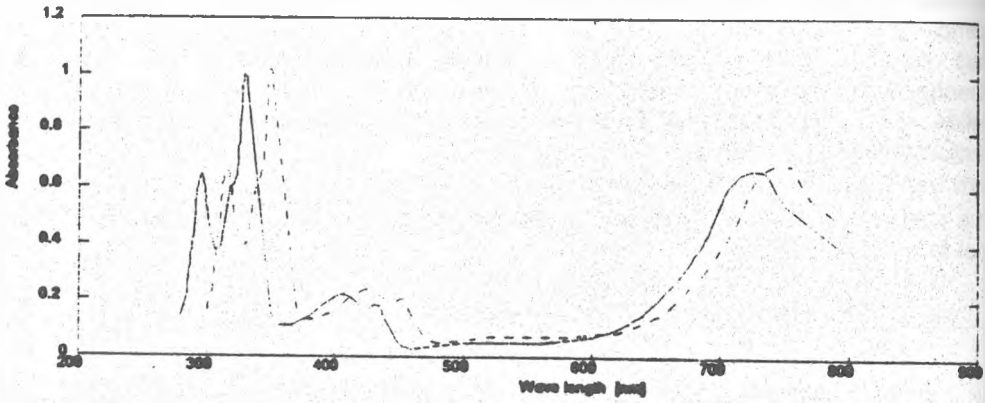

Fig. 1. UV-VIS absorption spectra for the 96% H_2SO_4 solutions of:
a. [-]1,4-Benzothiazino-[2,3-b]-phenothiazine, **3**
b. [...]16H, 18H-dibenzo-[c,l]-7,9-dithia-16,18-diazapentacene **4**

We attributed to the protonated cation radical of **3** the absorption maxima at 430 and 725 nm and the mesometric structures **3a** and **3b** from Scheme 2.

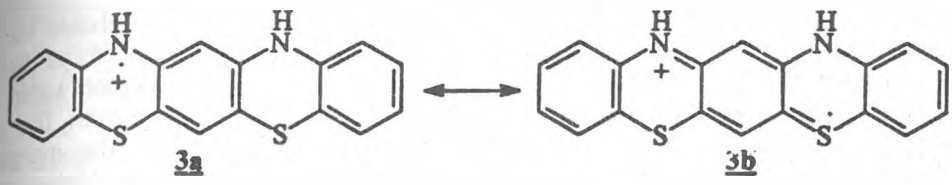

Scheme 2

The radicalic character of sulphuric acid solutions components has been proved by recording their ESR spectra which show a very broad band; the resolution was not good enough to allow the assignement of hyperfine splittings.

The cation radical salts of 1,4-benzothiazino-[2,3-b]-phenothiazine **3** and of its dibenzoderivative: 16H, 18H-dibenzo-[c,l]-7,9-dithia-16,18-diazapentacene, **4** with iodine solved in dimethysulfoxide (DMSO) showed absorption bands with maxima at 630 and 625 nm respectively (fig.2) attributed to the neutral radicals with the mesomeric structures **5a** and **5b** presented in the Scheme 3.

Scheme 3

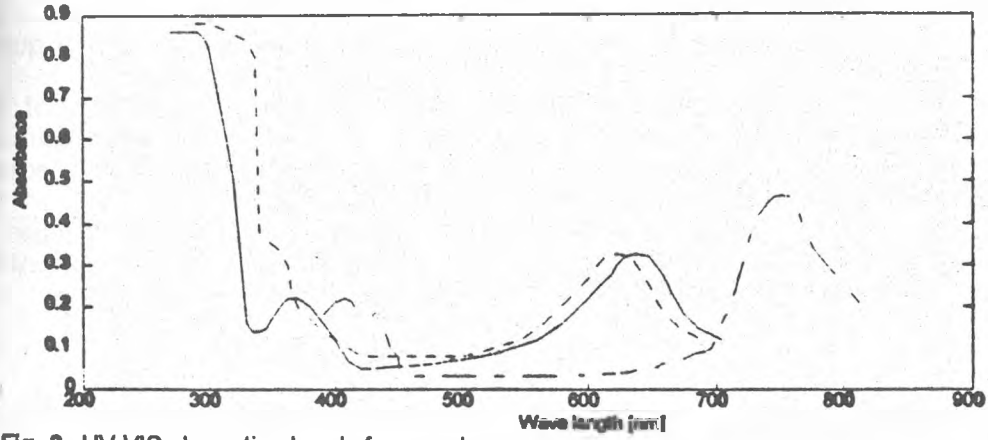

Fig. 2. UV-VIS absorption bands for complexes:

a. [-]1,4-benzothiazino-[2,3-b]-phenothiazine **3**: iodine, in DMSO

b. [...]16H, 18H-dibenzo-[c,l]-7,9-dithia-16,18-diazapentacene, **4**: iodine, in DMSO

c. [- -]1,4-benzothiazino-[2,3-b]-phenothiazine **3**: TCNE, in DMF

As iodine, most probably in the form of perhalide ions, I_3^-, should be the counterpart in this complexes, we assume that mesometric structures like 2 (Scheme 1) are a very good approximation of the electronic distribution within the organic moiety of the compound. This is in good agreement with the low electronegativity and high polarizability of iodine; consequently, the inorganic counterpart is best represented as $I_3^{\bullet}$ [6]. In view of the well-established importance of phenothiazine-iodine complexes [7] as cathodes for dry batteries, we find it of interest to further investigate these iodine charge transfer complexes.

The charge transfer complex of **3** with tetracianoethylene (TCNE) solved in dimethylformamide gave an absorption pattern shown in fig. 2c, with an absorption band situated at 750 nm, corresponding to the same species as the one in the sulfuric acid solutions: the protonated cation radical (with the mesometric structures **3a** and **3b** from Scheme 2). The strong electronoacceptor TCNE molecule determined the total one electron transfer from the molecule of **3**, so that mesomeric structures **3a** and **3b** contribute the most to the real state of the 1,4-benzothiazino-[2,3-b]-phenothiazine: TCNE CT complex. The bathochromic shift of the absorption maxima of the cation radical represented by the mesomeric structures **3a**, **3b** denotes a π conjugated sistem more extended than in the neutral radical case represented by the mesomeric structures **5a**, **5b**. These facts can be explained by the overwhelming importance of the delocalisation of the unpaired electron from nitrogen to sulfur (structure **3b**), and the importance of the localisation of the unpaired electron to nitrogen in the iodine complexes (structure **5a**). This explanation is also supported by the bathochromic shift observed in the series of phenothiazine itself: for the neutral phenothiazinyl radical an absorption band situated at 380 nm, anf for the protonated cation radical an absorption band situated at 516 nm [4].

EXPERIMENTAL

General: All commercial solvents were for spectral determinations quality grade. EPR spectrometer: IFA Bucharest. UV-VIS spectrometer Specord.

1. Iodine complexes general workup: a saturated solution of the heterocycle in benzene is mixed with a concentrated solution of iodine in benzene; the complex salt precipitated upon mixing is filtered. The dark precipitate is soluble in polar solvents. UV-VIS spectra were recorded (fig. 2).

2. CT complexes with TCNE general workup: a 5m M solution of heterocycle in CS_2 is carefully layered with a 5m M solution of TCNE in acetonitrile. The black powder obtained is filtered. UV-VIS spectra were recorded (fig. 2).

REFERENCES

1. R. Pummerer, S. Gassner, *Ber. deut.chem. Ges.*, 1913, 46, 2310
2. I. A. Silberg, C. Cristea, *Heterocyclic Communications*, 1996, 2, 117

3. H. J. Shine, E. E. Mach, *J. Org. Chem.*, 1965, 30, 2130.
4. P. Hanson, R. O. C. Norman, *J. Chem. Soc., Perkin Trans. II*, 1973, 264.
5. I. A. Silberg, M. Bossany, C. Molnariu, *Rev. Roum. Chim.*, 1993, 38, 10, 1215.
6. I. A. Silberg, in *Methodicum Chimicum*, 1976, vol. 7, 264, Georg Thieme Verlag, Stuttgart and Academic Press, New York.
7. M. Pampallona, A. Ricci, B. Scrosati, B. Vincent, *J. Appl. Electrochem.*, 1976, 6(3), 269, CA 1978, 85, 180.048h.

STUDIA UNIVERSITATIS BABEŞ-BOLYAI, CHEMIA, XLII, 1-2, 1997

BINDING STUDY OF 1-ANILINO-8-NAPHTALEN SULFONATE TO HUMAN SERUM ALBUMIN USING FLUORIMETRIC METHOD

MARIA DRONCA[1], COSMIN SĂVEANU[1], GHEORGHE JEBELEANU[1]

ABSTRACT. Double reciprocal plots of fluorescence intensity versus protein concentration are often used to obtain the intrinsic molar fluorescence (φ) of ligands bound to acceptor molecules such as albumin. These plots develop an upward concave curvature as the concentration of albumin increases. Thus linear extrapolation of such plots cannot be employed to provide accurate values of φ. In this paper we used an equivalent of Hanes transformation: a direct plot of the ratio of protein concentration / fluorescence intensity versus protein concentration which has the advantage that is the slope, not the extrapolated intercept, that estimate φ.

The 1-anilino-8-naphtalene sulfonate (ANS) binding to human serum albumin (HSA) revealed one tight and specific binding site (K_{d1} = 3 μM) and many other weak, nonspecific sites (N_2/K_{d2}=0.0043 μM^{-1}).

INTRODUCTION

Fluorescence spectroscopy is one of the most versatile and sensitive of the optical technique for studding the interaction between ligands and macromolecules [1]. Molecules whose fluorescence characteristics are dependent on the environment have been widely used as probes. Changes in the fluorescence characteristics associated with probe binding to macromolecules are similar to changes observed when these molecules are transferred from a polar to a nonpolar environment [2,3].

The fluorescent dye 1-anilino-8-naphtalene sulfonate (ANS) has been used commonly as probe in the investigation of the proteins' structure or the nonfluorescent substances binding [4,5]. The binding of this probe to hydrophobic regions of protein (i.e. HSA) is typically accompanied with the enhancing of fluorescent yield and the blue-shifted of the emission maximum [6].

In order to describe the ligand-protein interactions in a quantitative manner it is usually necessary to measure the intrinsic molar fluorescence of bound ligand (φ). To estimate φ it is common practice [7] to vary the concentration of protein (or acceptor molecule) at a fixed ligand concentration and then to extrapolate a double-reciprocal plot to infinite protein concentration. It is than assumed that all the ligand is bond so that the resultant fluorescence divided by the concentration of

[1] University of Medicine and Pharmacy, Department of Biochemistry, 6 Pasteur st., R-3400 Cluj-Napoca, Romania.

probe gives φ. Theoretical analysis of the relationship between fluorescence intensity and protein concentration has led Zierler [8] to suggest that double-reciprocal plots of fluorescence vs. protein concentration become nonlinear as the concentration of protein increases. Such plots develop an upward concave curvature as protein concentration increases and so, the desired value of φ cannot be obtained by simple linear extrapolation. Panjehshahin *et al.* [9] have proposed another method for φ estimation. They used a direct plot of fluorescence intensity (F) vs. log protein concentration (log [P]); as log [P] increases F approaches a plateau value (F_∞) which divided by the concentration of probe gives φ. This method is more valuable but needs many determinations for approaching the plateau value.

The purpose of the present communication was to obtain ANS-HSA binding parameters using φ estimated by plotting the ratio protein concentration/fluorescence intensity (F/[HSA]) versus protein concentration ([HSA]), an equivalent of Hanes transformation [10].

EXPERIMENTAL PROCEDURES

Chemicals

Essentially fatty acid free human serum albumin (HSA, Fraction V, < 0,1 mole fatty acid per mole of protein) was obtained from Sigma Chemical Co. The magnesium salt of 1-anolino-8-naphtalene sulfonate (ANS) was purchased from Serva Feinbiochemica Heidelberg.

The molar concentrations of HSA and ANS were calculated using absorption coefficient of 5.5 M^{-1} cm^{-1} at 280nm [11] and 4950 M^{-1} at 530nm [12] respectively. Molar mass of HSA 68.5 kDa was considered. All measurements were made in phosphate buffer 0.1M, pH 6.8.

Spectrophotometric measurements were performed on a Ultrospec III Pharmacia LKB spectrophotometer.

Fluorescence measurements were performed on a Eppendorf 1101 M photofluorimeter equipped with a termostated cell holder, using 0.5 cm path length fluorimetric cells. After temperature equilibration at 22^{0}C, fluorescence was measured at excitation/emission wavelengths 366nm and 470-3000nm respectively. All fluorescence measurements were done in triplicate and the mean values were corrected for inner effects using the approximate equation [13]:

$$F = F_{obs} * 2.303 * A / 1-T \qquad (1)$$

where F and F_{obs} are the corrected value and the actual reading (in relative units) of fluorescence respectively; A is the absorbance of the solution at excitation wavelength and T is the corresponding transmittance. Probes with absorbance up to 1.2 were considered. The absorbances at emission wavelength never exceeded 0.01 absorbance units and were neglected.

To obtain intrinsic molar fluorescence of bound ANS (φ), a solution of ANS (4.78μM) was titrated with a large molar excess of HSA (30-100μM). estimates of φ were obtained from plot of the ratio [HSA]/F vs. [HSA], using the following relation [10]:

$$[HSA]/F = K_d/N*F_\infty + [HSA]/F_\infty = K_d/N*[ANS]*9 + [HSA]/[ANS]*\varphi \quad (2)$$

where [HSA] and [ANS] were the micromolar concentrations of the albumin and ANS, respectively; K_d and N were the dissociation constant and the number of equivalent binding sites per mole of protein; F is the corrected fluorescence and F_∞ is the maximum fluorescence corresponding to infinite [HSA]. The value of φ was then used to calculate the concentrations of bound ($[ANS_b]$) and free ($[ANS_f]$), using the following relations:

$$[ANS_b] = F/\varphi; \quad [ANS_f] = [ANS_t] - [ANS_b] \quad (3)$$

where $[ANS_t]$ was the total concentration of ANS.

To study the binding of probe to a fixed concentration of albumin, we used a reverse titration of HSA with ANS. The concentration of HSA was kept constant (4.25μM) and the concentration of ANS was in the range 2.3 to 600μM. Results were plotted according to Scatchard [14], using the relation:

$$r / [ANS_f] = -r / K_d + N / K_d \quad (4)$$

where $r = [ANS_b] / [HSA]$.

The binding parameters of ANS were obtained by unweighted nonlinear least square regression analysis (computer fitting) using the following expression:

$$r = N_1 * [ANS_f] / (K_{d1} + [ANS_f] + N_2 * [ANS_f] / K_{d2} \quad (5)$$

which was obtained from equation proposed by Mendel *et al.* [15] when $K_{d2} >> [ANS_f]$:

$$r = N_1 * [ANS_f] / (K_{d1} + [ANS_f] + N_2 * [ANS_f] / (K_{d2} + [ANS_f]) \quad (6)$$

where N_1 and N_2 are the number of two classes of binding sites; K_{d1} and K_{d2} are the dissociation constants of the ligand for each classes of sites.

RESULTS AND DISCUSSIONS

Graph of ratio [HSA] / F vs. [HSA] is shown in Fig. 1. From the slope of this linear plot we obtained φ indicated in the legend of figure. The curvilinear shape of the Scatchard plot illustrated in Fig. 2 shows that ANS binds to two independent classes of sites: one for specific and another for nonspecific binding.

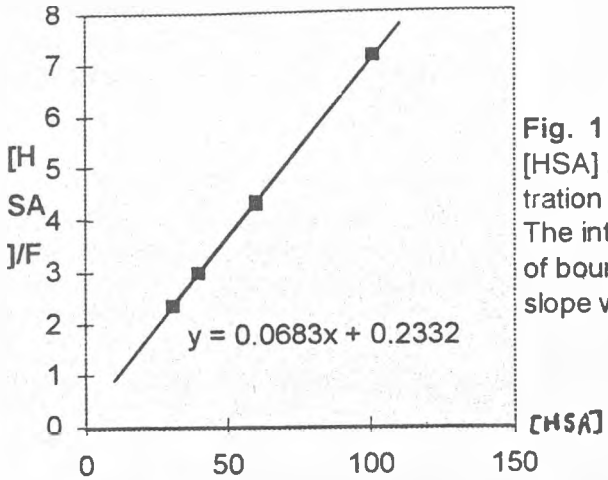

Fig. 1 Hanes direct plot of ratio [HSA] / F vs. [HSA]. The concentration of ANS was 4.78 microM. The intrinsic molar fluorescence of bound ANS obtained from the slope was 3.063 relative units.

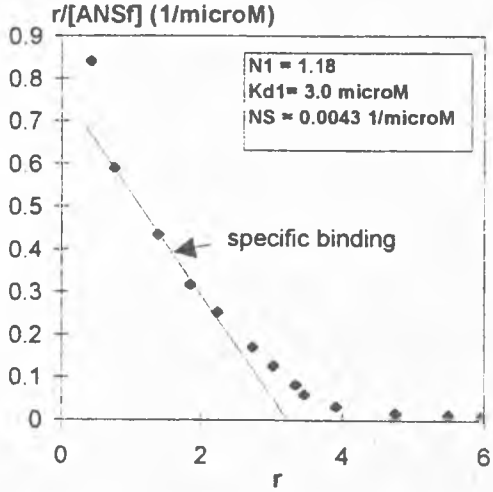

Fig. 2 Scatchard plot for the binding of ANS (2.3-600 microM) to HSA (4.25 microM).The insert icon gives the obtained values for binding parameters.

Least-square fitting was not able to give reliable estimates for N_1 and N_2 so we used equation (5) which gave estimates for N_1, K_{d1} and N_2 / K_{d2}. The values are presented in the insert icon Fig. 2. ANS binding to HSA revealed one tight binding site, with K_{d1} = 3 μM. These value disagree with the findings of Kolb *et al.* [16] but agree partially with the values presented by Sudlow *et al.* [5] which report one high affinity (K_d = 1.1 μM) and three lower affinity (K_d = 7.7 μM) binding sites. Panjehshahin *et al.* [9] reported 1.6 binding sites with K_d = 0.52 μM. These discrepancies may be the result of different experimental conditions and methods of data analysis.

REFERENCES

1. C. F. Chignell, *Ann. N. Y. Acad. Sci.*, 226, 45-59 (1973).
2. G. Weber & D. J. R. Laurence, *Biochem. J.*, 56, 31P (1954).
3. R. F. Chen, *Arch. Biochem. Biophys.*, 120, 609-620 (1967).
4. L. Brand & J. R. Gohlke, *Annu. Rev. Biochem.*, 41, 483-491 (1972).
5. G. Sudlow, D. J. Birkett, D. N. Wadi, *Mol. Pharmacol.*, 11, 824-832 (1975).
6. L. Stryer, *J. Mol. Biol.*, 13, 482 (1965).
7. E. A. Haigh, W. H. Sawyer, *Aust. J. Biol. Sci.*, 31, 1-5 (1978).
8. K. Zierler, *Biophys. Struct. Machanism*, 3, 275-289 (1977).
9. M. R. Panjehshahin, C. J. Bowmer, M. S. Yates, *Biochem. Pharmacol.*, 38(1), 155-159 (1989).
10. G. N. Wilkinson, *Biochem. J.*, 80, 324-332 (1961).
11. G. H. Beaven, S. H. Chen, A. d'Albis & W. B. Gratzer, *Eur. J. Biochem.*, 41, 539-546 (1974).
12. K. V. Ebner, *Biochim. Biophys. Acta*, 746, 87-96 (1983).
13. P. L. Luisi & R. Favella, *Eur. J. Biochem.*, 17, 91-94 (1970).
14. G. Scatchard, *Ann. N. Y. Acad. Sci.*, 51, 660-673 (1949).
15. C. M. Mendel & D. B. Mendel, *Biochem. J.*, 228, 269-272 (1985).
16. D.A. Kolb & G. Weber, *Biochemistry*, 14, 4476-4481 (1975).

STUDIA UNIVERSITATIS BABEŞ-BOLYAI, CHEMIA, XLII, 1-2, 1997

SYNTHESIS, STEREOCHEMISTRY AND NMR SPECTRA OF SOME NEW 2,5-SUBSTITUTED-1,3-DIOXANE DERIVATIVES

ION GROSU[1], SORIN MAGER[1], EUGEN MESAROS[1], LUMINITA MUNTEAN[1], CRINA SOCACI[1]

ABSTRACT. The stereochemistry of some new 1,3-dioxanes bearing phenyl, benzyl, methyl and ethyl substituents in the (a)cetal part of the heterocycle has been studied taking into account the data of conformational analysis and using complex NMR investigations.

INTRODUCTION

In pervious studies [1-8] on the stereochemistry of some 2,5-substituted-1,3-dioxanes the presence of flipping or anacomeric structures (Scheme 1), in correlation with the nature of substituents, has been discussed.

The conformational analysis of the 2,5-substituted-1,3-dioxanes shows flipping structures for the compounds displaying identical geminal substituents or bearing geminal substituents with very close conformational free enthalpies [4]. These compounds exhibit, at room temperature, a rapid inversion of the six-membered ring (A $\rightleftharpoons$ B), in their NMR spectra being observed unique signals (at mean values of the chemical shifts) for the axial and equatorial orientations of the protons of the rings or of the similar groups located in it.

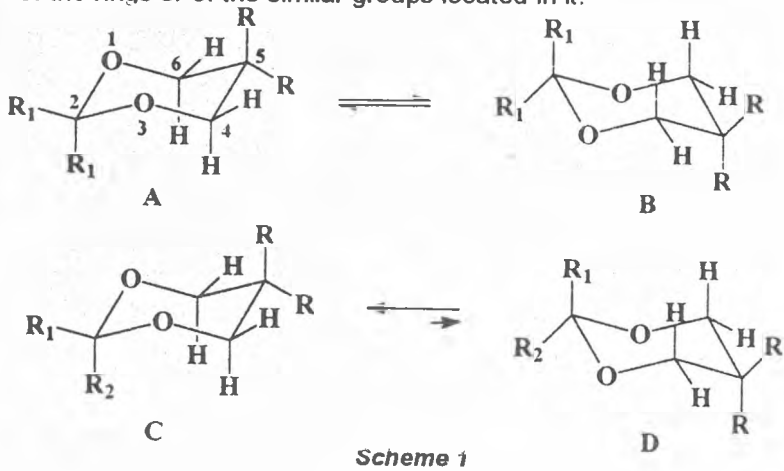

Scheme 1

[1] Facultatea de Chimie, Universitatea "Babeş-Bolyai", RO-3400, Cluj-Napoca, Romania

Contrarily, when different substituents are linked in the same position, the conformational equilibria are shifted towards the conformation (C) exhibiting the substituent with larger conformational free enthalpy (R_1, $\Delta G^0_1 > \Delta G^0_2$) in equatorial orientation ($C \rightleftarrows D$). The NMR spectra of these compounds show different signals for the axial and equatorial orientations of the protons of the heterocycle and of the protons and carbon atoms of the similar groups located in it.

It was considered of interest to study by means of NMR spectra the stereochemistry of some new 1,3-dioxanes displaying in the position 2 of the heterocycle aryl and (or) alkylaryl groups and to determine the anacomericity of the rings and the orientation of the substituents.

RESULTS AND DISCUSSION

New 1,3-dioxanes have been obtained (Scheme 2) by the condensation reaction of some aromatic ketones or aldehydes with 1,3-propanediols:

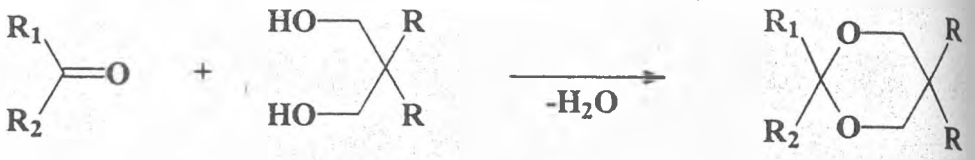

$R=CH_3$	$R_1=C_6H_5\text{-}CH_2$	$R_2=H$	1
$R=COOC_2H_5$	$R_1=C_6H_5\text{-}CH_2$	$R_2=H$	2
$R=CH_3$	$R_1=C_6H_5\text{-}CH_2$	$R_2=C_6H_5$	3
$R=COOC_2H_5$	$R_1=C_6H_5\text{-}CH_2$	$R_2=C_6H_5$	4
$R=CH_3$	$R_1=C_6H_5$	$R_2=C_2H_5$	5
$R=COOC_2H_3$	$R_1=C_6H_5$	$R_2=C_2H_5$	6

Scheme 2

All the investigated compounds exhibit anancomeric structures, the conformational equilibria being shifted towards the conformations that display the CH_2-X fragment (X = CH_3, C_6H_5) in equatorial orientation (Scheme 3).

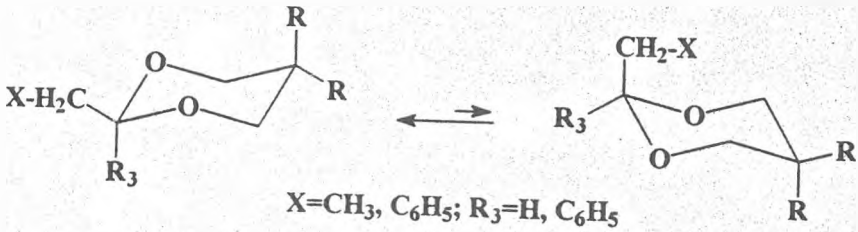

Scheme 3

The data of literature [9, 10] show a high conformational free enthalpy for the CH_3 group (ΔG_{Me} = 3.8-3.9 kcal/mol) as well as for the substituted methyl groups. The benzyl group, in compounds ***1*** and ***2*** shows an equatorial orientation. In comparison with the methyl group, the phenyl substituent displays lower value of

the conformational free enthalpy (ΔG_{ph} = 3.12 kal/mol, [11]). In 2,2-disubstituted-1,3-dioxanes bearing methyl (or substituted methyl) and phenyl groups, the preference of the phenyl group for the axial orientation is considerably higher (ΔG_{exp} = 2.42 kcal/mol, [12]) as that calculated by the addition of the values of the free conformational enthalpies measured for the two groups (methyl and phenyl) in monosubstituted compounds (ΔG_{calc} = 0.80 kcal/mol).

Compounds ***3*** and ***4*** show in position 2 equatorial benzyl groups and axial methyl substituents while compounds ***5*** and ***6*** exhibit axial phenyl groups and equatorial ethyl substituents.

The spectra of all investigated compounds exhibit different signals for the axial and equatorial orientations of the protons of the 1,3-dioxane ring and of the methyl or ethyloxycarbonyl groups located in the aliphatic part of the heterocycles (Tables 1 and 2).

As an example the ^{1}H NMR spectrum of compound ***2*** (Figure 1) shows for the aliphatic part of the molecule two doublets ($\delta_{4,6eq}$ = 4.71 and $\delta_{4,6ax}$ = 3.91 ppm) for the protons of positions 4 and 6 and two quartets (δ_{ax} = 4.32, δ_{eq} = 4.15 ppm) and two triplets (δ_{ax} = 1.30, δ_{eq} = 1.23 ppm) belonging to the protons of the methylene and methyl groups of the axial and equatorial ester groups of position 5. In the spectrum The triplet (δ = 4.69 ppm) belonging to the axial proton of position 2 is overlapped with the doublet pertaining to the equatorial protons of positions 4, 6. The spectrum also shows a doublet (δ = 2.92 ppm) which has been associated with the methylene protons of the benzyl substituent.

Table 1. NMR data (δ,ppm) for the protons and carbon atoms of positions 4 and 6 of the 1,3-dioxane ring

Compound	^{1}H			^{13}C
	4,6-eq	4,6-ax	$\Delta\delta$	4,6
1	3.62	3.41	0.19	77.34
2	4.71	3.91	0.80	69.34
3	3.42	3.35	0.07	71 63
4	4.48	3.91	0.57	63.64
5	3.70	3.26	0.44	71.61
6	4.48	3.93	0.55	63.64

The differences of the chemical shifts for the equatorial and axial protons of positions 4, 6 are higher ($\Delta\delta_{eq-ax}$ = 0.55-0.80 ppm) for the compounds displaying ester groups in the aliphatic part of the heterocycle then for the compounds exhibiting methyl substituents in the position 5 of the 1,3-dioxane ring ($\Delta\delta_{eq-ax}$ = 0.07-0 44 ppm). The stronger deshielding of the equatorial protons in compounds ***2, 4*** and ***6*** is due to the influences through space of the oxygen atoms of the ester group (Scheme 4) that create a deshielding area at the level of the equatorial protons of the heterocycle. The shown disposition of the axial ester group (ethyl "inside" rotamer) explains the stronger deshielding of the protons of the axial ester group, too.

Table 2. NMR data (δ,ppm) for the protons and carbon atoms of the substituents of position 5

Compound	^{1}H				^{13}C					
	$-CH_2-$ ax	$-CH_2-$ eq	$-CH_3$ ax	$-CH_3$ eq	-COO- ax	-COO- eq	$-CH_2-$ ax	$-CH_2-$ eq	$-CH_3$ ax	$-CH_3$ ax
1	-	-	1.21	0.71	-	-	-	-	23.07	21.91
2	4.32	4.15	1.30	1.23	168.05	166.94	62.03	62.03	14.09	13.98
3	-	-	1.07	0.53	-	-	-	-	22.77	21.90
4	4.15	4.04	1.26	1.15	167.88	166.97	61.88	61.83	14.08	13.89
5	-	-	1.24	0.16	-	-	-	-	22.71	22.33
6	4.35	4.06	1.34	1.16	167.01	167.01	61.98	61.98	14.21	13.90

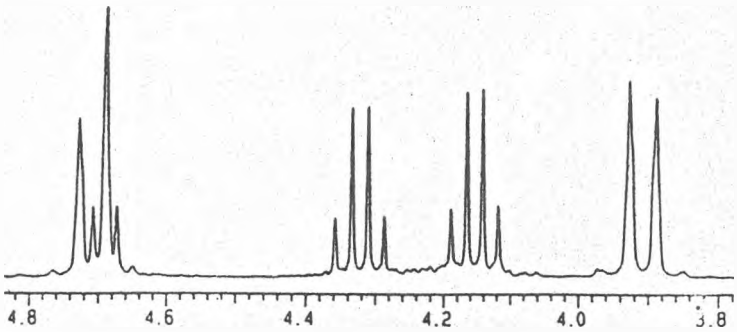

Figure 1. ^{1}H NMR spectrum of compound ***2*** (fragment)

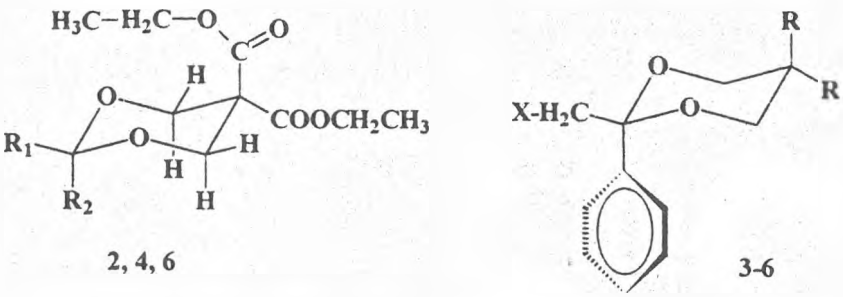

Scheme -

The differences between the chemical shifts of the protons of the axial and equatorial methyl groups (compounds ***1, 3*** and ***5***; ($\Delta\delta_{ax-eq}$ = 0.50-1.08 ppm) are higher as those recorded for the protons beloging to the methylene ($\Delta\delta_{ax-eq}$ = 0.11-0.29 ppm) or methyl ($\Delta\delta_{ax-eq}$ = 0.07-0.18 ppm) protons of the ester groups located in the aliphatic part of the heterocycle (compounds ***2, 4*** and ***6***). The ^{13}C NMR spectra exhibit higher differences ($\Delta\delta_{ax-eq}$ = 0.76-1.16 ppm) of chemical shift recorder for axial and equatorial groups for the compounds (***1, 3*** and ***5***) bearing methyl groups in the aliphatic part of the heterocycle then it was observed between the chemical shifts of the carbon atoms of the axial and equatorial ester groups. For compounds ***2, 4*** and ***6***, in some cases the differences between the magnetic environments of the axial equatorial carbon atoms were too small for being observed.

Compounds ***3-6*** exhibit axial phenyl groups. The rotation of the aromatic substituent around its bond with the heterocycle is hindered. The aryl group adopts a "rigid" orthogonal arrangement (Scheme 4). In this disposition the magnetic resonance of the protons and carbon atoms of the molecule is influenced by the magnetic anisotropy of benzene ring. This influence is stronger on the protons of the equatorial group of position 5 and could be observed by the shielding of their signals.

CONCLUSIONS

Compounds ***1-6*** exhibit anancomeric structures, the substituted methyl group (CH_2-X) prefers the equatorial orientation. The aryl groups determine by their magnetic anisotropy modifications of the pattern of the NMR spectra.

EXPERIMENTAL

^1H-and ^{13}C-NMR spectra were recorded at room temperature, using $CDCl_3$ as solvent, in 5 mm tubes, on a Varian Gemini 300 Fourier transform NMR spectrometer, equipped with a multinuclear head, operating at 300 MHz for protons and 75 MHz for carbon atoms. M. ps were measured with Electrothermal melting point apparatus and are uncorrected.

*New compounds **1-6**, general procedure.* - Equimolecular amounts of 1,3-diol and carbonyl compound (0.1 mol) with catalytic amounts of p-toluenesulphonic acid (0.1 g) were solved in 200 ml benzene. The mixture was refluxed and the water resulted in the reaction was removed using a Dean-Stark trap. When 80 % of the theoretical water was separated, after cooling at room temperature, the catalyst was neutralized (under stirring 0.5 h) with CH_3-COONa powder in excess (0.2 g). The reaction mixture was washed twice with 100 ml water. After drying (with Na_2SO_4) the benzene was removed and the 1,3-dioxane compounds were purified by crystallisation from ethanol or by vacuum distillation.

*2-Benzyl-5,5-dimethyl-1,3-dioxane **1**.*

Liquid, b.p.= 92-94^{0}C.(1 mm colHg). Yield 78%. $C_{13}H_{18}O_2$, M = 206.22. Found: C, 75.82; H, 8.98; required C, 75.69; H, 8.80. ^1H NMR ($CDCl_3$) δ 0.71[3H, s, 5-CH_3(eq)], 1.21[3H, s, 5-CH_3(ax)], 2.96(2H, d, J = 5.2 Hz, 2-CH_2-), 3.41(2H, d, J =

11.2 Hz, 4,6-H_{ax}), 3.62 (2H, d, J = 11.2 Hz, 4,6-H_{eq}), 4.62(1H, t, J = 5.2 Hz, 2-H_{ax}), 7.25-7.32 ppm(5H aromatic, m, overlapped peaks). ^{13}C NMR ($CDCl_3$) δ 21.91[5-CH_3(eq)], 23.07[5-CH_3(ax)], 30.16(C^5), 41.63(2-CH_2), 77,34($C^{4,6}$), 102.66(C^2), 126.46, 128.28, 129.68(tertiary aromatic carbon atoms), 136.70 ppm(quaternary aromatic carbon atom).

2-Benzyl-5,5-bis(ethyloxycarbonyl)-1,3-dioxane ***2***.
Liquid, b.p. = 156-158^{0}C (1mm colHg). Yield 60% $C_{17}H_{22}O_6$, M = 322.36. Found: C, 63.18; H, 6.72; required C, 63.34; H, 6.88. ^1H NMR ($CDCl_3$) δ 1.23[3H, t, J = 7.1 Hz, 5-$COOCH_2C\underline{H}_3$(eq)], 1.30[3H, t, J = 7.1 Hz, 5-$COOCH_2C\underline{H}_3$ (ax)], 2.92(2H, d, J = 5.1 Hz, 2-CH_2-), 3.91(2H, d, J = 11.0 Hz, 4,6-H_{ax}), 4.15[2H, q, J = 7.1 Hz, 5-$COOC\underline{H}_2CH_3$ (eq)], 4.32[2H, q, J = 7.1 Hz, 5-$COOC\underline{H}_2CH_3$ (ax)], 4.69(1H, t, J = 5.1 Hz, 2-H_{ax}), 4.71(2H, d, J = 11.0 Hz, 4,6-H_{eq}), 7.15-7.25 ppm(5H aromatic, m, overlapped peaks). ^{13}C NMR ($CDCl_3$) δ 13.98[5-$COOCH_2\underline{C}H_3$ (eq)], 14.09[5-$COOCH_2\underline{C}H_3$ (ax)], 41.24(2-CH_2), 53.29(C^5), 62.03[5-$COO\underline{C}H_2CH_3$ (ax and eq)], 69.34($C^{4,6}$), 102.90(C^2), 126.61, 129.52, 129.73(tertiary aromatic carbon atoms), 136.07 (quaternary aromatic carbon atom), 166.94[5-$\underline{C}OOCH_2CH_3$ (eq)], 168.05 ppm[5-$\underline{C}OOCH_2CH_3$ (ax)].

2-Benzyl-2-phenyl-5,5-dimethyl-1,3-dioxane ***3***.
Solid, white crystals, m.p. = 64-65^{0}C. Yield 64%. $C_{19}H_{22}O_2$, M = 282.38. Found: C, 81.01; H, 7.73; required C, 80.82; H, 7.85. ^1H NMR ($CDCl_3$) δ 0.53[3H, s, 5-CH_3(eq)], 1.07[3H, s, 5-CH_3(ax)], 3.01(2H, s, 2-CH_2-), 3.35(2H, d, J = 11.0 Hz, 4,6-H_{ax}), 3.42 (2H, d, J = 11.0 Hz, 4,6-H_{eq}), 7.00-7.30 ppm(10H aromatic, m, overlapped peaks). ^{13}C NMR ($CDCl_3$) δ 21.90[5-CH_3(eq)], 22.77[5-CH_3(ax)], 30.02(C^5), 50.82(2-CH_2), 71.63($C^{4,6}$), 101.52(C^2), 126.12, 127.27, 127,71, 128.01, 128.19, 131.22(tertiary aromatic carbon atoms), 135.98, 139.15 ppm(quaternary aromatic carbon atom).

2-Benzyl-2-phenyl-5,5-bis(ethyloxycarbonyl)-1,3-dioxane ***4***.
Solid, white crystals, m.p. = 87-88^{0}C. Yield 62%. $C_{23}H_{26}O_6$, M = 398.46. Found: C, 69.48; H, 6.43; required C, 69.33; H, 6.58. ^1H NMR ($CDCl_3$) δ 1.15[3H, t, J = 7.0 Hz, 5-$COOCH_2C\underline{H}_3$(eq)], 1.26[3H, t, J = 7.0 Hz, 5-$COOCH_2C\underline{H}_3$ (ax)], 2.97(2H, s, 2-CH_2-), 3.91(2H, d, J = 11.5 Hz, 4,6-H_{ax}), 4.04[2H, q, J = 7.0 Hz, 5-$COOC\underline{H}_2CH_3$ (eq)], 4.15[2H, q, J = 7.0 Hz, 5-$COOC\underline{H}_2CH_3$ (ax)], 4.48(2H, d, J = 11.5 Hz, 4,6-H_{eq}), 6.95-7.30 ppm(10H aromatic, m, overlapped peaks). ^{13}C NMR ($CDCl_3$) δ 13.89[5-$COOCH_2\underline{C}H_3$ (eq)], 14.08[5-$COOCH_2\underline{C}H_3$(ax)], 50.33(2-CH_2), 53.23(C^5), 61.83[5-$COO\underline{C}H_2CH_3$ (eq)], 61.88[5-$COO\underline{C}H_2CH_3$(ax)] 63.64($C^{4,6}$), 102.09(C^2), 126.21, 127.30, 127.45, 128.18, 128.54, 131.15(tertiary aromatic carbon atoms), 135.37 137.86(quaternary aromatic carbon atom), 166.97[5-$\underline{C}OOCH_2CH_3$ (eq)], 167.88 ppm[5-$\underline{C}OOCH_2CH_3$ (ax)].

2-Ethyl-2-phenyl-5,5-dimethyl-1,3-dioxane ***5***.
Liquid, b.p.= 101-102^{0}C.(1 mm colHg). Yield 62%. $C_{14}H_{20}O_2$, M = 220.31. Found: C, 76.15; H, 9.03; required C, 76.33; H, 9.15. ^1H NMR ($CDCl_3$) δ 0.16[3H, s, 5-

CH_3(eq)], 1.07(3H, t, J = 7.4 Hz, 2-CH_2-C$\underline{H_3}$), 1.24[3H, s, 5-CH_3 (ax)], 1.94(2H, q, J = 7.4 Hz, 2-C$\underline{H_2}$-CH_3), 3.26(2H, d, J = 10.7 Hz, 4,6-H_{ax}), 3.70(2H, d, J = 10.7 Hz, 4,6-H_{eq}), 7.27-7.35 ppm(5H aromatic, m, overlapped peaks). ^{13}C NMR ($CDCl_3$) δ 7.56(2-CH_2-$\underline{C}H_3$), 22.33[5-CH_3(eq)], 22.71[5-CH_3(ax)], 30.13(C^5), 37.48(2-$\underline{C}H_2$-CH_3), 71.61($C^{4,6}$), 101.93(C^2), 127.06, 127.91, 128.30(tertiary aromatic carbon atoms), 139.70 ppm(quaternary aromatic carbon atom).

2-Ethyl-2-phenyl-5,5-bis(ethyloxycarbonyl)-1,3-dioxane ***6***.
Liquid, b.p. = 162-164^{0}C (1mm colHg). Yield 67% $C_{18}H_{24}O_6$, M = 336.38. Found: C, 64.13; H, 7.05; required C, 64.27; H, 7.19. ^{1}H NMR ($CDCl_3$) δ 0.80[3H, t, J = 7.3 Hz, 2-CH_2-C$\underline{H_3}$), 1.16[3H, t, J = 7.1 Hz, 5-$COOCH_2C\underline{H_3}$ (eq)], 1.34[3H, t, J = 7.1 Hz, 5-$COOCH_2C\underline{H_3}$(ax)], 1.71(2H, q, J = 7.3 Hz, 2-C$\underline{H_2}$-CH_3), 3.97(2H, d, J = 11.2 Hz, 4,6-H_{ax}), 4.06[2H, q, J = 7.1 Hz, 5-$COOC\underline{H_2}CH_3$(eq)], 4.35[2H, q, J = 7.1 Hz, 5-$COOC\underline{H_2}CH_3$ (ax)], 4.48(2H, d, J = 11.2 Hz, 4.6-H_{eq}), 7.30-7.40 ppm(5H aromatic, m, overlapped peaks). ^{13}C NMR ($CDCl_3$) δ 7.25(2-CH_2-$\underline{C}H_3$), 13.90[5-$COOCH_2\underline{C}H_3$ (eq)], 14.21[5-$COOCH_2\underline{C}H_3$ (ax)], 37.08(2-$\underline{C}H_2$-CH_3), 53.32(C^5), 61.98[5-$COO\underline{C}H_2CH_3$ (eq and ax)], 63.64($C^{4,6}$), 102.48(C^2), 127.23, 128.01, 128.71(tertiary aromatic carbon atoms), 138.52(quaternary aromatic carbon atom), 167.01 ppm[5-$\underline{C}OOCH_2CH_3$ (eq and ax)].

REFERENCES

1. Mager S., Hopartean I., Horn M. and Grosu I., *Studia Univ. "Babes-Bolyai", Chemia*, (1979), 29, 31.
2. Mager S. and Grosu I., *Studia Univ. "Babes-Bolyai" Chemia*, (1988), 33, 47.
3. Mager S., Grosu I. and Horn M., *Stud. Univ. "Babes-Bolyai" Chemia* (1991) 36, 53.
4. Grosu I., Plé G. and Mager S., *Rev. Roum. Chim.*, (1996), 41, 259.
5. Mager S., Grosu I., Horn M., Hopartean I., Darabantu M., Puscas C., Kovacs D. and Plé G., *Roum. Chem. Quarterly Reviews*, (1995), 3, 201.
6. Grosu I., Mager S. and Plé G., *Tetrahedron*, (1995), 51, 2659.
7. Grosu I., Mager S., Plé G., Martinez R., Muntean L. and Mesaros E., *Heterocycles*, (1995), 41, 2233.
8. Grosu I., Mager S., Plé G., Muntean L. and Schirger I., *Heterocyclic Commun.*, (1996), 2, 432.
9. Pihlaja K. and Luoma S., *Acta Chim. Scand.*, (1968), 22, 2401.
10. Anteunis M.J.O., Tavernier D., Borremans F., *Heterocycles* (1976), 4, 293.
11. Nader F. W., Eliel E.L., *J. Am. Chem. Soc.*, 1970, 92, 3050-3055.
12. Bailey W.F. and Eliel E.L., *J. Am. Chem. Soc.*, (1974), 96, 1798.

STUDIA UNIVERSITATIS BABEŞ-BOLYAI, CHEMIA, XLII, 1-2, 1997

TAFT REVISITED

CORINA M. POP[1], MIRCEA V. DIUDEA[1], LJUPCO PEJOV[2]

ABSTRACT. A new topological descriptor, W_s, based on walks in graphs, is proposed for modeling the steric effect of alkyl substituents. It is tested on a set of twenty fragmental structures vs. the reaction rates of acid-catalysed esterification of carboxylic acids. The correlations obtained indicate that W_s can severe as a useful steric parameter in reactivity studies.

INTRODUCTION

In the field of chemical reactivity, quantitative structure-property relationships were examined by using free-energy-related physico-chemical parameters, [1] such as σ (Hammet) and E_s (Taft). The first proposal, in literature, of a substituent steric parameter, is due to Taft. [2] He tried to quantify the influence of a substituent located on the hydrocarbon part of organic esters in the acid-catalysed hydrolysis of aliphatic carboxylic, RCOOR'. He defined the steric parameter as

$$E_s = \log (k_R/k_{Me})_A \qquad (1)$$

where $(k_R/k_{Me})_A$ is the ratio of acid-catalysed hydrolysis rate constant of RCOOR' to that of MeCOOR'. By definition, $E_s(Me) = 0$.

Since the E_s parameters have been defined empirically, many subsequent studies tried to give a structural interpretation of these ones [3]. Taft himself recognised that E_s varies parallel to the group radius. Charton also found that this parameter is linearly dependent on the van der Waals radius, defining a new steric parameter, v. [4,5].

Murray (see [3], ref. 27) found correlations between the Taft parameter and the topological index (defined by Randic [6]) for a series of substituted alkyls Very recently, Ivanciuc and Balaban [3] have proposed a topological based descriptor, SVTI, which encodes the topological distances (i.e., the number of bonds/edges joining two atoms/vertices, on the shortest path) in a molecular graph, G. It is defined on the fragment F (i.e. an alkyl group) attached to the vertex i of G, as

[1] Facultatea de Chimie şi Inginerie Chimică, Universitatea "Babeş-Bolyai", 11 Arany Janos Str. 3400 Cluj, Romania.

[2] Institut za Hemija, PMF, Univerzitet "Sv. Kiril i Metodij" Arhimedova 5. P.O.Box 162, 91001, Skopje, Republic of Macedonia.

$$SVTI(F) = \sum_{j=1}^{N_F} [D]_{ij}\ ; \quad [D]_{ij} \leq 3 \tag{2}$$

The summation runs over all N_F vertices of F and the distance $[D]_{ij}$ is limited to 3, in agreement to the Charton's conclusion about the limit of the influence of the steric effect beyond the gamma carbon. [4] The calculation of SVTI is exemplified for the *sec*-butyl group (R = H) or higher homologues (R≠H):

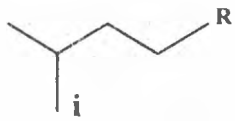

SVTI(s-Bu) = 1+ 2 + 2 + 3 = 8

In the present work, a new descriptor for the steric effect of an alkyl group is presented.

THE STERIC TOPOLOGICAL DESCRIPTOR, WS

The new descriptor herein proposed is based on the walks in a connected molecular graph. A walk W is defined [7] as a continuous sequence of vertices, v_1, v_2, ..., v_m; it is allowed edges and vertices to be revisited. If the two terminal vertices coincide ($v_1 = v_m$), the walk is called a closed (or self returning) walk, otherwise it is an open walk. If its vertices are distinct, the walk is called a path. The number e of edges traversed is called the legth of walk. Walks of length e, starting at the vertex i, ${}^eW_i$, can be counted by summing the entries in the row i of the eth power of the adiacency matrix *A* (whose nondiagonal entitres are 1 if two atoms are adjacent and zero otherwise).

$${}^eW_i = \sum_{j \in V(G)} [A^e]_{ij} \tag{3}$$

${}^eW_i$ is called the walk degree (of rank e) of vertex i (or atomic walk count [8,9]). Local and global invariants based on walks in graph were considered for correlating with physico-chemical properties. [8,9]

The steric descriptor, W_s, is defined as

$$W_s(F) = \sum_{j=1}^{j \leq 3} (1/j) \sum_{u \in F(u)_j} {}^3W_u \tag{4}$$

where ${}^3W_u$ is the walk number, of length 3, of the vertex u lying in the jth layer, $F(u)_j$, of the partition of the attachement point i, F(i), (see below). The summation in the first sum is limited to the first three layers (see the SVTI parameter) while in the

second sum it runs over all u vertices belonging to the jth layer. In fact, W_s is calculated on the (truncated) i^{th} row of the layer matrix, L^3W. For more details about the layer matrices, the reader can consult [8].

The calculation of the steric parameter, W_s, is exemplified for the fragment $CHiBu_2$:

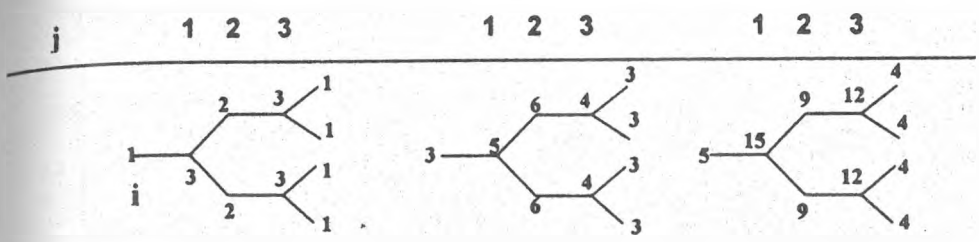

$L^3W(F(i)) = 5, [15, 18, 24], 16$

$W_s = 15 + 18\ (1/2) + 24\ (1/3) = 32$

CORRELATING TEST

The validation of the Ws descriptor was made on a set of twenty alkyl fragments (Table 1) involved in the reaction rate of esterification of alkyl substituted carboxylic acids with methanol [10-13]. Y_1 refers to the esterification rates catalysed by HCl, at 30^0C, while Y_2 were recorder at 40^0C, at a catalyst concentration of 0.05 N, for both series. The correlating results are listed in Table 2.

From Table 2, one can see that the best steric descriptor, in single variable, is W_s (entries 1 and 3). The quantitative structure-property relation, QSPR, for the reaction rates are given below

$$Y_1 = 0.552 + 0.097\ W_s \qquad (5)$$
$$n = 20;\ r = 0.9530;\ s = 0.303;\ cv\ (\%) = 13.08;\ F = 178.16$$

$$Y_2 = 0.350 + 0.094\ W_s \qquad (6)$$
$$n = 20;\ r = 0.9532;\ s = 0.294;\ cv\ (\%) = 14.23;\ F = 178.80$$

In the above relations, n is the number of samples in the set, r denotes the correlation coefficient, s is the dispersion, cv(%) is the coefficient variance (in percents) and F is the Fisher ratio. Fig. 1 shows the plot corresponding to eq. 5.

Table 1. Fragmental steric descriptors and experimental reaction rates

No.	Alkyl group	W_s	SVTI	E_s	v	N_C	VOL	Y_1	Y_2
1	Me	1	1	0.00	0.52	1	23.23	1.05	0.82
2	Et	5	3	0.07	0.56	2	37.68	1.12	0.88
3	Pr	8.5	6	0.36	0.68	3	50.26	1.43	1.19
4	iPr	12	5	0.47	0.76	3	44.51	1.58	1.35
5	Bu	11	6	0.39	0.68	4	66.99	1.38	1.15
6	iBu	13.66	9	0.93	0.98	4	65.99	2.06	1.87
7	sBu	16.33	8	1.13	1.02	4	65.76	2.14	1.88
8	tBu	22	7	1.54	1.24	4	65.51	2.57	2.31
9	CH_2Bu	11.83	6	0.40	0.68	5	78.65	1.37	1.14
10	CH_2iBu	14.16	6	-	-	5	77.94	1.42	1.2
11	CH_2sBu	16.50	9	-	-	5	80.06	2.03	1.84
12	CH_2tBu	20.50	12	1.74	1.34	5	77.59	2.8	2.51
13	$CHEt_2$	20.66	11	1.98	1.51	5	79.13	3.15	2.88
14	$CHPr_2$	25.67	11	2.11	1.54	7	106.31	3.2	2.91
15	$CHMeCH_2tBu$	25.83	8	1.85	1.41	7	107.53	2.95	2.69
16	C_6	12.16	6	-	-	8	123.39	1.42	1.19
17	CMe_2CH_2tBu	36.67	10	2.57	1.74	8	119.62	3.66	3.36
18	$CHBu_2$	27.33	11	-	-	9	138.26	3.26	2.96
19	$ChiBu_2$	32	11	2.47	1.70	9	135.24	3.55	3.26
20	$CH(CH_2tBu)_2$	33.33	11	3.18	2.03	11	158.35	4.25	3.94

Table 2. Statistics of Multivariable Regression ($Y = a + \Sigma_i b_i X_i$)

No.	Y	X_i	b_i	a	r	s	cv(%)	F
1	Y_1	W_s	0.097	0.552	0.9530	0.303	13.08	178.16
2		SVTI	0.279	0.133	0.8560	0.518	22.32	49.35
3	Y_2	W_s	0.094	0.350	0.9532	0.294	14.23	178.80
4		SVTI	0.271	-0.084	0.8593	0.497	24.06	50.78
5	Y_1	W_s SVTI	0.078 0.071	0.329	0.9609	0.285	12.31	102.30
6		W_s 1/Vol	0.111 21.365	-0.024	0.9606	0.286	12.35	101.56
7		W_s $1/N_c$	0.109 0.855	0.106	0.9612	0.284	12.25	103.24
8	Y_2	W_s SVTI	0.075 0.072	0.125	0.9618	0.274	13.26	104.78
9		W_s 1/Vol	0.107 19.760	-0.162	0.9600	0.280	13.54	100.10
10		W_s $1/N_c$	0.105 0.792	-0.062	0.9606	0.278	13.45	101.65
11	Y_1	W_s SVTI 1/Vol	0.090 0.129 39.478	-0.918	0.9811	0.205	8.86	137.27
12		W_s SVTI $1/N_c$	0.086 0.130 1.556	-0.668	0.9821	0.200	8.63	144.96
13	Y_2	W_s SVTI 1/Vol	0.086 0.128 37.631	-1.064	0.9813	0.199	9.61	138.34
14		W_s SVTI $1/N_c$	0.083 0.129 1.483	-0.826	0.9822	0.194	9.37	145.97

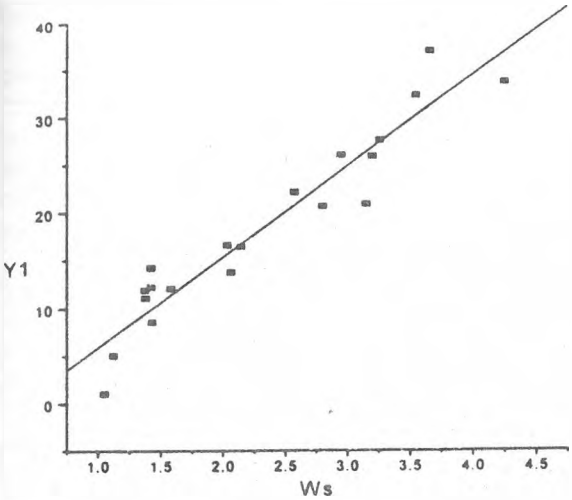

Figure 1. The plot corresponding to eq 5

W_s is far more better than the SVTI parameter (r = 0.8560; 0.593). The E_s and v are not discussed since they are defined just on such a set of fragments.

When added the fragmental volume, VOL, (for their calculation see below) or the number of carbon atoms, N_c, the correlation is improved (see Table 2). Note that the reciprocal of the volume or the number of carbons is here important, as a measure of the accessibility to the reaction centre. The two variable regressions are still unsatisfactory. When three variable regression is performed (Table 2, entries 11-14), the coefficient of variance becomes less than 10% and the F parameter increases (as compared to the two variable regressions, Table 2, entries 5-10) thus proving a good quality for the regression equations. The QSPRs for the entries 12 and 14 are given below

$$Y_1 = -0.668 + 0.086\, W_s + 0.130\, SVTI + 1.556\, 1/N_c \quad (7)$$
$$n = 20;\ r = 0.9821;\ s = 0.200;\ cv\ (\%) = 8.63;\ F = 144.96$$

$$Y_2 = -0.826 + 0.083\, W_s + 0.129\, SVTI + 1.483\, 1/N_c \quad (8)$$
$$n = 20;\ r = 0.9822;\ s = 0.194;\ cv\ (\%) = 9.37;\ F = 145.97$$

The plot for the calculated values by (7) and the experimental Y_1 data is presented in Fig. 2.

Table 3 shows the intercorrelation between the steric parameters (on a set of 16 data). One can see that W_s is far more correlated to the Taft, E_s, (0.9637), and Charton, v, (0.9587), parameters, (in comparison to the SVTI, fragmental volumes, and N_c), which is a promise in describing the steric effect of alkyl substituents.

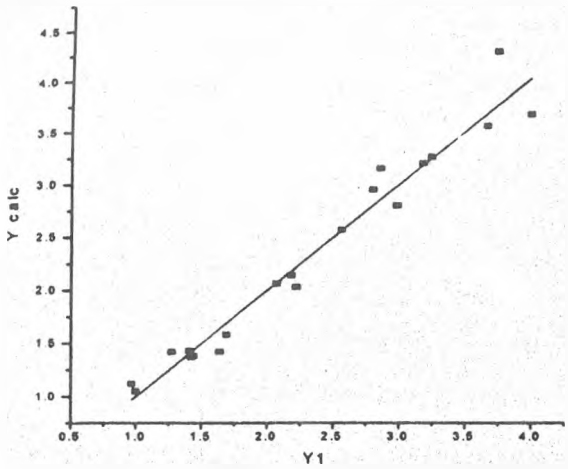

Figure 2. The plot corresponding to eq 7

It is noteworthy that W_s is a pure steric parameter, not affected by the electronic effects (which is the case of E_s). It is not degenerated in the considered set in opposition to the SVTI, v and N_c parameters. However, degeneracy (i.e. a same value for different structures - see Table 1, the shaded values) could appear in larger fragments. Ws is also better correlated to the fragmental volumes, among all the steric parameters herein discussed (see Table 3).

Also note that the volumes of fragments correlate 0.998 with the number of carbon atoms, N_c in the considered set. It is a consequence of the Monte Carlo method of calculation of the fragmental volumes. Both parameters do not exceed a correlation of 0.79 with the reaction rates herein discussed. The calculation of volumes (as a fragment size) seems to be not justified in sets of structures of various N_c, since the last parameter is trivially calculable.

Table 3. Intercorrelating relations among the steric parameters (16 data, in Table 2)

	E_s	W_s	SVTI	Vol	C	v
E_s	1.0000	0.9637	0.8564	0.9121	0.9133	0.9991
W_s		1.0000	0.8191	0.9209	0.9211	0.9587
SVTI			1.0000	0.7709	0.7669	0.8565
Vol				1.0000	0.9984	0.9044
C					1.0000	0.9061
v						1.0000

COMPUTATION OF FRAGMENTAL VOLUMES

The geometries of the hydrocarbon fragments (in fact, the corresponding radicals) were fully optimised at the Unrestricted Hartree-Fock (UHF) level of theory, using the 6-31G** (double zeta) basis set, which contains polarisation functions for better description of the radical wavefunctions. The Berny's optimisation algorithm was used (the derivatives were computed analytically). The method of initial guess of the second derivative matrix was applied. Standard harmonic vibrational analysis, using the Coupled Perturbed Hartree Fock (CPHF) method, was applied to test the optimised geometries (stationary points at the hypersurfaces).

Volume calculations were performed for the optimised structures (stationary points at potential energy hypersurfaces), by the Monte-Carlo method. All calculations were performed with Gaussian 94 series of programmes. Since Monte-Carlo method for calculating molecular volume (defined as the volume inside a contour of 0.001 electrons/bohr^3 density) is stochastically-based algorithm, it often leads to results accurate up to several percents. Therefore, 11 volume calculations per fragment were performed, and the arithmetic average value was taken as the closest approximation to the real one. In order to increase the density of points for a more accurate integration, the "Tight" option of the Gaussian "Volume" keyword was used.

CONCLUSIONS

W_s descriptor, based on the walks in graph, satisfactorily describes the steric effect of alkyl substituents in the esterification reaction. It is a pure steric parameter, not affected by the electronic effects. W_s correlates well to the fragmental volumes (over 0.92) and shows a lower degeneracy in comparison to the SVTI, v and N_c parameters. It is also well correlated to the Taft, E_s, (0.9637), and Charton, v, (0.9587), parameters, which makes from W_s a promising alternative in describing the steric effect of alkyl substituents.

REFERENCES

1. Gh. Surpăţeanu, *"Bazele teoretice ale reactivităţii chimice"*, Ed. Tehnică, Bucureşti, 1982.
2. R. W. Taft, *J. Am. Chem. Soc.* 74 (1952) 2729, 3120.
3. O. Ivanciuc, A. T. Balaban, *Croat. Chem. Acta*, 69 (1996) 75.
4. M. Charton, *J. Am. Chem. Soc.* 91 (1969) 615.
5. M. Charton, *J. Am. Chem. Soc.* 97 (1975) 1552, 3691, 3694, 6159.
6. M. Radic, *J. Am. Chem. Soc.* 97 (1975) 6609.
7. N. Trinajstic, *Chemical Graph Theory;* CRC Press, Inc.; Boca Raton, FL, 1983.
8. M. V. Diudea, M. Topan, A. Graovac, *J. Chem. Inf. Comput. Sci.* 34 (1994) 1072.
9. G. Rücker, C. Rücker, *J. Chem. Inf. Comput. Sci.*, 33 (1993) 683.

10. H. A. Smith, *J. Am. Chem. Soc.* 61 (1939) 254, 1176.
11. H. A. Smith, *J. Am. Chem. Soc.* 62 (1940) 1136.
12. H. A. Smith, C. H. Reichardt, *J. Am. Chem. Soc.* 63 (1941) 605.
13. K. L. Loening, A. B. Garrett, M. S. Newman, *J. Am. Chem. Soc.* 74 (1952) 3929.

STUDIA UNIVERSITATIS BABEŞ-BOLYAI, CHEMIA, XLII, 1-2, 1997

DYNAMIC SIMULATOR FOR A UOP MODEL FLUID CATALYTIC CRACKING UNIT

MIRCEA CRISTEA[1], ŞERBAN AGACHI[1]

ABSTRACT. The paper presents a new dynamic mathematical model for the simulation of a UOP type Fluid Catalytic Craching Unit. This model was developed to answer the need of a more detailed and realistic description of a complex and multivariable process, featuring significant nonlinearities. The reactor riser is described by a three lump kinetic scheme (Weekman and Nace) and the regenerator by a fluidized bed model. The model also includes the feed system, the catalyst circulation bands, the air blower and the wet gas compressor. The model offers the opportunity of studying the process behaviour in varying conditions but also the means for testing advanced control with real chances of industrial implementation.

INTRODUCTION

The FCCU process is one of the most important process in a modern refinery. It consists of cracking heavy hydrocarbon components into lighter and more valuable ones, from which gasoline is the most important. The attempt of describing this multivariable process has to face a very complex behaviour due to interactions, nonlinearities and operating constrains. The dynamic simulation reveals interesting features which can be later used in control studies for industrial implementation.

RESULT AND DISCUSSION

The gas oil mixed with wash oil and Diesel oil are preheated in a furnace and then mixed with slurry recycle from the bottom of the main fractionar and sent to the reactor riser, Fig. 1. Here, the feed streams are mixed with regenerated catalyst coming from the regenerator. This regenerated catalyst brings heat necessary for vaporising and cracking reactions that take place in the riser. The so named reactor vessel is in fact only a separating vessel where spent catalyst is separated from products. The products are evacuated at the top of the reactor, being sent to the main fractionar. Wet gases are suctioned by the wet gas compressor and sent for further work to other refinery units. The spent catalyst is stripped with steam. Due to the cracking reactions a large amount of coke (carbon + hydrogen) is produced and deposited on the catalyst, poisoning it. Therefore a

[1] Facultatea de Chimie şi Inginerie Chimică, Universitatea "Babeş-Bolyai", 11 Arany Janos, 3400 Cluj-Napoca, Romania.

regeneration procedure is necessary and takes place in the regenerator where carbon and hydrogen from spent catalyst are removed by burning. The oxygen necessary for the combustion reactions is supplied by the combustion air blower which is driven by a constant speed electric motor. Coke is burned in the regenerator in a fluidized bed. Stack gas is evacuated at the top of the regenerator. Entrained catalyst is separated in the cyclones and returns in the dense bed. Regenerated catalyst is sent again to the reactor riser where begins a new cycle.

The new dynamic model presented in this paper has as starting point the Model IV FCCU presented by McFarlane et al [1] and with certain adaptations by Morari and Agachi [2]. The main parts of the simulator are: the reactor (riser and stripper), the regenerator, the feed system, the catalyst circulation bends, the wet gas compressor and the combustion air blower.

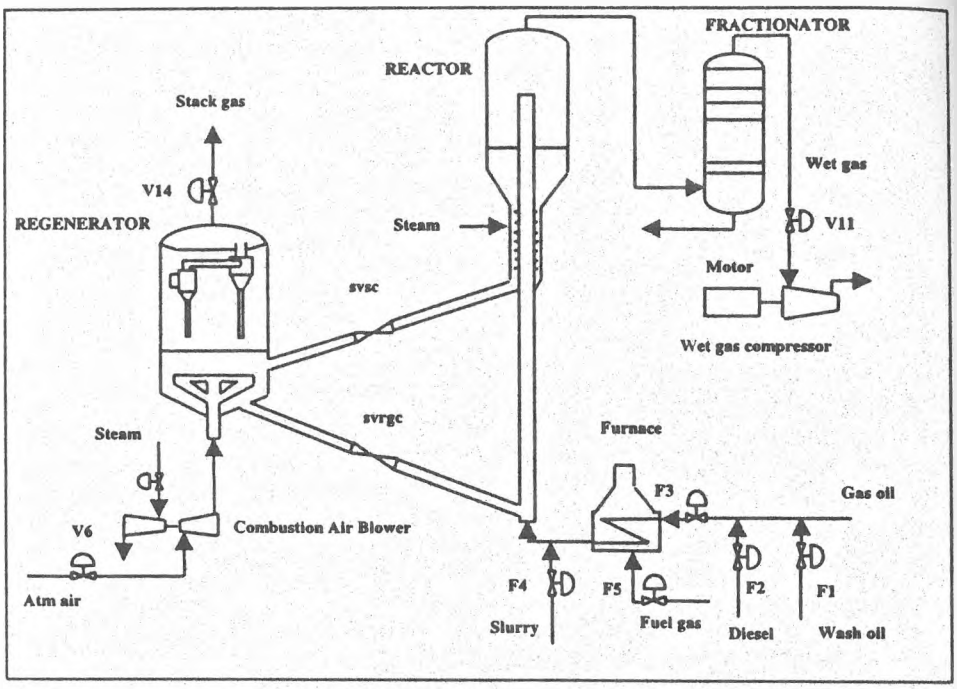

Figure 1. Schematic of the UOP FCCU

Compared with the models mentioned, the new UOP model has the following additions:

- the kinetics of the cracking reactions taking place in the riser replace the empirical formula used in McFarlane and Morari works
- two different phases are distinguished in the dense bed of the regenerator
- the reactor vessel is modeled as a CSTR using both mass and energy balance

- the catalyst is made by means of V pipes (for UOP model) and not through U-bends (Model IV) implying the change of pressure balance equations
- the reactor-regenerator relative position is changed, vessels and pipes dimensions updated according to a real UOP unit.

The reactor riser model is a static model described by an ideal plug flow (residence time in the riser is very short compared to other time constants) [1]. Material balance for gas oil and gasoline is provided, predinting the gasoline and coke + light gases yield based on a three-lump kinetic scheme of Weekman and Nace [3], [4], Fig. 2: it also predicts the amount of deposited coke and the cracking temperature (energy balance) [5], [6].

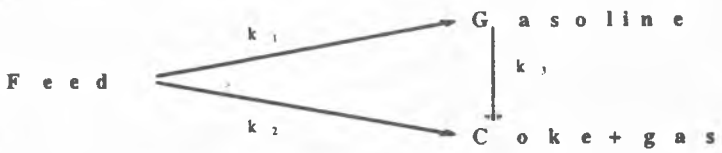

Figure 2. Three lump kinetic scheme

The stripper model is a CSTR (mass and energy balance); it predicts the stripper temperature and concentration of coke on spent catalyst.

The regenerator model assumes a fluidized bed consisting of two zones:

a) <u>the dense bed with</u>: a *bubble phase* (gaseous reactants and products moving up in the bed in plug flow) and a *dense phase* (gas and solid catalyst perfectly mixed). Mass transfer occurs between the two phases as gas moves up in the bed, but at regenerator temperatures the reaction rates are controlling rather than the mass transfer between the two phases. Due to perfectly mixed assumption the temperature is uniform in the dense bed and the bubble phase is in thermal equilibrium with the dense phase. Mass balance for: xO_2, xCO, xCO_2 (varying with time and distance) and carbon on catalyst (varying with time) are also accounted. Energy balance for regenerator temperature is provided (varying with time and distance in the disengaging zone and varying with time in the dense bed).

b) <u>the disengaging zone</u> appearing due to catalyst entrainment in the zone above the dense bed. Reaction with oxygen takes place here too. The volume fraction of catalyst and regenerator temperature are predicted (mass and energy balance).

The operating mode of the regenerator is total combustion mede which assumes that excess oxygen is present and virtually all CO is transformed to CO_2.

The feed system consists of a preheat furnace. The temperature of feed leaving the furnace is described by energy balance. The flow of the furnace is used to control the amount of heat transferred to the fresh feed.

The wet gas compressor is modeled as a single stage centrifugal compressor. The equation describing it relates polytropic heat to volumetric suction flow. It has a single surhe point being provided with a bypass line and a vent valve (flare vale).

The combustion air blower is also a single stage compressor driven by a constant speed electric motor. The performance curve is given relating suction volumetric flow to discharge pressure, with suction pressure at atmospheric pressure.

The catalyst circulation lines for spent and regenerated catalyst simulate the catalyst circulation described by force balance equations. Slide valves are used in order to manipulate the spent and regenerated catalyst flows. Pressure balances are also accounted for the riser, reactor and regenerator due to their importance in the general behaviour of the process.

The simulation was performed in MATLAB and SIMULINK software environment.

The simulation led to the following steady state values for the most important variables: temperature of fresh feed entering reactor riser T_2 = 362.98^{0}C, furnace firebox temperature T_3 = 877.77^{0}C, inventory of catalyst in the reactor W_r = 36396 kg, reactor fractionar pressure P_5 = 1.573 bara, wet gas compressor suction pressure P_7 = 1.498 bara, temperature of regenerator bed T_{reg} = 692.72^{0}C, weight fraction of coke on regenerated catalyst crgc = 4.4. 10^{-4}, inventory of catalyst in the regenerator W_{reg} = 175551 kg, inventory of carbon in the regenerator W_{reg} = 806.8 kg, mass fraction of gasoline y_G = 0.46, mass fraction of gas oil y_F = 0.29, regenerator pressure P_6 = 2.308 bara, combustion air blower discharge pressure P_2 = 2.928 psia, weight fraction of coke on spent catalyst csc = 7.87.10^{-3}, reactor temperature T_{st} = 533.45^{0}C, cyclone temperature T_{cyc} = 972.2^{0}C, molar ratio of oxygen to air in stack gas xO2sg = 0.03566, air flowrate into regenerator Ft = 42.01 kg/s.

The above steady state point was used as a starting state for demonstrating the dynamic characteristics of the model. Several dynamic runs were performed by implementing preprogrammed disturbances on coking characteristics of the fresh feed (Run 1) and ambient temperature (Run 2). A step change of +1% amplitude in coking rate constant at t = 1000 s was generated for Run 1 and a +17^{0}C ramp change (starting at t = 300 s and ended at t = 3900 s) was performed for Run 2. These disturbances are usually encountered in commercial FCS units. The simulation results for some of the most important variables of the process are presented in Fig. 1 for Run 1 and Fig. 2 for Run 2.

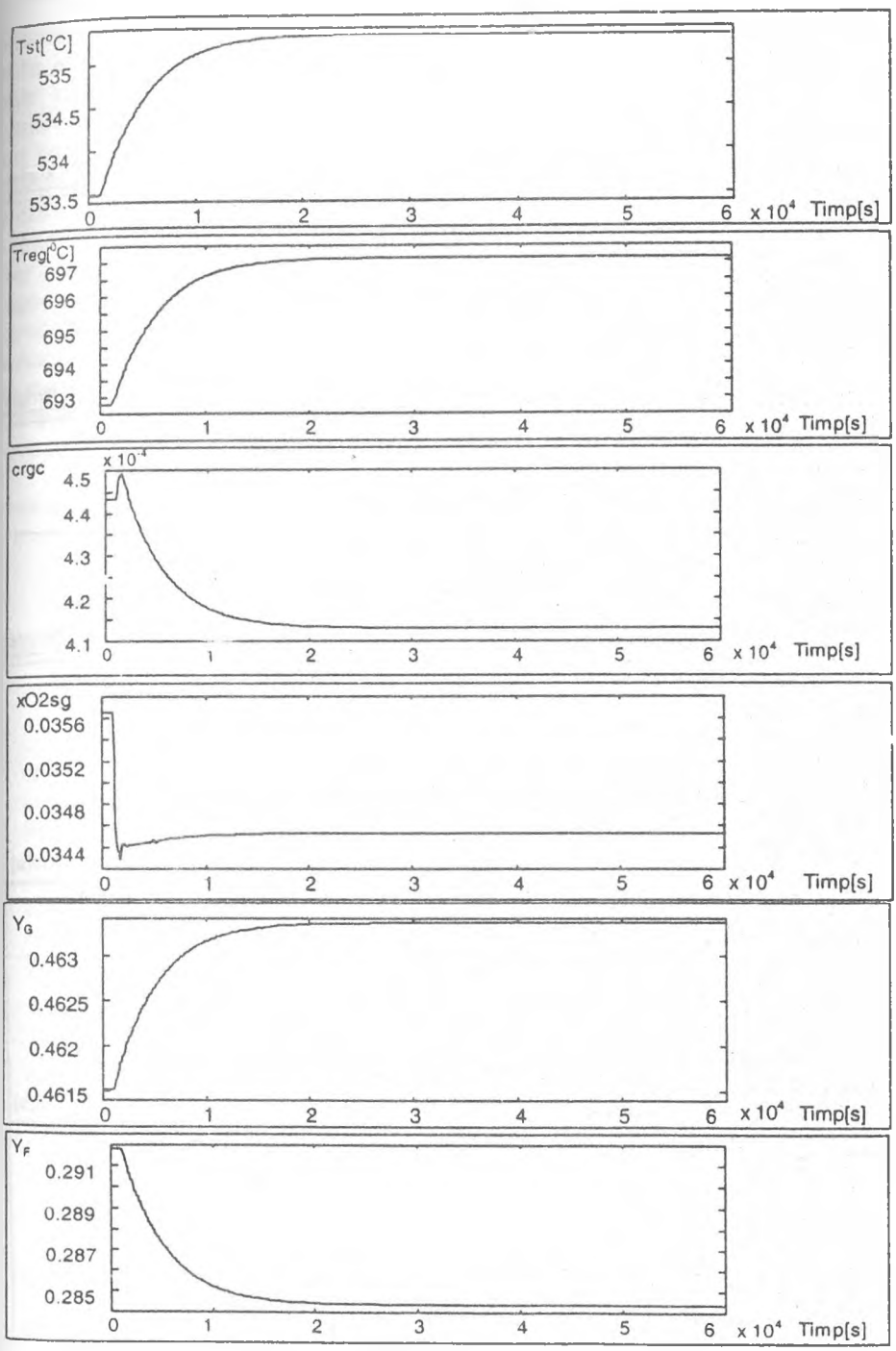

Figure 1. Simulation results for Run 1

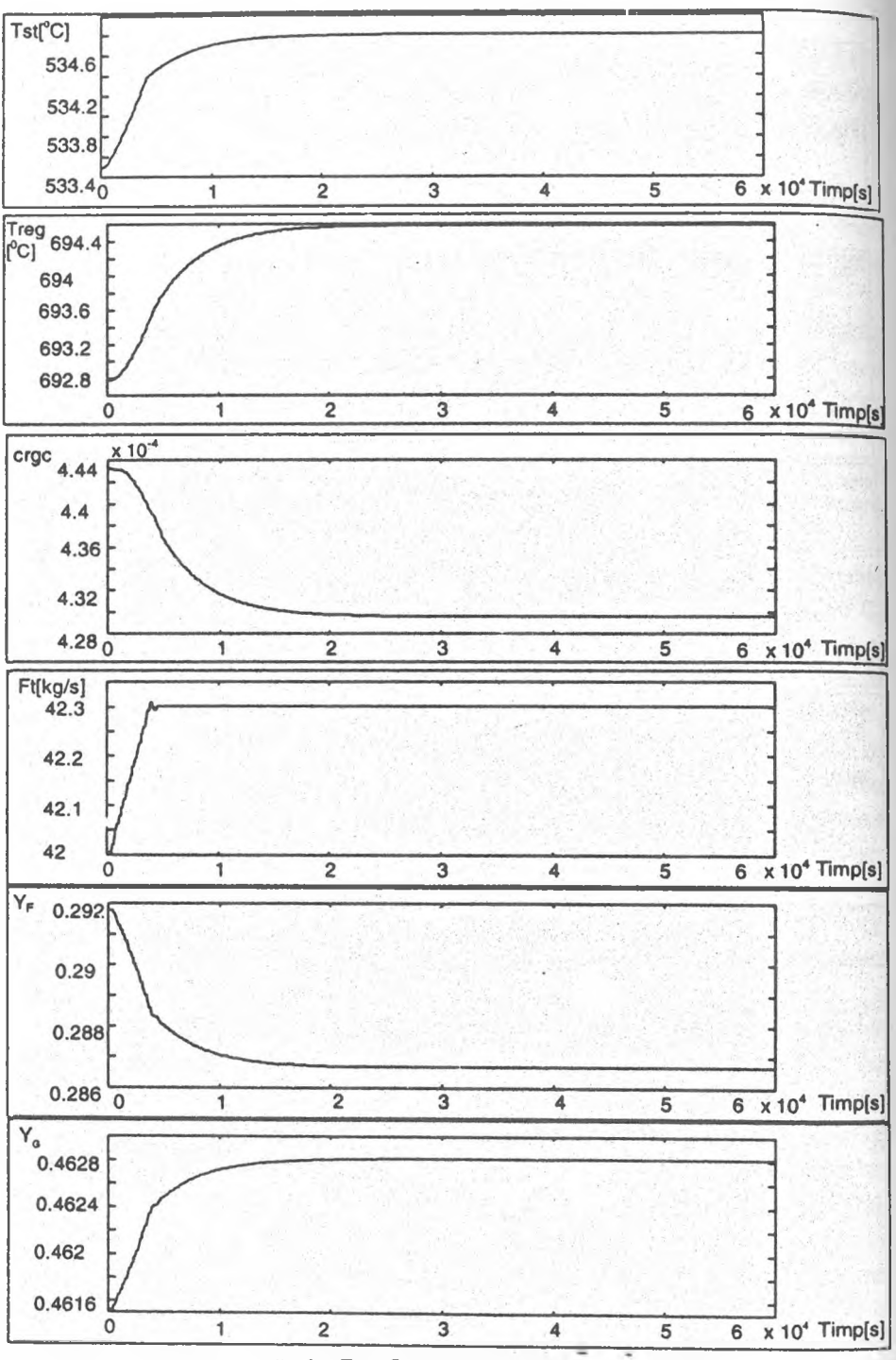

Figure 1. Simulation results for Run 2

The simulation reveals the complex dynamic behaviour that FCC process presents. For example in the case of Run 1, the increase in coking rate constant results in a rapid increase in coke deposition on spent catalyst which determines higher amounts of coke transported in the regenerator. The combustion in the regenerator intensifies resulting in higher regenerator temperature (T_{reg}). For a short time the concentration of coke on regenerated catalyst (crgc) peaks (small time constant), but as the combustion rate increases (larger time constant) more of the coke transported from the reactor is consumed and the concentration of coke on regenerated catalyst declines. As the inlet air flow is maintained constant, the molar ratio of oxygen to air in stack gas xO2sg decreases. Higher regenerator temperature generates an increase in bed height which results in higher regenerated catalyst flow. This increased material flow transports more heat to the reactor causing reactor temperature T_{st} to rise until a new steady state is reached. The mass fraction of gasoline y_G increases due to a higher cracking rate. All these main dynamic effects encountered in commercial FCCU's are well simulated by the above model.

The new dynamic model proves to be a useful tool for studying the complex dynamics of a large and difficult to control industrial unit offering the basis for studying advanced control strategies.

REFERENCES

1. McFarlane C., et al, *Computers and Chem. Engng.*, 3, 275-300.
2. Morari M., Agachi Ş., *Modeling and Control Studies on Model IV FCCUs*, Joint Research Project Between Chevron Research and California Institute of Technology, 1991.
3. Avidan A., Shinnar R., *Ind. Chem. Res.*, 1990, 29, 931-942.
4. Weekman V., *AIChE Journal*, 1970, 3, 397-404.
5. Hovd M., Skogestadt S., *AIChE Annual Meeting*, Nov., 1991.
6. Zheng Y., *Computers and Chem. Engng.*, 1994, 1, 39-44.

STUDIA UNIVERSITATIS BABEŞ-BOLYAI, CHEMIA, XLII, 1-2, 1997

MONOLACUNARY KEGGIN AND DAWSON-WELLS MOLYBDOTUNGSTO-PHOSPHATES WITH ORGANOMETALLIC FRAGMENTS[1]

MARIANA RUSU[2], LUMINIŢA SILAGHI-DUMITRESCU[2], CEZAR PAVEL[2], ADRIAN-RAUL TOMSA[2]

ABSTRACT. The reaction of Dawson and Keggin type polyoxometallates with organometallic chlorides $RECl_3$ (E = Sn, Si and R = butyl, phenyl, vinyl) lead to following complexes: $K_4[C_6H_5SnPMo_2W_9O_{39}]\cdot 14H_2O$ (1), $K_4[C_4H_9SnPMo_2W_9O_{39}]\cdot 14H_2O$ (2), $K_3[(C_2H_3Si)_2PMo_2W_9O_{40}]\cdot 17H_2O$ (3), $K_7[C_4H_9SnP_2MoW_{16}O_{61}]\cdot 15H_2O$ (5), $K_7[C_6H_5SnP_2MoW_{16}O_{62}]\cdot 14H_2O$ (4), $K_6[(C_2H_3Si)_2P_2MoW_{16}O_{62}]\cdot 15H_2O$ (6). Elemental analysis, thermal analysis, IR and UV spectra were used to characterise the new compounds.

INTRODUCTION

The remarcable structural properties of Mo, W and V containing polyoxometallates coroborated with properties permitting their use in ions exchange techniques, homogenous and heterogenous catalysis or in chemotherapy (antiviral or antitumor) stimulate the interest in the field. New interesting structures were reported lately on polyoxometallates with organometallic fragments [1-8, 10-14].

RESULTS AND DISCUSSION

Dawson and Keggin-type polyoxometallates were reacted with $RECl_3$ (E = Sn; R = Bu,Ph and E = Si, R = vinyl) in aqueous media. We obtained new polyoxometallates containing organometallic fragments of the type $[\{P\}ER]^{n-}$ (where {P} is $[PMo_2W_9O_{39}]^{7-}$ (P^1) and $[P_2MoW_{16}O_{61}]^{10-}$ (P^2)) as following equations:

$$K_7[PMo_2W_9O_{39}] + PhSnCl_3 \rightarrow K_4[PhSnPMo_2W_9O_{39}] + 3KCl$$

$$K_7[PMo_2W_9O_{39}] + BuSnCl_3 \rightarrow K_4[BuSnPMo_2W_9O_{39}] + 3KCl$$

$$K_7[PMo_2W_9O_{39}] + 2C_2H_3SiCl_3 + H_2O \rightarrow K_3[(C_2H_3Si)_2PMo_2W_9O_{40}] + 4KCl + 2HCl$$

---

[1] Dedicated to the distinguish Professor Ionel Haiduc on the occasion of his 60-th anniversary.

[2] Facultatea de Chimie şi Inginerie Chimică, Universitatea "Babeş-Bolyai", RO-3400 Cluj-Napoca, Romania.

$$K_{10}\left[P_2MoW_{16}O_{61}\right] + PhSnCl_3 \rightarrow K_7\left[PhSnP_2MoW_{16}O_{61}\right] + 3KCl$$

$$K_{10}\left[P_2MoW_{16}O_{61}\right] + BuSnCl_3 \rightarrow K_7\left[BuSnP_2MoW_{16}O_{61}\right] + 3KCl$$

$$K_{10}\left[P_2MoW_{16}O_{61}\right] + 2C_2H_3SiCl_3 + H_2O \rightarrow K_6\left[(C_2H_3Si)_2P_2MoW_{16}O_{62}\right] + 4KCl + 2HCl$$

During the reaction a MO^{4+} unit (M = Mo,W) is replaced by a RE^{3+} organometallic moiety; the hole is acting as a tridentate/pentadentate ligand, the element E becoming tetra- or hexa-coordinated, respectively.

The composition of the new compounds was establihed on the basis of the elemental analysis (the content in K, Mo, W, Si, Sn determined by AAS) and thermal analysis (the content in water).

The IR spectra exibit the characteristic bands for both polyoxometallates units [1,2] and organometallic fragments [18]. The assignement and the position of the important bands are presented in Table 1.

Table 1. IR Spectra of the title compounds

	Compund							
	P^1	1	2	3	P^2	4	5	6
	ν (cm^{-1})	ν (cm^{-1})	ν (cm^{-1})	ν (cm^{-1})	ν (cm^{-1})	ν (cm^{-1})	ν (cm^{-1})	ν (cm^{-1})
ν_{as} P-O(1)	1065 1022	1090 1040	1085 1035	1085 1025	1087 1055 1022	1090 1070 1025	1100 1070 1025	1095 1065 1025
ν_{as} M-$O_{(4)}$ or ν_{as} M-$O_{(6)}$	940 900	965 910	965 930	960 940	945 920	940 910	955 920	950 920
ν_{as} M-$O_{(2)}$-M	880 830	890 810	870 820	890 835	890 820	880 820	895 825	885 820
ν_{as} M-$O_{(3)}$-M	795 750 730	790 740 720	800 750 725	790 750 715	770 740 705	785 740 710	805 730	790 750 700
δ $O_{(1)}$-P-$O_{(1)}$	625	620	605	620	605 575	610 580	600 570	605 565
δ M-O-M	510	515	510	515	530 495 475	550 520 480	535 485 475	535 475
δ (phenyl)	-	460	-	-	-	460 480	-	-
ν_{as} Sn-O-Sn	-	790 740 705	800 745 720	-	-	660	665	-
ν_{as} C-Sn-O	-	-	665 630 615	-	-	-	600	-
ν_{sym} C-Sn-O	-	407	425	-	-	410	425	-
ν_{as} C-Si-O	-	-	-	1120	-	-	-	1120
ν_{as} O-Si-O	-	-	-	1060	-	-	-	1060
ν C=C	-	-	-	1640	-	-	-	1640

The UV spectra recorded in the range 50000-28000 cm^{-1} (350-200 nm) on aqueous solution exhibit bands atom expected positions for polyoxometallates, as shown in Table 1.

The electronic transitions of the phenyl group (around 38000 cm^{-1}) are superposed with the transitions characteristic for the polyoxometallate fragment. The other organic groups (butyl and vinyl) do not exibit electronic transitions in the range of the recorded spectra.

Thermal behavior. Thermogravimetric curves were recorded for all the polyoxometalates with organometallic fragments. The first important process is the weight loss accompanied by endothermal effect at temperatures in the range 40-240^{0}C. This corresponds to the elimination of water molecules; the loss of zeolitic-type molecules of water and the loss of nonzeolitic-type molecules, without the possibility to evaluate in a quantitative way their individual contribution. Therefore the weight loss noticed in this part of curves was used to calculate the total wather content (see experimental part).

Table 1. UV Spectra of the title compounds

	Compund			
	P^1	1	2	3
	ν (cm^{-1})	ν (cm^{-1})	ν (cm^{-1})	ν (cm^{-1})
ν_1 (charge transfer M-O-M)	41600 37700	42700 38000	42200 27800	42600 38200
ν_2 (charge transfer M-$O_{(4)}$)	46800	47500	47400	47400
	P^2	4	5	6
	ν (cm^{-1})	ν (cm^{-1})	ν (cm^{-1})	ν (cm^{-1})
ν_1 (charge transfer M-O-M)	41700 33300	40800 34000	41100 34500	41400 34600
ν_2 (charge transfer M-$O_{(4)}$)	46416	46900	47080	46950

The next important process observed at 200-350^{0}C is related to changes in the polyanionic moiety, as reported for other reprezentatives of this class of compounds [9].

After 380^{0}C in all cases, after the combustion of the organic components, the inorganic residue exhibits some minor exothermal effect probably due to polymorphic transformation.

EXPERIMENTAL

The heteropolyoxometallates $K_7[PMo_2W_9O_{39}]\cdot 13H_2O$ (P^1) and $K_{10}[P_2MoW_{16}O_{61}]\cdot 19H_2O$ (P^2), were prepared according the literature data [15-17]. Organostatic and silicoorganic derivatives are comercial samples (Aldrich).

Thermal analysis was performed using a OD-102 System Paulik-Paulik-Erdely derivatograph. UV spectra were recorded on a SPECORD UV-75 in aqueous solution and IR spectra using a SPECORD IR-75 spectrophotometer on KBr pellets. Atomic absorbtion was used to determine the composition of the synthesised compounds (K, W, Mo, P, Si, Sn). The content in water was estimated on the basis of thermal analysis.

General procedure. Heteropolyoxometallates and organometallic stananes and silanes were reacted in 1:1 molar ratio, in water. The solution of organometallic compounds in water was treated with AcONa to get a pH value of 1.5. For some experiments an opalescence occured wich did not affect the reactivity. The soechiometric amount of solid heteropolioxometallates was added to the above prepared solution under vigurous stirring. A clear solution are obtained after several minutes. The pH of mixture rise up to 4.5 for Dawson type compounds and 5 for Keggin type compounds. Unreacted ligand was filtered after 10 to 30 minutes. Fine powder of potasium chloride was added to filtrate until no precipitation was observed. The white crystals were filtered and the precipitates washed with satured solution of KCl and dried in a vacuum desicator. The compounds were recrystallized from water at 40-50^{0}C. The filtrates afforded crystalline products by treatement with EtOH (diffusion method).

$K_4[C_6H_5SnPMo_2W_9O_{39}]\cdot 14H_2O$; $K_4C_6H_{33}SnPMo_2W_9O_{53}$ (3106,579)
Calcd.: K 5,02%; W 53,28%; Mo 6,18%; P 0,99%; Sn 3,82%; H_2O 8,18% .
Found : K 5,20%; W 50,45%; Mo 5,89%; P 0,68%; Sn 3,86%; H_2O 8,02%.

$K_4[C_4H_9SnPMo_2W_9O_{39}]\cdot 14H_2O$; $K_4C_4H_{37}SnPMo_2W_9O_{53}$ (3086,591)
Calcd.: K 5,06%; W 53,63%; Mo 6,22%; P 1,00%; Sn 3,25%; H_2O 8,23%.
Found: K 5,15%; W 51,10%; Mo 6,02%; P 0,89%; Sn 3,90%; H_2O 8,10 %.
$K_3[(C_2H_3Si)_2PMo_2W_9O_{40}]\cdot 17H_2O$; $K_3C_4H_{40}Si_2PMo_2W_9O_{57}$ (3051,995)
Calcd.: K 4,27%; W 60,28%; Mo 6,99%; P 1,13%; Si 2,04%; H_2O 11,15%.
Found : K 4,40%; W 58,26%; Mo 6,80%; P 1,06%; Si 1,98%; H_2O 11,00%.
$K_7[C_6H_5SnP_2MoW_{16}O_{61}]\cdot 14H_2O$; $K_7C_6H_{33}SnP_2MoW_{16}O_{75}$ (4798,344)
Calcd.: K 5,69%; W 61,33%; Mo 2,00%; P 1,29%; Sn 2,47%; H_2O 5,26%.
Found: K 5,78%; W 58,80%; Mo 1,75%; P 1,08%; Sn 2,35%; H_2O 5,10%.
$K_7[C_4H_9SnP_2MoW_{16}O_{61}]\cdot 15H_2O$; $K_7C_4H_{39}SnP_2MoW_{16}O_{76}$ (4796,732)
Calcd.: K 5,85%; W 61,36%; Mo 1,80%; P 1,29%; Sn 2,48%; H_2O 5,65%.
Found: K 5,85%; W 59,65%; Mo 1,80%; P 1,15%; Sn 2,28%; H_2O 5,45%.
$K_6[(C_2H_3Si)_2P_2MoW_{16}O_{62}]\cdot 15H_2O$; $K_6C_4H_{36}Si_2P_2MoW_{16}O_{77}$ (4707,728)
Calcd.: K 4,98%; W 62,50%; Mo 2,04%; P 1,32%; Si 1,19%; H_2O 5,74%.
Found: K 5,02%; W 60,90%; Mo 1,90%; P 1,22%; Si 1,06%; H_2O 5,58%.

CONCLUSIONS

The spectral data suggest that both, Keggin and Dawson heteropolyoxometallates reacted with organometallic chlorides to give six new heteropolyoxometallates with organometallic fragments.

REFERENCES

1. F. Xin, M. T. Pope, *Organometallics*, 1994, 13, 4881.
2. F. Xin, M. T. Pope, *Inorg. Chem.*, 1996, 35, 1207.
3. B. H. Rapko, M. Pohl, R. G. Finke, *Inorg. Chem.*, 1994, 33, 3625.
4. M. Pohl, D. K. Lyon. N. Mizuno, K. Nomiya, R. G. Finke, *Inorg. Chem.*, 1995, 34, 1413.
5. M. Pohl, I. Lin, T. J. R. Weakley, K. Nomiya, M. Kaneko, H. Weiner, R. G. Finke, *Inorg. Chem.*, 1995, 34, 767.
6. F. Xin, M. T. Pope, *Inorg. Chem.*, 1996, 35, 5693.
7. A. Mazeaud. N. Aminari, F. Robert, R. Thouvenot, *Angew. Chem. Int. Ed. Engl.* 1996, 35(17), 1961-1964.
8. K. Nomya, M. Kaneko, N. C. Kasuga, R. G. Finke and M. Pohl, *Inorg. Chem.*, 1994, 33, 1469.
9. G. A. Tsiganos, C. J. Hullada, *J. Inorg. Chem.*, 1978, 17, 134.
10. W. H. Knoth, *J. Am. Chem. Soc.*, 1979, 101, 2211.
11. F. Zonnevijlbe, M. T. Pope, *J. Am. Chem. Soc.*, 1979, 101, 2731.
12. R. G. Finke, D. K. Lyon, K. Nomiya, S. Sur, N. Mizuno, *Inorg. Chem.*, 1990, 29, 1784.
13. R. G. Finke, C. A. Gren, B. Rapko, *Inorg. Synth.*, 1990, 27, 128.
14. W. H. Knoth, *J. Am. Chem. Soc.*, 1979, 101, 759-760.
15. R. Contant, J. M. Fruchart, G. Hervé, A. Tézé, *C.R.(Paris)*, 1974, C 278, 195.
16. J. P. Massart, R. Contant, J. M. Fruchart, J. P. Ciabrini, M. Fourier, *Inorg. Chem.*, 1977, 16, 2916.
17. R. Contant, J. P. Ciabrini, *J. Chem. Res. (M)*, 1977, 2601.
18. N. B. Colthup, L. H. Daly, S. E. Wiberley, *"Introduction to Infrared and Raman Spectroscopy"* Academic Press, New York, 1964.

STUDIA UNIVERSITATIS BABEŞ-BOLYAI, CHEMIA, XLII, 1-2, 1997

THE MASS-SPECTROMETRY STUDY OF SOME SPIRO-1,3-DIOXANE ESTERS

MIHAI HORN[1], SORIN MAGER[1], ION GROSU[1], NICOLAE PALIBRODA[2]

ABSTRACT. The electron impact-induced fragmentation of a series of spiro 1,3-dioxanes has been studied by exact mass measurements and metastable ion analysis. A comparison with the fragmentation pattern of monocyclic 1,3-dioxane compounds bearing similar ester groups has been developed.

INTRODUCTION

Many 1,3-dioxane derivatives have been synthesised and their structure has been investigated by NMR spectra, dipole-moments measurements, I.R. spectrometry and thermodynamic methods [1]. However the interest for the mass-spectrometry investigations of this type of compounds has been small, few papers [2-11] being published in this field.

As a continuation of our investigations [12-14] on the mass-spectrometry of some monocyclic 1,3-dioxane it was considered of interest to study the E. I. (electron impact) fragmentation pathways of some ethyloxycarbonyl-spiro-1,3-dioxane derivatives (Scheme 1). The synthesis and the investigations on the stereochemistry of these compounds have been already reported [15-17].

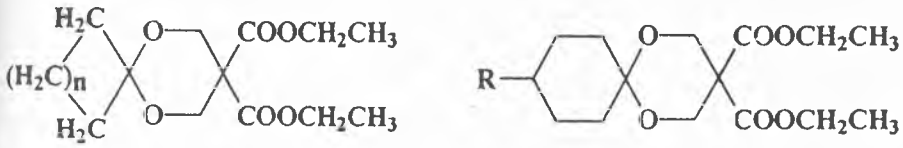

n=1	1	R=H	3
n=2	2	R=CH_3	5
n=3	3	R=*t*-C_4H_9	6
n=4	4	R=C_6H_5	7

Scheme 1

[1] "Babeş-Bolyai" University, Organic Chemistry Department, 11 Arany Janos str., RO-3400, Cluj-Napoca, România.
[2] Institute of Isotopic and Molecular Technology, P. O. Box 700, Cluj-Napoca, România.

EXPERIMENTAL

The EI mass spectra have been recorded at 70 eV with a MAT 311 mass spectrometer. Samples were introduced through the indirect inlet system at temperatures between 100 and 150°C, the ion source temperature was 150°C. Accurate mass measurements were made at a resolution $\Delta m/m$ = 5000. Metastable transitions were registered using the mass-analysed ion kinetic energy (MIKE) technique for metastable ion transitions in the second field-free region before the electrostatic deflection and highvoltage techniques.

RESULTS AND DISCUSSION

The relative abundance of the ions formed in the fragmentation process (E.I. at 70 eV) of compounds ***1-7*** are shown in Table 1.

Based on exact mass measurements [ions: g(g'), 245; b, 244; p, 173; c, 172; o, 145; h, 129; r(r'), 99; m(m'), 55] and metastable transitions (12-16, 20, 31, 33) the principal mass spectral fragmentations of compound ***1*** are interpreted according to schemes 2-4. Common routes with those observed for monocyclic compounds [14] could be recovered in these schemes.

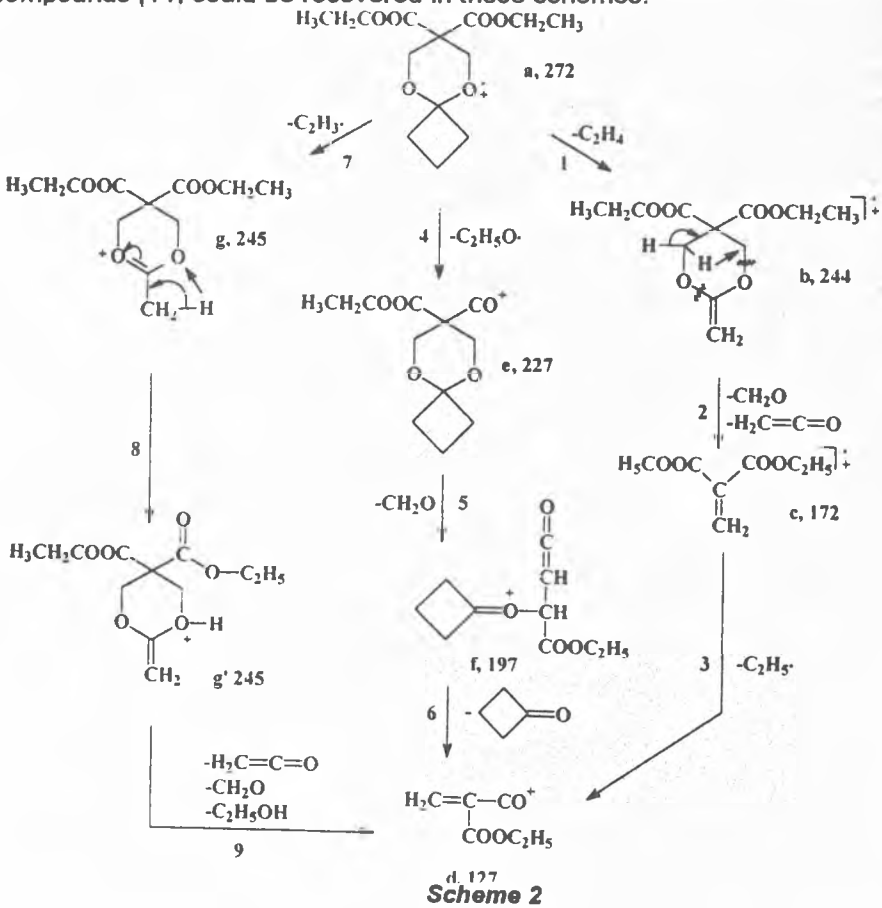

Scheme 2

Table 1. 70 eV mass-spectra of compounds 1-7: m/z(relative intensity, %)

Compound	M^{+}	$(M-45)^{+}$	$(M-75)^{+}$	257	Base peak	Other important peaks
1	272 (0.0)	227 (13.0)	197 (0.0)	(1.5)	59	245(12.5), 244(60.0), 173(12.5), 172 (33.5), 157(4.0), 127(66.5), 113(14.0), 101(20.5), 99 (33.5), 85(22.0), 83(20.5), 73(5.5), 70(11.5), 55 (34.5).
2	286 (18.0)	241 (8.0)	211 (2.0)	(87.5)	55	258(24.0), 173(13.5), 157(2.5), 145(2.5), 139 (6.0), 129(7.0), 127(70.5), 113(7.0), 101 (6.0), 99(27.0), 85(26.5), 84(32.5), 83(23.0), 73(3.5), 71(3.0), 69(5.0), 67(5.0), 59(92.0), 57(13.0).
3	300 (30.5)	255 (7.0)	225 (3.0)	(98.0)	55	271(12.5), 258(23.0), 172(11.0), 157(2.0), 145 (2.0), 139(4.5), 129(9.0), 127(7.0), 113 (5.5), 101(5.5), 99(29.5), 98(23.0), 97(5.5), 85 (11.0), 83(12.5), 81(6.5), 73(3.0), 70 (12.5), 69(34.0), 59(81.0), 57(9.0), 56(22.5).
4	314 (24.5)	269 (7.0)	239 (2.0)	(75.0)	55	285(5.0), 258(15.0), 173(20.0), 157(2.0), 145(2.0), 139(5.0), 129(9.0), 128(7.0), 113 (9.0), 112(21.0), 105(11.5), 101(5.5), 99 (29.0), 97(5.5), 95(5.5), 85(23.0), 84(25.0), 83(23.0), 81(4.5), 73(5.5), 71(3.5), 70(6.0), 69(26.5), 68(33.5), 67(8.0), 59(85.0), 57 (15.0), 56(35.0).
5	314 (6.1)	269 (4.9)	239 (1.8)	(100)	257	285(2.2), 173(3.5), 139(2.7), 129(4.47), 128 (2.2), 127(30.4), 113(2.2), 112(2.3), 99(5.3), 85 (2.5), 84(1.5), 83(4.0), 69(2.9), 67(1.3), 59 (16.1), 57(2.1), 56(2.7), 55(16.5).
6	356 (1.9)	311 (4.1)	281 (1.1)	(100)	257	341(1.0), 299(4.6), 285(7.7), 259(2.3), 258 (13.8), 203(3.4), 173(2.8), 139(1.5), 138 (1.4), 129(3.6), 128(1.8), 127(23.3), 113 (1.3), 101 (1.0), 99(4.6), 98(4.0), 97(2.4), 85(2.2), 83(2.6), 81(1.6), 69(3.9), 67(1.3), 59(11.4), 57(7.3), 56 (1.3), 55(8.2).
7	376 (0.7)	331 (6.3)	301 (2.1)	(100)	257	332(1.4), 299(2.1), 259(4.7), 258(31.2), 244(9.63), 243(1.47), 175(1.1), 174(5.8), 173(5.4), 172(4.5), 167(1.1), 157(3.8), 149 (3.1), 146(1.3), 145(3.9), 139(2.5), 131(2.8), 130(5.8), 129(16.6), 128(4.4), 127(46.9), 119 (5.7), 118(3.3), 117(5.6), 113(2.2), 105(2.8), 104(14.7), 103(2.7), 101(2.3), 99(9.1), 91 (11.5), 85(3.2), 83(3.0), 81(1.1), 78(1.9), 77(1.6), 73(1.6), 71(1.5), 69(2.7), 59(23.6), 57(3.7), 56(2.1), 55(14.8).

Notes:

Intensity as % of the base peak (into brackets).
Ions below m/z 50 and lower than 2% are not included, except mechanistically relevant peaks.

Based on exact mass measurements [ions: g(g'), 245; b, 244; p, 173; c, 172; o, 145; h, 129; r(r'), 99; m(m'), 55] and metastable transitions (12-16, 20, 31, 33) the principal mass spectral fragmentations of compound ***1*** are interpreted according to schemes 2-4. Common routes with those observed for monocyclic compounds [14] could be recovered in these schemes.

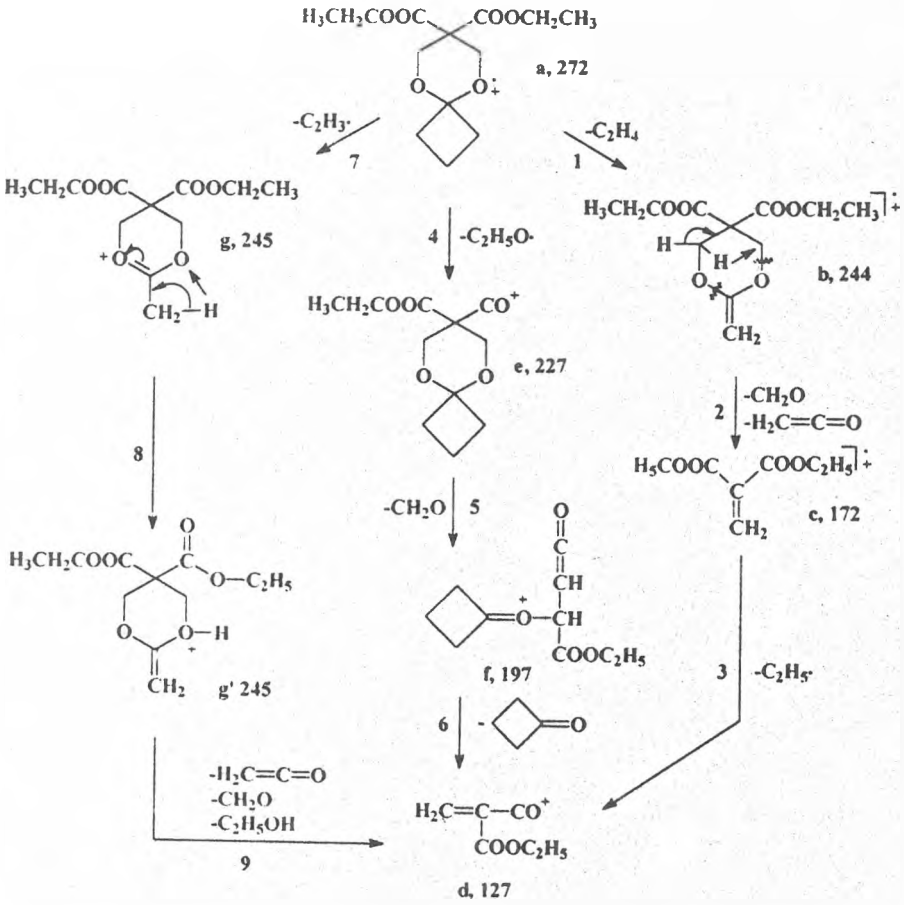

Scheme 2

The mass spectral fragmentation of the other investigated spiro 1,3-dioxanes involves some other peculiar aspects (Schemes 5 and 6).

The fragmentations 41 and 42 has a low importance for compound ***1*** [the abundance of ion m/z = 257 is small (1.5%)], but their importance increases with the number of atoms of the carbocycle (compounds ***2-4***) arriving to generate the base peak (m/z = 257) for the compounds bearing substituted cyclohexane rings. The increasing of the number of carbon atoms in the carbocycle stabilises the molecular peak (the relative intensity are ***1***: 0.0%, ***2***: 18.0%, ***3***: 30.5% and ***4***:

24.5%), while the substitution of the carbocycle leads to smaller intensities for the molecular peak (e.g. compound 7: 0.7%). This diminution is associated with a rapid fragmentation of the substituent located on the cyclohexane ring and its value is correlated with stability of the radical generated by the substituent of the cyclohexane ring [the peak $(M-R)^+$ was observed in the spectra of these compounds, Table 1].

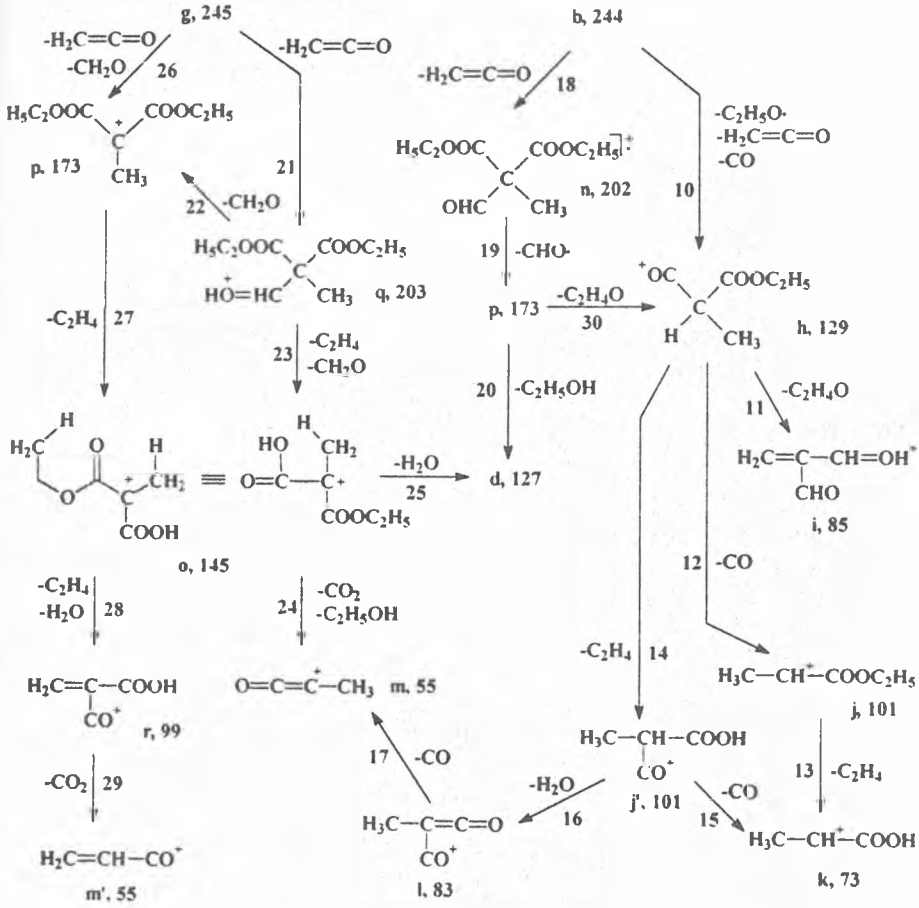

Scheme 3

Elimination of CH_2O and/or CO is a common process (showed for monocyclic 1,3-dioxanes too) for obtaining ions that keep unaltered the 1,3-dioxane system. The ions showing the OC_2H_5 group exhibit three competitive fragmentations: the loss of ethylene (probably, through a McLafferty process), elimination of a molecule of C_2H_4O and the expulsion of a molecule of ethanol.

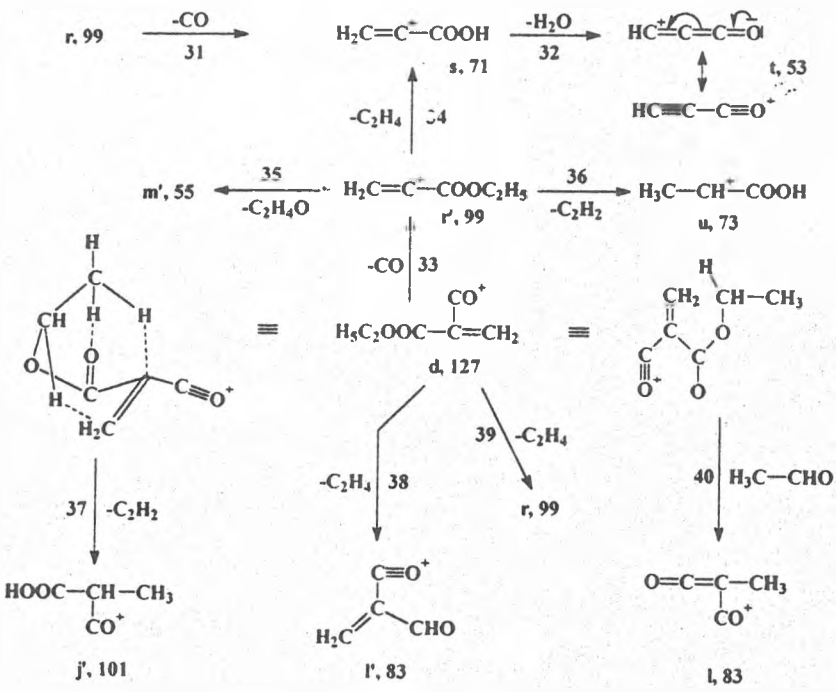

Scheme 4

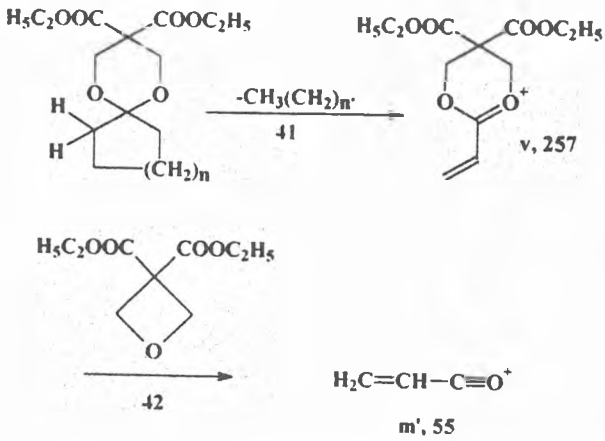

Scheme 5

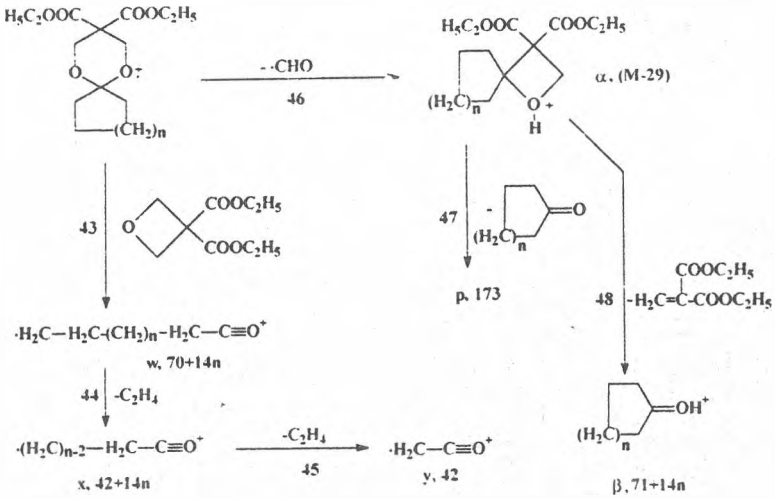

Scheme 6

THE MASS-SPECTROMETRY STUDY OF SOME SPIRO-1,3-DIOXANE ESTERS

The mass-spectrometry of some spiro-1,3-dioxanes is discussed using a comparison with the results obtained on the study of some similar monocyclic 1,3-dioxane derivatives.

Mihai Horn, Sorin Mager, Ion Grosu and Nicolae Palibroda

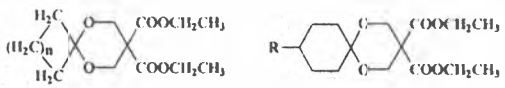

n=1-4 R=Me, Ph, *t*-Bu

REFERENCES

1. M. J. O. Anteunis, D. Tavernier and F. Borremans, Heterocycles, (1976), 4, 293.
2. J. E. Collin and G. Conde, Bull. Acad. R. Belg., (1966), 52, 978.
3. M. Vandewalle, N. Schamp and K. van Cauwenberghe, Bull. Soc. Chim. Belg., (1968), 33, 77.
4. F. Borremans and M. Anteunis, Bull. Soc. Chim. Belg., (1971), 80, 595.

5. D. Jeremic, V. Vajs, J. Bihalovic and S. Milosavijevic, Bull. Soc. Chim. Beogr., (1979), 44, 406.
6. D. Jeremic, V. Vajs, P. Rajkovic and S. Milosavijevic, Bull. Soc. Chim. Beogr., (1981), 46, 1.
7. D. Jeremic, V. Vajs, Z. Jovicic, P. Rajkovic and S. Milosavievic, Bull. Soc. Chim. Beogr., (1981), 46, 403.
8. D. L. Rakhmankulov, E. G. Galkin, E. M. Vyrpaev, R. K. Nurieva, A. M. Syrkin and E. A. Kantor, Zh. Prikl. Khim. (Leningrad), (1978), 51, 1356.
9. G. B. Chalova, E. G. Galkin, E. M. Vyrypaev, E. A. Kantor, A. I. Naimushin, A. M. Syrkin and D. L. Rakhmankulov, Zh. Prikl. Khim. (Leningrad), (1981), 54, 369.
10. J. Witowska, H. Malikowska and H. Otwinowska, Chem. Anal. (Warsaw), (1985), 30, 853.
11. K. Pihlaja and J. Jalonen, Org. Mass Spectrom., (1971), 5, 1363.
12. S. Mager, R. Taranu, M. Horn and N. Palibroda, Studia Univ. "Babeş-Bolyai", Chem., (1982), 27, 45.
13. S. Mager, N. Polibroda, I. Grosu and M. Horn, Stud. Univ. "Babeş-Bolyai", Chem., (1983), 28, 14.
14. M. Horn, S. Mager, N. Palibroda and M. Culea, Org. Mass Spectrom., (1991), 26, 649.
15. S. Mager, I. Hopartean, M. Horn and I. Grosu, Stud. Univ. "Babeş-Bolyai", Chem., (1979), 24, 32.
16. I. Grosu, S. Mager, G. Plé and M. Horn, J. Chem. Soc. Chem. Commun., (1995), 167.
17. I. Grosu, S. Mager and. G. Plé, J. Chem. Soc. Perkin Trans. 2, (1995), 1351.

STUDIA UNIVERSITATIS BABEŞ-BOLYAI, CHEMIA, XLII, 1-2, 1997

AN EXTENDED HUCKEL MOLECULAR ORBITAL STUDY OF THE STRUCTURE OF MOO_2^{n+} (n = 1,2) GROUP

IOSIF GERGEN[1], IOAN SILAGHI-DUMITRESCU[2], IONEL HAIDUC[2]

ABSTRACT. Extended Huckel molecular orbital calculations on MoO_2^{+1} fragment show that the MoO bonds should have different lenghts, in variance to the MoO_2^{2+} units containing Mo(VI). The elongation of one of the MoO bonds is correlated with the shape of the HOMO and explain the transfer of the oxygen atom in certain redox reactions involved in biological systems.

INTRODUCTION

Modern EXAFS (extended X-ray absorbtion fine structure spectroscopy) studies performed on Mo containing enzymes like: xantin-oxydaze [1,2], xantin-dehidrogenaze [3] sulfit-oxydaze [3,4] and nitrat-reductaze [5], have shown that, in their oxidized form, the coordination sphere of Mo (VI) contains ligands with O, S or N in a pseudoctahedral environment. As models of these enzymes various MoO_2L_2 (L = polydentate ligands with oxygen, sulfur or nitrogen donor atoms) have been synthetized and characterized by spectral and crystallographic methods [6-9].

All of the MoO_2L_2 compounds and the above mentioned enzymes contain the MoO_2^{2+} group which is considered responsible for the reversible redox processes the Mo compounds or oxydo-reductazic enzymes can produce.

The structure of the MoO_2 unit in MoO_2L_2 compounds resembles that of the same group in oxydo-reductazic enzymes [3,8]. The lenght of the Mo = O bonds is about 1.70 A and the angle O = Mo = O is of 106^0 +/- 3^0 [8,9]. The group $[MoO_2]^{2+}$ has an angular structure, irrespective other L ligand are coordinated to Mo [8,9]. Due to this specific structure, in the compounds with octahedral coordination at Mo like MoO_2L_2 (L: bi-tri dentated with O, S, N ligand), the two oxygen atoms from the $[MoO_2]^{2+}$ group are always in a cis position.

The cis structure of $[MoO_2]^{2+}$ is due to the Mo (VI) specific electronic configuration, and is not influenced by other ligands. In order to see the influence of the OMoO bond angle on the properties of the group, EH molecular orbital calculations [10] have been undertaken on MoO_2^{2+}. The electronic structure of MoO_2^{2+}.moieties (M = U, Mo) has already been addressed by Hoffmann [11] which showed that the linear geometry of UO_2^{2+} is due to the inner shell 6p orbitals of U.

[1] Facultatea de Tehnologia Produselor Agroalimentare, Universtatea de Ştiinţe Agricole a Banatului, RO-1900, Timişoara, Romania.

[2] Facultatea de Chimie, Universitatea Babeş-Bolyai, RO-3400 Cluj-Napoca, Romania

Since in the oxydo-reductazic processes Mo^{VI} is transformed to Mo^{V} and probably a MoO_2^+ unit is intermediary formed, it would be of interest to investigate this cation to some more extent. In the present MO calculations we took advantage of the excellent graphical capabilities of the C.A.C.A.O. package of programs made available by Mealli and Proserpio [12].

RESULTS AND DISCUSSION

The experimental MoO bond length in MoO_2L_2 compounds varies between 1.683 and 1.709 A and the OMoO angle are in the 107.3-109.5^0 range [8,9]. In the model used in calculations we chose an average value of 1.700 A for the MoO bond and the OMO angle has been varied from 90 to 170^0 (see Figure 1 for the definition of the coordinates).

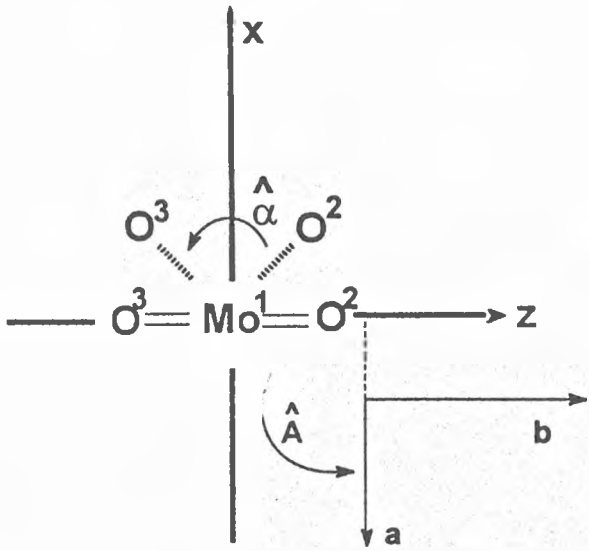

Figure 1. The orientation of the MoO_2 unit as required by C.A.C.A.O. Angle Â has been varied in 10 steps from 95° (α=170°) to 135° (α=90°).

Table 1 lists the changes in the total energy (E_{tot}) and in the reduced Mulliken population (Mo = O) with the OMoO bond angle.

These data show that the total energy has the lowest value at an OMoO angle of 110^0, where the reduced population is maximum. This angle is good agreement with the above cited experimental values [8,9] and confirms that the geometry of the MoO_2^{2+}. unit is determined rather by the electronic properties of the metal than by the surrounding ligands.

Table 1. The variation of total energy (Etot) and Mulliken Reduced Population (MRP) of $[MoO_2]^{2+}$ with the bond angle.

Step	OMoO angle (α)	$E_{tot.}$ (eV)	MRP Mo==O2 (3)
1	170	-312.797	.717
2	140	-312.915	.729
3	130	-312.967	.732
4	126	-312.985	.733
5	120	-313.007	.733
6	116	-313.016	.734
7	110	-313.017	.734
8	106	-313.006	.730
9	100	-312.965	.725
10	90	-312.788	.710

The $[MoO_2]^{2+}$ group from the compounds like MoO_2L_2 (L: ligant, tetradentated with 2N and 2O or 2S) can participate in redox reactions ***1*** when one the oxygen atoms is transferred to a proper acceptor X[5].

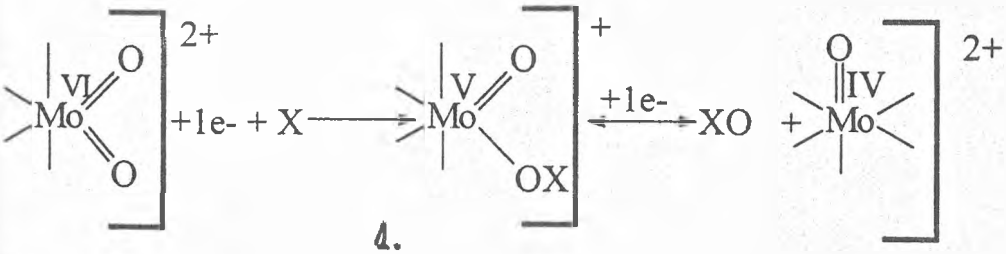

1.

Figure 2 gives the Walsh diagram for a hypothetical $OMo^{V}O$ unit (when the bond angle varies as above 135 to 95^0).

As can be noticed no minimum of the total energy is attained in case ***a***. An elongation of one of the MoO bonds (taken as 2.1 A to simulate a single bond) afforded however, the detection of a flat minimum for α = $115\text{-}130^0$. INDO and ab initio molecular orbital calculations on model MoO_2L (L = tetradentale ligands) [13] support this finding. In other words, the angular MoO_2^+ unit is stabilized if the MoO bonds become non equivalents (see Figure 2b for corresponding Walsh diagram).

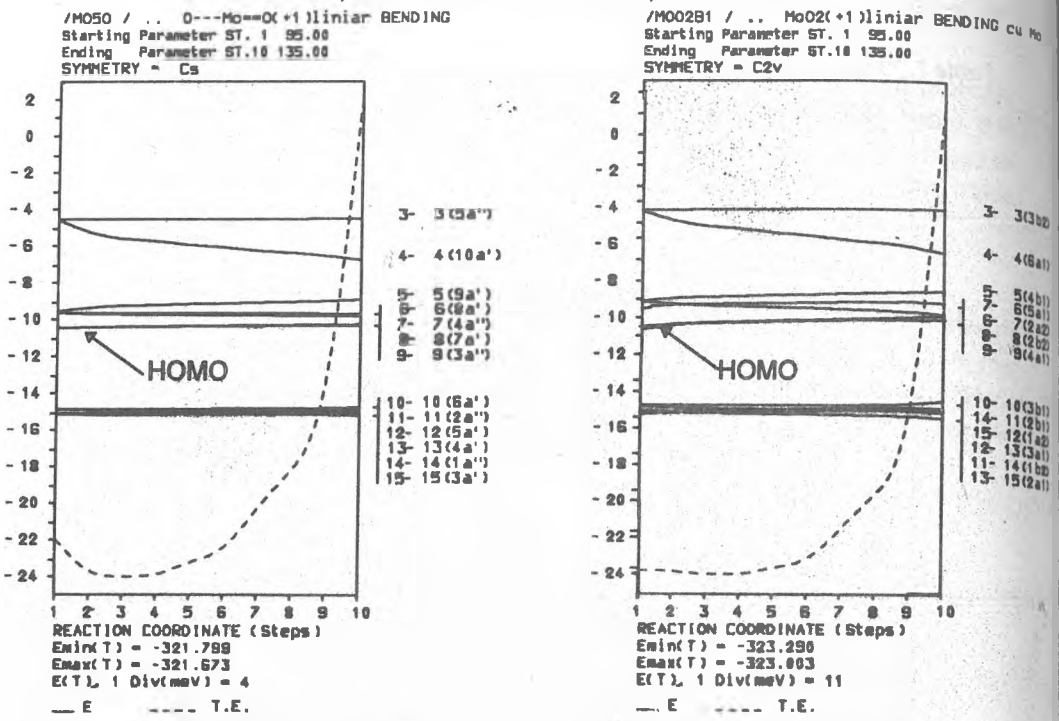

Figure 2. The Walsh diagram of OMo^{v}O system: ***a***) equal MoO bonds and ***b***) unequal MoO bonds

The HOMO of this system **2** (of π type) is located on molybdenum (d orbital) and on the oxygen atom (p orbital) of the longer MoO bond. This orbital is Mo-O antibonding and makes easier the breaking of this bond during a transfer like that mentioned in scheme ***1***.

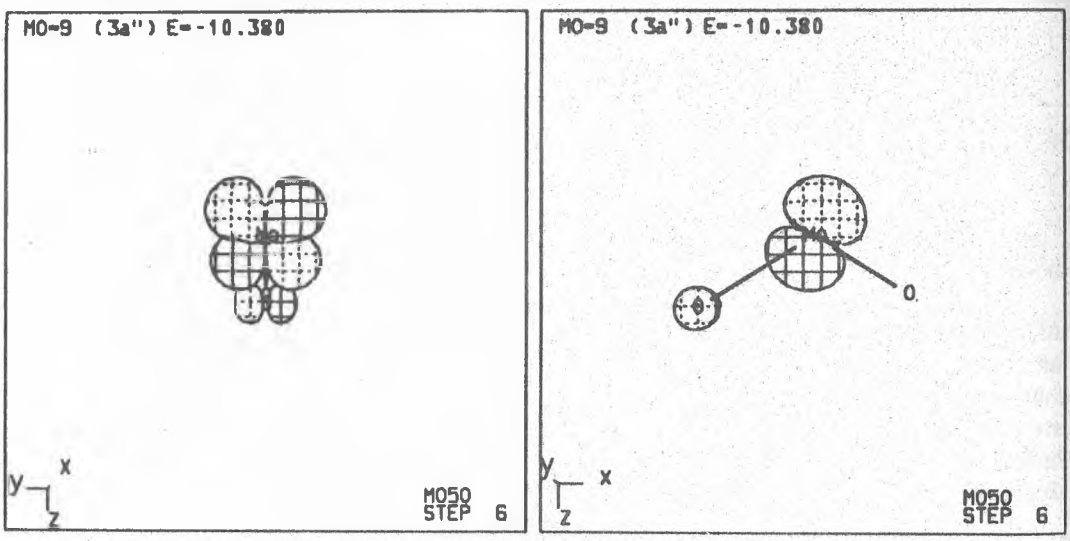

2

CONCLUSIONS

Both the structural data and the calculated geometries of MoO_2 group show that the optimal angle for the $[O = Mo = O]^{2+}$ group is 110^0, and is not influenced by the presence of another ligands attached to Mo. If the oxydation state of Mo changes from +5 to +6, the system is stabilized if the two MoO bonds are non equivalents and bond angle increases to $120\text{-}140^0$.

ACKNOWLEDGEMENTS

We thank dr. Mealli for providing us a copy of the C.A.C.A.O. package of programs.

REFERENCES

1. T. D. Tullius, D. M. Kurtz, S. D. Coradson and K. O. Hodgson, *J. Am. Chem. Soc.*, 1979, 101, 2776.
2. Bordas, R. C. Bray, C. D. Garner, S. Gutteridge and S. S. Hosnain, *Biochem. J.*, 1980, 191, 499.
3. S. P. Cramer, R. Wahl, and K. V. Rajagopalan, *J. Am. Chem. Soc.*, 1981, 103, 772.
4. S. P. Cramer, H. B. Gray and K. V. Rajagopalan, *J. Am. Chem. Soc.*, 1979, 101, 2772.
5. R. Hille, V. Massey, *Molybdenum Enzymes;* Spiro T. G. Editor; Wiley, New-York, 1985, p. 519.
6. J. L. Corbin, K. F. Miller, K. Pariyadath, S. Wherland, A. E. Bruce and E. I. Stiefel, *Inorg. Chim.* Acta, 1984, 90, 41.
7. J. H. Berg, D. Spiro, K. Wo, B. Mc Cord, B. Lye, M. S. Co, J. Belmont, C. Barnes, K. Kosydar, S. Roybuck, K. O. Hodgson, A. E. Bruce, J. L. Corbin, and E. I. Stiefel, *Inorg. Chim. Acta,* 1984, 90, 35.
8. J. H. Berg and K. O. Hodgson, *Inorg. Chim. Acta,* 1984, 90, 25.
9. C. J. Hinshaw, G. Peng, R. Singh, J. T. Spence, J. H. Enemark, M. Bruck, J. Kristofzski, S. L. Merbs, R. B. Ortega and P. A. Wexler, *Inorg. Chem.*, 1989, 28, 4483.
10. R. Hoffmann, J. Chem. Phys., 1969, 39, 1397.
11. K. Tasumi, and R. Hoffmann, Inorg. Chem., 1980, 19, 2656.
12. C. Mealli and D. M. Proserpio, *J. Chem. Ed.*, 1990, 67, 399.
13. G. Peng, J. Nichols, Ed. A. McCullough Jr. and J. T. Spence, *Inorg. Chem.*, 1994, 33, 2857.

STUDIA UNIVERSITATIS BABEȘ-BOLYAI, CHEMIA, XLII, 1-2, 1997

CONTRIBUTIONS TO THE KINETICS AND MECHANISM OF LACTIC AND MALIC ACIDS OXIDATION BY CHROMIC ACID

IOAN BÂLDEA[1], CLAUDIA MUREȘANU[1], ALEXANDRA RUSTOIU-CSAVDARI[1]

ABSTRACT. The stoichiometry, kinetics and mechanisms of chromium (VI) oxidation of lactic acid (H_2L) and malic acid (H_3M) have been studied under a relative high $HClO_4$ concentration. Keto acids are the reaction products. The oxidation has been found to follow a first-order dependence on both Cr(IV) and substrate and two parallel ways, first-order and second-order with respect to the hydrogen ion. Some free radicals are involved during the oxidation, formed in one-equivalent electron transfer between Cr(VI) and α-hydroxy acid. Activation parameters have been determined. The results are compared with those of related studies.

INTRODUCTION

The oxidation of various alcohols [1,2], α-hydroxy acids [3,4] and cooxidation of these classes of organic compounds and oxalic acid [5] by chromate in acidic media has been extensively studied. The mechanism elaborated by Westheimer and his co-workers [1a,2] for Cr(VI) oxidation of 2-propanol has served as a model for the oxidation of alcohols, aldehydes and acids for a long time. The oxidations of α-hydroxy acids as glycolic, lactic, malic, tartric, 2-hydroxy-2-methylpropionic yield keto acids under condition of a large excess of organic substrate, following the patterns of the oxidation of 2-propanol.

Srinavasan and Rocek [6] investigated the oxidation of oxalic acid by chromic acid and proved the formation and disappearance of a relatively stable chromium(V) intermediate during the reaction. They showed that chromium(V) resembles chromium(VI) in most of its kinetic properties, being only two to three times more reactive towards oxalic acid.

Krumpolc and Rocek [7] searched the direct involvement of Cr(V) into the oxidation of lactic acid. Another group of researchers [8] reported about Cr(VI) oxidation of lactic acid.

Haight and co-workers [9] in a study on lactic acid oxidation have presented kinetics and mechanism of the reaction of Cr(V) intermediates with a reducing substrate. The significant build up of chromium(V) has consequences for the interpretation of Cr(VI) oxidations. The way Cr(V) appears during Cr(VI)

[1] Universitatea "Babeș-Bolyai", Facultatea de Chimie și Inginerie Chimică, Str. Arany Janos nr. 11, 3400-Cluj-Napoca, Romania.

oxidation of α-hydroxy acids or other organic substrates involves an initial three-electron reduction of $HCrO_4^-$, producing the product by biequivalent path and free radicals that reduce additional Cr(VI) to Cr(V).

$$Cr(VI) + 2S \rightarrow CrS_2 \rightarrow Cr(III) + P + R^{\bullet} \quad (1)$$
$$R^{\bullet} + Cr(VI) \rightarrow P + Cr(V) \quad \text{fast} \quad (2)$$
$$Cr(V) + S \rightarrow Cr(III) + P \quad (3)$$

Rate laws for Cr(VI) decay usually involve terms first-order in substrate S at low concentrations, where reactions (1) requires two steps:

$$Cr(VI) + S \rightarrow Cr(IV) + P \quad (4)$$
$$Cr(IV) + S \rightarrow Cr\ (III) + R^{\bullet} \quad \text{fast} \quad (5)$$

and terms second-order in substrate at high concentrations in which reaction(1) may involve a one-step three-equivalent reduction of Cr(VI) by two molecules of coordinated substrate [4]. The step (5) differs from that suggested by Westheimer [1a,2] of creation of Cr(V) by the step:

$$Cr(VI) + Cr(IV) \rightarrow 2Cr(V) \quad (6)$$

This study using lactic and malic acids as substrates was undertaken to compare previous results [3,8,9] and to search for the involvement of free radicals. Unfortunately, the growth and decay of Cr(V) during the reaction cannot be monitored. Activation parameters were considered for comparison.

EXPERIMENTAL

Analytical grade potassium dichromate, perchloric acid, sodium perchlorate and high purity lactic and malic acids were used without further purification. Stock solutions of $HClO_4$, $NaClO_4$ and $KHCrO_4$ were prepared in twice distilled water, standardized by usual procedures and diluted to the requested concentration of each kinetic run. Fresh prepared solutions of lactic and malic acids were used for each set of runs.

The oxidation was followed spectrophotometrically at 350 nm in an 1 cm path length cell, maintained in the cell-holder provided with a temperature jacket and connected to a thermostat. Temperature was kept constant(± 0.05^{0}C). The reaction was started by injecting a known volume of Cr(VI) solution into the cell, containig α-hydroxy acid, $NaClO_4$ and $HClO_4$. Absorbance decay was read as a function of time.

The involvement of free radicals during the oxidation process was cherked by using the systems to initiale polymeration of buthylacrylate [10]. The stoichiometry of the reaction was found by spectrophotometrical titration [11]. Different mixtures with the molar ratio α-hydroxy acid: Cr(VI) between 0 and 5 were allowed to react for at least 10 half-lives and unreacted Cr(VI) was measured spectrophotometrically.

RESULTS AND DISCUSSION

Stoichiometry. The results of the experiments performed to establish the redox stoichiometry of Cr(VI) oxidation of lactic acid and hydrogen ion concentration of 0.0582 mol·dm^{-3} are shown in figure 1. Based on the break in absorbance at 350 nm, the molar ratio is lactic acid: Cr(VI) = 1.5: 1, proving that the product is pyruvic acid. A similar result has been obtained in the case of malic acid oxidation under the acidity of 0.87 mol·dm^{-3}. Thus, the formal, overall stoichiometry is:

$$CH_3CH(OH)CO_2 + 2Cr(VI) \rightarrow 3CH_3COCO_2H + 2Cr(III) \quad (7)$$

$$HO_2CCH_2CH(OH)CO_2H + 2Cr(VI) \rightarrow 3HO_2CCH_2COCO_2H + 2Cr(III) \quad (8)$$

with pyruvic acid and oxalacetic acid as the product of the oxidation respectively under the conditions of a quite high hydrogen ion concentration.

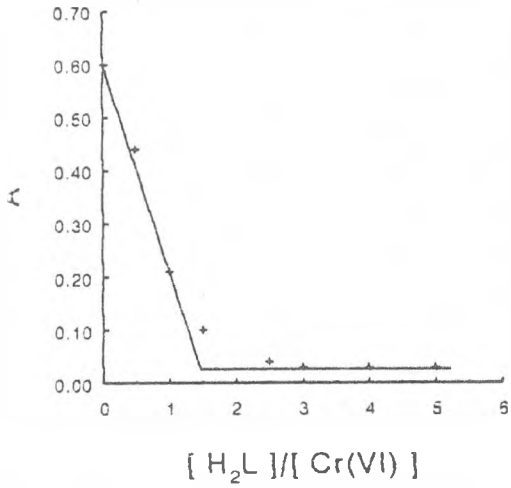

Fig. 1. The dependence of final absorbance on lactic acid: Cr(VI) molar ratio

Free radicals involvement. Although Bakore and Narain failed to identify free radicals using the induced reduction of mercury chloride [3a,12] when α-hydroxy acids were oxidated, Hasan and Rocek [4a] evidentiated the involvement of free radicals during the oxidation of glycolic acid by Cr(VI). Our results, using the initiation of polymerization of acrylic monomer confirms the involvement of free radicals during the oxidation of both the α-hydroxy acids investigated here.

Kinetics. Pseudo-first rate constants were obtained from the slope of the semilogarithmic plots, from absorbance measurements,

$$\ln(A - A_\infty) = \ln(A_0 - A_\infty) - k_{obs} \cdot t \quad (8')$$

for more than 95% of the reaction for both the α-hydroxy acids used, under a large excess of substrate and hydrogen ion concentration. Replicate runs gave the same slope. Three to four individual runs were performed under the same experimental conditios, giving rate constants within ± 3.0%. First-order rate coefficients were

determined using a least square procedure. The linear dependence (9) proves the first order with respect to the oxidizing species. Using large excesses of substrate (16.8-62.5 fold excess for malic acid and 140-563 fold excess for lactic acid) we did not obtain a reaction order larger than one with respect to the substrate, different from the work of Haight *at all* [9]. This is illustrated by the data in table 1.

The plot of k_{obs}, as a function of α-hydroxy acid concentration, are straight lines passing though the origin (figure 2). Therefore, the oxidation reaction follows a first order dependence with respect to the substrate for both cases. The lines in the graph in figure 2 are described by the equations:

$$k_{obs} = (2.32 \pm 4.74)\cdot 10^{-5} + (2.30 \pm 0.08)\cdot 10^{-2} \text{ for lactic acid } (r = 0.9993) \quad (9)$$
$$k_{obs} = (1.37 \pm 3.2)\cdot 10^{-5} + (3.76 \pm 0.05)\cdot 10^{-2} \text{ for malic acid } (r = 0.9999) \quad (10)$$

The intercepts could be considered zero, and the slopes give the second-order rate constants.

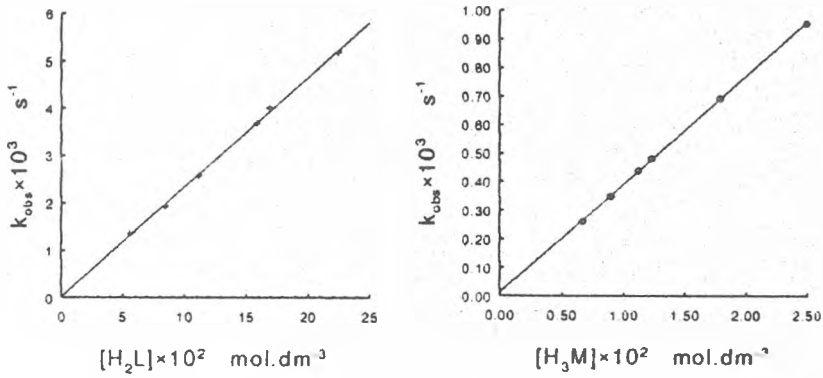

Fig. 2. The effect of α-hydroxy acid concentration on the pseudo-first-order rate coefficient

Table 1. The effect of α-hydroxy acid concentration on the first order rate coefficient. T = 298K, μ = 1.5 mol·dm^{-3}

$[H^+]$ mol·dm^{-3}	[Substrate]·10^2 mol·dm^{-3}	$10^3\cdot k_{obs}$ s^{-1}
0.582	Lactic acid	
	5.6	1.35
	8.5	1.93
	11.2	2.57
	15.9	3.67
	16.9	4.00
	22.5	5.17
1.46	Malic acid	
	0.67	0.261
	0.895	0.348
	1.12	0.438
	1.23	0.48
	1.79	0.689
	2.50	0.95

Table 2 reports the data concerning the effect of total hydrogen ion concentration on the rate. Because lactic and malic acids have the first acid dissociation constant of the order of 10^{-4} [13], we ignored the contribution of them to the total acidity, even at the lowest experimental values chosen.

Table 2. The effect of hydrogen ion concentration on the rate at 298K and μ = 1.5 $mol \cdot dm^{-3}$

Substrate and concentration $mol \cdot dm^{-3}$		$[H^+]$ $mol \cdot dm^{-3}$	$10^3 \cdot k_{obs}$ s^{-1}	$10^2 \cdot k$ $dm^3 \cdot mol^{-1} \cdot s^{-1}$
Lactic	0.048	0.086	0.049	0.102
	0.169	0.290	1.18	0.698
		0.436	2.47	1.46
		0.582	4.00	2.37
		0.775	6.79	4.02
		0.925	9.55	5.64
	0.048	1.15	4.09	8.53
Malic	0.00895	0.29	0.0317	0.354
		0.52	0.072	0.801
		0.87	0.145	1.62
		1.00	0.184	2.06
		1.25	0.265	2.96
		1.46	0.348	3.89
		1.5	0.365	4.08

A complex dependence has been found. The plots of $k/[H^+]$ (using second-order rate coefficient) versus $[H^+]$, presented in figure 3, fit linear functions, with intercepts, having the following equations(least-square):

$$k/[H^+]=(7.21\pm0.91)\cdot10^{-3}+(5.82\pm0.014)\cdot10^{-2}\cdot[H^+] \quad \text{for lactic acid} \quad (11)$$

$$k/[H^+]=(8.60\pm0.74)\cdot10^{-3}+(1.22\pm0.068)\cdot10^{-2}\cdot[H^+] \quad \text{for malic acid} \quad (12)$$

It shows the involvement of two parallel ways, one first-order and the other second-order with respect to the hydrogen ion, within the acid concentration range investigated. This finding is different from the rate law found in the case of alcohols oxidation as benzyl alcohol or cyclohexanol, where only one term, second-order on H^+ was obtained [10].

The effect of temperature on the rate was initially studied at constant α-hydroxy acids and hydrogen ion concentration over the range 288-308K. Table 3 presents the data. The experimental activation energies are somewhat larger than those found by Bakore and Narain [3a] in 10% acetic acid-water solutions, and similar to that for tartric acid [3b] oxidation in aqueous solution.

In order to deduce more information from the activation parameters, the dependence of the second-order rate coefficient on the hydrogen ion (see fig. 3) has been investigated again at 288 and 308 K and intercepts and slopes have been obtained. The results are included in Table 4. The accuacy has been evaluated by the errors propagation [14].

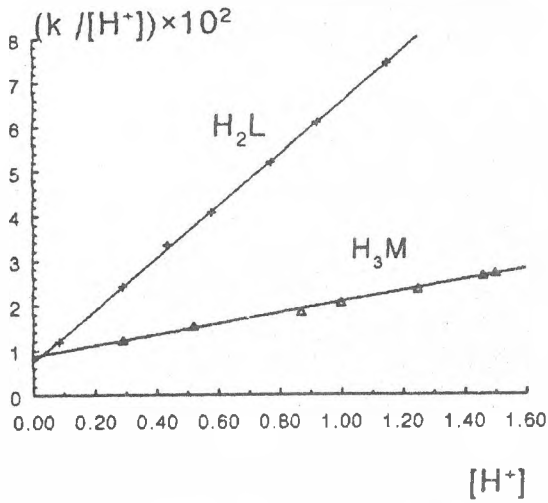

Fig. 3. Plot of $k(dm^3 \cdot mol^{-1} \cdot s^{-1})/[H^+]$ vs $[H^+](mol \cdot dm^{-3})$ at 298K

Table 3. The influence of temperature upon the rate coefficient

Substrate	[S] mol·dm^{-3}	[H$^+$] mol·dm^{-3}	T K	$10^3 \cdot k_{obs}$ s^{-1}	$10^2 \cdot k_2$ dm^3·mol^{-1}·s^{-1}	E_a kJ·mol^{-1}
Lactic acid	0.169	0.582	288	2.12	1.26	
			291	2.74	1.62	
			293	2.96	1.75	
			298	4.00	2.37	45.3±0.7
			303	5.35	3.16	
			308	7.68	4.55	
Malic acid	0.00875	0.87	288	0.0644	0.719	
			293	0.0962	1.08	
			298	0.145	1.12	49.2±0.8
			303	0.185	2.07	
			308	0.243	2.72	

Quite close activation enthalpies were found for the two studied reactions, and large negative activation entropies, close to those for the oxidation of secondary alcohols or other hydroxy acids. The second order-order with respect to the H^+ process have smaller activation enthalpies as compared to those of first-order on H^+. The large negative activation entropies are in agreement with to the formation of a condensed species prior to the electron transfer, with a hydrogen ion assistance.

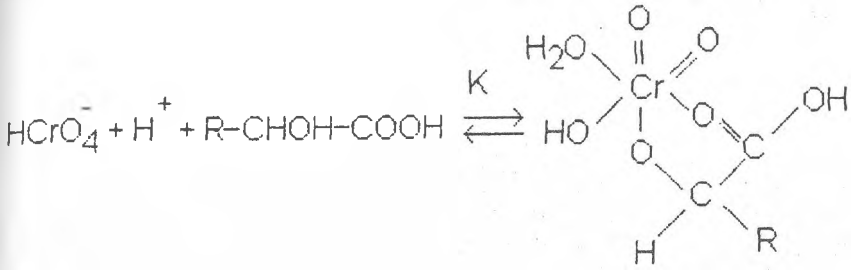

(13)

Under our experimental conditions, no second-order term with respect to lactic or malic acid was found, that is an unique three-electron step is not possible. Our data support a rate determining bi-equivalent step yielding Cr(IV) and keto-acid as first products, with and without the involvement of a second hydrogen ion.

Table 4. The rate coefficients for the ways having first-order and second order dependence on H^+

T K	Lactic acid		Malic acid	
	$10^3 \cdot k_1$ $dm^6 \cdot mol^{-2} \cdot s^{-1}$	$10^2 \cdot k_2$ $dm^9 \cdot mol^{-3} \cdot s^{-1}$	$10^3 \cdot k_1$ $dm^6 \cdot mol^{-2} \cdot s^{-1}$	$10^2 \cdot k_2$ $dm^9 \cdot mol^{-3} \cdot s^{-1}$
288	3.71±0.09	3.13±0.008	4.14±0.28	0.64±0.01
298	7.21±0.47	5.82±0.014	8.60±0.44	1.22±0.07
308	13.43±0.25	10.33±0.05	17.04±0.92	2.24±0.08
$\Delta H^{\#}$ $kJ \cdot mol^{-1}$	45.1±3.6	42.6±2.5	49.6±4.0	43.8±2.2
$\Delta S^{\#}$ $J \cdot mol^{-1} \cdot K^{-1}$	-134.8±10.8	-125.9±7.3	-118.2±9.5	-134.6±6.2

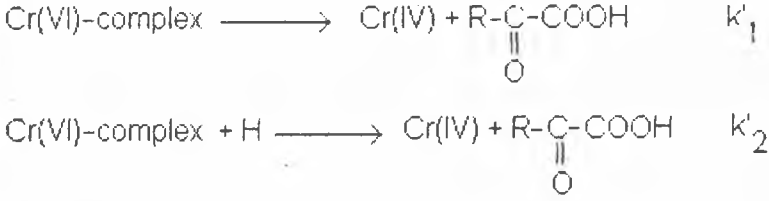

(14)

(15)

From these steps, the rate law, in accord with the experiment, is:

$$-\frac{d[Cr(VI)]}{dt} = \{k_1' \cdot K + k_2' \cdot K \cdot [H^+]\} \cdot [RCHOHCOOH] \cdot [HCrO_4^-] \cdot [H^+] \quad (16)$$

The generation of free radicals during the process suggests the involvement of an one-equivalent step where Cr(IV) formed in the rate determining step oxidizes a new α-hydroxy acid molecule.

$$\mathrm{Cr(IV)} + \mathrm{R{-}CHOH{-}COOH} \longrightarrow \mathrm{Cr(III)} + \mathrm{R\dot{C}(OH)COOH} + \mathrm{H}^+ \quad (17)$$

$$\updownarrow$$

$$\mathrm{RCH(\dot{O})COOH}$$

Two rapid reactions give Cr(V), as proved by Rocek and Srinavasan [6] at the oxalic acid oxidation, or by Haight et al [9] at the lactic acid oxidation.

$$\mathrm{Cr(VI)} + \mathrm{RCH(\dot{O})COOH} \longrightarrow \mathrm{Cr(V)} + \mathrm{R{-}\underset{\underset{\mathrm{O}}{\|}}{C}{-}COOH} + \mathrm{H}^+ \quad (18)$$

$$\mathrm{Cr(VI)} + \mathrm{Cr(IV)} \longrightarrow 2\mathrm{Cr(V)} \quad (19)$$

Chromium (V) acts in the same way as Cr(VI). Because of the presence of a large excess of α-hydroxy acid, either Cr(VI) or Cr(IV) are bound to the substrate, the reaction product is a Cr(V)- α-hydroxy acid complex, which seems to be quite stable [6-8] and have a smaller absorption coefficient than the Cr(VI)-homologue. Following the decay of the coloured species as a function of time, it came out that the absorbance values, namely the extrapolated to zero time one, were lower than those corresponding to Cr(VI). It means that some Cr(V) is formed and it probably reacts by a two-electron transfer yielding Cr(III) and keto-acid. It is possible that Cr(V) reacts by the same way as Cr(VI) does. Haight and co-workeres [9] suggested the rate law is:

$$-\frac{d[Cr(VI)]}{dt} = \{k_A + k_B \cdot [H^+]^2\} \cdot [H_2L] \cdot [H_2CrO_4^-] \quad (20)$$

with a zero and second-order with respect to hydrogen ion and rate constants of the same order of magnitude as rate constants for Cr(VI). It is worth mentioning that these authors found two ways, one zero-order and the other first order with respect to hydrogen-ion for the disappearance of Cr(VI) [9], along with a second order term on lactic acid. Our data revealed two pathways, one first-order, and the other second-order on H^+. It is possible that Cr(V) behaves similarly. Unfortunately, without any experimental means to record the evolution of Cr(V) species, it is not

possible for us to assign the effect of hydrogen-ion on its electron-transfer step. The reaction of chromium (V) cannot be separated from the chromium (VI) reaction. More data are required to elucidate the role of Cr(V) and the effect of the acidity on the α-hydroxy acids oxidation.

REFERENCES

1. a) F. H. Westheimer, *Chem. Rev.*, 1949, 95, 419.
   b) K. B. Wilberg, *"Oxidation in Organic Chemistry"* Part A. Academic Press, New York, 1965, 69.
2. F. H. Westheimer, N. Nicolaides, *J. Amer. Chem. Soc.*, 1949, 71, 25; A. Novick, F. H. Westheimer, *J. Chem. Phys.*, 1973, 11, 506.
3. a) G. V. Barkore, S. Narain, *J. Chem. Soc.*, 1963, 3419.
   b)*Z. Physik. Chem.* (Leipzic), 1964, 227, 8; 14.
4. a) F. Hasan, Rocek, *J. Amer. Chem. Soc.*, 1975, 97, 1444.
   b) M. Krumpolc, J. Rocek, *J. Amer. Chem. Soc.*, 1977, 99, 137.
   c) D. Ip, J. Rocek, *J. Amer. Chem. Soc.*, 1979, 101, 6311.
5. F. Hasan, J. Rocek, *J. Amer. Chem. Soc.*, 1972, 94, 3181; 8946; 1973, 95, 5421.
6. V. Srinavasan, J. Rocek, *J. Amer. Chem. Soc.*, 1974, 96, 127.
7. M. Krumpolc, J. Rocek, *Inorg. Chem.*, 1985, 24, 617.
8. P. C. Samal, B. B. Pattnaik, S. C. D. Ravand, S. N. Mahapato, *Tetrahedrn*, 1989, 39, 143.
9. G. P. Haight, G. M. Jursich, M. T. Kelso, P. J. Merill, *Inorg. Chem.*, 1985, 24, 2740.
10. I. Bâldea, M. Giurgiu, *Studia Univ. Babeș-Bolyai Chem.*, 1992, 37(1,2), 35.
11. D. W. J. Kwong, D. E. Pennington, *Inorg. Chem.*, 1984, 23, 2528.
12. P. Levesly, W. A. Waters, *J. Chem. Soc.*, 1955, 217.
13. M. Eden, R. G. Bates, *J. Res. Nat. Bur. Standards*, 1959, 62(4), 161; C. W. Davies, C. B. Monk, *Trans. Faraday Soc.*, 1954, 50, 132;
    ***, *Handbook of Chemistry and Physics*, David R. Lide Editor, Ed. 71st, 1990-91, 8-36.
14. R. C. Petersen, J. M. Markgraf, S. D. Ross, *J. Amer. Chem. Soc.*, 1961, 83, 3819.

STUDIA UNIVERSITATIS BABEŞ-BOLYAI, CHEMIA, XLII, 1-2, 1997

INTERACTION OF CHOLESTEROL WITH BILE SALTS AT THE CCl_4/WATER INTERFACE

EMIL CHIFU[1], JÁNOS ZSAKÓ[1], MARIA TOMOAIA-COTIŞEL[1], AURORA MOCANU[1], AURELIA VOINA[1]

ABSTRACT. By measuring the liquid/liquid interfacial tension between CCl_4 (or CCl_4 solution of cholesterol) and aqueous solution of bile salts at pH 8.6, viz. of sodium cholate (NaC), deoxycholate (NaDC) and ursodeoxycholate (NaUDC), critical micelle concentration (CMC) have been determined. As observed, the presence of cholesterol in the organic pfase entails diminishing of CMC and increasing of maximum adsorption at the interface. Correlation between the effects observed and the number of OH groups in the molecule is discussed.

INTRODUCTION

Numerous studies are done on the self-association properties of the acids molecules in aqueous solutions [1-13]. The findings offer a major advance in the understanding of the physical chemistry of some biological systems such as bile [2,9].

The fundamental importance of functional lipid associations which may exist in the structure of hepatocyte membrane, the constitution of lipoproteins, the absorption of fats through the intestinal wall, also stimulates further studies on aqueous lipid dispersions (vasicles and liposomes) and lipid monolayers at fluid interfaces in the absence and presence of bile acids/bile salts.

In our days an increasing attention is paid to mixed systems containing bile salts and other surfactants, since most of the biological functions of bile salts are based upon their capacity to associate with cholesterol and lecithin like molecules, by forming some structures with mixed micellar aggregates. Therefore, mixtures of bile salts with anionic, cationic and non-ionic type surfactants have been studied by means of miscellaneous methods and their micellar characteristics have been described for different molar ratios [14-16].

The solubilizing effect of the bile salts upon cholesterol is rather reduced. Thus, about 30-100 bile salts molecules are needed for the solubilization of a single cholesterol molecule [4].

[1] Department of Chemistry, "Babeş-Bolyai" University, Cluj-Napoca, Romania.

Over the last decade, ursodeoxycholic acid has been used to dissolve cholesterol gallstones in bile [12, 13, 17-19], and is spite of the relative large data on the biochemical, metabolic and clinical aspects and its therapeutic efficacy, the information on the physico-chemical properties of this bile acid species is limited [4, 11] and controversial.

In the present paper critical micelle concentrations (CMC) have been determined by means of interfacial tension measurements at the CCl_4 aqueous solution interface. The aqueous solution contained bile salts of different concentrations and measurements have been performed both in the absence and in the presence of cholesterol in the organic phase. The structure of cholesterol and of the studied bile acids molecules are presented in figure 1.

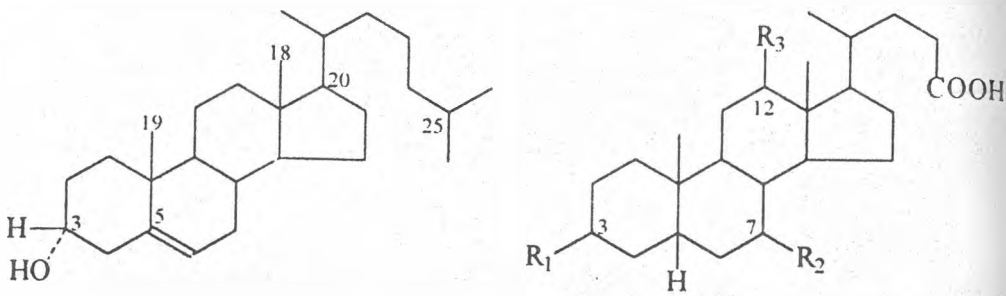

(5-colesten-3βol)

Figure 1. Molecular structure of cholesterol and of the investigated C_{24} bile acids: cholic acid (3α', 3α, 12α trihydroxyl 5β cholic acid) (CA); deoxycholic acid (3α, 12α dihydroxyl 5β cholic acid) (DCA); and ursodeoxycholic acid (3α, 7α dihydroxyl 5β cholic acid) (UDCA).

RESULTS AND DISCUSSIONS

The interfacial tension (γ) vs the logarithm of the bile salt concentration plots are given in figures 2-4. The CMC values are given by the intersection of the two linear portions.

In the case of cholesterol/bile salt mixed systems, at each measurement the concentration of the aqueous solution of bile salts was the same as the concentration of cholesterol in the CCl_4 phase.

It is worth mentioning, that while in the case of both NaC and NaUDC a simple CMC value has been obtained, with NaDC the formation of two types of micelles has been abserved, viz. of primary and secondary ones. This phenomenon has been also reported by ather authors [20] on the basis of X ray measurements. These authors presumed that in the first stage micelles of 30-120 mM are formed and in the second stage the size of the micelles becomes larger (120-300 mM).

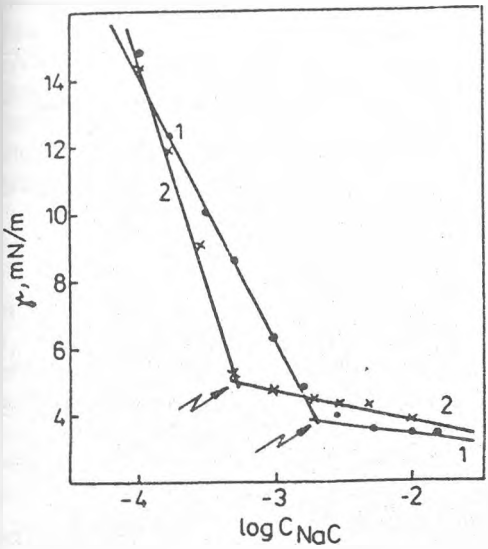

Fig. 2. Interfacial tension (γ) as function of C_{NaC} at the: (1) CCl_4/aqueous solution of NaC; (2) cholesterol (CCl_4)/aqueous solution of NaC interfaces

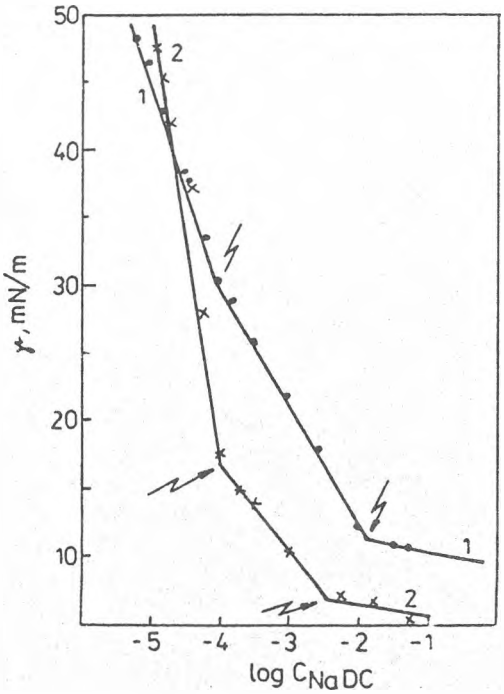

Fig. 3. Interfacial tension (γ) as function of C_{NaDC} at the : (1) CCl_4/aqueous solution of NaDC; (2) cholesterol (CCl_4)/aqueous solution of NaDC interfaces

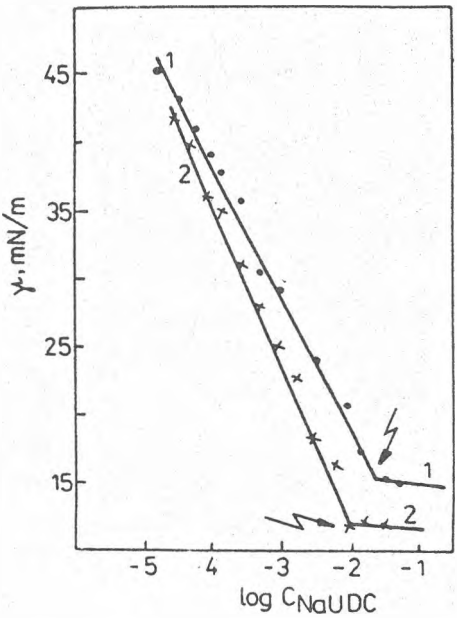

Figure 4. Interfacial tension (γ) as function of C_{NaUDC} at the: (1) CCl_4/aqueous solution of NaUDC; (2) cholesterol (CCl_4)/aqueous solution of NaUDC interfaces ·

The CMC values of the 6 studied systems are presented in table 1.

Table 1. CMC values of the bile salts in aqueous both in the presence and absence of cholesterol. T = 23°C, pH = 8.6, phosphate buffer

Bile salt	Type of micelles	$CMC \times 10^4$
NaC	simple	17.4
	mixed	8
NaDC	simple primary	1.41
	simple secondary	141
	mixed primary	1
	mixed secondary	30
NaUDC	simple	300
	mixed	100

By inspecting table 1, one may observe that:

- CMC values of the mixed system are always lower as compared to the simple ones, in agreement with literature data [21];
- CMC of UDC is higher than that of NaC in the case of both types of micelles, at least at the same temperature and pH and by using the same method;
- The number of the OH groups has an important effect upon the CMC. Thus, the CMC of the dihydroxy salts (NaDC and NaUDC) is higher than that of the trihydroxy salt (NaC).

Meanwhile, the CMC of NaUDC is comparable to the CMC in the secondary stage [22].

By using the $\gamma = f(\log c)$ curves given in figures 2-4, the maximum adsorption (Γ_{max}) at the liquid/liquid interface, as well as the molecular area A_0 can be derived. For this purpose Gibbs' equation is used and the procedure described elsewhere [23]. Results are presented in table 2.

Table 2. Maximum adsorption and moecular area of bile salts at the liquid/liquid interface in the absence and presence of cholesterol. T = 23°C, pH = 8,6, phosphate buffer

Bile salt	Type of the interfacial film	$\Gamma_m \times 10^{10}$ ($mol \cdot cm^{-2}$)	A_0 ($Å^2$)
NaC	simple	1.54	107.7
NaUDC	simple	1.71	96.68
NaC	mixed	1.99	83.05
NaUDC	mixed	2.23	74.42

Obviously, the presence of cholesterol entails the increase of the maximum adsorption revealing a specific interaction between cholesterol and the bile salts. This enhanced adsorption is observed with both trihydroxy and dihydroxy bile salts. At the other hand, both in the presence and in the absence of cholesterol, the maximum adsorption is higher and consequently the molecular area is lower in the case of the dihydroxy type NaUDC as compared to the NaC, having three OH groups. This result is completely resonable taking into account the enhanced area necessity due to the presence of one more highly hydrated OH group in the molecule.

EXPERIMENTAL

The cholesterol (3β-ol 5-cholestan) used was a commercial Merck product, of 98% purity, disolved in CCl_4, "Reactivul" București.

The bile salts investigated have been obtained by neutralizing the corresponding bile acids with 0,1N sodium hydroxide solutions. The used bile acids were commercial Merck and Flucka products.

Aqueous solutions of the bile salts, their concentration being comprized between $3x10^{-6}$ and $5x10^{-2}$M, have been prepared by using twice distilled water and a phosphate buffer in order to ensure an alkaline pH (8-9).

CCM determinations have been performed at room temperature (22^0C), by measuring the interfacial tension. For this purpose the weight method, or the drop volume method has been used [8].

ACKNOWLEDGEMENT

Authors thank Merck and Fluka for the bile acids offered us free of charge.

REFERENCES

1. D. M. Small, M. C. Bourges, D. G. Dervichian, *Biochim. Biophys. Acta,* 1996, 125, 563.
2. D. M. Small, in "The Bile Acids: Chemistry, Physiology and Metabolism", vol. 1, Ed. by P. P. Nair and D. Kritchovsky, Plenum Press., New York, 1971, p. 249.
3. N. A. Mazer, G. B. Benedek, M. C. Carey, *Biochemistry,* 1980, 19(4), 601.
4. D. J. Cabral, D. M. Smmal, Phys. Chem. of Bile - in *Handbook of Lipid Research,* ed. by D. Hanahan, Plenum Press., New York, 1986.
5. J. C. Hauton, H. Lafont, *Biochemie,* 1987, 69, 177.
6. H. Igimi, M. C. Carey, *J. Lipid Research,* 1980, 21, 72.
7. A. Roda, A. Minutello, M. A. Angellotti, A. Fini, *J. Lipid Research,* 1990, 31, 1433.
8. J. C. Montel, Path. Biol., 1991, 39(6), 621.
9. M. C. Carey, in *Bile Acids in Health and Disease: Update on Cholesterol Gallstones and Bile Acid Diarrhoea,* Ed. T. Northfield, R. Jazrawi and P. Zentler - Munro, Kluwer Academic Publishers, Dordrecht, Boston, London, 1988, p. 61-82.

10. O. Shibata, H. Miyoshi, S. Nagadome, G. Sugihara, H. Igimi, *J Colloid Interface Sci.*, 1991, 146, 594.
11. H. Miyoshi, S. Nagadome, G. Sugihara, H. Kagimoto, Y. Ikawa, H Igimi, O. Shibata, *J. Colloid Interface Sci.*, 1992, 149, 216.
12. H. Igimi, M. C. Carcy, *J. Lipid reseacrh*, 1981, 22, 254.
13. G. S. Tint, G. Salem, S. Shefer, *Gastroenterology*, 1986, 91, 1007.
14. G. V. Shilnikov, A. P. Sarvazyan, *J. Colloid Interface Sci.*, 1990, 93, 140.
15. P. K. Jana, S. P. Moulik, *J. Phys. Chem.*, 1991, 95, 9525.
16. M. Ueno, Y. Kimoto, Y. Ikeda, R. Zana, *J. Colloid interface Sci.*, 1987, 117 179.
17. M. Sackmann, J. Pauletzki, U. Aydemir, J. Holl, T. Sauerbruch, J. Hasford, G. Paumgartner, *Hepatology*, 1991, 14(6), 1136.
18. S. Sahlin, P. Thyberg, J. Ahlberg, B. Angelin, K. Einarsson, *Hepatology*, 1991, 13, 104.
19. C. B. O'Brien, J. R. Senior, R. Arora-Mirchandani, A. K. Batta, G Salen, *Hepatology*, 1991, 14, 838.
20. P. Zakrzewska, A. Markovic, M. Vucelic, *J. Phys, Chem.*, 1990, 94, 5078.
21. K. Ryu, L. M. Lowery, D. F. Evans, *J. Phys. Chem.*, 1983, 87, 5015.
22. A. Roda, H. F. Hofmann, K. J. Mysels, *J. Biol. Chem.*, 1983, 258, 6362
23. J. Zsakó, A. Mocanu, Cs, Rácz, K. Rácz, E. Chifu, *Studia Univ. "Babes-Bolyai" Chem* (in press).
24. I. Mândru, D. M. Ceacăreanu, "Chimia coloizilor și suprafețelor - Metode experimentale", Ed. Tehnică, București, 1976, pp. 255-277

STUDIA UNIVERSITATIS BABEŞ-BOLYAI, CHEMIA, XLII, 1-2, 1997

SZEGED INDICES: VERTEX AND FRAGMENTAL DESCRIPTORS

ANTON A. KISS[1], IRINA E. KACSO[1], OVIDIU M. MINAILIUC[1], MIRCEA V. DIUDEA[1], SONJA NIKOLIC[2], IVAN GUTMAN[3]

ABSTRACT. Novel fragmental Szeged indices, defined on unsymmetric property matrices, which collect various fragmental properties, are proposed. Classical vertex Szeged indices and fragmental descriptors are tested for correlating ability with physico-chemical properties of two sets of cycle-containing organic structures. Some QSPR models are proposed.

INTRODUCTION

Wiener index, ***W***, [1] one of the most studied topological indices, (see the recent reviews [2-4]) is defined, in acyclic structures, by

$$W = \sum_e N_{i,(i,j)} N_{j,(i,j)} \tag{1}$$

where $N_{i,(i,j)}$ and $N_{j,(i,j)}$ denote the number of vertices lying on the two sides of the edge/path, e/p (having the endpoints i and j). The summation runs over all edges (i,j) in graph. When (i,j) represents a path, then *a hyper-Wiener* index, ***WW***, [5] can be calculated

$$WW = \sum_p N_{i,(i,j)} N_{j,(i,j)} \tag{2}$$

The products $N_{i,(i,j)}$ $N_{j,(i,j)}$ represent the edge/path contribution to the global index ***W/WW*** and are just the (i,j)-entries in the Wiener matrices, [6,7] $\mathbb{W}_{e/p}$, from which the index can be calculated as half sum of their entries

$$W / WW = (1/2) \sum_i \sum_j [\mathbb{W}_{e/p}]_{ij} \tag{3}$$

Note that the vertices i and j must be adjacent in $\mathbb{W}_e$, otherwise its non-diagonal entries are zero. Relations (1) - (3) are valid only in acyclic graphs. In cycle-containing graphs, the Wiener indices are calculated by means of the distance-type matrices. [8,9].

---

[1] Facultatea de Chimie şi Inginerie Chimică, Universitatea "Babeş-Bolyai" Arany Janos 11, 3400 Cluj, Romania.

[2] Rudjer Boskovic Institute, P.O.B. 1016, Hr-11001, Zagreb, Croaţia.

[3] Faculty of Science, University of Kragujevac, 34000 Kragujevac, Yugoslavia

In the view of extending the validity of the above relations in cycle-containing graphs Gutman has proposed the *Szege index, **SZ***, [10] as a Wiener index analogue.

SZ index is defined according to eq **1** but the quantities $N_{i,(i,j)}$ and $N_{j,(i,j)}$ are now

$$N_{i,(i,j)} = |\{v \mid v \in V(G);\ D_{iv} < D_{jv}\}| \tag{4}$$

$$N_{j,(i,j)} = |\{v \mid v \in V(G);\ D_{jv} < D_{iv}\}| \tag{5}$$

where V(G) denotes the set of vertices in a graph and D_{iv}, D_{jv} are the topological distances (i.e., the number of edges on the shortest path joining the vertices i and j, respectively, with a vertex v). $N_{i,(i,j)}$ and $N_{j,(i,j)}$ represent the cardinality of the sets of vertices closer to i and to j, respectively; vertices equidistant to i and j are not counted. Thus, ***SZ*** index is calculated by summing all the edhe contributions in graph

$$SZ = \sum_e N_{i,(i,j)} N_{j,(i,j)} \tag{6}$$

Since ***SZ*** index is defined on edges, in the followings it will be symbolizsd by SZ_e.

By analogy to the Wiener matrices, Szeged matrices, $\mathbb{SZ}_{e/p}$, [11] can be defined by the aid of edge/path contributions

$$[\mathbb{SZ}_{e/p}]_{ij} = N_{i,(i,j)} N_{j,(i,j)} \tag{7}$$

on which the Szeged indices can be calculated by

$$SZ_{e/p} = (1/2) \sum_i \sum_j [\mathbb{SZ}_{e/p}]_{ij} \tag{8}$$

When the Szeged matrix is defined on paths, the index calculated on it is the *hyper-Szeged index, **SZ**$_p$*. [11].

SZ_e can be obtained by the Hadamard product [12] (i.e., $[M_a \bullet M_b]_{ij} = [M_a]_{ij} [M_b]_{ij}$) between SZ_p and A (the adjacency matrix, whose entries are 1 if two vertices are adjacent and zero, otherwise)

$$\mathbb{SZ}_e = \mathbb{SZ}_p \bullet \mathbb{A} \tag{9}$$

By analogy to the Cluj matrix,[13] Cj_u, a Szeged unsymmetric matrix, SZ_u, was defined by Diudea [11] (Figure 1).

$$[\mathbb{SZ}_u]_{ij} = N_{i,(i,j)} \tag{10}$$

SZ_u is a square array of dimensions **N** x **N**, in general unsymmetric. It allows the construction of the symmetric matrices SZ_e and SZ_p by relation

$$[\mathbb{SZ}_{e/p}]_{ij} = [\mathbb{SZ}_u]_{ij}[\mathbb{SZ}_u]_{ji} \tag{11}$$

and the derivation of two Wiener-type indices, as

$$SZ_{e/p} = \sum_{e/p} [\mathbb{SZ}_u]_{ij}[\mathbb{SZ}_u]_{ji} \tag{12}$$

In tree graphs, $SZ_e = CJ_e = W$. Note that, in the above discussion, the Cluj matrix, CJ_u, was defined on the shortest path (i,j). The symbol used for it in [14] is CJD_u.

Analitical relations for calculating the Szeged indices in paths, P_N, and simple cycles, C_N, are derived [15].

$$SZ_e(P_N) = N(N^2 - 1) / 6 \tag{13}$$

$$SZ_p(P_N) = (5N^4 - 10N^3 + 16N^2 - 8N - 6zN + 3z) / 48 \tag{14}$$

$$SZ_e(C_N) = N(N-z)^2 / 4 \tag{15}$$

$$SZ_p(C_N) = N(N-1)^{(2z+1)}(N^2 - 2N + 4)^{(1-z)} / 8 \quad ; z = N \bmod 2 \tag{16}$$

In the present paper, some extensions of the Szeged index, which account for fragments and their chemical nature are presented.

SZEGED PROPERTY MATRICES

By analogy to Sz_u (see eqs 4 and 10), Szeged property matrices are defined [16]

$$[\mathbb{SZ}_u\mathbb{P}]_{ij} = P_{i,(i,j)} \tag{19}$$

$$P_{i,(i,j)} = m \sum_v P_v \tag{20}$$

$$P_{i,(i,j)} = \left(\prod_v X_v\right)^{1/N_{i,(i,j)}} \tag{21}$$

Entries in a Szeged property matrix are evaluated on the set of vertices v which obey the Szeged index condition (see eq 4). In fact, such a set of vertices can be viewed as a fragment (i.e., a subgraph) since a molecular graph is alwais a connected one. The summation on the right-hant side of eq 20 goes over all vertices of the graph G which have the property $D_{iv} < D_{jv}$. A similar consideration is true for the product in eq 21.

Some special cases of the above definition deserve special attention:

(a) $P_v = 1$; $m = 1$ (classical matrix, SZ_u)

(b) $P_v = \sum_u A_u$; $m = 1/12$ (mass matrix, $\mathbb{SZ}_u\mathbb{A}$)

(c) X_v = group electronegativities [17] (electronegativity matrix, $\mathbb{SZ}_u\mathbb{X}$)

The case (a) is obvious: $P_{i,(i,j)}$ represents the cardinality of the set of vertices v (see above). In case (b) A_u is the atomic mass and the summation runs over all atoms u which are represented by the same vertex v. The factor m = 1/12 indicates that $P_{i,(i,j)}$ is a fragmental mass, relative to the carbon atomic mass.

In case (c) $P_{i,(i,j)}$ is just the geometric mean of vertex values, X_v, of group electronegativities.

The above matrices are illustrated, for the graph G_1 (2,3-Dymethilpentane) in Fig. 1.

Indices are calculated on these matrices by the general relation

$$I_{e/p} = \sum_{e/p} [SZ_uP]_{ij} [SZ_uP]_{ji} \quad ; I = SZ;\ SZA;\ SZX \qquad (22)$$

Indices calculated in the cases (b) and (c) are useful in discriminating chemical graphs which contain heteroatoms and multiple bonds.

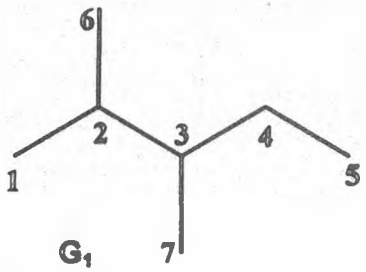

SZ_u; $P_v = 1$; $m = 1$

0	1	1	3	3	1	3
6	0	3	3	5	6	3
4	4	0	5	5	4	6
4	2	2	0	6	4	2
2	2	1	1	0	2	2
1	1	1	3	3	0	3
4	1	1	1	5	4	0

$SZ_e = 46$; $SZ_p = 151$

SZ_uA; $P_v = A_v$; $m = 1/12$

0.000	1.250	1.250	3.583	3.583	1.250	3.583
7.083	0.000	3.583	3.583	5.917	7.083	3.583
4.750	4.750	0.000	5.917	5.917	4.750	7.083
4.750	2.417	2.417	0.000	7.083	4.750	2.417
2.417	2.417	1.250	1.250	0.000	2.417	2.417
1.250	1.250	1.250	3.583	3.583	0.000	3.583
4.750	1.250	1.250	1.250	5.917	4.750	0.000

$SZ_eA = 66.736$; $SZ_pA = 217.729$

SZ_uX; $P_v = EVG_v$; $m = 1$

0.000	0.958	0.958	0.962	0.962	0.958	0.962
0.963	0.000	0.962	0.962	0.963	0.963	0.962
0.962	0.962	0.000	0.963	0.963	0.962	0.963
0.962	0.960	0.960	0.000	0.963	0.962	0.960
0.960	0.960	0.958	0.958	0.000	0.960	0.960
0.958	0.958	0.958	0.962	0.962	0.000	0.962
0.962	0.958	0.958	0.958	0.963	0.962	0.000

$SZ_eX = 5.538$; $SZ_pX = 19.383$

Figure 1. Szeged Property Matrices; Vertex and Fragmental Indices in G_1

APPLICATIONS

Two correlation tests have been performed: (a) for the vertex descriptors and (b) for both vertex and fragmental descriptors.

(a) A dozen of cycloalkanes (Table 1) was selected for correlating their boiling points, BP, and chromatographic retention index, RI, with the classical hyper-Szeged index, Sz_p.

For comparison, Wiener and hyper-Wiener indices are includet. Statistics of single variable regression are shown in Table 2. In such a set, the simplest descriptor is, of course, the number of carbon atoms, NC. Any acceptable correlation must surpass the correlation shown by NC. Thus, in Table 2, one can see that the correlation coefficient, r, shown by the topological indices is inferior to that supplied by NC (0.965). However, by applying the logarithmic function, all descriptors showed increased values of r, with a maximum for ***ln*** $\boldsymbol{SZ_p}$ (0.980) and a significant dropp in the standard error of estimate, s.

The crude descriptor, that is NC, is far less sensitive to logarithmation, proving a low structural information.

Tab. 1. Boiling Points,BP[18] Chromatographic Retention Index, RI and Topological Indices

Graph	BP/N	RI	SZ_p	*W*	*WW*	Graph	BP/N	RI	SZ_p	*W*	*WW*
1 	35.9 5	510.0	40	17	26	7 	100.9 7	725.8	182	42	71
2 	49.3 5	565.0	40	15	20	8 	103.5 7	733.8	159	43	75
3 	70.7 6	621.1	92	29	49	9 	126.4 8	812.1	247	61	110
4 	71.8 6	627.9	79	26	39	10 	131.0 8	830.3	230	58	99
5 	80.7 6	662.7	105	27	42	11 	131.8 8	834.3	296	61	110
6 	105.0 8	723.6	308	64	122	12 	136.6 9	840.4	447	82	152

(b) A set of 15 structures of explosives [19] (Figure 2 and Table 3) was tested for the correlation of two properies: with the topological descriptors $\boldsymbol{SZ_e}$, $\boldsymbol{SZ_p}$, $\boldsymbol{SZ_eA}$, $\boldsymbol{SZ_pA}$, $\boldsymbol{SZ_eX}$ and $\boldsymbol{SZ_pX}$. (Table 4). Statistics of single variable regressions and cross validation test ("leave one out") are shown in Table 5.

Table 2. Statistics of Single Variable Regression (y=a+bx) of Parameters from Table 1

Y	X	r	s	F
BP	SZ_p	0.9305	12.9426	64.5455
	W	0.9553	10.4518	104.3108
	WW	0.9533	10.6742	99.5966
	NC	0.96518	9.2434	136.1513
	ln SZ_p	0.9840	6.2945	305.172
	ln W	0.9757	7.7414	198.369
	ln WW	0.9721	8.2956	171.454
	ln NC	0.9725	8.2247	174.599
RI	SZ_p	0.9240	44.6232	58.384
	W	0.9455	37.9846	84.375
	WW	0.9470	37.4987	86.837
	NC	0.9512	36.0009	95.062
	ln SZ_p	0.9733	26.7664	180.061
	ln W	0.96241	31.6953	125.545
	ln WW	0.9597	32.8101	116.490
	ln NC	0.9580	33.4446	111.737

Table 3. Name of Compunds in the Graphs G_2-G_{16}

graph	Name	DC water $*10^{-6}$ (cm^2/s)	DC air (cm^2/s)
2	Trinitrotoluene	6.71	0.0639
3	2,4-Dinitrotoluene	7.31	0.0670
4	2,6- Dinitrotoluene	7.31	0.0670
5	1,3- Dinitrobenzene	7.94	0.0729
6	1,3,5- Trinitrobenzene	7.20	0.0679
7	Hexahydro-1,3,5-trinitro-1,3,5-triazine	7.15	0.0739
8	Octahydro-1,3,5,7-tetranitro-1,3,5,7-tetrazocine	6.02	0.0629
9	N-2,4,6-Tetranitro-N-methylaniline	5.99	0.0590
10	Picric acid	7.03	0.0660
11	Pentaerythrytol tetranitrate	5.61	0.0570
12	Nitroglycerin	6.95	0.0700
13	Nitroguanidine	10.40	0.1019
14	Ethylene glycol dinitrate	8.72	0.0839
15	Diethylene glycol dinitrate	7.05	0.0689
16	Propylene glycol dinitrate	7.93	0.0769

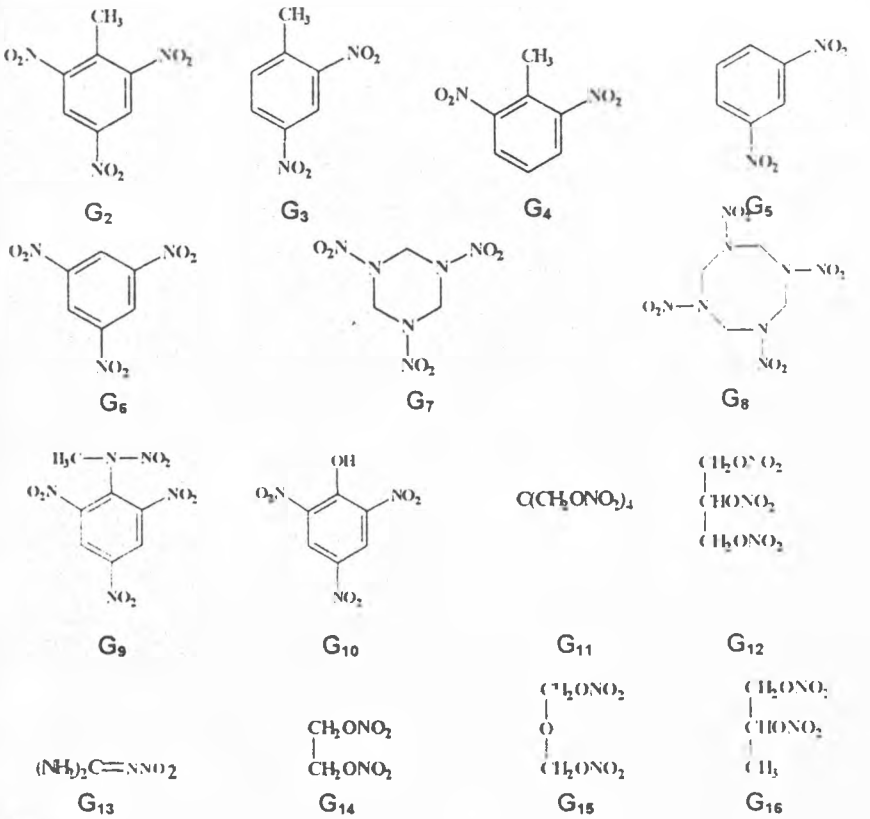

Figure 2. Molecular Formulas of Explosive Compounds

Table 5. Statistics of Single Variable Regression: Y = a + bX for Explosives and Cross Validation Test (Leave One Out)

No	Y	X	a	b	r	s	F	r_{cv}	s_{cv}
1	CD_{air}	ln SZ_e			0.943	0 0037	105 09		
2		1/ln SZ_eA	0.00073	0.4157	0.960	0.0031	155.21	0.951	0 0035
3		1/ln SZ_pA			0.954	0.0034	133.61		
4		1/W			0.942	0.0038	102.87		
5	CD_{water}	ln SZ_e	15.60561	- 1.3934	0.973	0.2801	231.72	0.960	0 338
6		ln SZ_eA	16.31334	- 1.4915	0.979	0.2443	310.57	0.968	0.302
7		ln SZ_pA	15.82862	-1.0766	0.984	0.2123	413 59	0.975	0 266
8		1/SZ_pX			0.961	0.3321	160.95		

Table 4. Topological Indices for Explosives (Figure 2 and Table 3)

Graph	SZ_e	SZ_p	SZ_eA	SZ_pA	SZ_eX	SZ_pX
2	594	4348	601.049	4169.958	74.949	510.786
3	360	2050	378.451	2049.049	57.524	333.915
4	348	1993	366.007	1978.160	49.430	290.101
5	296	1542	303.292	1500.896	49.076	268.231
6	516	3450	509.917	3239.271	66.837	431.457
7	516	3450	555.083	3528.729	68.038	439.675
8	1156	11794	1228.833	12083.000	100.785	824.478
9	1014	10342	1022.236	9969.632	99.907	820.577
10	594	4348	613.896	4248.014	78.289	528.620
11	968	11514	1083.000	12479.986	94.923	832.585
12	424	3677	475.729	3961.931	68.805	455.598
13	48	159	61.389	194.514	36.330	133.953
14	151	827	172.771	904.382	43.192	206.946
15	344	2518	408.569	2913.472	45.670	270.017
16	184	1153	214.278	1274.937	50.820	262.697

Table 5 indicated a good estimative and predictive ability of the regression equations. It appears that the fragmental descriptors are more suitable for QSPR studies.

Concluding, the novel Szeged fragmental indices are promising tools in correlating studies.

REFERENCES

1. H. Wiener, *J. Am. Chem. Soc.*, 1947, 69, 17.
2. I. Gutman, Y. N. Yeh, S. L. Lee, Y. L. Luo, *Indian J. Chem.* 1993, 32A, 651.
3. S. Nikolic, N. Trinajstic, Z. Mihalic, *Croat. Chem. Acta.* 1995, 68, 105.
4. M. V. Diudea, I. Gutman, *Croat. Chem. Acta.* (submitted).
5. M. Randic, *Chem. Phys. Lett.* 1993, 211, 478.
6. M. Radic, X. Guo, T. Oxley, H. Krishnapriyan, *J. Chem. Inf. Comput. Sci.* 1993, 33, 700.

7. M. Randic, X. Guo, T. Oxley, H. Krishnapriyan, L. Naylor, *J. Chem. Inf. Comput. Sci.* 1994, 34, 361.
8. H. Hosoya, *Bull. Chem. Soc. Jpn.* 1971, 44, 2332.
9. M. V. Diudea, *J. Chem. Inf. Comput. Sci.* 1996, 36, 535.
10. I. Gutman, *Graph Theory Notes New York,* 1994, 27, 9.
11. M. V. Diudea, O. M. Minailiuc, G. Katona, I. Gutman, *Commun. Math. Comput. Chem. (MATCH),* 1997, 35, 129.
12. R. A. Horn, C. R. Johnson, *Matrix Analysis.* Cambridge Univ. Press, Cambridge, 1985.
13. M. V. Diudea, *J. Chem. Inf Comput. Sci.* 1997, 37, 300.
14. M. V. Diudea, B. Pârv, I. Gutman, *J. Chem. Inf. Comput. Sci.* (submitted).
15. M. V. Diudea, *J. Chem. Inf. Comput. Sci.* 1997, 37, 292.
16. M. V. Diudea, "Wiener-Type Indices", lecture at the Rudger Boskovic institute, July 7, 1996.
17. M. V. Diudea, I. E. Kakso, M. Topan, *Rev. Roum. Chim.* 1996, 41, 141.
18. R. Gautzsch, P. Zinn, *J. Chem. Inf. Comput. Sci.* 1994, 34, 791.
19. S. Nikolic, M. Medic-Saric, S. Rendic, N. Trinajstic, *Drug Metabolism Reviews,* 1994, 26, 717.

STUDIA UNIVERSITATIS BABEȘ-BOLYAI, CHEMIA, XLII, 1-2, 1997

SEPARATION AND CHARACTERIZATION OF METHYL-FLUORENYL DERIVATIVES OF Si(IV) AND Ge(IV)[1]

T. HODIȘAN[2], LUMINIȚA SILAGHI-DUMITRESCU, CLAUDIA CIMPOIU

ABSTRACT. The synthesis of difluorenyl derivatives of group 14 elements by treating the corresponding diorganodihalide with fluorenyl-lithium affords together with the main product, $R_2E(CHR_2')$ where R = Me, CHR_2' = fluorenyl, E = Si(IV), Ge (IV)) several secondary products. The thin layer chromatography was used to find the conditions to separate this products further used to obtain pure samples by column chromatography. The products were characterized by their ^{1}H-NMR and ^{13}C-NMR.

INTRODUCTION

The fluorenyl group is very interesting due to its special electronic (possibility of strong conjugation) and steric (large size, but flat group) properties [1,2]. Groups of this type appeared particularly suitable for the stabilisation of double-bounded main group elements, such as germenes [3-5], >Ge=C<, and stannenes [6], >Sn=C<, they were also used for the preparation of a synthetic equivalent of a sililene [7]. The introduction of two fluorenyl groups on the group 14 elements was found interesting in order to study the synthesis, reactivity and physic - chemical properties of the resulted compounds as well as for the possibility to transform them in polymeric or cyclic structures such as:

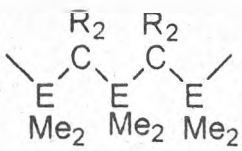

E=Si, Ge, Sn

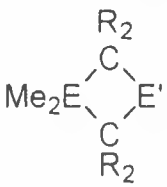

E': SiR_2, GeR_2, NR, PR, AsR

This paper presents the analysis of the reaction mixtures obtained in the synthesis of $Me_2E(CHR_2)_2$ (E = Si, Ge) and some of their derivatives.

Dimethyldiflourenylsilane and germane were prepared according the next equation [1]:

---

[1] Dedicated to prof. dr. Ionel Haiduc on the occasion of his 60-th aniversary.

[2] Facultatea de Chimie și Inginerie Chimică, Universitatea "Babeș-Bolyai", str. Arany Janos nr. 11, 3400 Cluj-Napoca, România.

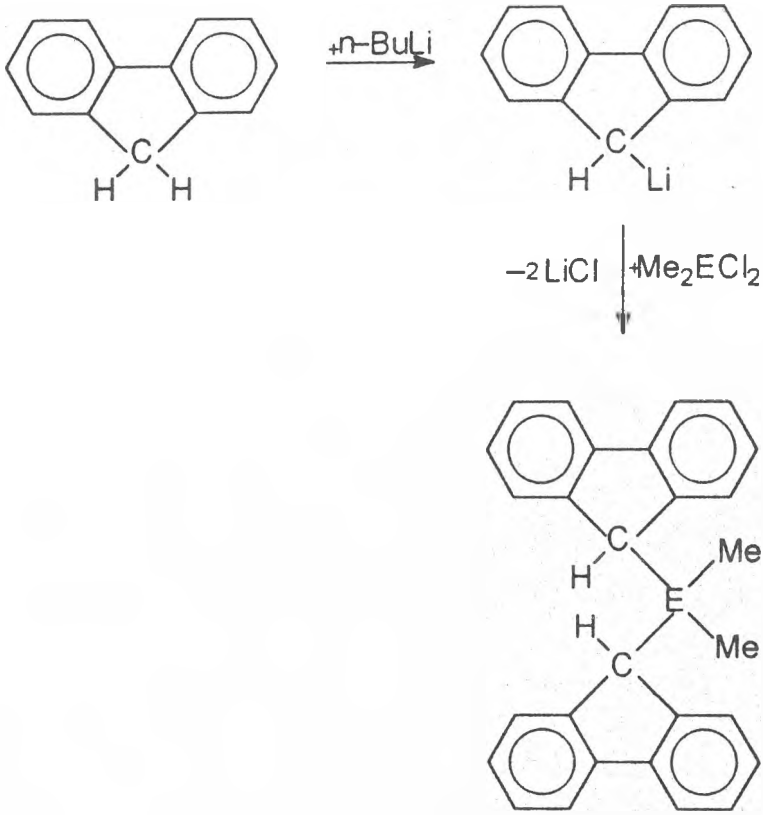

I

After the white crystalline major product was filtered off (yield 50-60% in pure compound), the filtrate was concentrated. This fraction contains 50-60% $Me_2E(CHR_2)_2$ accompanied by different other products.

The possible secondary products (further identified as such) are II and III, formed as follows:

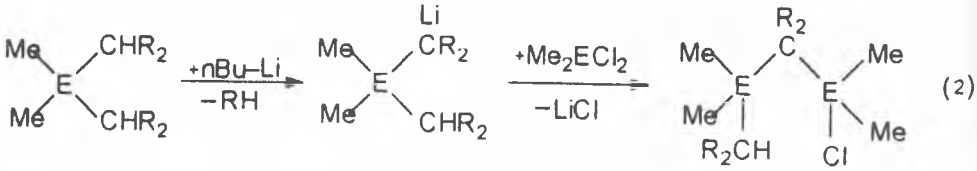

II

III

In order to have pure samples of II and III, the products were synthesised according (2) and (3) reactions (only for Si(IV)) [1]. Compound II was transform into IV and V by treating it with water and HF, respectively.

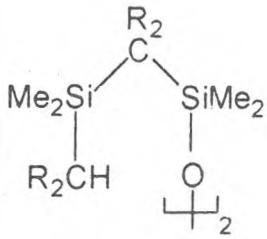

IV

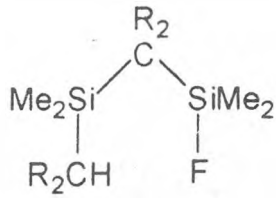

V

In order to perform the synthesis of $Me_2Ge(CHR_2')_2$ a mixture of the composition 71% Me_2GeCl_2 and 29% $MeGeCl_3$ (as obtained by direct syntheses) was also used. We expected to be easier to separate the fluorenyl derivatives than the halides. The synthesis afforded pure $Me_2Ge(CHR_2')$ with 54% yield (white crystals form in the reaction mixture). According the ^{1}H-NMR spectra the remaining white solid contains more $Me_2Ge(CHR_2')_2$ and $MeGe(CHR_2')_2Cl$.

The conditions to separated this mixture were established by thin layer chromatography and the separation performed on a column using the appropriate eluent.

EXPERIMENTAL

The above mentioned mixtures were solved in benzene (0.1%) and 1μL was applied to the thin layer plates using silicagel F_{254} as stationary phase. The preliminary attemps to optimise the mobile phase composition (eluotrope serie of Snyder) indicated the mixture benzene-petroleum ether (3:1 v/v) as the best eluent. The plates were photodensitometred.

The samples containing $Me_2E(CHR_2)_2$ (E = Si(IV), Ge(IV)) and secondary products II and III was passed through a column (20x2 cm with chromatographic silica using the same mobile phase. Pure components were obtained using this technique.

RESULTS AND DISCUSSION

The ^{1}H and ^{13}C-NMR spectra, and the interactions between the components of the mixture and the stationary phase were used to identify the peaks.

The highest R_f was formed for $Me_2E(CHR_2)_2$ (E = Si(IV), Ge(IV)) the less polar compound, with no possibility of interactions with the stationary phase. The strength of the product- stationary phase interactions lead to the distribution of the accompanying components (see Figure 1).

The ^{1}H-NMR spectra of the compounds are presented in Table 1 and ^{13}C-NMR spectra in Table 2. The spectra are similar with those reported earlier [1].

Table 1. ^{1}H-NMR spectra of fluorenyl derivatives, (ppm), J(Hz)

Compound	$(CH_3)_2E$		R_2CH	R_2C
$Me_2Si(CHR_2')_2$	-0.49 s		4.25 s	7.29-7.99 m
$Me_2(CHR_2)Si(CR_2)$	0.07 s	0.40 s	2.81 s	6.41(d,$^{3}J_{HH}$:6.0)
$SiMe_2Cl$		(Me_2SiCl)		6.85-8.03 m
$Me_2Si(CHR_2')Cl$	0.21 s		4.12 s	7.33-7.90 m
$[Me_2Si(CHR_2')_2]_2O$	-0.48 s	0.12	3.95 s	6.90-8.00 m
		(Me_2SiO)		
$Me_2Si(CHR_2')_2F$	0.30	0.11	2.79 s	6.41(d,$^{3}J_{HH}$:8)
	(d,$^{3}J_{HF}$:0.8)	(d,$^{3}J_{HF}$7.2)		6.84-8.06 m
		(Me_2SiF)		
$Me_2Ge(CHR_2')_2$	-0.28 s		4.26 s	7.30-7.95 m
$MeGe(CHR_2')_2Cl$	-0.53 s		4.16 s	7.30-7.95 m
$Me_2Ge(CHR_2')_2Cl$	0.33 s		4.20 s	7.30-7.95 m
$Me_2(CHR_2)Ge(CR_2)$	0.35 s	0.38s	3.05 s	6.39(d,$^{3}J_{HH}$:9)
$GeMe_2Cl$		(Me_2GeCl)		6.87-8.00 m

Table 2. ^{13}C-NMR spectra, (ppm), J(Hz)

	Me_2Si		R_2CH	$C_{4,5}$	$C_{1,2,3,\ 6,7,8}$	$C_{10,11,12,13}$	
I	-6.63		40.47	120.29	124.37		140.92
					125.74		
					126.39		145.09
II	0.74	1.35	39.13	119.51	124.63	125.75	140.29
		(Me_3SiCl)		120.63	124.94	126.43	140.84
					125.41		144.09
							145.18
III	-0.19		43.58	120.19	124.80		140.96
					126.32		
					126.56		142.96
V	0.17	-2.26	39.20	119.50	124.69	125.50	140.28
		($^{2}J_{CF}$: 14.6)		120.66	124.94	126.50	140.73
		Me_2SiF			125.42		144.25
							145.23

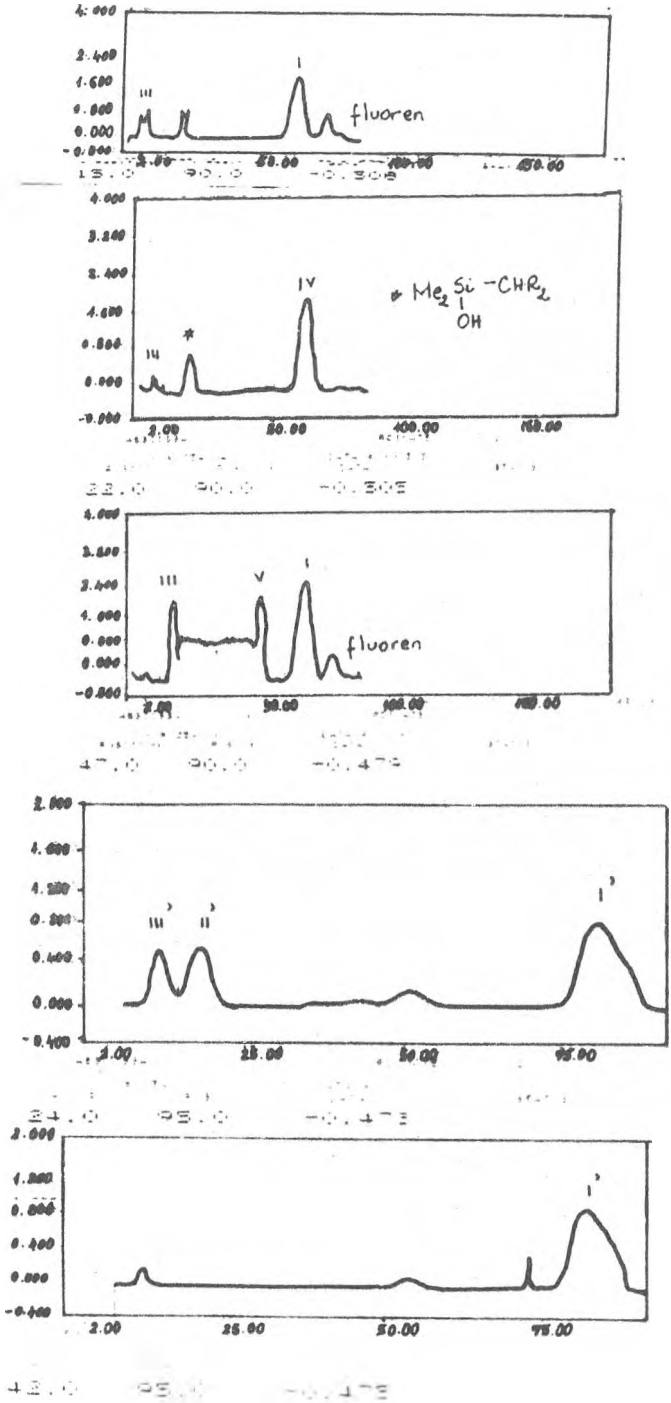

Figure 1. The distribution of the components (I-V-derivatives of Si; I'-III'-derivatives of Ge)

CONCLUSIONS

The qualitative separation and identification of the products resulted in the attempt of preparation of $Me_2E(CHR_2)_2$ (E = Si(IV), Ge(IV)) was performed using TLC and NMR spectroscopy. The components of the reaction mixture were obtained as pure products by column liquid chromatography and used for further structural investigations. The technique is suited to separate any mixture of the above mentioned compounds.

ACKNOWLEDGEMENT

One of the authors (Luminița Silaghi-Dumitrescu) is greatful to European Community and Paul Sabatier University, Toulouse for the financial support through a LOST (PECO) grant.

REFERENCES

1. Silaghi-Dumitrescu, I. Haiduc, J. Escudie, C. Couret and J. Satge, *Synth. React. Inorg., Met-Org. Chem.*, 25. 575.
2. Silaghi-Dumitrescu, I.Silaghi-Dumitrescu, R.Cea-Olivares, C. Couret, J. Escudie and I. Haiduc, *J. Organometal. Chem.*, 1997, in press.
3. a) C. Couret, J. Escudie, J. Satge and M. Lazraq, *J. Am. Chem. Soc.*, 1987, 109, 4411.
   b) M. Lazraq, J. Escudie, C. Couret, J. Satge, M. Drager and R. Dammel, *Angew. Chem. Int. Ed. Engl.*, 1988, 25, 828.
4. G. Anselme, J. Escudie, C. Couret and J. Satge, *J. Organomet. Chem.*, 1991, 403, 93.
5. M. Lazraq, C. Couret, J. Escudie, J. Satge and M. Soufiaoui, *Polyhedron*, 1991, 10, 1153.
6. G. Anselme, H. Ranaivonjatovo, J. Escudie, C. Couret and J. Satge, *Organometallics*, 1992, 11, 3176.
7. C. Couret, J. Escudie, G, Delpon-Lacaze and J. Satge, *J. Organomet. Chem.*, 1992, 440, 233.

STUDIA UNIVERSITATIS BABEŞ-BOLYAI, CHEMIA, XLII, 1-2, 1997

THE APPLYING OF ORGANIC ABSORBENTS IN THE ABSORPTION OF SULFUR DIOXIDE, USING A CCLUMN OF LIQUID FILM TYPE

J.VODNAR[1], S. DRĂGAN[1], MIHAELA DRĂGAN[2]

ABSTRACT. The paper presents a lot of experimental results, obtained by studying the absorption of sulfur dioxide from different industrial gases, using aqueous solutions of triethanolamine (TEA). The apparatus used was a three plated column of Vodnar type. Industrial gases having different sulfur dioxide content appear in the sulfuric acids plants, in a series of metallurgical plants, in all industrial works where the Claus procedure is applied a.s.o. The apparatus used enables to make absorption in an ascending turbulent film of the absorbent and a uniform and self distribution of the absorbent and the gas in the contacting tubes. The absorbent and gas were used in a counter current, but the film producing phenomenon took place in a common tide.

INTRODUCTION

The paper presents a lot of experimental results obtained by studying the absorption of sulfur dioxide from different industrial gases, using aqueous solutions of triethanolamine (TEA), triethanolamine sulfite (TEAS) and N-methyl-pyrrolidone (NMP) [1]. The apparatus used was a three plated column of Vodnar type [2]. Industrial gases having different sulfur dioxide content appear in the sulfuric acids plants, in a series of metallurgical plants, in all industrial works where the Claus procedure is applied a.s.o. [3-5]. The apparatus used enables to make absorption in an ascending turbulent film of the absorbent and a uniform and self distribution of the absorbent and the gas in the contacting tubes. The absorbent and gas were used in a counter current, but the film producing phenomenon took place in a common tide. The total inner surface of the gas-liquid contacting tubes is equal of 1.149385 m^2. The best coefficient of absorption (C_a) obtained, using the mentioned three absorbents were as following: with TEA 1.155, with TEAS 1.1493 and using NMP was 1.1 kg SO_2/m^2h when the absorbent flows in the same order were: 1.15, 2.9 and 9.8 dm^3/h. Temperature was 20°C.

EXPERIMENTAL

Experiments were made in above mentioned column of Vodnar type, having three contacting segments. Some structural data of the apparatus were

[1] University "Babeş-Bolyai" of Cluj-Napca, Faculty of Economical Sciences, Department of Technology and Merceology.

[2] University "Babeş-Bolyai" of Cluj-Napoca, Faculty of Chemistry and Chemical Engeneering.

describerd in [2]. The ascending turbulent film of the absorbent was formed continuously on the inner surface of the absorption tubes. The absorbents (TEA, TEAS, NMP) were fed with an adequate pump, continuously. The necessary sulfur dioxide was taken from a steel cylinder vessel and the air with a compressor was ensured. The sulfur dioxide content of the gas mixture was determined iodometrically. Temperature was maintained at 19-20°C. The absorbent was introduced continuously in the upper part of the column and the solution resulted was eliminated from the lowest contacting segment of the apparatus. The contacting of the phases took place in a counter current, but the liquid film formation was made in a common tide. Gas flow varied between 3 and 12.3 m^3/h and that of the absorbents between 0.85 and 9.8 dm^3/h. Sulfur dioxide content of the gas was maintained constant on 0.5% v/v in all experiments.

The absorption of sulfur dioxide takes place by the following physical and chemical phenomena:

1) 

(NMP)

2) $N(CH_2CH_2OH)_3 + SO_2 + H_2O \rightleftharpoons HN(CH_2CH_2OH)_3HSO_3$

(TEA)

3) $[HN(CH_2CH_2OH)_3]_2SO_3 + SO_2 + H_2O \rightleftharpoons 2[HN(CH_2CH_2OH)_3]HSO_3$

At 80-100°C the resulted products decompose, elaborating sulfur dioxide which can be recycled in the technological installation or can be used in different chemical purposes.

RESULTS AND DISCUSSION

In the first series of experiments the dependence of the absorption degree (D_a[%]), versus the absorbent flow (Q_a[dm^3/h]) was studied. The experimental results obtained are illustrated in figures 1-3.

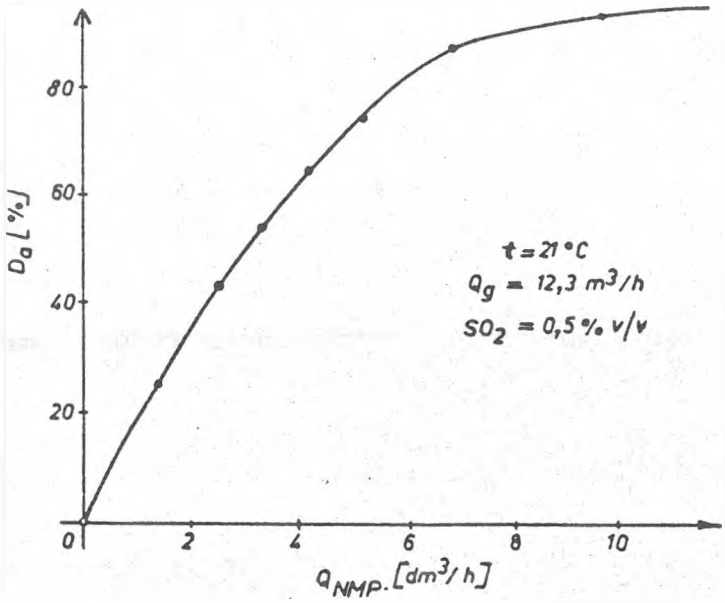

Fig. 1. The dependence of the absorption degree (D_a), versus the NMP flow (Q_{NMP})

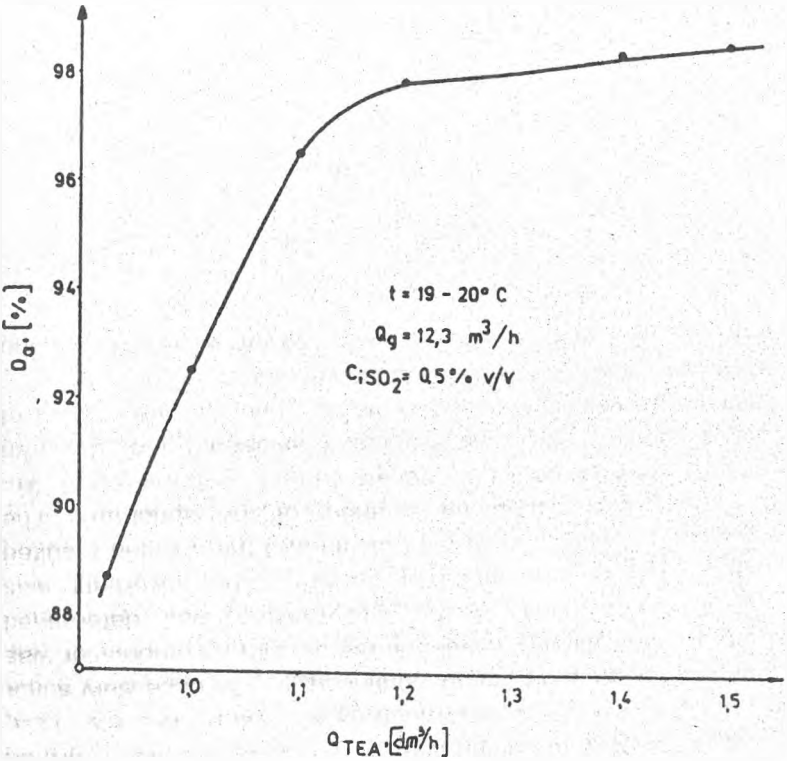

Fig. 2. The dependence of the absorption degree (D_a), versus the TEA flow (Q_{TEA})

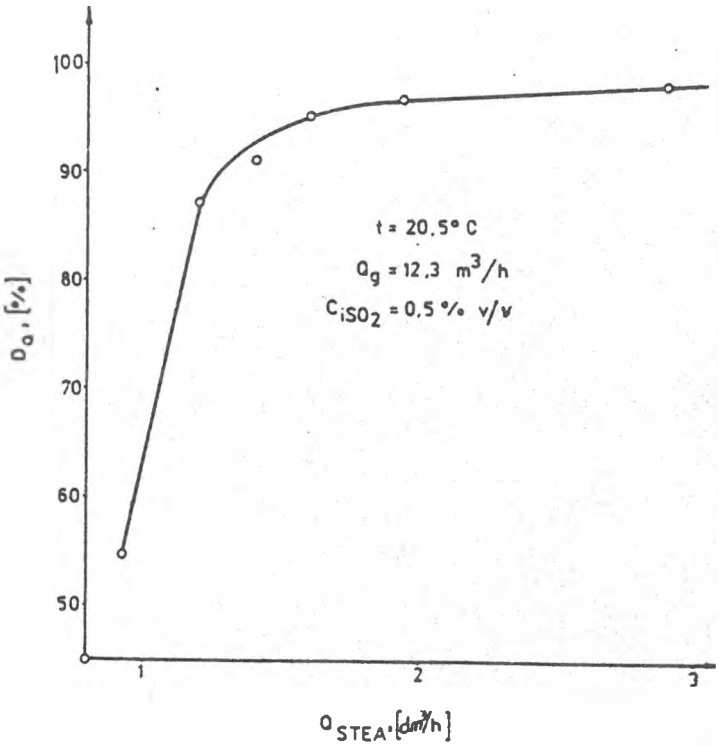

Fig. 3. The dependence of the absorption degree (D_a), versus the TEAS flow (Q_{TEAS})

Figures 1-3 show that at 20-21°C, using a total gas flow of 12.3 m^3/h and the initial sulfur dioxide content of the gas mixture being 0.5% v/v the absorption degree values in NMP, TEA and TEAS were in the same order the followings: 94% by 9.8 dm^3/h, 98% by 1.2 dm^3/h and 98%when the absorbent flow was 2.9 dm^3/h.

The more important aspects of the absorption are illustrated in figures 4-6, where the dependence between the coefficients of the absorbtion (C_a[Kg SO_2/m^2 h]) and the absorbents flow are given, corresponding to NMP, TEA and TEAS, in the above mentioned conditions of work: 1.1, 1.155 and 1.027 [$KgSO_2/m^2h$] (respectively 128 [g SO_2/dm^3h] when Q_{TEAS}=1.2 dm^3/h).

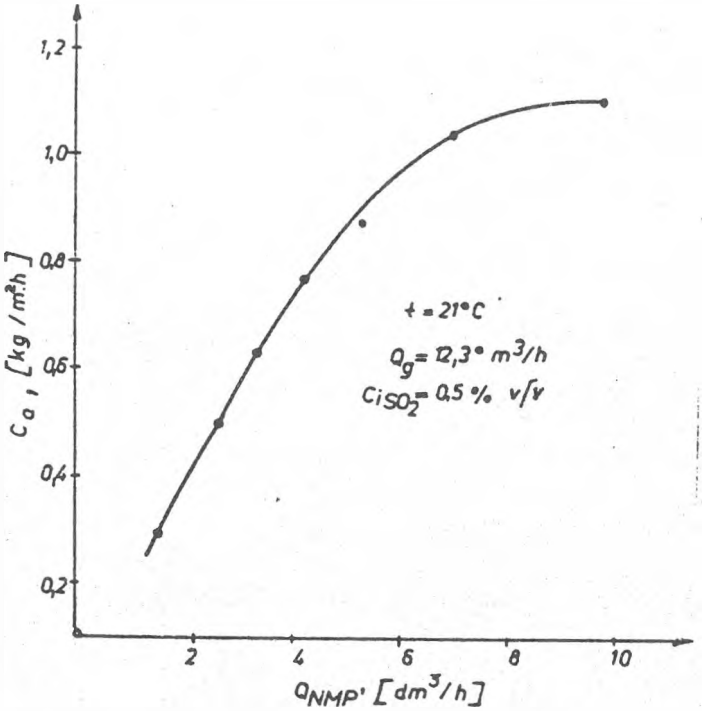

Fig. 4. Variation of the coefficient of absorption (C_a), versus the NMP flow (Q_{NMP})

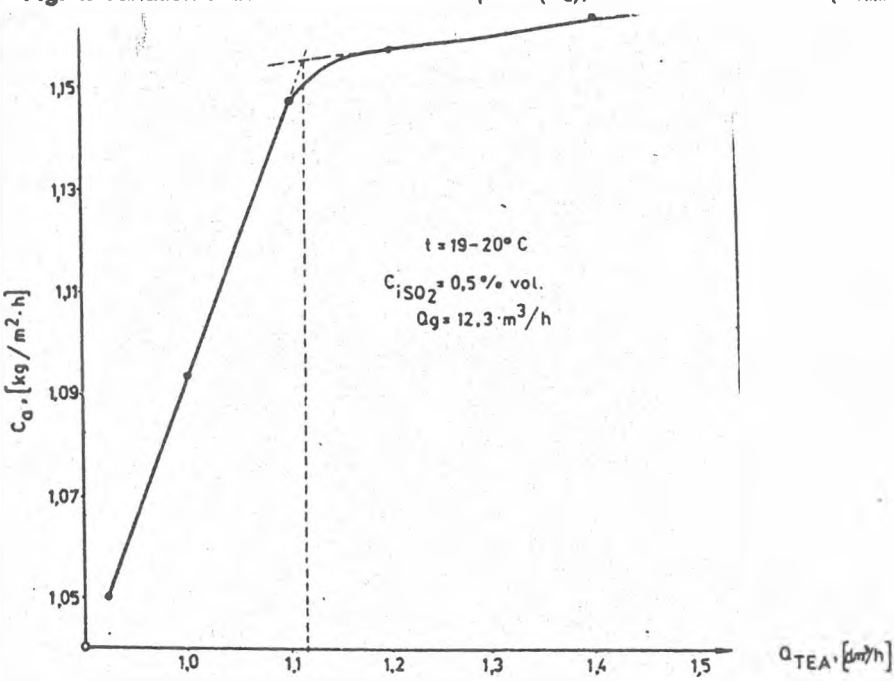

Fig. 5. Variation of the coefficient of absorption (C_a), versus the TEA flow (Q_{TEA})

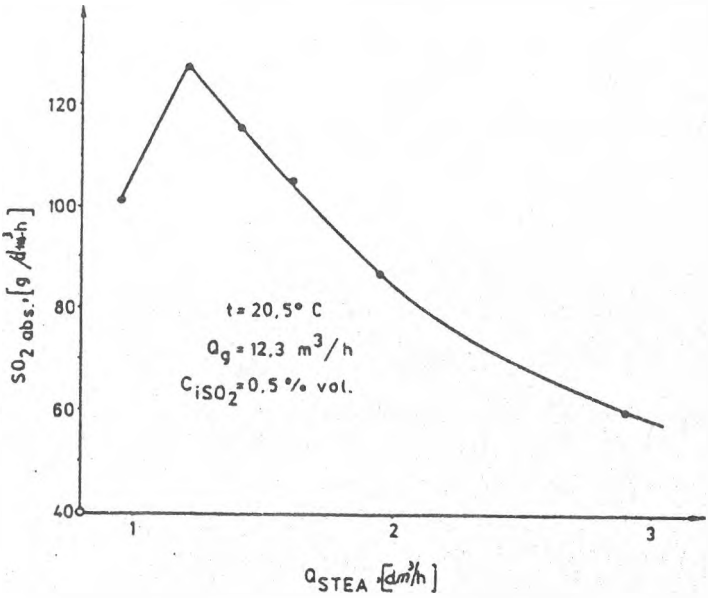

Fig. 6. Variation of sulfur dioxide quantity, versus the TEAS flow (Q_{TEAS})

In the figures 7 and 8 are illustrated the variation of sulfur dioxide content of the purified gas (%v/v), versus the absorbent flow (dm^3/h), in the above mentioned conditions of work. The obtained values are: 0.33% SO_2 if the flow of NMP is 9.8 dm^3/h, 0.007% when TEA flow is 1.5 dm^3/h.

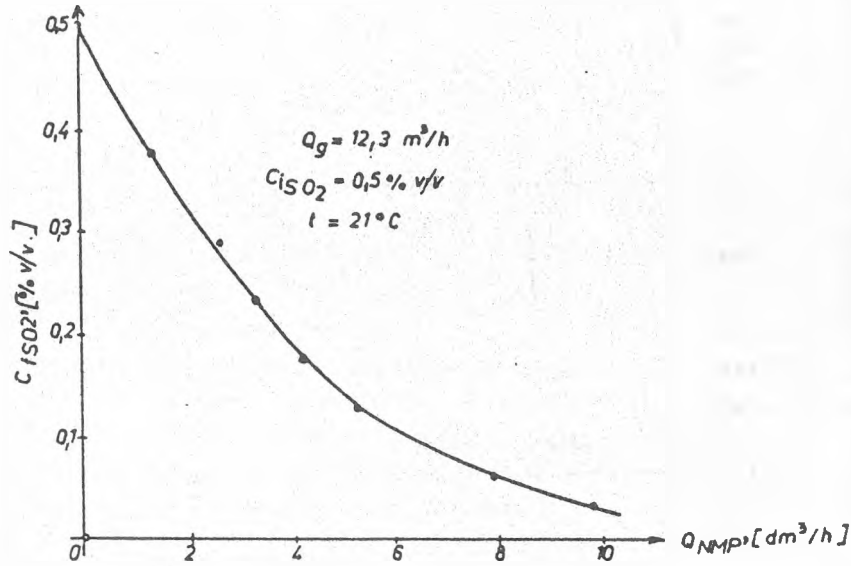

Fig. 7. Variation of sulfur dioxide content of the purified gas (C_f), versus the NMP flow (Q_{NMP})

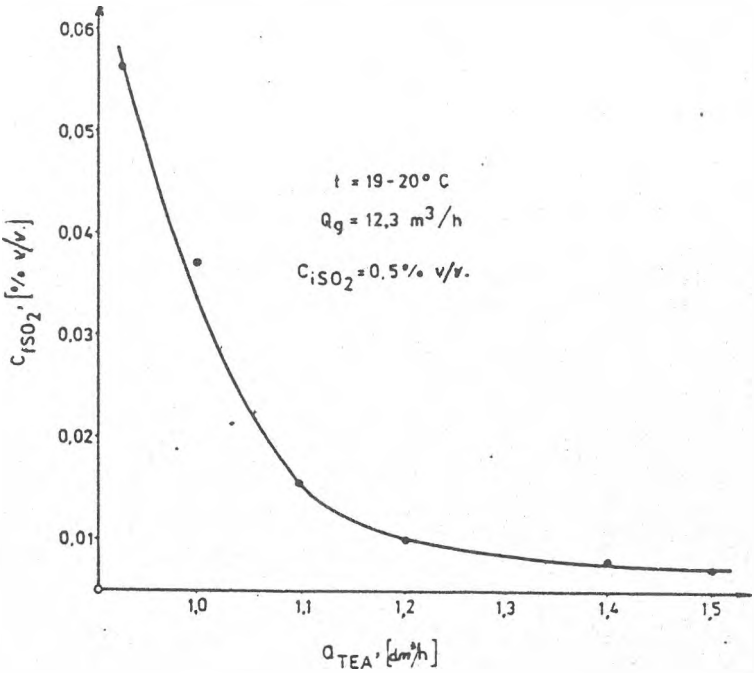

Fig. 8. Variation of sulfur dioxide content of the purified gas (C_f), versus the TEA flow (Q_{TEA})

The values of the coefficient of absorption (C_a) were calculated using the best experimental results obtained in the case of the utilized absorbents: NMP, TEA and TEAS. These are - in the same order - as followings: 112, 1115 and 862 [g SO_2/m^2 h dm^3].

REFERENCES

1. J. Vodnar, *RO Patent*, No. 93128, 1987. C.A. vol. 109:60718u.
2. J. Vodnar, *RO Patent*, No. 89508, 1986. C.A. vol. 108:77737b.
3. J. Vodnar, *Studia Univ. Babeş-Bolyai, Chemia*, 1985, 30, 59.
4. J. Vodnar, *Rev. Chem.*, Bucureşti, 1986, 37(2), 499.
5. J. Vodnar, *Studia Univ. Babeş Bolyai, Chemia*, 1986, 31, 37 and 44.
6. G. Astarita, D.W. Savage, A. Bisio, *Gas Treating with chemical Solvents* Wiley-Interscience, New-York, 1983.
7. Menig, H., *Emissionsminderung und Recycling - Grundlagen, Technologien, Verordnungen und Richlinien.* Ecomed Verlag 1987.

STUDIA UNIVERSITATIS BABEŞ-BOLYAI, CHEMIA, XLII, 1-2, 1997

THE STUDY OF CHEMICAL REACTIONS, ABSORPTION AND EXTRACTION, USING APPARATUSES WITH SERPENTINE PIPE FOR PELLICLIZING-BUBBLING. IX. THE THERMAL AND INITIATED HYDROPEROXIDATION OF p-DIISOPROPYLBENZENE

JANOS VODNAR[1], ALEXANDRU CHIŞ[1], ANDREI BIRO[1], SÁNDOR BEKASSY[2], SIMION DRĂGAN[3], MIHAELA DRĂGAN[1]

ABSTRACT. The paper presents the experimental results obtained by thermal and initiated hydroperoxidation of p- diisopropylbenzene, using one of the Vodnar type apparatuses [1-5] with discontinuous working. The p- diisopropylbenzene was used after a purifying by two different methods: the first was a fractional distillation and the second was a washing with concentrated sulfuric acid followed by a vacuum distillation in nitrogen atmosphere. As oxidizing agent molecular oxygen was used. Temperature varied between 110 and 130° C. The oxygen flow rate was always 10 dm^3/h. p- Diisopropylbenzene fed in the apparatus was 80 cm^3. The best results were obtained at 120°C, using p- diisopropylbenzene purified by the above mentioned second method, when the hydroperoxide content of the sample, after six hours, attained the value of 1,4 $mole/dm^3$.

Based on the experimental results, the activation energy was calculated and mathematical models for calculation the quantity of hydroperoxides yielded up to time t were deduced. The efficiency of the apparatus by the liquid recycling number "α" was determined. This way we concluded that the apparatus used is a chemical reactor making the mixing to be perfect.

INTRODUCTION

Hydroperoxides may be obtained by thermal and initiated hydroperoxidation of hydrocarbons and their derivatives. During the hydroperoxidation of p-diisopropylbenzene one can obtained the corresponding mono- and dihydroperoxides which are used as raw material in p-isopropylphenol and hidroquinone production. Both are widely used chemical substances. The first is, for instance, a good antioxidizer and the second is a commonly used photography developer and monomer stabilizer. This paper presents the

[1] Facultatea de Ştiinţe Economice, Catedra de Tehnologie şi Merceologie, Universitatea "Babeş-Bolyai", Cluj-Napoca.

[2] Department of Organic Chemical Technology, Technical University of Budapest (Hungary).

[3] Facultatea de Chimie şi Inginerie Chimică, Catedra de Inginerie Chimică, Universitatea "Babeş-Bolyai", Cluj-Napoca.

experimental results obtained by the thermal and initiated hydroperoxidation of p-diisopropylbenzene, using a Vodnar-1 type apparatus [1-5] with discontinuous working. p-Diisopropylbenzene, the most raw material of the process was purified by two different methods: the first was a fractional distillation and the second consisted of a washing with concentrated sulfuric acid which followed by a vacuum distillation in nitrogen atmosphere. These two varieties of the mentioned hydrocarbon were hydroperoxidized separately with a view to determine the influence of the impurities of the hydroperoxidation process.The best results were obtained at 120°C using oxygen as oxidizing agent and p-diisopropylbenzene purified by the above mentioned second method, when the hydroperoxide content of the sample, after six hours, attains the value of 1,4 mole/dm^3.

Based on the experimental results the activation energy was calculated, and mathematical models to calculate the quantities of hydroperoxides yielded up to time t were deduced. The efficiency of the apparatus by the recycling number "α" was determined. On this way we concluded that the used apparatus in a chemical reactor with perferct mixing [6].

In the chemical literature there are described many procedures for hydroperoxidation of p-diisopropylbenzene using oxygen or air as oxidizing agents [7-15]. In this paper is described the hydroperoxidation of p-diisopropylbenzene by bubbling and in a liquid film which forms on the internal surface of the serpentine pipe with which the apparatus is provided [5].

EXPERIMENTAL

Experiments were performed by means of a Vodnar-1 type apparatus which permits hydroperoxidation in a discontinuous flow. Purified oxygen was used as hydroperoxidizing agent. p-Diisopropylbenzene used as most important raw material was purified by the above mentioned two different methods.

The general scheme of the laboratory installation is presented in Fig.1.

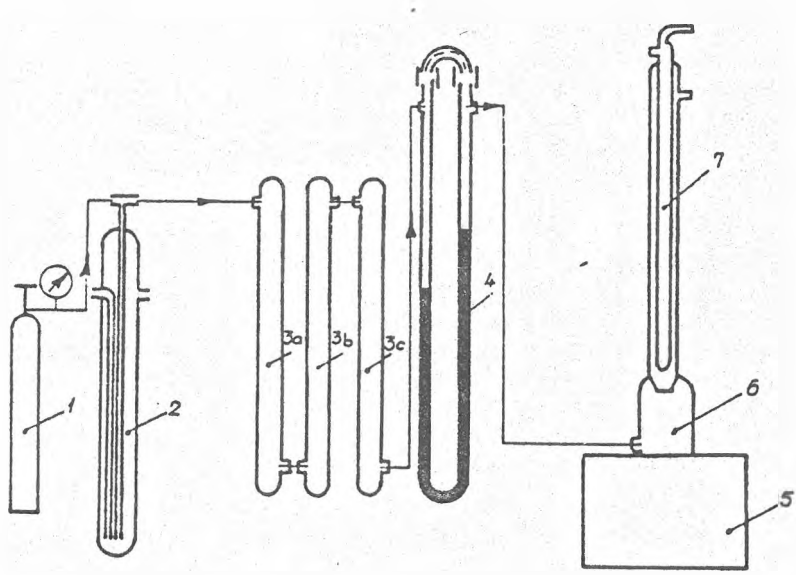

Fig.1. The scheme of the laboratory installation

The oxygen coming from a steel reservoir 1 pass through excess pressure safety 2, adsorption columns 3, a-3 b-3; c-3 (contain in the same order: calcium hydroxide, calcium chloride and active carbon), rheometer 4 (having the aim to determine the gas flow rate), and then get into Vodnar-1 type apparatus 6, provided with reflux refrigerator 7. Constant temperature was maintained with the ultrathermostat 5. The quantities of p-diisopropylbenzene samples subjected to hydroperoxidation were always 80 cm^3. Cumene hydroperoxide as initiator was used. Hydroperoxidation took place by bubbling the purified oxygen through p-Diisopropylbenzene, when a liquid pellicle (film) is produced within the serpentine pipe (spiral shape tube) of the apparatus. Tests for dosing hydroperoxides are taken from the reaction mixture periodically. The flow rate of oxygen was generally 10 dm^3/h.

RESULTS AND DISCUSSION

The experimental results are illustrated in figures 2-5. In the first series of experiments was studied the dependence between the hydroperoxide content of the samples on different temperatures and the reaction time, without the use of any initiators. Figure 2 illustrates the kinetic curves at three temperature values: 110°C; 120°C and 130°C. The p-diisopropylbenzene was purified by the first method. We can state that when the temperature is higher than 120°C, the reaction rate increases considerably. Nevertheless, the hydroperoxide contents after six hours remain relatively low: 0,24 at 110°C, 0,253 at 120°C and 0,563 mole/dm^3 at 130°C.

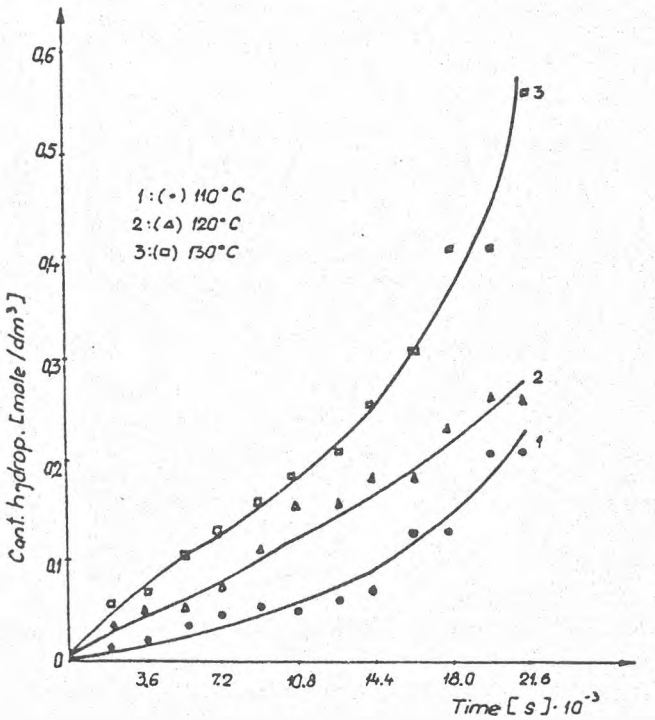

Fig. 2. The dependence of the hydroperoxide content, versus the reaction time: 1- 110°C; 2- 120°C; 3- 130°C

The influence of the initiator (cumene hydroperoxide) content of samples, which is an important parameter of the hydroperoxidation process of hydrocarbons was studied in the following series of experiments, illustrated in figure 3. The results obtainde at 120°C using 0,229; 0,433 and 0,569 mole/dm^3 cumene hydroperoxide as initiator, show that the rate of hydroperoxidation and the maximum concentration of hydroperoxide which may be achieved, are not high enough even if we use 0,569 mole/dm^3 initiator. Nevertheless, the positive effect of the initiator is obvious. The maximum concentration of hydroperoxide which can be obtained at 128°C, after four hours of hydroperoxidation is about 1,8 mole/dm^3. Without initiator (thermal hydroperoxidation) at the same temperature, the concentration of hydroperoxide was only 0,253 mole/dm^3.

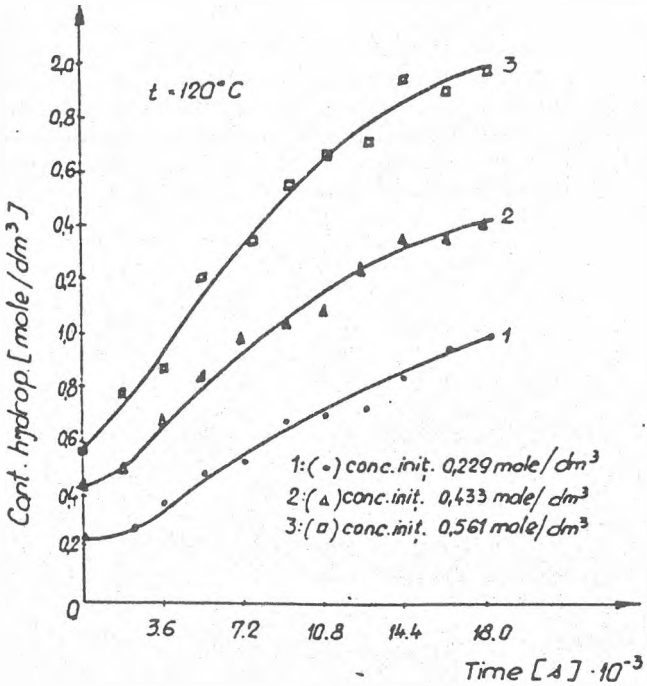

Fig.3. Variation of hydroperoxide content, versus the reaction time, at 120°C, using different quantities of initiator (mole/dm^3): 1- 0,229; 2- 0,433; 3- 0,561 mole/dm^3

Another series of experiments were made at 110°C, 120°C and 130°C, using constant quantities of cumene Hydroperoxide as initiator equal with 0,433 mole/dm (see Fig.4). It was stated that after 4,5 hours of hydroperoxidation at 120°C was achieved a concentration of hydroperoxide equal with 1,122 mole/dm^3. In the same time, at 130°C, after 2,5 hours, when the hydroperoxide content of the sample was 0,867 mole/dm^3, began the thermal decomposition of the hydroperoxide. Consequently, in some practical applying of this process the accepted temperature limit is at 120°C.

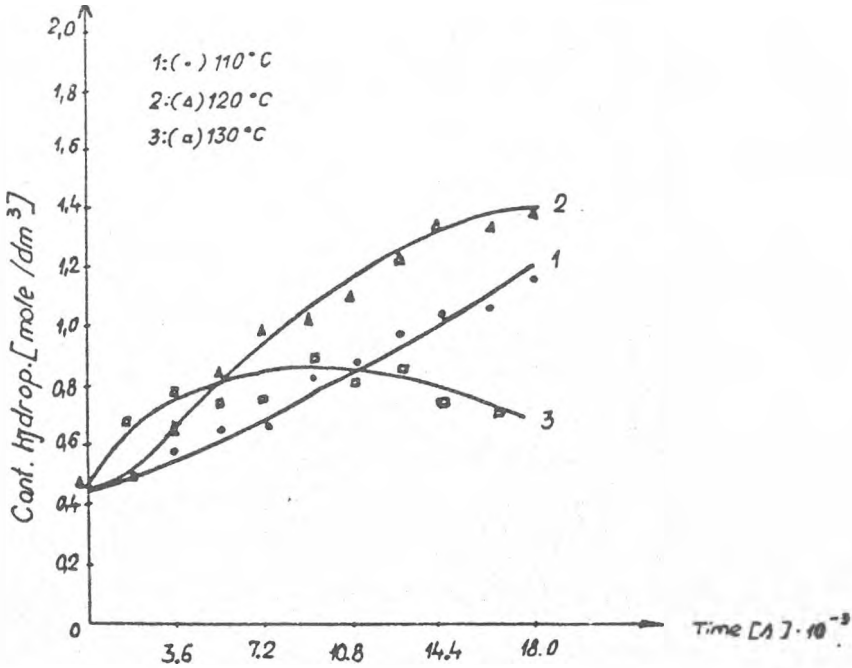

Fig.4. Variation of hydroperoxide content, versus the reaction time, using 0,433 mole/dm^3, at different temperatures: 1- 110°C; 2- 120°C; 3- 130°C

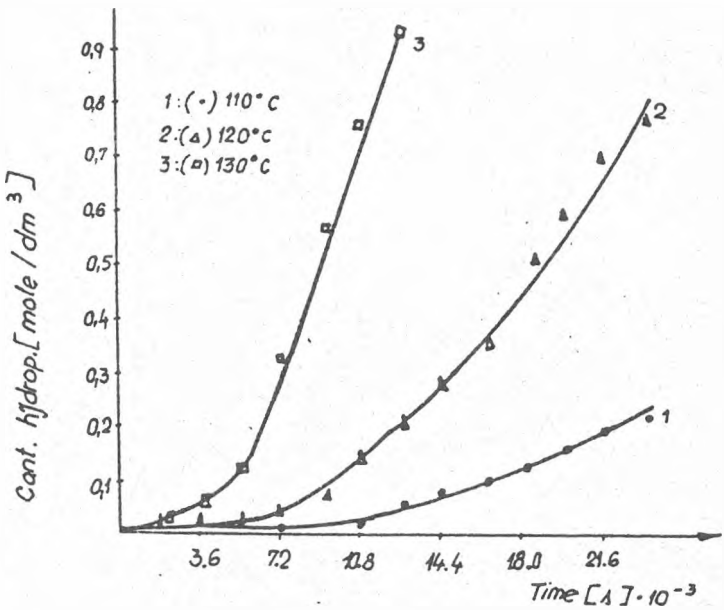

Fig.5. The dependence of the hydroperoxide content, versus the reaction time, without initiator, at different temperatures: 1- 110°C; 2- 120°C; 3- 130°C

To point out the importance of the purifying of p-diisopropylbenzene in the next series of experiments we used as raw material p-diisopropylbenzene purified by washing with concentrated sulfuric acid, followed by a vacuum distillation in nitrogen atmosphere. Figure 5 illustrates the experimental results obtained by hydroperoxidation of the p-diisopropylbenzene purified according to the second method (mentioned above), without any initiator.

Experiments were made at 110°C; 120°C and 130°C. We stated that at 120°C, after six hours of hydroperoxidation the maximum concentration of hydroperoxide attained 0,786 mole/dm^3 value, in comparison with that obtained using p-diisopropylbenzene purified only by fractional distillation, which was equal with 0,355 mole/dm^3.

In the last series of experiments was tested the effect of the oxygen flow rate, on the hydroperoxidation process. It was stated that at 120°C, using an oxygen flow rate equal with 12 dm^3/h, the hydroperoxide content of the sample attained the value of 1,4 mole/dm^3, which is with 0,6 mole/dm^3 higher than that obtained with 10 dm^3/h oxygen flow rate. That underlines the importance of the oxygen flow rate, which determines the recycling flow rate of the liquid within the apparatus used.

On the basis of the experimental results obtained, we concluded that the hydroperoxidation process has an autocatalytic character and the rate constant k can be described with the following mathematical equation:

$$k = \frac{1}{t} \cdot \frac{1}{a+b} \cdot \ln \frac{a(b+x)}{b(a-x)}$$

where a is the concentration of the p-diisopropylbenzene [mole/dm^3];
b - concentration of the initiator [mole/dm^3];
x - p-diisopropylbenzene transformed into hydroperoxide up to time t [mole/dm].

The activation energy was calculated from pairs of lnk and 1/T values in the temperature region between 110°C and 130°C and it is equal with 26,34 kJ/mole, respectively 110,10 kJ/mole.

Mathematical models for the calculation of hydroperoxide content at different temperature, corresponding to time t were deduced.

These are the followings:

- at 110°C: $C^{t}_{HDPB} = 1{,}001 \cdot C^{o}_{HDPB} \cdot e^{3{,}25 \cdot 10^{-3} \cdot t}$
- at 115°C: $C^{t}_{HDPB} = 1{,}0092 \cdot C^{o}_{HDPB} \cdot e^{4{,}4 \cdot 10^{-3} t}$
- at 120°C: $C^{t}_{HDPB} = 1{,}001 \cdot C^{o}_{HDPB} \cdot e^{5{,}55 \cdot 10^{-3} t}$

where c^{t}_{HDPB} is the concentration of hydroperoxide at time t [mole/dm^3];
c^{o}_{HDPB} - the quantity of the initiator [mole/dm^3];
t - the reaction time [min].

The efficiency of the apparatus was determinated by the liquid recycling number "α". This way we have concluded that the apparatus is a chemical reactor

with perfect mixing. For such a determination must calculate the contact time (t_c) of p-diisopropylbenzene in the hydroperoxidizing apparatus [6]:

$$t_c = \frac{1}{k(C^o_{DIB} + C^o_{HDIB})} \cdot \ln[\frac{c^0_{DIB}(c^0_{DIB} + c^0_{HDIB} - c_{DIB})}{c_{DIB} \cdot c^0_{HDIB}}]$$

where t_c is the contact time of p-diisopropylbenzene in the apparatus of hydroperoxidation [min];
k - reaction rate constant [dm^3/mole.min];
c^O_{DIB} - the initial concentration of p-diisopropylbenzene [mole/dm^3];
c_{DIB} - the final concentration of p-diisopropylbenzene [mole/dm^3];
c^O_{HDIB} - the initial concentration of hydroperoxide [mole/dm^3];
c_{HDIB} - the final concentration of hydroperoxide [mole/dm^3].

$$c^o_{DIB} + c^o_{HDIB} - c_{DIB} = c_{HDIB}$$

Using the experimental data we can calculate the value of t_c, as following:

$$t_c = \frac{1}{2{,}27 \cdot 10^{-4}(4{,}49 + 0{,}561)} \cdot \ln[\frac{4{,}49(4{,}49 + 0{,}561 - 3{,}913)}{3{,}913 \cdot 0{,}561}] = 736\,\text{min}.$$

In the same time we must know that:

$t_c = V_A / D_V$ and $D_V = V_A / t_C = 80 / 736 = 0{,}108696$ cm^3 / min = 6,5217 cm^3 / h.

Consequently: $\alpha = d_V / D_V = 12{,}000 / 6{,}5217 = 1{,}840$.

Where V_A is the useful volume of the apparatus [cm^3];
D_V - the flow rate of p- diisopropylbenzene [cm^3/h];
d_v - the recycling flow rate of the liquid within the apparatus [cm^3/h];
α - the recycling number.

By such a high value of "α" the apparatus may be considered as a reactor with perfect mixing.

REFERENCES

1. J. Vodnar, *J. Appl. Chem.*, London, 1970, 20, 99.
2. J. Vodnar, *Revista de Chimie*, București, 1992, (1-2), 60-63.
3. J. Vodnar, *Magy. Kem. Lapja*, Budapest, 1993, XLVIII, 3sz, 125.
4. J. Vodnar, *RO Patent, No.53332*, 1971, C.A. vol. 78:29200m.
5. J. Vodnar, *RO Patent, No. 96372*, 1989, C.A. vol. 115:138742t.
6. R. Mihail, O. Munteanu, *Reactoare chimice*, Editura did. și ped. București, 1983.
7. T. Shigeru, O.V. Yoshinobu, T. Todahiko, *J. Fuel Soc. Japan*, 1956, 35, 32-36.
8. S.V. Zavgorodni, O.V.Sigov and I.F. Baev, *Zl. Obshch. Khim.*, 1958, 28, 1279-1284.
9. B.D. Kruzhalov and V.V. Federova, *Khim. Nauka I Prom.*, 1958, 3, 687.
10. S.V. Zavgorodnii, I.N. Novicov, *Izvest. Vysshikh Ucheb. Zvedenii, Khim., Khim. I Khim. Teknol.*, 1968, 3, 863-867.

11. T. Shigeru, *Japan*, 1960, 6, 7558, C.A. vol. 62:8027 g.
12. V.V. Federova, M.S. Belinskii and I.D. Sinovich, C.A., 1965, 62, 6419c.
13. G.P. Pavlov, I.E. Pokravskaya and I.B. Shmakova, *Otkrutya Izobret. Prom. Obrazttsy, Tovamye Znaky*, 1973, 50(16), 49.
14. K. Hashimoto, H. Nambu, K. Watari, *Eur. Pat. Appl.*, 1981, 21, 848.
15. J. Vodnar, *The second conference on the Applied Chemistry*, 1971, 2/2, 593, Veszprem (Hungary).

STUDIA UNIVERSITATIS BABEŞ-BOLYAI, CHEMIA, XLII, 1-2, 1997

ELECTROCHEMICAL ASSAY OF CREATINE KINASE ACTIVITY IN SERUM WITH A MINIATURIZED BIOSENSOR

MARCEL B. MĂDĂRAŞ[1], RICHARD P. BUCK[1]

ABSTRACT. A miniaturized, disposable amperometric creatine biosensor (biochip) has been used for the electrochemical assay of creatine kinase (ATP: creatine N-phosphotransferase, EC 2.7.3.2) in human serum. The formation rate of creatine was linearly proportional to the activity of creatine kinase (CK) up to 0.8 U mL^{-1} (r^2 = 0.9997) in buffer, with a detection limit of 0.005 U mL^{-1} when tested in buffered control serum. The biochip was applied to the assay of creatine kinase in human control serum. At 37°C and using N-acetyl-L-cysteine (NAC) as reactivator of CK catalytic activity, the measured CK activity for a human control serum was 0.187 ± 0.012 U mL^{-1}, which was not statistically different from the assigned value of 0.165 ± 0.040 U mL^{-1}. This disposable sensor may be integrated into a portable analyzer that allows reliable and relatively fast assay of CK as a molecular marker of acute myocardial infarction (AMI).

INTRODUCTION

Measurement of creatine kinase and creatine kinase - MB isoform are presently used as biochemical markers of acute myocardial infarction [1]. The approved method recommended by the International Federation of Clinical Chemistry (IFCC) is based on a spectrophotometric method, using a sequence of enzymatic reactions with a NADPH-forming indicator reaction [2]. Recent studies have shown the importance of measuring and recording the time changes (slopes) of CK activity in addition to the discrete values, over a period of at least 12 h (better 24-30 h) after the onset of chest pain in hospitalized patients [3, 4]. The normal CK values in serum are 0.015 - 0.10 U mL^{-1}, while they can increase up to 0.8 - 1.0 U mL^{-1} in the first 24 h after the onset of AMI.

In recent years a new class of portable clinical analyzers has been designed to provide rapid turnaround time with precision and accuracy comparable to the bench-top analyzers. These systems require integrated and miniaturized sensing elements. We have recently described [5, 6] creatine and creatinine amperometric biosensors fabricated using immobilized enzymes and microelectronics technology. Here we present preliminary results for the use of the miniaturiazed creatine sensors in the electrochemical assay of creatine kinase. These biosensors have the potential advantage of reducing the cost of this test, especially if several repetitive determinations are to be made in a narrow time frame.

[1] Department of Chemistry, University of North Carolina at Chapel Hill, Chapel Hill, NC 27599-3290, USA

The principle of the assay is based on the following reaction:

$$\text{Creatine phosphate} + \text{ADP} \xrightarrow{\text{CK}} \text{Creatine} + \text{ATP} \quad (1)$$

The formation rate of creatine is proportional to the activity of CK in the sample, provided the substrate concentrations are not rate-limiting.

The detection method for creatine is based on an enzyme catalytic sequence, using co-immobilized creatine amidinohydrolase (CI) and sarcosine oxidase (SO):

$$\text{Creatine} + H_2O \xrightarrow{\text{CI}} \text{Sarcosine} + \text{Urea} \quad (2)$$

$$\text{Sarcosine} + H_2O + O_2 \xrightarrow{\text{SO}} \text{Glycine} + HCHO + H_2O_2 \quad (3)$$

The hydrogen peroxide formed in the enzyme layer is amperometrically detected at the working electrode polarized at + 0.6 V vs. Ag/AgCl reference electrode.

A few other enzyme-electrode based schemes were proposed for the quantitation of CK activity. Hill and Sanghera [7] have used a ferrocene mediated glucose electrode and soluble hexokinase for this purpose and Shubert *et al.* [8] have used a multienzyme membrane containing immobilized pyruvate kinase, lactate dehydrogenase and lactate monooxygenase. These systems are rather complicated; different reagents and/or enzymes had to be added to the assay solution increasing the cost of the analysis. Pfeiffer *et. al.* [9] have summarily described a similar approach with the one proposed here, using a classical macroelectrode.

EXPERIMENTAL

Reagents

Creatine kinase (type I from rabbit muscle), creatine phosphate (disodium salt, hydrate), adenosine 5'-diphosphate (ADP), N-acetyl-L-cysteine (NAC), creatine hydrate, 1,3-diaminobenzene (DAB), acetaminophen, L-ascorbic acid, uric acid and Accutrol® normal control serum were purchased from Sigma Chemical Co (St. Louis, MO). Nafion (perfluorosulfonic acid, 5% solution in a mixture of low molecular weight aliphatic alcohols and water) was from Aldrich (Milwaukee, WI) and poly-(2-hydroxyethylmethacrylate) (p-HEMA) with MW = 300,000 was obtained from Scientific Polymer Products, Inc. (Ontario, NY). Dade Moni-Trol® level I control serum was from Baxter (McGaw Park IL). All other chemicals were analytical reagent grade. Double distilled water was used for all the solutions.

Solutions

The amperometric measurements were performed in isotonic phosphate buffer saline (PBS, pH 7.4) containing 0.053 M Na_2HPO_4, 0.051 M NaH_2PO_4, 0,051 M NaCl, 1.5 mM $MgNa_2EDTA$, 1 mM NaH_2PO_2 and 0.2 nM NaN_3. The following reagent stock solutions were prepared: 10 mM ADP (in PBS), 0.345 M creatine phosphate (aqueous) and 0.5 M NAC (in PBS). The creatine phosphate stock solution was stable for 3 months at 4°C, whereas ADP and NAC solutions were freshly prepared before use. A stock solution of 1000 U mL^{-1} CK in PBS was

prepared and stored frozen at -20°C. Aliquots were used periodically to prepare a 100 U mL^{-1} solution used in the assay.

Equipment

Electrochemical measurements were performed using a PINE RDE4 potentiostat The miniaturized biochip incorporating the working, counter and pseudo-reference electrodes on the same wafer was fabricated as described below. The batch-type experiments used a thermostatable Plexiglas cell (5 mL volume) and the solutions were stirred at constant speed using a Fisher magnetic stirrer. The noise due to the magnetic stirring was removed using an analog 0.7 Hz Butterwoth-type low pass filter.

Preparation of microfabricated biosensors

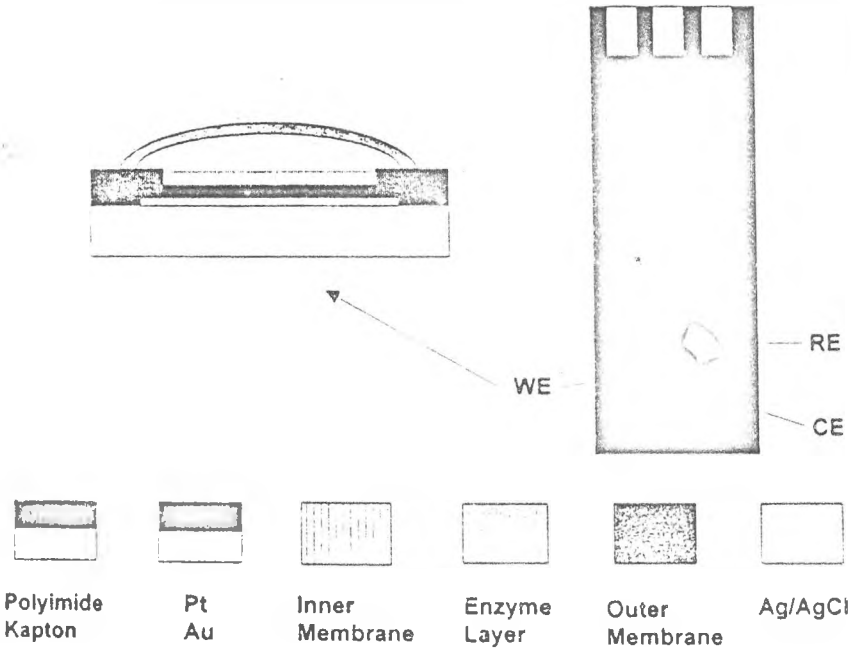

Fig.1. Schematic drawing of the miniaturized, planar-type, biochip: WE = working electrode (d = 1.5 mm); CE = counter electrode; RE = reference electrode Biochip dimensions: 20 x 6 (mm x mm)

The fabrication of the film structure for the base electrodes comprises several steps described in more detail elsewhere [10]. Before the Pt deposition, the surface of the working electrode was electrochemically cleaned using a current density of 0.5 mA/cm^2 for 30 seconds, with the polarity of the electrodes reversed. Then, Pt was galvanostatically deposited using 12.7 mA/cm^2 for 6.5 minutes. After Pt electrodeposition, the inner membrane was prepared as described below, then the chips were individually cut from the larger wafer and the electrical connections

were made. The pseudo-reference Ag/AgCl electrode on each biochip was prepared after the individual chips were cut from the wafer. First, Ag deposition was performed from a 1% $KAg(CN)_2$ aqueous solution, using a current density of 5 mA/cm^2 for 10 minutes. Then, a portion of the electrodeposited Ag was converted to AgCl by inserting each chip in a 0.1 M HCl solution and anodizing using 5 mA/cm^2 for 2.5 minutes. The schematic diagram of the biochip design with all three electrodes incorporated on the chip is shown in Figure 1.

To provide the desired chemical sensitivity and selectivity, a structure consisting of a three layer system subsequently described, was built on the working electrode:

Inner membrane (IM). An inner permselective layer on the Pt electrode was used to diminish simultaneous oxidation of interferences such as ascorbate, urate, acetaminophen and other electroactive molecules likely to be present in the serum. The inner layer was formed by electropolymerization from 0.1 M PB (pH 7) solutions containing 1,3-DAB. The electropolymerization was done by cyclic voltammetry between +0.2 and +0.8 V vs. Ag/AgCl, using different scan rates and electropolymerization times. The oxidation of the monomer at the surface of the electrode produces an anodic peak (at +0.5 V vs. Ag/AgCl) which gradually decrease in amplitude in subsequent cycles indicating that a non-conducting film forms at the electrode surface. Preliminary trials have used deoxygenation of the monomer(s) solution before and during electropolymerization using N_2, but this approach produced gas bubbles on the surface of the electrode which could alter the uniformity of the electrodeposited layer. No deaeration was therefore used in our subsequent studies.

Enzime layer (EL). The enzymatic layer was obtained by crosslinking the enzymes with GA in the presence of BSA. For a typical preparation, 3.8 mg CI (12 U/mg), 1.2 mg SO (45 U/mg) and 0.6 mg BSA were dissolved in 60 µL PBS (pH 7.4) in a small conical vial and mixed together. The appropriate amounts of 1% glutaraldehyde aqueous solution (freshly prepared) were added to the vial to start the crosslinking process. 2 µL of the resulting mixture was quickly deposited on the working electrodes of the creatine sensors using a micro syringe. The EL obtained was allowed to crosslink in air, at room temperature, for one hour. The amount of immobilized enzymes was estimated from the activity of the lyophilized enzymes, as specified by the manufacturer. No measurement of the residual activity after the immobilization was performed.

Outer membrane (OM). To complete the preparation of the biosensors, an outer membrane was deposited above the enzymatic layer. Stock solutions of p-HEMA (5 and 10% by weight) were prepared by dissolving the p-HEMA beads in methanol (99,9%). The deposition solutions were prepared by mixing equal volumes of the 5% p-HEMA and Nafion solutions to yield a mixture with 2.5% p-HEMA-2.5% Nafion or by diluting the p-HEMA and Nafion stock solutions with methanol. The outer membrane was fabricated by placing 1-3 µL (depending on the area of the WE) of the chosen mixture on top of the enzymatic layer with a micro syringe. The solvent evaporation at room temperature produced a

transparent and compact outer layer. After solvent evaporation and when not in use, these biosensors were stored at 4°C in PBS.

Assay procedures

For the optimization studies of the assay conditions, the biochip was initially inserted in the cell into the buffer solution containing the desired amounts of ADP and creatine phosphate. After the potential was applied to the working electrode (+ 600 mV vs. Ag/AgCl) and the background current was allowed to stabilize, the appropriate volume of CK solution (100 U mL^{-1}) solution was injected in the cell and the sensor output (current) increase was recorded in time. Creatine kinase in serum is rapidly inactivated. The loss of catalytic activity is caused by exposure to light, thermal inactivation or oxidation of the reactive thiol groups. To ensure full catalytic activity, the enzime must be reactivated using a reducing compound. NAC has been recommended by IFCC for this purpose [2].

Serum assay of CK was performed in a similar manner with the buffer assay, except that this time the cell was thermostated at 37°C and NAC was used for the reactivation of CK. After the stabilization of the background current in 2.0 mL PBS solution containing ADP and NAC, 1 mL control serum was injected in the cell and after incubation for 2 minutes, 0.3 mL creatine phosphate stock solution was added to initiate the reaction. The current increase due to the CK activity in serum was recorded for about 4 minutes to obtain the slope; then an aliquot of 100 U mL^{-1} CK solution was injected and the new slope of the creatine sensor response was recorded for another 4 minutes.

RESULTS AND DISCUSSION

Before the actual measurements of the CK activity were performed, the miniaturized biosensors for creatine were tested for ptential interferences such as ascorbate, urate and acetaminophen, likely to be found in serum. Because the surface of the Pt electrode is covered with a permselective film as described before, the effect of the interferences is highly diminished. Moreover, because the electrochemical assay follows the response of the sensor in time, the signal due to the remaining interferences reaches a constant value in about 60 seconds and does not influence the slope of the current response after this initial response period. This is the reason the slope of the response is measured after 2-4 minutes from the initiation of the reaction.

In preliminary experiments, there was no response at the creatine sensor when injecting CK in a solution containing ADP in the absence of creatine phosphate or in a solution containing creatine phosphate in the absence of ADP. These results indicate that both substrates should be present in order for the enzyme catalyzed reaction to take place. An optimization study of the assay conditions was performed to ensure that the sensor response is dependent only on the activity of CK.

Effect of substrate concentrations

The dependence of the sensor's response on the concentration of creatine phosphate in the sample was studied first. From the data presented in Fig. 2, it is clear that the reaction rate reaches a maximum for creatine phosphate concentrations above 30 mM. The other substrate, ADP, shows a similar behaviour

(Fig. 3), with no significant increase in the reaction rate beyond 4 mM, the value that was chosen for the assay. In both cases, the final activity of CK in the tested solutions was high, to account for the abnormal values.

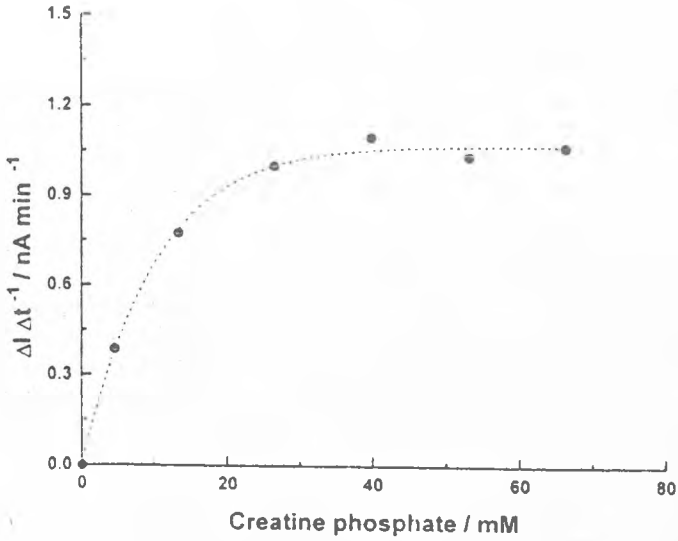

Fig. 2. Dependence of the current increase at the creatine blosensor on the concentration of creatine phosphate in the assay solution; measurements in PBS (pH 7.4), 25°C; [CK] = = 0.77 U mL^{-1}; [ADP] = 7.7 mM

CK assay in buffer solution

The assay of CK in buffer was done to determine the sensitivity of the assay and the linearity of the response. For this part no reactivation of the CK activity was used and the measurements were performed in PBS (pH 7.4) at room temperature (25°C). The selection of the buffer type, additives and pH was done according to the optimized conditions for the response of the biosensor and they are not necessarily the optimum conditions for the CK assay. Further studies are needed to find a compromise between the recommended conditions for the catalytic conversion of creatine phosphate and the optimal response conditions for the creatine biosensor.

The linear range of the response extended up to at least 0.8 U mL^{-1} (r^2 = 0.9997), as shown in Fig.4. The linearity of the response is appropriate for measurements of CK activity in serum samples from patients suspected of acute myocardial infarction.

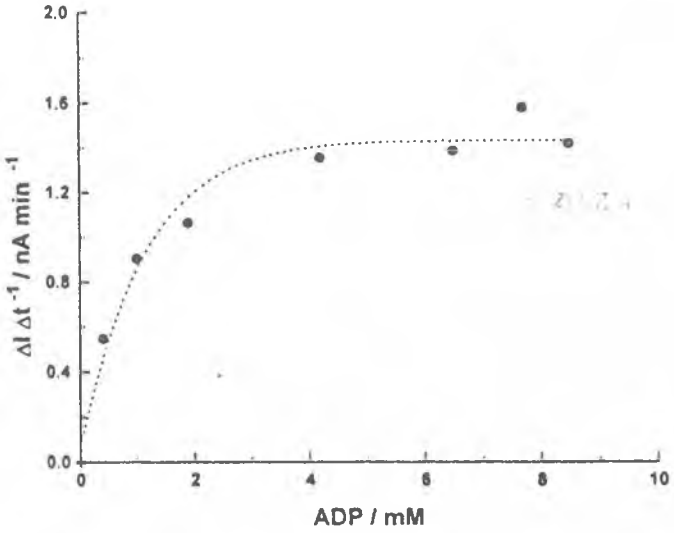

Fig. 3. Dependence of the current increase at the creatine biosensor on ADP concentration in the assay solution; measurements in PBS (pH 7.4), 25°C; [CK] = 0.77 U mL^{-1}; [creatine phosphate] = 39.8 mM

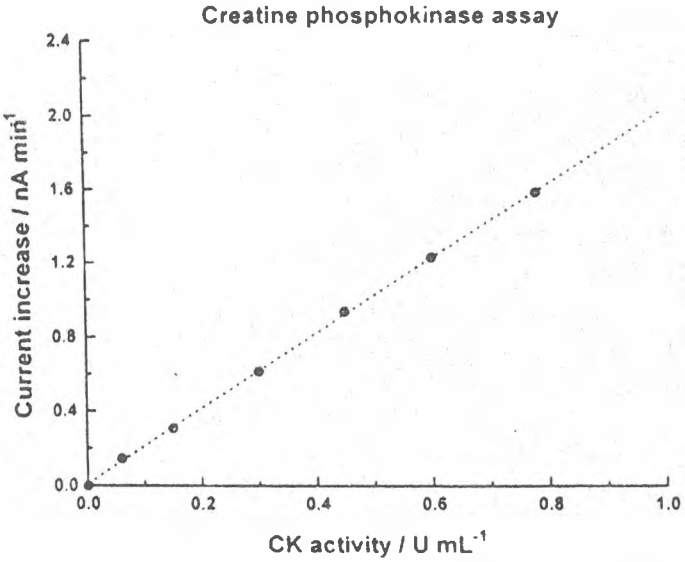

Fig. 4. Calibration curve for the CK assay; measurements in PBS (pH 7.4) at 25°C. No reactivation of CK activity was used. Substrate concentrations used in the assay: [creatine phosphate] = 31 mM; [ADP] = 4 mM

CK assay in control serum

The determination of CK activity in serum was performed using a standard addition procedure. When the concentration of the substrates (creatine phosphate and ADP) is kept in excess (at the levels determied before), the rate of increase in current at the creatine biosensor is directly related to the CK activity in the sample. Preliminary measurements of CK activity without adding NAC yielded recoveries 30-50% lower than the expected values, due to the inactivation of CK catalytic activity. Using 10mM NAC in the assay solution, the measured value using a human control serum was in statistical agreement with the assigned value by the manufacturer (Table 1).

Table 1. CK activity measurements in human control sera

Control serum	Measured* ($U\ L^{-1}$) at 37°C	Assigned ($U\ L^{-1}$) at 37°C
Moni-Trol (no reactivation)	58.4 ± 1.2	115.2 ± 5.9**
Accutrol (reactivation with NAC)	186.7 ± 30.3	165.0 ± 40.0

* $[CK] = [CK]_{avg} \pm CL$ (n=3)

** mean value of 10 different clinical analyzers

ACKNOWLEDGEMENTS

We thank Stefan Ufer and Bruce R. Ash (North Carolina State University, Biomedical Microsensors Laboratory) for the microfabrication of the electrodes used in this work. This research was supported by NSF Engineering Research Center Grant CDR-8622201.

REFERENCES

1. Adams, D.R. Abendschein and A.S. Jaffe, *Circulation*, 1993, 88, 750.
2. Horder, R.C. Elser, W. Gerhardt, M. Mathieu and E.J. Sampson, *Eur. J. Clin.Chem. Clin. Biochem.*, 1991, 29, 435.
3. Bakker, M.J.W. Koelemay, B. van Vlies, J.P.M.C. Gorgels, R. Smits, J.G.P. Tijssen and F.D.M. Haagen, *Eur. J. Clin. Chem. Clin. Biochem.*, 1995, 33, 351.

4. Lott, J.W. Heinz and K.A. Reger, *Eur. J. Clin. Chem. Clin. Biochem.*, 1995, 33, 491.
5. Mădăraș, I.C. Popescu, S. Ufer and R.P. Buck, *Anal. Chim. Acta*, 1996, 319, 335.
6 Mădăraș and R.P. Buck, *Anal. Chem.*, 1996, 68, 3832.
7. Hill and G.S. Sanghera, in *Biosensors: a practical approach*, ed. Cass, A.E.G., Oxford University Press, New York, 1990, pp. 30-32.
8. Weigelt, F. Schubert ano F. Scheller, *Anal. Lett.*, 1988, 21, 225.
9. Pfeiffer, K. Setz, N. Klimes, A. Makower, T. Schulmeister and F. Scheller, in *Biosensors: fundamentals, technologies and applications*, ed. F. Scheller and R.D. Schmid, vol. 17, GBF Monographs, Braunschweig, 1992, pp. 11-18.
10. Cosofret, M. Erdosy, T.A. Johnson, R.P. Buck, R.B. Ash and M.R. Neuman, *Anal. Chem*, 1995, 67, 1647.

STUDIA UNIVERSITATIS BABEŞ-BOLYAI, CHEMIA, XLII, 1-2, 1997

NORMAL PHASE THIN LAYER CHROMATOGRAPHY AND A LIPOPHILICITY STUDY BY REVERSED PHASE THIN LAYER CHROMATOGRAPHY OF SOME 2-AMINO-3-CYANO-4,5-DIPHENYLFURANE DERIVATIVES

GABRIELA CÎMPAN[1], VASILE MICLĂUŞ[1]

ABSTRACT. Several new compounds (2-amino-3-cyano-4,5-diphenylfurane derivatives) were studied by normal phase thin layer chromatography (NP-TLC), on silica gel plates, and by reversed phase thin layer chromatography (RP-TLC), on RP-C18 plates. The optimum separation was obtained in NP-TLC by using methanol-benzene-chloroform (48:48:4, v/v) as mobile phase, and the corresponding performance index was I_p=0.70. The RP-TLC was performed in order to establish the cogeneric nature of compounds, with methanol-water as eluent system. Good linear correlations were obtained between the R_M values and X, the methanol molar fraction in the mobile phase. The logP values were calculated from fragmental constants (Rekker's system) and were correlated with the extrapolated values, R_{MO}, for zero organic modifier in the mobile phase.

INTRODUCTION

Chromatographic methods can be successfully applied for the analysis of furane derivatives. Thin layer chromatography (TLC) and high performance liquid chromatography (HPLC) methods were reported in the literature for these compounds [1, 2]. Some azomethinic nitrofurans were separated and purified on a silica gel column [3]. Usually, normal phase chromatography (NP-TLC) is performed in order to obtain a good separation of the compounds in a given sample mixture. Different algorithms for the optimisation of the mobile phase composition are given in the literature, as the Simplex [4] or the Prisma [5] methods.

Reversed phase thin layer chromatography (RP-TLC) was applied for lipophilicity studies of substances. Lipophilicity can be determined directly by the "shake-flask" partition method between n-octanol and water [6, 7]. The practical difficulties of this method can be overcome by using reversed phase liquid chromatography, one of these methods being RP-TLC [8-10]. The retention parameters, logk in RP-HPLC or R_M in RP-TLC can be correlated with the logP values, experimentally determined or calculated. The calculated logP values can

[1] Faculty of Chemistry and Chemical Engineering, "Babeş-Bolyai" University, 11 Arany Janos street, 3400 Cluj-Napoca, Romania.

be obtained by different methods (Rekker's system [11, 12], Pomona College data base [13] or various software).

The first part of this study contains the optimisation of the separation by NP-TLC of some 2-amino-3-cyano-4,5-diphenylfurane derivatives. The second part it is a lipophilicity approach for the same compounds on RP-TLC plates in order to establish a congenerity in the series, or in other words, a linear correlation between the retention parameter, R_M, and the calculated logP values.

EXPERIMENTAL

The structures of the studied compounds are shown in Figure 1. Normal-Phase Thin-Layer Chromatography (NP-TLC) was performed on 10 x 10 cm plates precoated with a 0.25 mm layer of silica gel $60F_{254}$, and for Reversed-Phase Thin-Layer Chromatography (RP-TLC), RP-18 F_{254} plates (10 x 10 cm) were used (both plate types from Merck, Darmstadt, Germany).

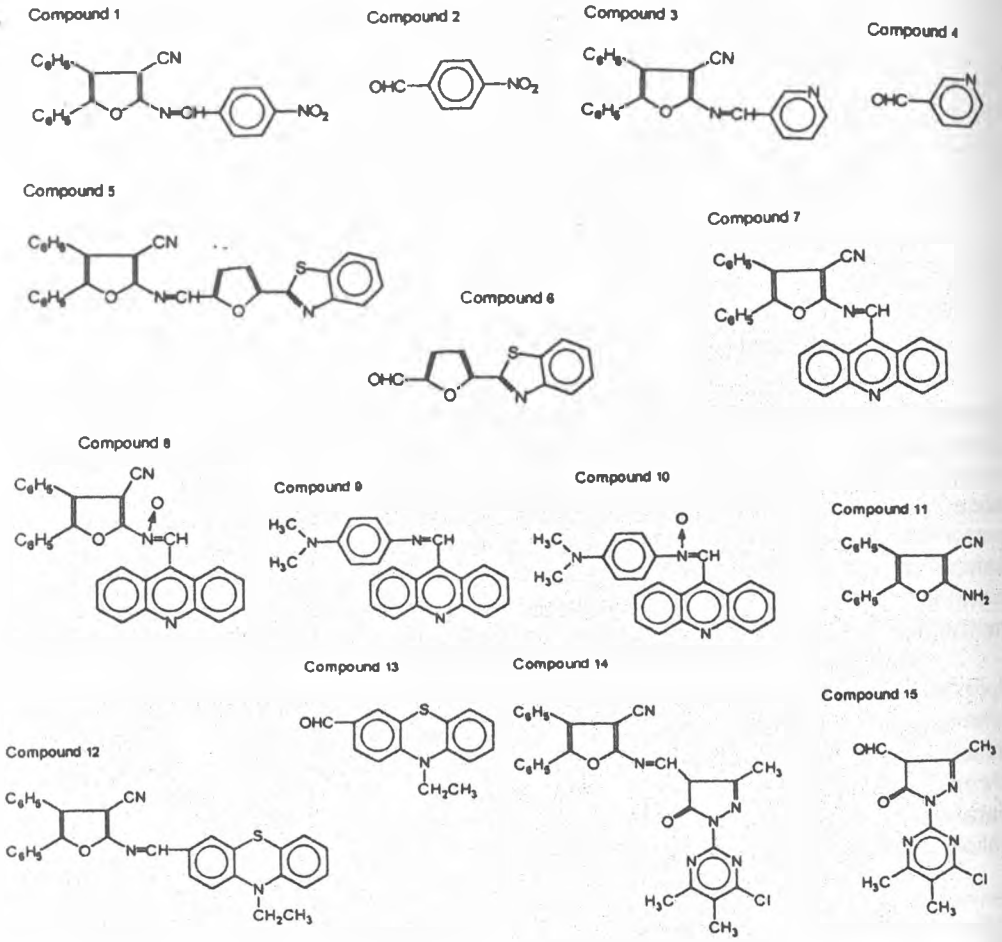

Figure 1. The structures of the studied 2-amino-3-cyano-4,5-diphenylfurane derivatives

The plates were developed in the ascending mode in previously equilibrated chambers for 30 minutes. The solvents for chromatography: chloroform, benzene, methanol, were obtained from "Chimopar" (Bucharest, Romania). The sample solutions were prepared as 1 mg in 8 ml methanol or a mixture methanol-chloroform (5:3, v/v) in order to improve the solubility (0.12 mg/ml). The samples were applied as spots onto the plates, 15 mm from the bottom edge, using 5 µL calibrated micropipettes. The eluent migration distance was 8 cm in all cases.

After development, the plates were dried in a gentle air stream and evaluated in UV light at 254 nm (by quenching the fluorescence of the layer) or at 366 nm for the compounds which have native fluorescence (compounds 1, 3, 5-13). The migration distances of substances and of the eluent font were measured by densitometry, using a CS-9000 Shimadzu dualwavelength flying spot scanner, in reflexion mode, at 245 nm.

RESULTS AND DISCUSSION

1. NP-TLC

The separations on silica gel plates were carried out in order to optimize an eluent system which can provide the best separation for all compounds. The compounds shown in Figure 1 are 2-amino-3-cyano-4,5-diphenylfurane derivatives and some other reagents which can be found the first group. The first type of compounds are new substances, synthesized in our laboratory, which were expected to have antibacterial and antifungical activity [14]. The optimization of the mobile phase composition has taken into account the Snyder's classification of all solvents in 8 groups, according to their proton-donor, proton-acceptor or dipolar characteristics [15, 16]. Preliminary experiments were performed by using a representative solvent from each of the 8 groups of polarity. Methanol, chloroform and benzene were the chosen solvents for the optimization of the mobile phase composition. The optimization process has involved 6 steps, following a Simplex procedure [17]. The degree of separation was evaluated by calculating the performance index, I_p [18].

$$I_p = \sqrt{\frac{\Sigma(\Delta hR_{f,i} - \Delta hR_f)^2}{n(n+1)}}$$

where,

$hR_f = 100 \times R_f$

$\Delta hR_{f,i}$ = the difference between 2 successive hR_f values, experimentally obtained and arranged in the increasing order.

ΔhR_f = the difference between 2 successive hR_f values for an ideal separation, when all the spots were situated equidistant between the start and the front line.

n = the total number of substances.

The hR_f data and the corresponding I_p values are shown in Table 1. The best separation was obtained by using methanol-benzene-chloroform (48:48:4,

v/v), when the performance index I_p has the lowest value. Further experiments, obtained by modifying the concentration of each solvent have lead to an increasing of I_p values, so that the separations were not improved.

Table 1. The hR_f and I_p values for the compounds 1-15, obtained by NP-TLC, using methanol-benzene-chloroform as mobile phase (the volume percents are given at each column top)

Compound	43:55:2 (v/v)		52:46:2 (v/v)		48:50:2 (v/v)		48:48:4 (v/v)		36:60:4 (v/v)		42:54:4 (v/v)	
	hR_f	I_p	hR_f	I_p	hR_f	I_p	hR_f	I_p	hR_f	I_p	hR_f	I_p
1.	96		93		97		57		41		38	
2.	84		78		85		84		77		79	
3.	42		40		52		76		54		55	
4.	26		25		30		50		30		32	
5.	83		81		80		94		85		88	
6.	67		65		71		82		71		72	
7.	73	1.01	69	0.90	74	0.84	84	0.70	64	0.94	62	0.98
8.	56		55		60		76		21		22	
9.	53		51		57		70		73		72	
10.	45		45		51		62		22		22	
11.	41		39		40		54		41		40	
12.	97		96		98		96		34		29	
13.	91		89		91		93		85		87	
14.	84		84		83		91		80		81	
15.	79		78		78		90		72		74	

2. RP-TLC

C18-bonded silica gel was used as a non-polar stationary phase and methanol-water as a polar mobile phase. The experimentally measured R_f and R_M values ($R_M = \log(1/R_f^{-1})$, for different concentrations of methanol (in terms of the molar fraction, X) are shown in Table 2. In binary aqueous organic eluents, e.g. methanol-water, methanol has a decisive influence on the overall chromatographic distribution reflected in the R_M values of the investigated solute.

A good linear correlation:

$$R_M = a_0 + a_1X \tag{2}$$

was found between the R_M and X values, characterized by high values of the correlation coefficient, r (Table 2). The extrapolated R_M values, $R_{M0} = a_0$, to zero content of organic modifier in the aqueous phase, are different and depend on structures. The R_{M0} values can be used as a lipophilicity parameter, which can be correlated with the partition coefficient of a certain compound between n-octanol and water, logP. The slope, a_1, of the equation 2 can be considered as a measure of the strength of mobile phase contribution to solute retention.

The compounds 7-8 and 9-10 cannot be separated, probably because the partition equilibrum in RP-TLC it is based on a hydrophobic exclusion of compound from the mobile phase, and not on a specific interaction between the compound and the non-polar stationary phase.

The logP values were calculated according to the method described by Rekker [12] using the fragmental constants and the relationship:

$$logP = \Sigma f_i n_i + \Sigma k_n C_m \tag{3}$$

where f_i isfragmental constant for fragment i, n_i is the number of identical fragments, k_n is the number of identical proximity effect corrections and C_m is the proximity effect correction type m. The logP values cannot be calculated for compounds 14 and 15 because some structural fragments are not estimated in Rekker's tables. The extrapolated R_{M0} (=a_0) values from Table 2 were correlated with the calculated logP values in order to check if the compounds are congeners (with similar chromatographic behavior) (Table 3).

Table 2. The R_f (first value in each row) and R_M (second data) values obtained by RP-TLC for the studied compounds with methanol/water as eluent (molar fractions at each column top). Parameters of the correlation equation $R_M = a_0 + a_1X$, s_{a0}, s_{a1} - standard errors, F - statistic and r - correlation coefficient

methanol/water=X/(1-X)

	0.800/ 0.200	0.716/ 0.284	0.640/ 0.360	0.509/ 0.491	0.400/ 0.600	a_0	a_1	F	r
1.	0.66 -0.283	-	0.60 -0.179	0.38 -0.205	0.24 -0.501	1.245 ±1.048 s_{a0}=0.243	0.402 ±1.729 s_{a1}=0.402	25.168	0.962
2.	0.80 -0.604	-	0.67 -0.303	0.52 -0.040	0.38 -0.213	1.009 ±0.173 s_{a0}=0.040	-2.031 ±0. 2 86 s_{a1}=0.066	934.812	0.999
3.	0.43 0.129	0.24 0.501	0.16 0.706	0.03 1.502	-	3.803 ±2.831 s_{a0}=0.329	-4.643 ±2.098 s_{a1}=0.487	90.702	0.989
4.	0.79 -0.580	-	0.71 -0.392	0.66 -0.283	0.54 -0.070	0.385 ±0.362 s_{a0}=0.084	-1.219 ±0.597 s_{a1}=0.139	77.267	0.987
5.	0.30 0.357	0.14 0.788	0.07 1.103	0.01 1.912	-	4.571 ±0.863 s_{a0}=0.201	-5.301 ±1.279 s_{a1}=0.297	318.032	0.997
6.	0.65 -0.274	-	0.48 0.041	0.28 0.417	0.15 0.753	1.746 ±0.500 s_{a0}=0.116	-2.575 ±0.825 s_{a1}=0.192	180.559	0.994
7.	0.69 -0.352	-	0.51 -0.014	0.42 0.136	0.32 0.327	0.995 ±0.357 s_{a0}=0.083	-1.653 ±0.590 s_{a1}=0.137	145.340	0.993
9.	0.67 -0.302	-	0.50 0.001	0.31 0.353	0.22 0.550	1.331 ±0.480 s_{a0}=0.111	-2.066 ±0.792 s_{a1}=0.184	126.152	0.992
11.	0.80 -0.607	-	0.63 -0.241	0.42 0.145	0.15 0.753	1.949 ±1.294 s_{a0}=0.301	-3.297 ±2.136 s_{a1}=0.496	44.133	0.978
12	0.43 0.116	0.25 0.480	0.14 0.790	0.03 1.523	-	3.941 ±0.784 s_{a0}=0.182	-4.824 ±1.161 s_{a1}=0.270	319.479	0.997
13.	0.50 -0.002	0.38 0.713	0.28 0.407	0.11 0.911	-	2.472 ±0.743 s_{a0}=0.173	-3.137 ±1.101 s_{a1}=0.256	150.260	0.993
14.	0.24 0.500	0.10 0.954	0.05 1.288	0.01 2.212	-	5.129 ±1.201 s_{a0}=0.279	-5.839 ±1.780 s_{a1}=0.414	199.231	0.995
15.	0.60 -0.186	-	0.44 0.112	0.24 0.509	0.12 0.865	1.875 ±0.635 s_{a0}=0.148	-2.639 ±1.049 s_{a1}=0.244	117.251	0.992

Table 3. The extrapolated R_{M0} values (Table 2) and the calculated logP data (Rekker's system) for the studied compounds

Compound	R_{M0}	LogP	Compound	R_{M0}	LogP
1.	1.245	4.719	7.	0.995	6.828
2.	1.009	1.325	9.	1.331	5.559
3.	3.803	4.252	11.	1.949	3.878
4.	0.385	0.201	12.	3.941	8.422
5.	4.571	7.502	13.	2.472	4.371
6.	1.746	2.794			

The compounds from Table 3 are not congeners because the correlation coefficient for a linear relationship, $R_{M0} = A + B \log P$, has not a high value ($r = 0.634$), but the substances can be included in further investigations of compounds with similar structures. The compounds 3, 7 and 9 have been excluded from the correlation because they are suspected to interact strongly with the residual silanol groups on the alkylated silica surface due to the aromatic nitrogen and extended conjugation. The linear relationship between the remaining substances is shown in equation 4:

$$R_{MO} = 0.206 + 0.472 \log P, \quad r = 0.918 \qquad (4)$$

The satisfying linearity encourages further investigations on similar groups of substances, splitting the series of compounds by the main structure and including different substituents.

ACKNOWLEDGMENTS

The authors are deeply grateful to prof. dr. V. Fărcășan and to prof. dr. S. Gocan for helpful comments.

REFERENCES

1. J. P. Abjean, *J. Planar Chromatogr.-Mod. TLC*, 1993, 6(4), 319.
2. D. Saleeno, C. Suibutean, V. Acedo, C.A. Corea, *J. Chromatogr. A*, 1997, 764(2), 243.
3. W. Baik, J.L. Han, K.C. Lee, N.H. Lee, B.H. Kim, J.T. Hahn, *Tetrahedron Letters*, 1994, 35(23), 3965.

4. X. Tomas, L.G. Sabate, *Anal. Chim. Acta*, 1986, 191, 439.
5. Harmala, *J. Planar. Chromatogr.-Mod TLC*, 1991, 4(6), 460.
6. Hansch, S.M. Anderson, *J. Org. Chem.*, 1967, 32, 2583.
7. Smith, C. Hansch, M.A. Ames, *J. Pharm. Sci.*, 1975, 64, 599.
8. Gullner, T. Cserhati, B. Bordas, K. Valko, *J. Liq. Chromatogr.*, 1989, 12, 957.
9. Dross, C. Sonntag, R. Mannhold, *J. Chromatogr. A*, 1994, 673, 113.
10. Gocan, F. Irimie, G. Cîmpan, *J. Chromatogr. A*, 1994, 675, 282.
11. Rekker, *The Hydrophobic Fragmental Constant*, Elsevier, Amsterdam, 1977.
12. Rekker, R. Mannhold, *Calculation of Drug Lipophilicity. The Hydrophobic Fragmental Constant Approach*, VCH, Weinheim, 1992.
13. Biobyte Corporation, 201 W-4th st. 204, Claremont, CA91711 USA.
14. Miclăuș, G. Damian, E. Făgărășan, G. Cîmpan, S. Stamate, S. Paizs, C. Afloroaei, *Proceedings Supplement of Balkan Physics Letters*, 1997, 5, accepted for publication.
15. Snyder, *J. Chromatogr.*, 1974, 92, 223.
16. Snyder, *J. Chromatogr. Sci.*, 1978, 16, 223.
17. Berridge, E.G. Morissey, *J. Chromatogr.*, 1984, 316, 69.
18. Gocan, V. Liteanu, *Studia Univ. "Babeș-Bolyai", Chemia*, 1988, 33, 82.

STUDIA UNIVERSITATIS BABEŞ-BOLYAI, CHEMIA, XLII, 1-2, 1997

RHEOLOGY OF SOME ADHESIVES WITH DEXTRIN[1]

MARIANA SORA[2], LIDIA TAUBERT[3], SEPTIMIA POLICEC[3], A. RUS[2]

ABSTRACT. In the paper are presented the results of an experimental study concerning the rheological behaviour of some adhesive pastes with dextrin and carboxymethyl-cellulose (CMC) content. The rheograms of adhesives containing 50-45% dry substance, with 40% dextrin and 10-5% CMC, indicate a pseudoplastic behaviour. The material rheological indices have been determined at different temperatures and compositions, as well as the flow activation energies at a constant deformation rate, respectively at constant shearing stress.

INTRODUCTION

Various synthetic adhesives are extensively used in different fields due to their properties which often surpass those of natural, vegetal or animal glues [1,2]. In food industry there are some requirements for adhesives, especially concerning their nontoxic imposed characteristics and also other ones, particularly related to mechanical paper application for wrapping purposes. In the cigarettes industry, for instance, adhesives based on starch and dextrins [3] are still used and prepared empirically.

As the efficiency of an adhesive depends on several factors, it is impossible to predict its performances in a new application, the specific testing being therefore the most reliable method for selection.

In the cigarettes industry mechanical packing the sticking quality depends mainly on the adhesive affinity for paper, on the thickness and flexibility of the adhesive layer, its continuity between the two glueing materials and on its rapid drying capacity after the package formation. Therefore besides the quality and stability tests concerning the paper link, some specific determinations for the adhesive characterization are also recommended, namely the dry substance content and the viscosity. The last is an important characteristic as it has an influence on the pellicle thickness set on the paper and obviously of that on the cylinder of the industrial equipment [4-6].

In the present paper an experimental study is performed concerning the influence of different factors on the rheological behaviour of some adhesive pastes with dextrin, animal glue and carboxymethyl-cellulose content. The rheological properties depend on the adhesive's composition, its dry substance content, the preparation working conditions (as temperature, homogenization time) and on the application process temperature.

---

[1] Dedicated to Prof. dr. Ionel Haiduc on the occasion of his 60-th anniversary.

[2] Technical University of Timişoara, Department of Chemical Engineering.

[3] Romanian Academy - Timişoara Branch, Inorganic Chemistry Laboratory.

EXPERIMENTAL

The adhesive pastes are aqueous compositions of yellow dextrin and animal glue, respectively dextrin and carboxymethyl-cellulose (CMC), heated at 80°C, under stirring, during 1-3 hours. The first adhesive D with a dry substance content of 65%, mainly contains dextrin (about 96%) and only a small amount of animal glue. The pastes in the series dextrin - CMC (C_1D - C_6D), characterized by a dry substance content varying between 50 and 45% contain the same amount of dextrin (40%) and a decreasing content of CMC.

The viscosity has been determined by means of a Rheotest-2 rotational viscosimeter, which allows to obtain a large range of the experimental data and using the deformation variation, between 0 and 1300 s^{-1}, in 24 steps. By means of the apparatus constants, the shearing stress, τ_f, and the deformation rate, γ, were calculated and thus the $\tau_f = f(\gamma)$ dependence has been established.

RESULTS AND DISCUSSION

The experimental results are graphically representing, the shearing stress (τ_f) dependence on the deformation rate (γ) respectively the apparent viscosity dependence ($\eta_a = \tau_f / \gamma$) on the deformation rate or the shearing stress.

Concerning the rheological behaviour, adhesive D presents a slight tixotropy. Curves (τ_f - γ) which exhibit the shearing stress as a function of the deformation rate (Fig. 1) are different for the increasing, respectively decreasing sense of the deformation rate, a hysteresis loop being thus obtained. The apparent viscosity decrease in time, at the same deformation rate, is given in Figure 2.

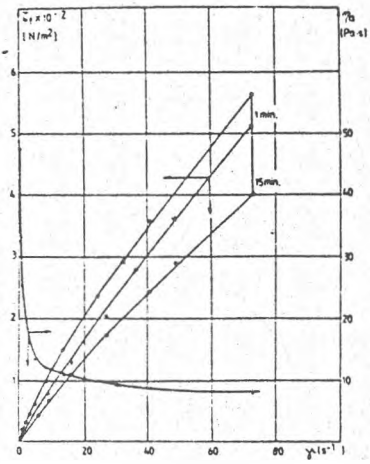

Fig. 1. Shearing stress and apparent viscosity dependence of the deformation rate for adhesive D at 20°C

In case of the products with adhesive properties C_1D - C_6D, the rheograms (Fig. 3) indicate for each a pseudoplastic behaviour. As a result, the apparent viscosity decreases as the deformation rate, respectively the shearing stress increases (Fig. 4a,b and Fig. 5a,b) being independent of time. The viscosity

decrease is more pronounced at small deformation rates. At great deformation rate values, the viscosity tends to a minimum value, due to particle orientation in the sense of flow, so that resistance to the shearing force should be minimum.

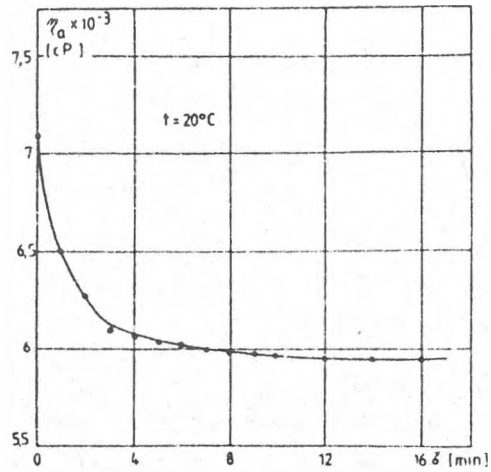

Fig. 2. Apparent viscosity variation, for adhesive D in time, at constant deformation rate ($\gamma = 72{,}9\ s^{-1}$)

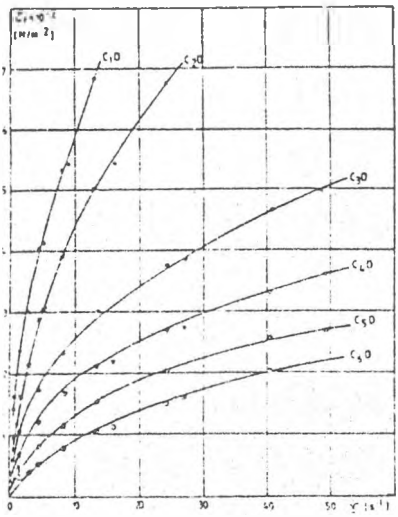

Fig. 3. Flow curves for adhesive C_1D - C_6D, at 22°C

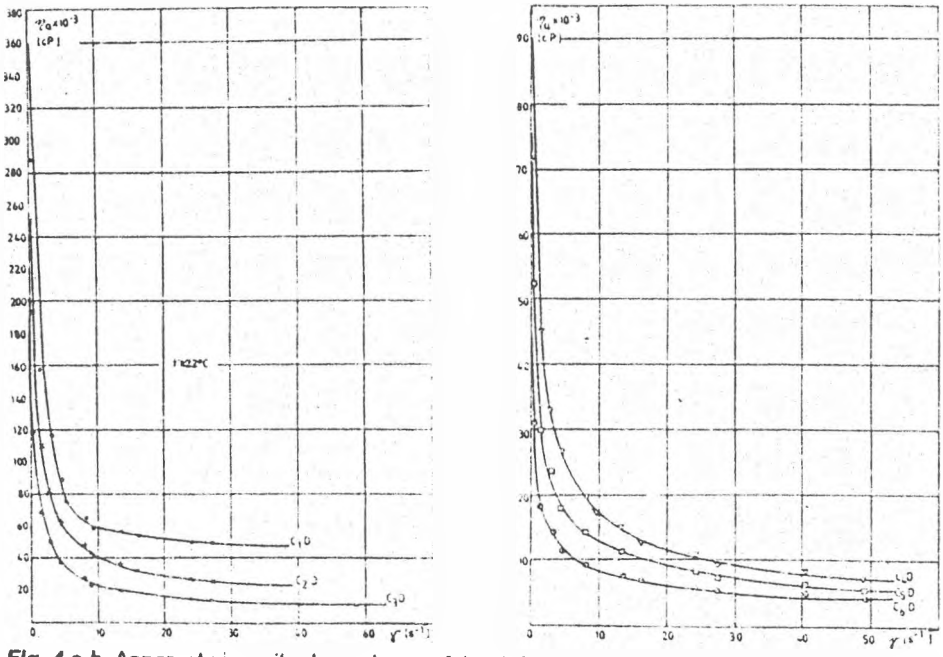

Fig. 4 a,b. Apparent viscosity dependence of the deformation rate for products C_1D - C_6D at 22°C

In order to describe the nonnewtonian behaviour of products C_1D - C_6D, the Ostwald-de-Waele rheological model has been considered:

$$\tau_f = k \cdot \gamma^n \qquad (1)$$

The values of the material rheological indices, n - the flow index, nondimensional and k - the consistence index, have been determined by linearisation of equation (1) through logarithmation. The values obtained are given in Tables 1 and 2. Knowing the material rheological values allows the calculation of the apparent viscosity of the product by means of the relation:

$$\eta_a = k \cdot \gamma^{n-1} \qquad (2)$$

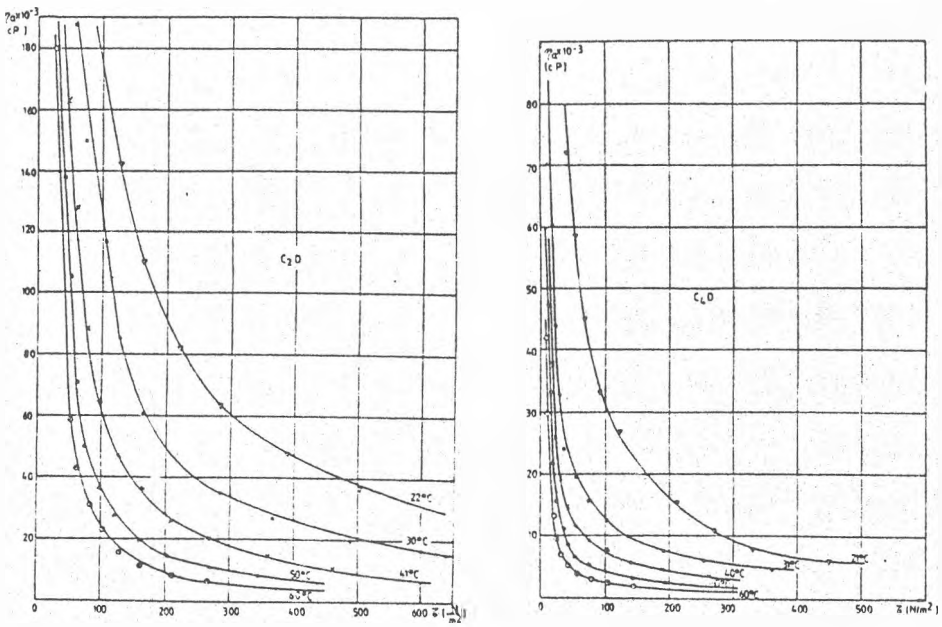

Fig. 5 a,b. Viscosity dependence of the shearing stress, at various temperatures

Table 1. Material rheological indices, at 22°C

Product	Composition		Flow index	Consistence index
	Dextrin %	CMC %		Ns^n/m^2
C_1D	40	10	0.4796	188.81
C_2D	40	9	0.5010	132.07
C_3D	40	8	0.4849	77.893
C_4D	40	7	0.5081	51.404
C_5D	40	6	0.5243	34.826
C_6D	40	5	0.5648	22.761

Table 2. Material rheological indices, at various temperatures

Temperature °C	Product					
	C_2D		C_4D		C_6D	
	n	k Ns^n/m^2	n	k Ns^n/m^2	n	k Ns^n/m^2
22	0.5010	132.07	0.5481	51.40	0.5648	22.76
30	0.4917	100.53	0.508**	31.74**	0.5262	16.79
40	0.4518*	80.89*	0.517	25.65	0.4904*	13.67*
50	0.4206	66.96	0.4763	21.55	0.4563	11.82
60	0.3999	56.87	0.4368***	18.53***	0.4175	10.53

* t = 41.5 °C;
** t = 31 °C;
*** t = 61 °C.

From Table 1 it is noticed that the consistence index values increase considerably with the CMC content, respectively with the dry substance content increase; at the same time, the flow index values are less influenced. Consequently the products with a greater CMC content, respectively dry substance, have a greater apparent viscosity, at the same deformation rate value, as it can be seen in figure 4. As the deformation rate increases, at constant temperature, the apparent viscosity decrease is more important for pastes with a greater dry substance content, fact which may be explained by the higher orientation degree of the flow elements, compared to the pastes less concentrated in dry substance.

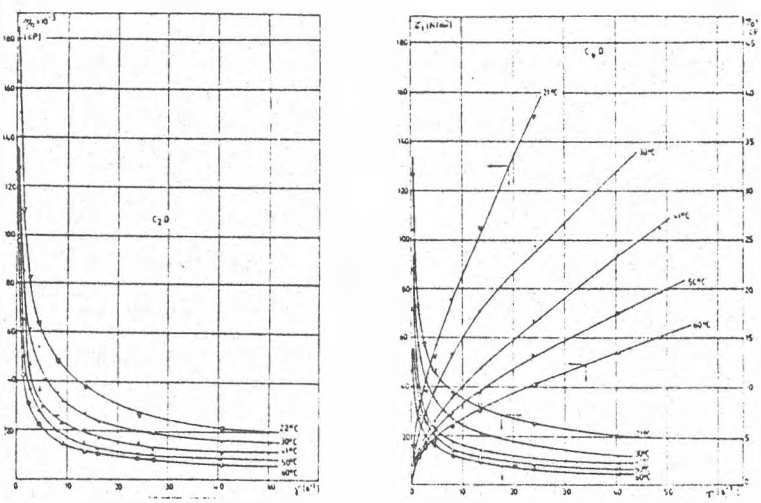

Fig. 6 a,b. Viscosity dependence of the deformation rate, at various temperatures

The temperature increase determines a viscosity decrease for all products, the pseudoplastic behaviour being present in all cases. The viscosity decrease as the temperature increases, at constant deformation rate, is more pronounced in the case of adhesives with a higher dry substance content (Fig. 6a,b).

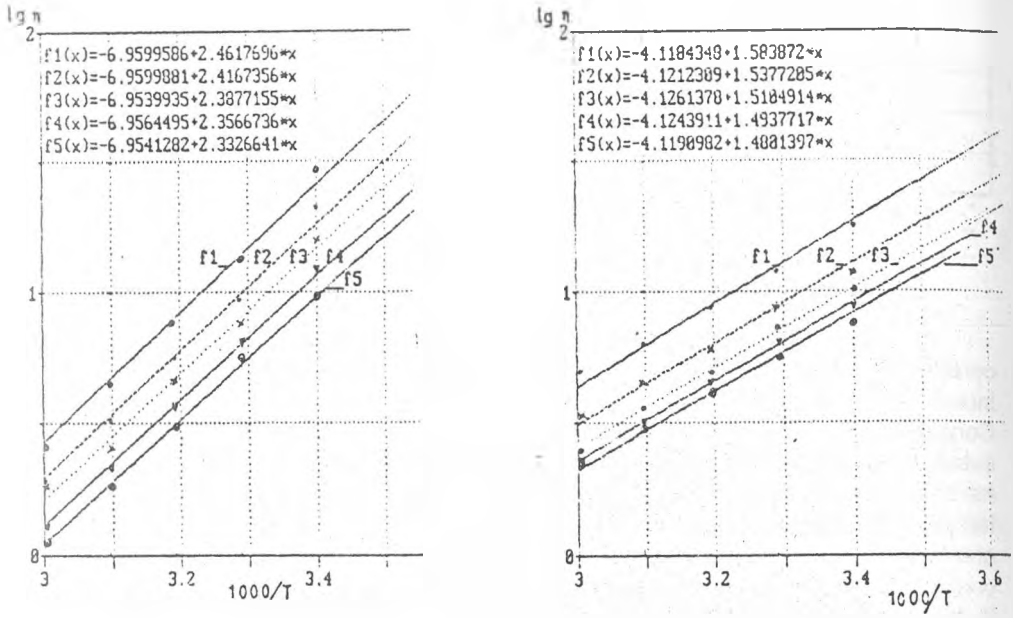

Fig. 7. Flow activation energies determination

The pronounced dependence of liquids visciosity on temperature is owed to the flow activation energy. In the case of nonnewtonian liquids, the empirical Arrhenius type relation between viscosity and temperature may be written:

$$\eta_a = A \cdot e^{-E_\gamma/RT} \quad (3) \qquad \eta_a = A \cdot e^{-E_\tau/RT} \quad (4)$$

In relation (3) and (4) E_γ and E_τ are the flow activation energies, at constant deformation rate, respectively at constant shearing stress, R = 8310 J/kmol.K - the univarsal gas constant, T - the absolute temperature and A - the constant frequency factor having the same dimension as viscosity.

Logarithmation of relations (3) and (4) and plotting in semilogarithmic coordinates (Fig. 7) the viscosity variation versus 1/T, allows the determination of the flow activation energies and the frequency factor. The automatic processing of the experimental data has allowed to obtain, with good precision, the frequency factor values, respectively those of the flow activation energy which are given in tables 3 and 4.

Table 3. Flow activation energy and frequency factor, at constant deformation rate

Deformation rate s^{-1}	Product					
	C_2D		C_4D		C_6D	
	$A \cdot 10^3$ Pa·s	$E_r \cdot 10^{-6}$ J/kmol	$A \cdot 10^5$ Pa·s	$E_r \cdot 10^{-6}$ J/kmol	$A \cdot 10^5$ Pa·s	$E \cdot 10^{-6}$ J/kmol
10	1.0250	26.106	7.613	30.312	3.33	30.669
20	1.0212	25.188	7.564	29.429	3.288	29.93
30	1.0206	24.661	7.479	28.908	3.277	29.428
40	1.0199	24.382	7.509	28.588	3.270	29.119
50	1.0156	24.256	7.603	28.327	-	-

Table 4. Flow activation energy and frequency factor, at constant shearing stress

Shearing stress Pa	Product					
	C_2D		C_4D		C_6D	
	$A \cdot 10^7$ Pa·s	$E_r \cdot 10^{-6}$ J/kmol	$A \cdot 10^7$ Pa·s	$E_r \cdot 10^{-6}$ J/kmol	$A \cdot 10^9$ Pa·s	$E_r \cdot 10^{-6}$ J/kmol
50	-	-	-	-	6	52.811
100	2.42	50.444	1.10	47.113	5	51.542
150	2.38	49.282	1.10	46.251	5	50.667
200	2.35	48.396	1.11	45.695	-	-
250	2.33	47.786	1.11	45.102	-	-
300	2.33	47.311	1.11	44.642	-	-

As a practical conclusion concerning the study of the experimental data, namely of the viscosity variation curves, it can be seen that adhesive C_4D at 20°C and adhesive C_2D at 50°C exhibit viscosity values close to that of adhesive D; in consequence, from this point of view, the first adhesive C_4D could replace adhesive D, at the mechanical packing in the cigarettes industry.

CONCLUSIONS

Experimental results regarding the rheology of adhesive pastes containing dextrin and carboxymethyl-cellulose indicate a nonnewtonian behaviour of pseudoplastic type, independent of temperature and dry substance content between the limits of 45-50%. The material rheological indices have been determined at different temperatures as well as the flow activation energies at a constant deformation rate, respectively at constant shearing stress, which permits the calculation of the product's viscosity in various conditions.

REFERENCES

1. Bischof C., Possart W., *Adhasion*, Akademie-Verlag Berlin, 1983, p. 9.
2. Kirk R. E., Othmer D. F., *Encyclopedia of Chemical Technology*, The Interscience Encyclopedia New York, 1978, vol. 1, p. 505.
3. Haciadur O., Nicolau A., *Fabricarea amidonului, glucozei și dextrinei*, Ed. Tehnica Bucuresti, 1966, p. 38, 301.
4. Tudose R. Z., Volintiru T., Asandei N., Lungu M., Merica E., *Reologia compușilor macromoleculari. Reologia stării lichide*, Ed. Tehnică București, 1984, vol. II., p. 82.
5. Tudose R. Z., *Procese și utilaje în industria de prelucrare a compușilor macromoleculari*, Ed. Tehnică București, 1976, p. 94.
6. Petrea I. C., Ionescu L. M., *Fizica elastomerilor. Reologie*, E.D.P. București, 1981, p. 168, 136.

STUDIA UNIVERSITATIS BABEŞ-BOLYAI, CHEMIA, XLII, 1-2, 1997

ARGENTOMETRIC TITRATION OF THIOSULFATE WITH CONDUCTOMETRIC AND POTENTIOMETRIC END-POINT DETECTION

E. FORIZS[1], E. VERESS[2], F. MIHĂLCIOIU[3], CS. MUZSNAY[1], G. SZABO[1]

ABSTRACT. Argentometric titration of thiosulfate has been investigated using conductometric and potentiometric end-point detection. The conductometric titration of thiosulfate with silver ions using non-conventional conductivity cells equipped with sintered titanium or antimony electrode is described. Conductometric titration curves displayed two stoichiometrically well defined end-points at 1:1 and 2:1 silver/thiosulfate ratios. Potentiometric titration curves give the same results. Accurate conductometric determination can be made in the range of thiosulfate concentrations 10^{-2}-10^{-4}M.

INTRODUCTION

The determination of sulfur containing anions has generally been performed by argentometric or mercurimetric titration with potentiometric end-point detection, using sulfide-sensitive membrane electrodes, or mercury, silver, and carbon indicator electrodes [1-4]. The conductometric end-point detection of argentometric titration of thiosulfate was not recommended by Kolthoff, due to the irregular conductivity variations durring titration [5]. Argentometric titration of thiosulfate by means of conductometric method is possible using non-conventional conductivity cells [6]. In a previous paper we presented the results obtained in the titration of thiosulfate with silver ions by using some new-type conductivity cells equipped with silver, amalgamated silver, stainless steel and polished platinum electrodes [6-11]. The aim of the present work was to study the behavior of conductivity cells with antimony and sintered titanium electrodes in argentometric titration of thiosulfate. The acid generation in the course of titration was followed by potentiometric pH measuring.

EXPERIMENTAL

A Radelkis OK/102 type conductometer equipped with laboratory-made dip-type conductivity cells with circular-plate electrodes was used. Plate types electrodes were made from antimony or sintered titanium of 99% purity. The diameter of the plate is 4 mm and the distance between the center of the two circular electrodes is 16 mm. The value of cell constant is 1.54 cm^{-1} for titanium electrodes and 1.70cm^{-1} for antimony electrodes.

---

[1] Universitatea Babeş-Bolyai, Facultatea de Chimie şi Inginerie Chimică, 3400 Cluj-Napoca, România
[2] Institutul de Chimie Raluca Ripan, Cluj-Napoca, România
[3] Societatea de Metrologie şi Ecologie, Cluj-Napoca, România

A pH-100 Otopeni-type digital pH-meter, silver-sensitive Ag-ISE electrode, pH-sensitive glass electrode, a home made platinum with electrode and a calomel electrode with a salt bridge (saturated potassium nitrate) were employed in potentiometric measurements.

All the solutions were prepared from analytical-grade reagents and distilled water was used. Sodium thiosulfate solutions were standardized iodometrically in the usual way. Silver nitrate solutions were standardized by potentiometric titration with sodium chloride. 0.1 M stock solutions were used and further diluted as required.

The conductance and potential values were read at fixed time intervals of 60 s after each titrant portions was added.

50 ml thiosulfate samples of 10^{-2}-10^{-4} M concentration were titrated with 10^{-1}-10^{-2} M solutions of $AgNO_3$. All titrations were performed at room temperature.

RESULTS AND DISCUSSION

Some examples of conductometric titration curves are shown in Fig. 1. Two distinct sharp end-points occurred at 1:1 and 2:1 silver/thiosulfate ratios.

In the first part of curves the conductance values slightly decrease due to the formation of $[Ag(S_2O_3)_x]^{1-2x}$, x=1-3, especially for x = 1, complex ions with lower mobilities than the thiosulfate ion.

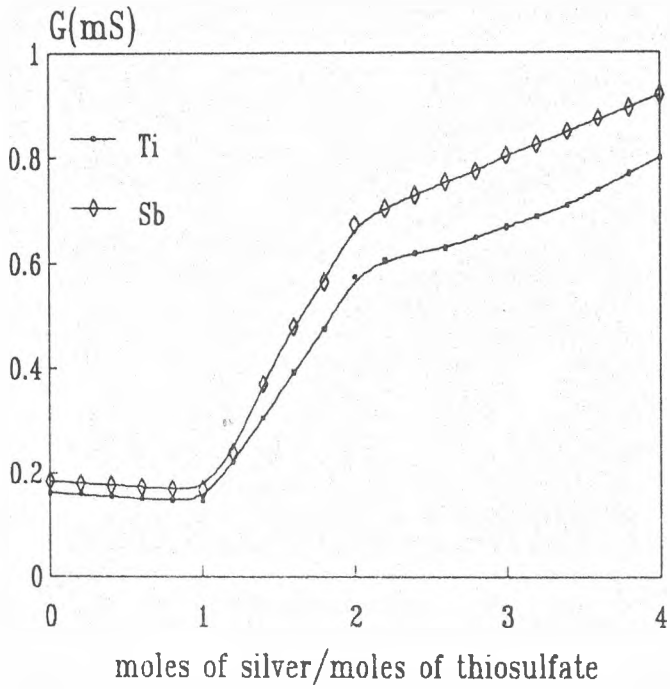

Fig. 1. Conductometric titration curves of 50 ml 1 mM $Na_2S_2O_3$ with 0.1 M $AgNO_3$ using conductivity cell equipped with titanium (Ti) and antimony (Sb) electrodes

The recoveries calculated from the first equivalence pints are satisfactory only in more dilute solution than 10^{3} M and above this concentration show an error of about +8%. Some analytical data are given in Table 1.

Table 1. Conductometric titration data of thiosulfate with silver nitrate at 1:1 ratio of Ag/S_2O_3

Electrode	Taken (mg/ml)	Found* (mg/ml)	Relative error (%)
Ti	0.0249	0 0240	-3.61
	0.2475	0.2497	+0.89
Sb	0.0249	0.0246	-1.20
	0.2491	0.2487	-0.16

* Mean of three determination

Addition of titrant after 1:1 ratio of Ag/S_2O_3 cause a sharp increase of conductance values due to the formation of sulfuric acid, on the basis of the following reaction:[1]

$$AgS_2O_3^- + Ag^+ + H_2O = Ag_2S + H_2SO_4$$

At the 2:1 ratio of Ag/S_2O_3 a well-resolved break point is observed corresponding to the complete precipitation of the silver sulfide. Further addition of titrant increases the concentration of silver nitrate in solution increasing the conductance. The equivalence points obtained coincide with the theoretical ones (Table 2). The equivalence points were calculated from the intersection of the most probable straight lines.

Table 2. Conductometric titration data of thiosulfate with silver nitrate at 2:1 ratio of Ag/S_2O_3

Electrode	Taken (mg/ml)	Found (mg/ml)	Recovery	RSD (%)
Ti	0.0249	0.0248	99.60	0.19
	0.2475	0 2497	100.89	0.10
	1.4719	2.4564	99.37	1.38
Sb	0.0249	0.0249	100.00	0.25
	0.2491	0.2512	100 84	0.79
	2.4931	2.4870	99.76	0.78

* Average of 3 determination

The recoveries listed in Table 2 are good, with an error less than ±1%, thus the precision of the conductometric method is satisfactory for the argentometric determination of thiosulfate.

In the argentometric titration of thiosulfate good results were obtained using potentiometric detection of the end-point. Potentiometric titration curves are shown in Fig. 2.

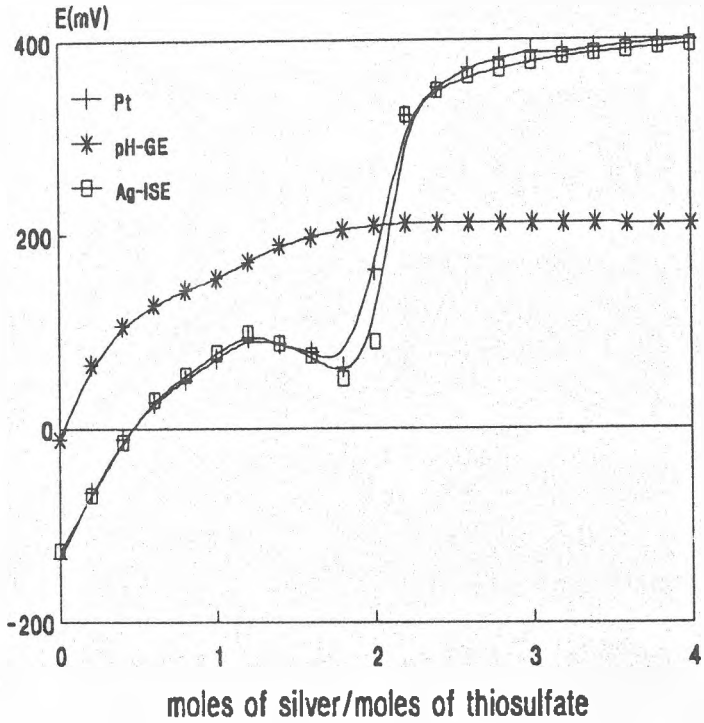

Fig. 2. Potentiometric titration curves of 50 ml of 10^{-3} M $Na_2S_2O_3$ with 0.01 M $AgNO_3$

At the 1:1 ratio of Ag/S_2O_3 a maximum in the curves indicates the formation of $AgS_2O_3^-$. The second equivalence point occurred at the 2:1 ratio of Ag/S_2O_3, when the silver sulfide precipitation is complete. The determinations of the equivalence points by Hosteller and Roberts method give an error of about ±3%. The general shape of the potentiometric titration curves indicates many similarities and differences for those presented by Piccardi et al [1]. The observed differences are connected with the different experimental conditions. The acidity of solution increases in the course of titration and the pH of solution remain practically constant after the 2:1 ratio of Ag/S_2O_3 (Fig. 2).

In conclusion accurate conductometric determinations can be made, using the second break-points of the titration curves as equivalence points. The simplicity, accuracy and precision of conductometric titrimetry using conductivity

cells equipped with sintered antimony and titanium electrodes indicate that this method is suitable for argentometric determination of thiosulfate. Comparison of the conductometric and potentiometric titration data suggests that the conductometric method should be preferred.

REFERENCES

1. G. Piccardi, R. Udisti and P. Cellini-Legittimo, *Microchim. Acta*, 1989, Part III, 7.
2. V. I. E. Schmidt and E. Pungor, *Magy. Kem. Foly.*, 1970, 76, 307.
3. E. Pungor, *Anal. Chem.*, 1967, 39, 28A.
4. V. I. Berestetskii and F.M. Tulyupa, *Zh. Anal. Khim.*, 1989, 44, 328.
5. I. M. Kolthoff, Konduktometrische Titrationen, Th., Steinkoff, Dresden, Germany, 1923.
6. E. Forizs and Cs. Muzsnay, *Talanta*, 1996, 43, 1639.
7. E. Hopîrtean, F. Mihălcioiu, E. Forizs and F. Kormos, *Sens. Actuat. B*, 1994, 317.
8. Cs. Muzsnay, *Magy. Kem. Foly.*, 1987, 92, 23.
9. Cs. Muzsnay, E. Forizs, M. Hanga and A. Szabo, Rom. Pat. 111589, 1989.
10. Cs. Muzsnay and A. Szabo, Rom. Pat. 72123, 1979.
11. Cs. Muzsnay and E. Forizs, *Studia Univ. Babeş-Bolyai, Ser. Chem.*, 1986, 31, 55.

STUDIA UNIVERSITATIS BABEȘ-BOLYAI, CHEMIA, XLII, 1-2, 1997

ANALYSIS OF A SOIL SAMPLE WITH HIGH CONTENT OF TRIAZINIC HERBICIDES USED TLC-FOTODENSITOMETRY

SIMONA GOCAN[1], SIMONA COBZAC[1]

ABSTRACT. The present paper deals with the determination of atrazine, simazine and propazine recovery from purified sea sand and two different types of soil. Also a soil sample with high atrazine concentration has been analysed. The triazine herbicides were extrated in methanol, analysed by TLC and scanned in UV. The limit of detection LOD for simazine, atrazine and propazine are 38.96, 25.46, 76.19ng/spot respectively. The recovery is situated 75-99,6%. The quantity determined in soil sample was 0.4 ppm.

INTRODUCTION

The triazine herbicides are chemical compound used for herbs elimination in crops. The treatment with this compounds must take in to account the type of soil and the residuals herbicides. Because the time for decomposition is long it possible to have problems with alternative crops. A higher quantity than 400g active compound/ha do not allowed growing [1].

In literature are presented many possibilities of herbicides extraction and analyses. The extraction can be done with methanol for 2 hours and continuous mixing [2], methanol - water (80:20, v/v) [3], acetonitril - HCl, 0.2M (9:1, v/v) [4], ultrasonication with methanol, SPE - C_{18} purification and preconcentration [5] and superfluid extraction with CO_2 [6]. The influence of temperature extraction [7], granulometry and type of soil [8,9] on recovery was also studied. The analysis may be done with GC, with limit of detection LOD 0,5 ppm [10], GC-MS with LOD is situated between 1-24pg [11], HPLC with LOD 100µg/g [12] and TLC [13,14].

The present paper concern with a study of simazine, atrazine and propazine recovery from purified sea sand and the influence of soil type on recovery. The quantitation of atrazine from a soil sample was determined. The analysis include extraction in methanol, TLC and scanning at 222nm.

EXPERIMENTAL

Solvents as toluen, methanol and acetone (Chimopar - București), Sil G F_{254} plates (Merck, Darmstadt), purified sea sand (Roth, Germany) ant atrazine, simazine and propazine (Atlas) were used for experiment. A methanol stock solution were prepared as 0,115mg/mL simazine, 0,108mg/mL atrazine, 0,103mg/mL propazine. For recovery determination 10g sand were spiked with

[1] Facultatea de Chimie și Inginerie Chimică, Universitatea "Babeș-Bolyai", 3400 Cluj-Napca, Romania.

1mL stock solution and dried for 2 hours at 60°C. Three extractions have been carried out with 15mL methanol for 10 minutes each. After settling the liquid was centrifuged 5 minutes. The obtained solutions were mixed together and methanol vaporised at 60°C. The residue was solved in 1mL methanol, resulting S_1 sand sample. In the same time a blank sand sample (B_1) was also performed. Soil samples (10g) from greenhouse and garden were allso prepared in the same manner resulting S_2 and B_2 and B_3 respecyively. A representative field soil sample (40g) was weighted for the determination of atrazine. The soil was sampled from the end of the crops field where the atrazine has a higher concentration due to the turning of spraying machine. The sample was prepared in the same way as it was before described resulting the soil sample solution S_4. 10µL from spiked samples and 20µL from soil sampled from the field were automatically spotted as lines (5mm long) with a Desaga applicator on Sil G F_{254} plates. The plates were developed with toluene - acetone (90:10, v/v) and evaluated, with a Shimadzu CS-9000 dual wavelength flying - spot scanner at 222 nm.

RESULTS AND DISCUSSION

The densitogram for stock solution containing simazine, atrazine and propazine is shown in figure 1. In figures 2-4 are presented the densitograms for spiked and blank samples for sand and soil, for 11.3 ppm simazine, 11.0 ppm atrazine and 10.5 ppm propazine. In figure 5 is presented the densitogram field soil sample.

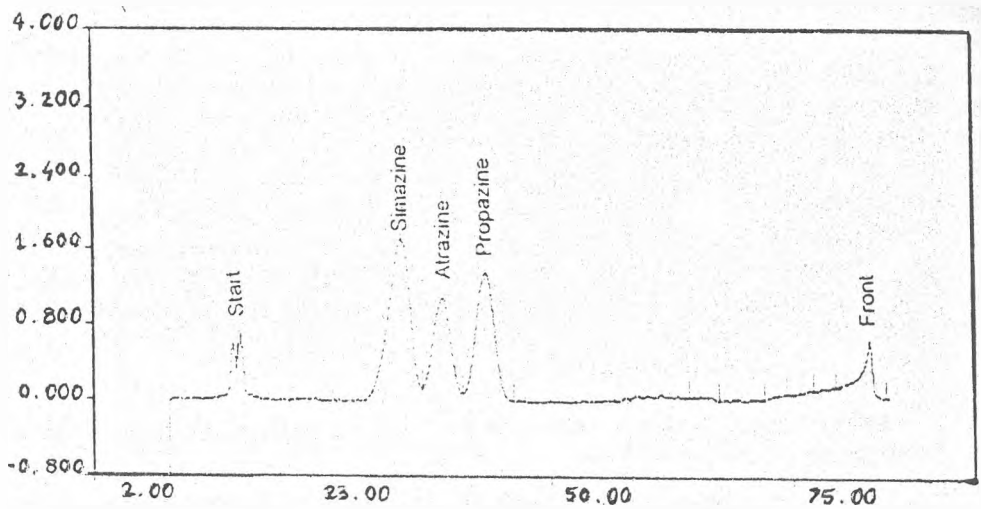

Figure 1. Reflectance scann of the cromatografic track obtained from a mixture containing simazine as 115 µg/mL and propazine as 113 µg/mL

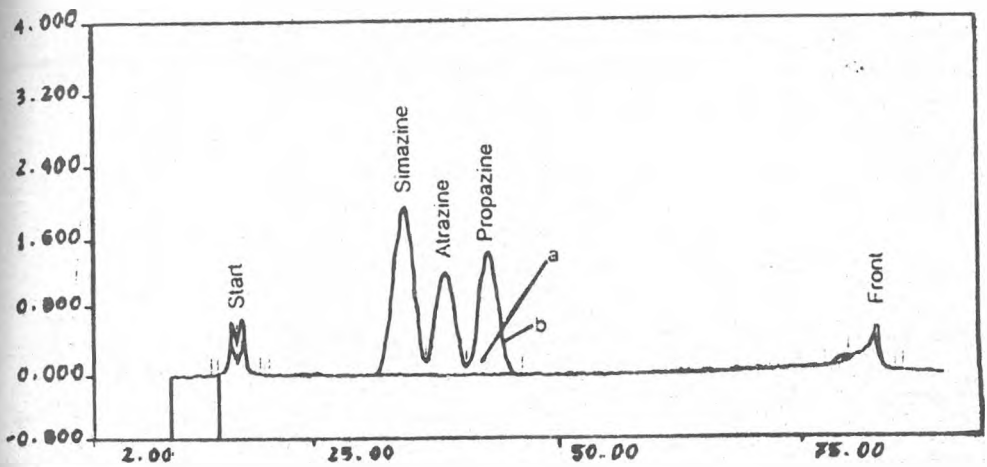

Figure 2. Typical densitograms obtained from: a - blank sand (B_1) and b - spiked sand (S_1)

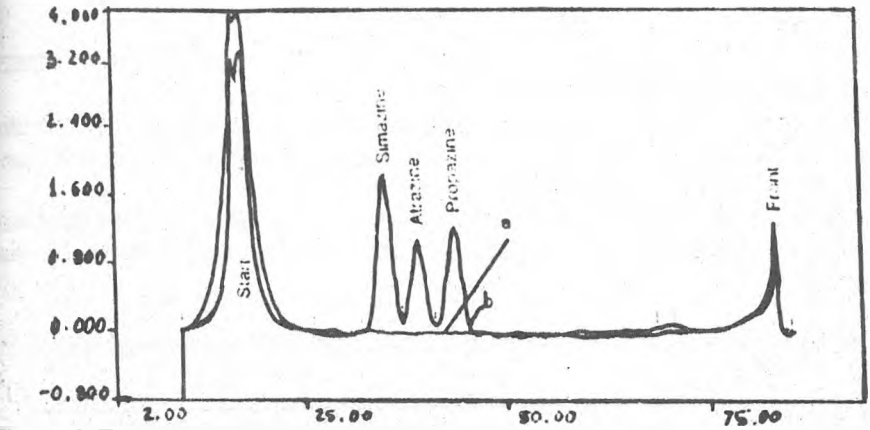

Figure 3. Typical densitograms obtained from: a - blank soil (B_2) and b - spiked soil (S_1)

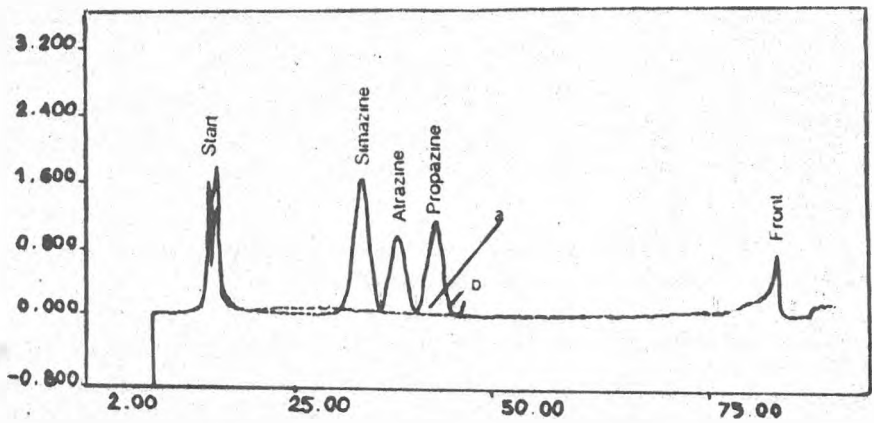

Figure 4. Typical densitograms obtained from: a - blank soil (B_3) and b - spiked soil (S_3)

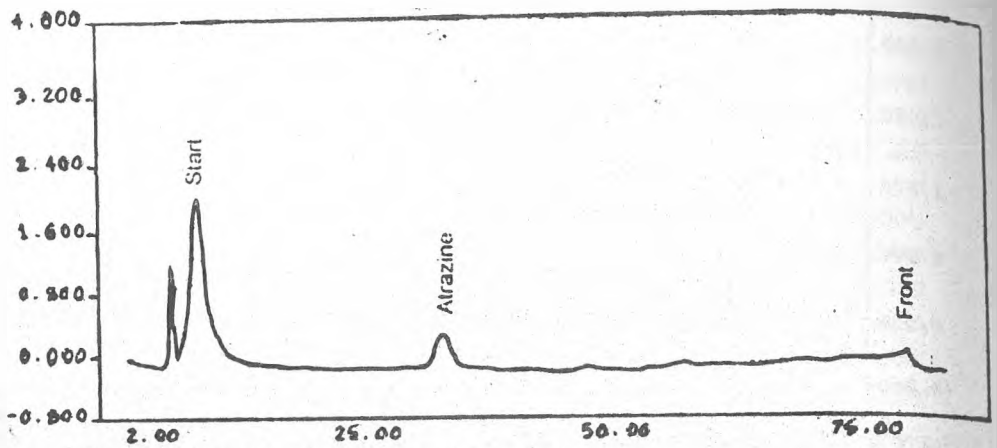

Figure 5. Densitogram of field soil sample (S_4)

The R_f value for the given chromatographic system for simazine, atrazine and propazine are 0.27, 0.34, 0.41 respectively.

In the R_f zone corresponding to simazine, atrazine and propazine the blank samples do not contain compounds. This fact makes possible the quantitation of triazines by simple extraction, TLC separation and UV scanning.

In table 1 are given the spots area for simazine, atrazine and propazine from the spiked sample and stock solution and the recovery values for each triazine compound.

Table 1. The spots area for simazine, atrazine and propazine and recovery values

Sample	Area			Recovery (%)*		
	simazine	atrazine	propazine	simazine	atrazine	propazine
stock	112466	55050	71839	—	—	—
S_1	112063	54877	71561	99.6	99.7	99.6
S_2	94042	50220	64375	83.6	91.2	89.6
S_3	84567	43572	60408	75.2	79.2	84.0

* The recovery value was calculated by reporting the spiked sample spot area to spot area of the same compound from stock solution.

The results show that the recovery value for the garden sample (S_3) with high content of clay is smaller as for the greenhous soil (S 2). This fact can be explained by the adsorption phenomena that are different for the two types of soil. In the case of sea sand (S1) this phenomena are limited, the differences can be explained by normal experimental errors.

The calibration curves for the simazine, atrazine and propazine are presented in figures 6, 7 and 8 respectively.

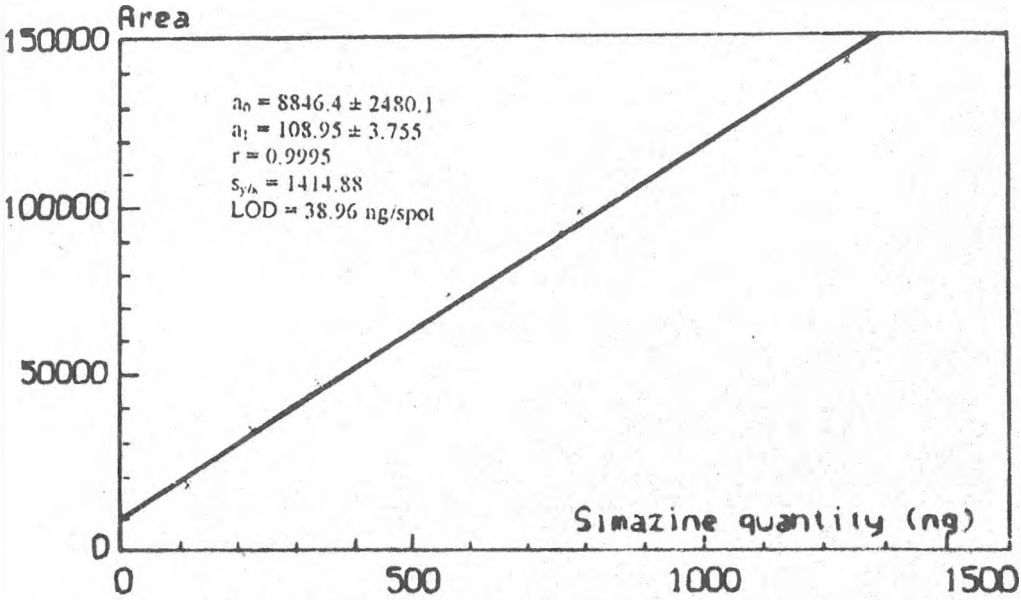

Figure 6. The calibration curve for simazine

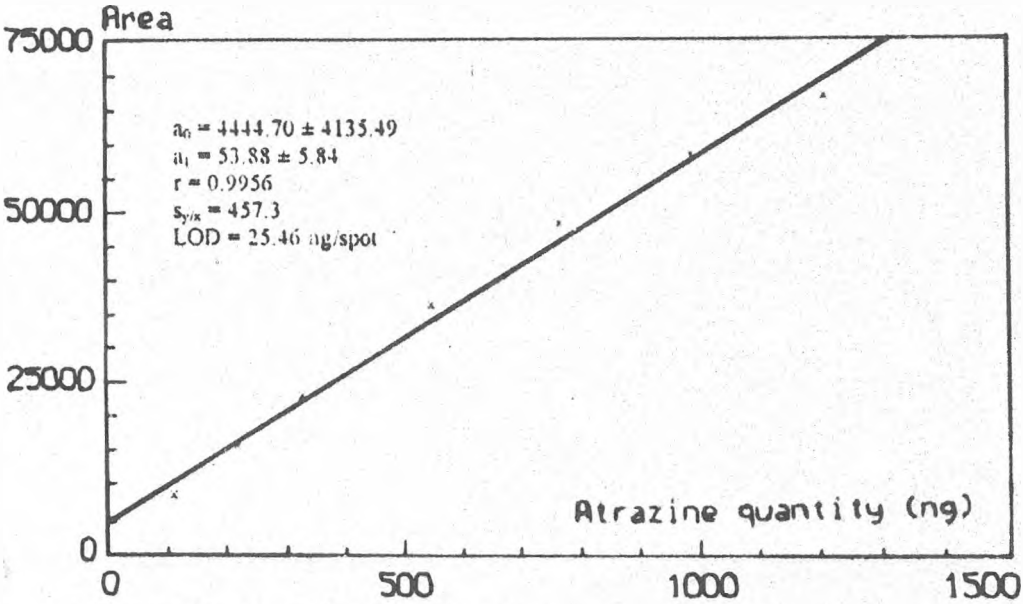

Figure 7. The calibration curve for atrazine

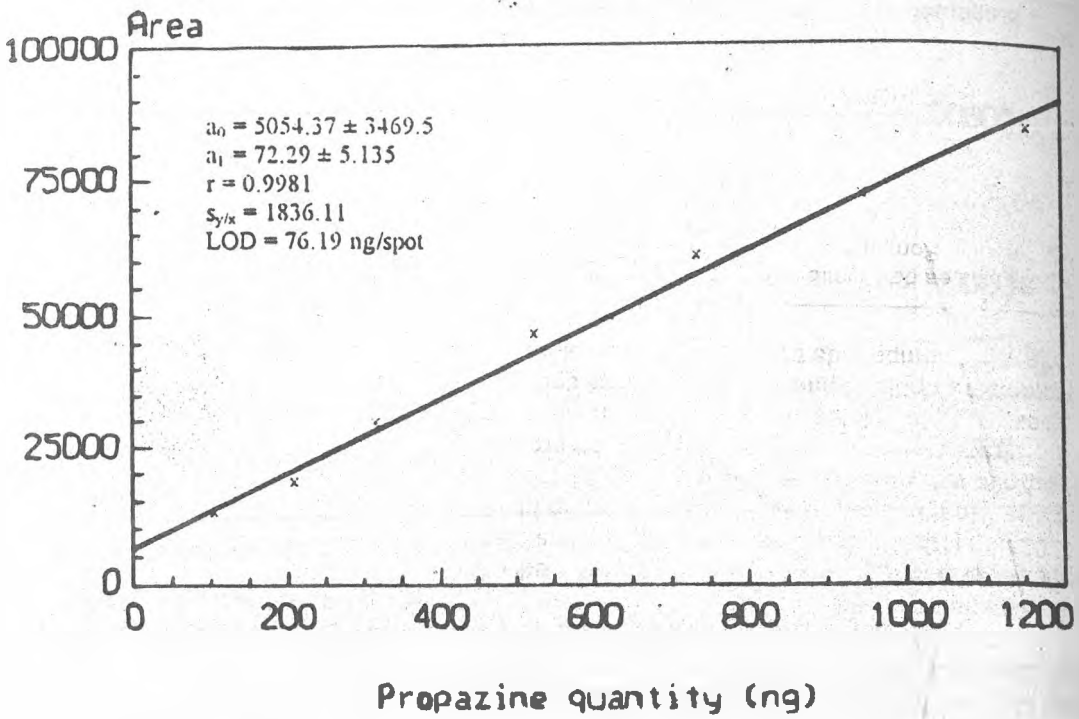

Figure 8. The calibration curve for propazine

The limit of detection LOD were calculated conform [15].

The quantity of atrazine, corresponding to the spot area from calibration curve was founded to be 317,447ng. The content of atrazine in analysed soil sample was found to be 0.4ppm.

CONCLUSIONS

The determination of triazine herbicides from soil can be performed by mathanol extraction followed by TLC - densitometry, if the soil contains more than 0.1ppm herbicides.

REFERENCES

1. Ghinea, I. Vlăduţu, M. Berca, *Efectele reziduale ale erbicidelor,* Ed Academiei, Bucureşti, 1989, 91-99.
2. R. M. Jhonson, F. Halaweish, J. J. Fuhrmann, *J. Liq. Chromatogr.*, 1992, 15(7), 294.

3. L. Q. Huang, J. J. Piinatello, *J. Ass. Off. Anal. Chem.*, 1990, 73(3), 443.
4. Q. Wenheng, N. Schultz, J. D. Stuart, J. C. Hogan, *J. Liq. Chromatogr., 1991*, 14(7), 1367.
5. G. Karlaganis; R. Von Arx, H. Ammon, R. Comenzind, *J. Chromatogr.*, 1991 549(1-2), 229.
6. S. Ashford, K. D. Bartle, A. Cliford, R. Moulder, W. M. Raynor, F. G. Shilstone, *Analyst*, 1992, 117(11), 1697.
7. H. Steinwandter, *Fresenius J. Anal. Chem.*, 1991, 304(6), 389.
8. Li Jinke, H. Cooper, D. S. Gamble, *J. Agric. Food Chem.*, 1996, 44, 3672.
9. Li Jinke, H. Cooper, D. S. Gamble, *J. Agric. Food Chem.*, 1996, 44, 3679.
10. P. Duc, *Analusis*, 1992, 20(suppl.7), 511.
11. G. Durand, P. Gille, D. Fraisse, D. Barcelo, *J. Chromatogr.*, 1992, 603(1-2), 175.
12. G. Durand, R. Forteza, D. Barcelo, *Chromatographia*, 1989, 28(11-12), 597.
13. N. Judge, D. E. Mullins, R. W. Joung, *J.P.C.-Mod. TLC*, 1993, 6(4), 300.
14. Z. Lin, S. A. Clay, D. E. Clay, S. H. Harper, *J. Agricol. Food Chem.*, 43, 1995, 815.
15. J. C. Miller, J. N. Miller, *Statistic for Analytical Chemistry*, Ellis Horwood Limited, England, 1986, 90-100.

STUDIA UNIVERSITATIS BABEŞ-BOLYAI, CHEMIA, XLII, 1-2, 1997

PARAMETRIC INVESTIGATION OF SODIUM BICARBONATE DECOMPOSITION IN ROTARY DRUM REACTOR

ALEXANDRU OZUNU[1], RADU MISCA[1], LIVIU LITERAT[1]

ABSTRACT. Residence time distribution measurements were carried out at different values of operating parameters by use of a step signal. The investigation did show that the particle movement can be described using the plug-flow model at moderate rotational speed. As the investigations of global kinetics did show the decomposition cannot be described as a simple chemical reaction. Different mechanisms have to be taken into account: at low temperatures the limiting rate is determined by chemical reaction while at higher temperatures additional resistances of heat and mass transfer limite the rate of decomposition. The analysis of scanning electron microscop did show that a simple shrinking core model is suitable to describe the conversion of single particles. The influence of operating conditions on the decomposition of sodium bicarbonate in a continuously working rotary kiln was studied experimentally and theoretically. The model developed matches the experimental results well. The grade of conversion increases with rising wall temperature, gas temperature and gas mass flow while an increasing rotational speed leads to a decrease of conversion.

INTRODUCTION

Because of their flexibility, large solid throughputs, simple construction and relative inexpensive, rotary drum reactors are employed in a variety of processes involving combinations of particulate mixing and gas-solid reaction with intensive heat and mass transfer. In spite of this, reaction engineering investigation of chemical reactions in rotary kilns are just a few. Most papers which have been published only recommended methods of calculations without publishing experimental reaction engineering data. An example of use in inorganic chemical industry for the manufacture of soda, is the decomposition of sodium bicarbonate. Therefore, sodium bicarbonate is present in technological processes as trona. The decomposition follows according to the reaction:

$$2\left(NaHCO_3 \cdot Na_2CO_3 \cdot 2H_2O\right)\ (s) \rightarrow 3\ Na_2CO_3\ (s) + 5H_2O(g) + CO_2(g) \qquad (1)$$

Recently, Keener showed (1993) that the use of sodium carbonate as a solid sorbent for the removal of SO_2 has many attractive features. It has been well

[1] Facultatea de Chimie şi Inginerie Chimică, Str. Arany Janos 11, Universitatea "Babeş-Bolyai", 3400 Cluj-Napoca, România

established that thermal decomposition of $NaHCO_3$ particles can produce a highly porous Na_2CO_3 product that reacts rapidly with SO_2 in waste gases [4].

Another studied example was the gypsum dehidration process.

For this work, our objective was to establish the influence of operating parameters on the decomposition process and to analyse it with a simple model which was developed [5].

EXPERIMENTAL

The experiments performed in this study were conducted to determine the influence of a number of rotary drum operating variables on the conversion of the decomposition reaction in continuously working. A secondary purpose was to characterize the particle movement in rotary drum. The operating variables considered were the temperature of the wall and gas, air mass flow rate, rotational speed, drum slope and the number of lifting flights.

A schematic diagram of the experimental system used is shown in Figure 1. It has three primary components: the material feeding system, the air feeding system and the rotary drum. The material feeding system consists of a bulk storage bin and a constant feeder. The air feeding system consists of a route to take and to transmit the atmospherical air at the expected parameters (F-filter, A-adsorber, V-ventil, R-rotameter, H-heating).

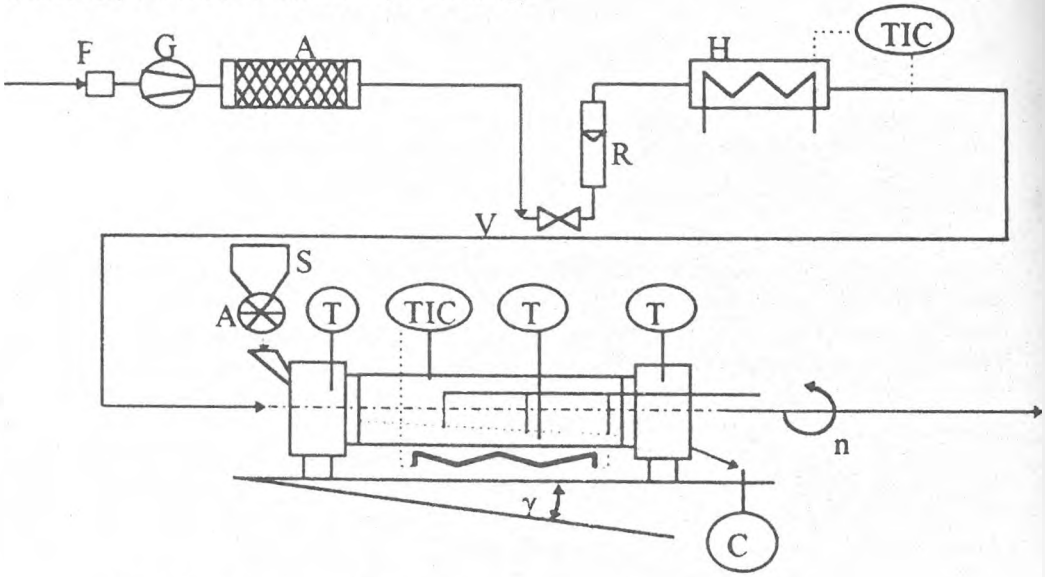

Figure 1. Experimental setup

The rotary drum was constructed from a stainless tube. It was 1 meter in length and had a diameter of 100 mm. Along the interior surface of the drum, parallel to its longitudinal axis, eight or five equally spaced lifter bars can be fitted. The outlet flange has an opening of 70 mm diam. The drum could be rotated at speeds between 1 and 10 min^{-1}. The slope of the drum is adjustable and the wall

can be heated with an electrical heater. In the wall, there are 8 thermoelements incorporated whereas the belonging to its electrical comparison point in the tube is assembled. It was used a Funk signal for all transmisions. The air temperature were measured at inlet and outlet of drum. For solids temperature measurements were 3 thermoelements over the length distributed in contact with material. With a sampler one can evaluate the locale composition in these alternative points. A thermal gravimetric method was used to measure rates of decomposition of $NaHCO_3$ particles in a dryer plank. In addition to the kinetics experiment, pore-volume data were obtained for solid reactant and product in order to evaluate changes in pore structure as a result of reaction. A sampler of 1.5 g in a very thin layer was used to prevent the contamination with gaseous products of decomposition (reducing the possibility of negative mass transfer effects in the layer).

RESULTS AND DISCUSSION

The process modelling

In every continuously working experiment, steady state flow conditions were assured before starting the measurements.

The most important assumptions are:

- The velocity and mass of the solid and gas are constant throughout the lentgh of the kiln.
- Specific heats, latent heats and heats of reaction are independent of temperature and position.
- The solids are in radial and transversal direction stirred. The gradients of measured variables are important in axial direction.
- The decomposition reaction is:

$$2\ NaHCO_3\ (s) \rightarrow Na_2CO_3\ (s) + H_2O\ (g) + CO_2\ (g) \qquad (2)$$

and, as Hu [3] indicated the decomposition was first-order in mass of $NaHCO_3$ with the formal kinetic:

$$dM_{NaHCO3} / dt = k(T)M_{NaHCO3} \qquad (3)$$

- The heat transfer due to release of water vapor and CO_2 into the gas can be treated as convective heat transfer.
- The wall temperature has a constant value

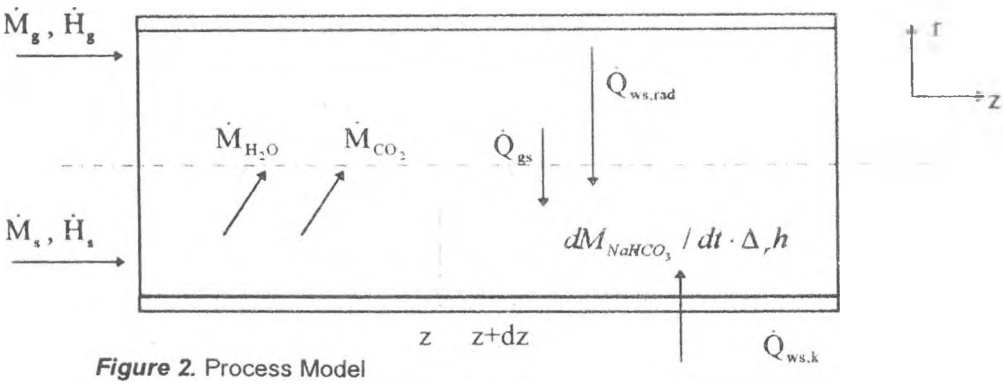

Figure 2. Process Model

By means of the material and energy balances, the longitudinal conversion and temperature profiles can been evaluated for diferential balance elements. Through integration over the reactor length ones can evaluate the outlet conversion.

Material and Gas Flow Rates

Drying of solids and evolution of carbon dioxide and water vapors due to decomposition of trona results in an increase in the gas flow rate, and a decrease in the material flow rate, down the length of the calciner. Considering the stoechiometry of the reaction, the material and gas flow rates are given by:

$$\frac{d\dot{M}_s}{dz} = -\frac{d\dot{M}_{NaHCO_3}}{dz} - \frac{d\dot{M}_{Na_2CO_3}}{dz} = \frac{d\dot{M}_{NaHCO_3}}{dz}\left(-1 + \frac{\tilde{M}_{Na_2CO_3}}{2\tilde{M}_{NaHCO_3}}\right) \tag{4}$$

$$\frac{d\dot{M}_g}{dz} = -\frac{d\dot{M}_{H_2O}}{dz} - \frac{d\dot{M}_{CO_2}}{dz} = \frac{d\dot{M}_{Na_2CO_3}}{dz}\left(+\frac{\tilde{M}_{Na_2CO_3}}{2\tilde{M}_{H_2O}} + \frac{\tilde{M}_{Na_2CO_3}}{2\tilde{M}_{CO_2}}\right) \tag{5}$$

with:

$$\frac{d\dot{M}_g}{dz} = -\frac{d\dot{M}_s}{dz} \tag{6}$$

Heat transport equations

Because of different material distribution in the bare sections and in the lifting flight section of the rotary reactor it is necessary to evaluate the various heat transfer coefficients and fluxes separately for each of these situations [1]. The most important assumption were made (1-3). Heat fluxes considered in the development of the mathematical model are shown in Figure 2. For this work a bare section is considered. In Appendix are given some parametric corelations for bare and lifting flight sections. Heat fluxes (Q_{gs}, from gas to material; Q_{ws} from wall to material) can be expressed as follows:

$$\dot{Q}_{gs} = \alpha_{konv}\, E_A\, A_{gs}(\vartheta_g - \vartheta_s) \tag{7}$$

$$\dot{Q}_{ws} = \dot{Q}_{ws,k} + \dot{Q}_{ws,rad} = \left(\alpha_{rad}\, A_{ws,rad} + \alpha_k\, A_{ws,k}\right)\left(\vartheta_w - \vartheta_s\right) \tag{8}$$

The heat transport rate due to the reaction enthaply are given by

$$\dot{Q}_{rkt} = -\frac{d\dot{M}_{NaHCO_3}}{dz}\,\Delta_r\tilde{H} \tag{9}$$

with:

$$\frac{d\dot{M}_{NaHCO_3}}{dz} = -k(T) * \dot{M}_{NaHCO_3} * \frac{1}{v} \tag{10}$$

In steady state the following energy balances are valid:

$$-d\dot{H}_g - \dot{Q}_{gs} + \dot{Q}_{vap} + \dot{Q}_{H2O} + \dot{Q}_{CO2} = 0 \tag{11}$$

$$-d\dot{H}_S - \dot{Q}_{vap} - \dot{Q}_{H2O} - \dot{Q}_{CO2} + \dot{Q}_{gs} + \dot{Q}_{ws} + \dot{Q}_{reac} = 0 \tag{12}$$

The required parameters to solve the model were taken from literature. In special those for heat and mass transfer coefficients from the works by Evripidis [2] and Blumberg [1].

Reaction kinetics

Decomposition experiments were caried out with particles (ca. 100 μm in diameter) at constant temperature in range from 80 to 140°C. Conversion was calculated from the decrease in sample weight:

$$X = \frac{N_{NaHCO_{3,t=0}} - N_{NaHCO_3}}{N_{NaHCO_{3,t=0}}} \tag{13}$$

and data plotted according to eq. 13 are shown in Figure 3. For lower temperatures than 90°C, the limitative stage is chemical reaction. One can see that the present

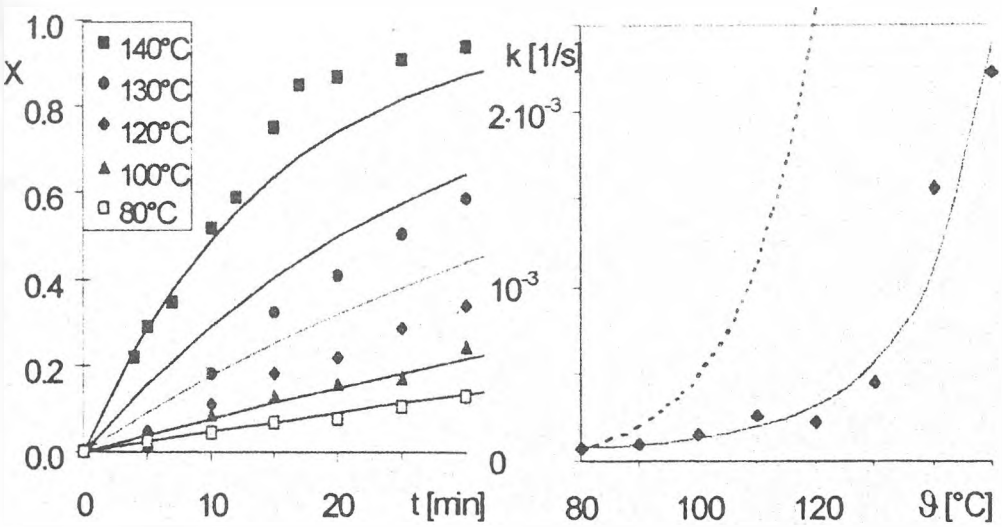

Figure 3. a) Conversion-time curve at different temperatures. b) Arrhenius plot of rate constant *k* with Hu[3] values (interrupt line), mathematical interpolation (continuously line) and measurements values (points).

works values are smaller than Hu [3]. gave in Arrhenius form ($k=k_0\exp(-E_a/RT)$ with preexponential factor, k_0 = 1.44 10^{11} and activation energy, E_a = 102 kJ/mol. Analyses carried out with the raster electron microscope (REM) on natrium bicarbonate and soda samples show that the first is nonporous and the second is porous. Since the original $NaHCO_3$ particles are nonporous, the reaction should take place at the surface of its unreacted core of $NaHCO_3$ as expressed by shrinking unreacted core model [4].

The influence of some operating parameters in continuously working

The influence of temperature and the type of heat transfer is shown in Figure 4. As can be seen the effect of increasing temperature is the same in every

case. The optimum is placed in the field 150-160°C. The role played by the conductive heat transfer is evident. The presence of lifting flight is important but the number of is not (4 or 8).

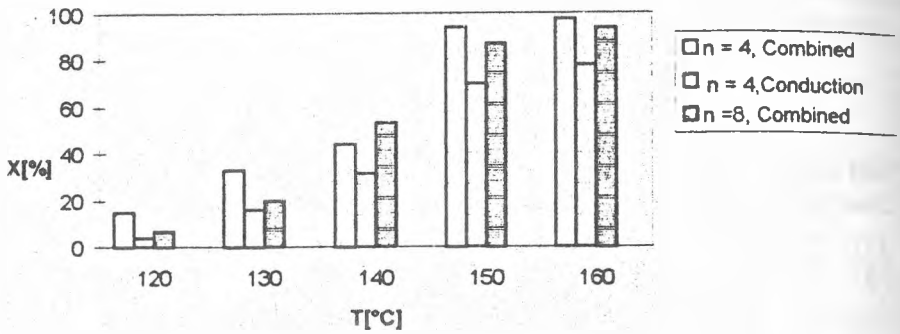

Figure 4. The influence cf temperature and heat transfer mechanism on the outlet conversion (T_g=150°C, M_g=5,9kg/h, M_s=1,4kg/h, z=3min^{-1})

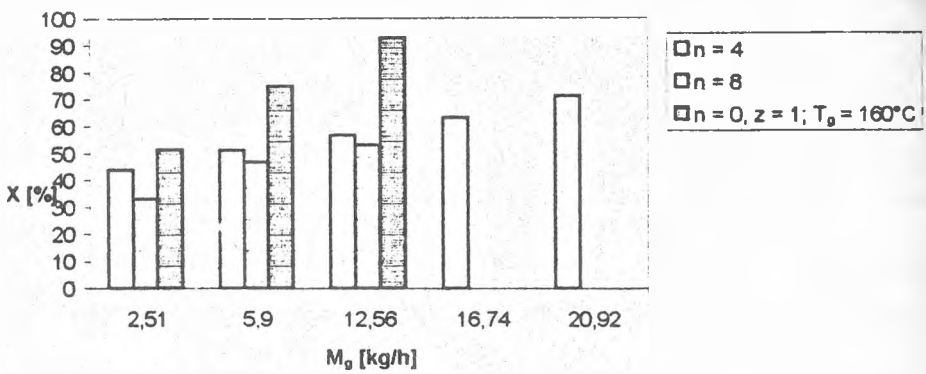

Figure 5. The influence of air flow rate on the outlet conversion (T_g=150°C, T_w=140°C, M_s=1,4kg/h, z=3min^{-1})

Figures 5 and 6, present two important effects on the process in our experimental conditions. A comparison between experiments and calculated values with process model are given in Figure 7. One can recognize the agreement between calculated and measured profiles.

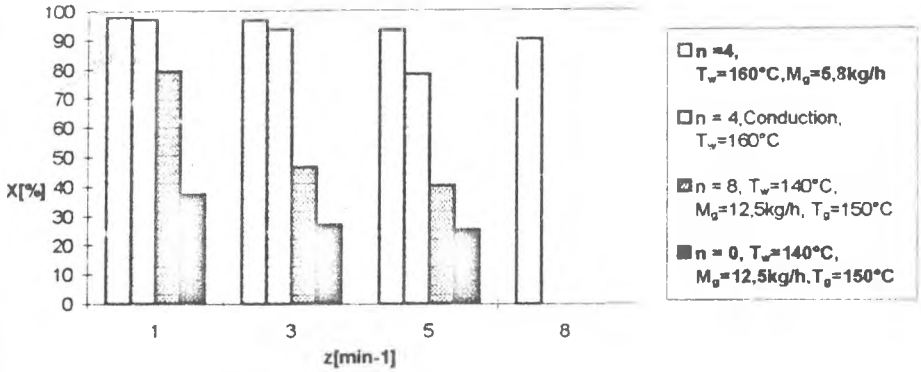

Figure 6. The influence of rotational speed on the outlet conversion

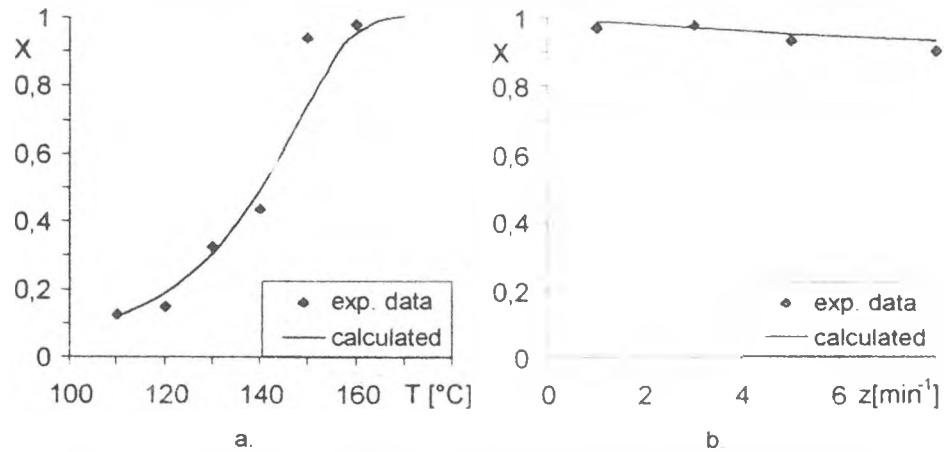

Figure 7. Conversion of reaction in continuously working as a function of wall temperature (a) and rotational speed (b)

APPENDIX. Heat Transfer Coefficients.

a) *α_c* ***(bare section)*** *is estimated by using the relations [2]:*

$$Nu = Nu_{min} + [Nu^2_{lam} + Nu^2_{turb}]^{1/2} \quad (14)$$

$$Nu_{lam}=0.664Pr^{1/3}Re^{1/2} \quad (15)$$

$$Nu_{turb}=(0.037Re^{4/5}Pr)/[1+2.44(Pr^{2/3}-1)Re^{-1/10}] \quad (15)$$

$$\alpha_c=\alpha\cdot K_d\cdot K_z\cdot K_D \quad (16)$$

α^*_c for lifting flight section:

$$\alpha^*_c=(\alpha_c(A_o+A_{FF})+\alpha_{c,fall}A_{fall})/(A_o+A_{FF}+A_{fall}) \quad (17)$$

b) α_K is estimated by using the relations [1]:

$$1/\alpha_K = 1/\alpha_{WS} + 1/\alpha_{SB} \quad (18)$$

where:

$$\alpha_{SB}=2\pi^{-1/2}[(\lambda\rho c_P)^{1/2}/(t_K N_{mix})^{1/2}] \quad (19)$$

c) α_{rad} is calculated by using the relation [1,2]:

$$\alpha_{rad}=4C_{12}[(T_W+T_s)/2]^3 \quad (20)$$

with: $C_{12}=C_S/[1/\varepsilon_s+A_o/A_K(1/\varepsilon_W-1)]$ (21)

DATA USED FOR SIMULATION

The data are follows: $\Delta_r H = 1.75 \cdot 10^6$ J/kg; $A_w = 0.314 m^2$; $A_{ws,rad} = 0.207 m^2$; $A_{ws,k} = 0.107\ m^2$; $v = 8.33 \cdot 10^{-4}$ m/s; $\alpha_{gs} = 18$ W/(m^{2}K); $\alpha_{ws,rad} = 15$ W/(m^{2}K); $\alpha_{ws,k} = 146$ W/(m^{2}K); $\alpha_{wg} = 6$ W/(m^{2}K); $d_p = 120 \cdot 10^{-6}$ m; $c_B = 1144$ J/(kg•K).

ACKNOWLEDGMENTS

The authors gratefully acknowledge the financial and scientific support of DAAD, International Seminar and Institute of Thermal Process Engineering at the University of Karlsruhe, Germany [5].

NOMENCLATURE

c_p	specific heat [J/kg/K]
k	rate constant [1/s]
r	radial coordinate [m]
v	solid velocity [m/s]
z	axial coordinate [m]
A	surface [m²]
E_A	Ackermann correction
$\Delta_r H$	reaction enthalpie [J/kg]
$\dot{M}$	flow rates [kg/s]
$\tilde{M}$	molecular weight
$\dot{Q}_{ik}$	heat fluxes from i to k [W]
α	heat-transfer coefficients [W/m²/K]
ϑ	temperature [°C]

Indices

g	gas phase
k	conduction
rad	radiation
s	solid
w	wall
c	convectiv
SB	first solid layer in contact with the wall
FF	fitted-flights
o	bare section

REFERENCES

1. W. Blumberg, *Selektive Konvektions- und Kontakttrocknung im Drehrohr*. Dissertation, VDI-Verlag, Dusseldorf, 1995.
2. I. Evripidis, *Kombinierte Kontakt-und Konvektionstrocknung in einem Trommeltrockner*. Dissertation, VDI-Verlag, Dusseldorf, 1991
3. W. Hu, *Kinetics of Sodium Bicarbonate Decomposition*, AIChEJ (1986) *32*, 1483-1490.
4. T. C. Kenner, S.J. Khang, *Kinetics of the Sodium Bicarbonate-Sulfur Dioxide Reaction*, Chem. Eng. Sci. (1993) *48*, 2859-2865.
5. A. Ozunu, J. Zank, E. U. Schlunder, *Untersuchung der Zersetzung von Natriumhydrogencarbonat in einem Drehrohrreaktor*, Wiss. Abbschlussber. 32. Int. Sem. Univ. Karlsruhe (1997), 128-138

STUDIA UNIVERSITATIS BABEȘ-BOLYAI, CHEMIA, XLII, 1-2, 1997

THE RECOVERY OF LEAD FROM SCRAP AS LEAD CARBONATE

LIVIU ONICIU[1], LUCIA ZADOR[1]

ABSTRACT. Lead was extracted from the scrap obtained after leaching with H_2SO_4 the non-ferrous sulphide calcination products as $PbCO_3$ and subsequent dissolution with proper acids, followed by electrolysis. The treatment of the scrap with Na_2CO_3 was more efficient than with $(NH_4)_2CO_3$ or ammonia/ammonium sulphate. Extraction with some mono and diethanolamines does not improve the yield of lead recovery. The influence of reaction time, $PbSO_4/Na_2CO_3$ molar ratio, solid/liquid mass ratio and particle size on the conversion of $PbSO_4$ from scrap to $PbCO_3$ were also analysed.

INTRODUCTION

In recent years the recovery of lead from scrap focused considerable research efforts because of economic and environmental reasons. The limited natural resources below increasing consumption, especially for manufacture of lead-acid storage batteries, have created the situation that half of the world's total output of lead is obtained by recovery from scrap [1].

Hydrometallurgical processes are advantageous relative to the pyrometallurgical methods due to the reduced costs as well as the absence of pollution problems. In scrap, lead is mainly present as sulphate or oxides, which (in order to be converted into carbonate) are dissolved in H_2SiF_6 or HBF_4 and the resulted soluble salts of lead are subjected to electrolysis. The extraction of lead from scrap can be performed by complexes formation with organic reagents [2,3], by dissolution in ammonia/ammonium sulphate [4], or by alkaline dissolution, when the complex ion $[Pb(OH)_4]^{2-}$ is formed [5-8]. The cementation of lead from sulphate with zinc is known as an efficient method when the scrap contains Pb beside Zn; $ZnSO_4$ resulted from the reaction can serve for electrolytical recovery of metallic zinc.

We report now the results regarding the optimal conditions for the transformation of lead compounds formed in the calcinating of non-ferrous sulphides into a soluble compound which allows electrolytical deposition.

RESULTS AND DISCUSSION

The scrap originates from the "SOMETRA COPȘA-MICĂ" enterprise. By leaching with H_2SO_3 almost all the zinc and iron are dissolved, leaving an insoluble

[1] Facultatea de Chimie și Inginerie Chimică, Universitatea "Babeș-Bolyai', RO-3400 Cluj-Napoca, România

grey powder. Most of the lead is present as $PbSO_4$ (from the reaction of PbO with H_2SO_4), but some PbS and metallic Pb resulted from some reduction processes can also be present:

$$PbS + 2\,PbO \longrightarrow 3\,Pb + SO_2 \quad (1)$$

$$PbS + PbSO_4 \longrightarrow 2\,Pb + 2\,SO_2 \quad (2)$$

The chemical composition of scrap, determined by atomic absorption and the granulometric distribution obtained by sifting, is given in Table 1:

Table 1. Chemical and granulometric composition of scrap powder

Element	Pb	Zn	Fe	Cu	Cd	Sb	Bi
%	32.7	11	5.8	0.95	0.035	0.03	0.04
Granule size	>0.5	0.5-0.4	0.4-0.315	0.315-0.25	0.25-0.2	0.2-0.18	
%	26.5	51.6	11.6	7.5	2.3	0.5	

The major granulometric fraction (particle size 0.4-0.5 mm) of this powder was treated under magnetic stiring with 5% or 15% aqueous solution of Na_2CO_3, in order to obtain different Na_2CO_3:Pb molar ratios and different solid/liquid (S/L) mass ratios. Depending on the solution pH and the reaction time, $PbCO_3$ or basic lead carbonates were formed, according to the equations:

$$PbSO_4 + HCO_3^- \longrightarrow PbCO_3 + SO_4^{2-} + H^+ \quad (3)$$

$$PbSO_4 + CO_3^{2-} \longrightarrow PbCO_3 + SO_4^{2-} \quad (4)$$

$$3\,PbSO_4 + 2\,Na_2CO_3 + 2\,H_2O \longrightarrow Pb_3(CO_3)_2(OH)_2 + 2\,Na_2SO_4 + H_2SO_4 \quad (5)$$

$$Pb_3(CO_3)_2(OH)_2 + 2\,Na_2CO_3 \longrightarrow 3\,NaPb_2(CO_3)_2(OH) + NaOH \quad (6)$$

As the reaction between pure Na_2SO_4 and $PbCO_3$ has a low activation energy (only 15.8 kJ/mol [10]) the temperature influence upon the reaction rate is negligible and therefore the work was carried out at room temperature.

The first set of experiments was performed with a S/L mass ratio of 1:20 and a $PbSO_4/Na_2CO_3$ molar ratio of 1:1. Figure 1 illustrates the conversion curve.

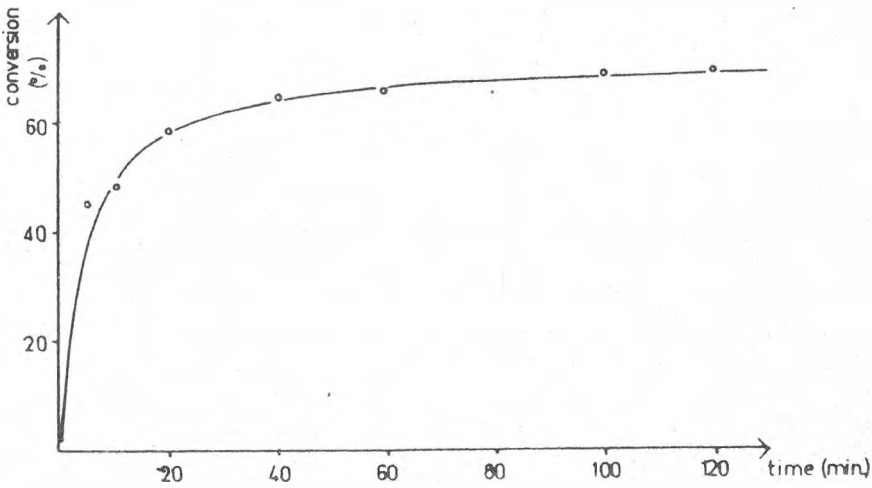

Figure 1. Conversion versus reaction time

The reaction is fast during the first 10-15 minutes (when conversion attains 60%), but afterwards it develops slowly. Table 2 shows that excess of sodium carbonate increases the conversion time:

	Molar ratio PbSO4/Na2CO3	Time (min.)	Particle size (mm)	Conversion (%)
a	1:1	60	0.4-0.5	66.3
a	1:2	60	0.4-0.5	74.2
a	1:3	60	0.4-0.5	72.3
a	1:1	5	0.4-0.5	45.75
a	1:2	5	0.4-0.5	64.4
a	1:3	5	0.4-0.5	70.6
b	1:1	60	>0.5	61.0
b	1:1	60	0.4-0.5	66.3
b	1:1	60	0.2-0.25	68.3

Table 2. The influence of Na_2CO_3 concentration (a) and particle size (b) on conversion in $PbCO_3$ at a S/L ratio of 1:20

Because the reaction takes place heterogeneously the rate increases with the specific surface area of the solid reagents (see Table 2). The effect of the solid/liquid mass ratio is also obvious. in table 3 results are given for the experiments carried out at different S/L ratio, at constant molar ratio of the reagents and particle dimension.

Table 3. The influence of S/L ratio on the reaction efficiency (f) $PbSO4/Na_2CO_3$ 1:1 molar ratio after 60 minutes

S/L ratio	1:40	1:20	1:10	1:5
f (%)	54.75	66.30	70.10	68.80

Another set of determinations was performed at S/L=1:5 in view of the fact that it would be economically advantageous to reduce water consumption, and the yield is higher than for 1:40 or 1:20 S/L ratios. Figure 2 shows the conversion curves at 1:5 S/L ratio at different $PbSO_4/Na_2CO_3$ molar ratios.

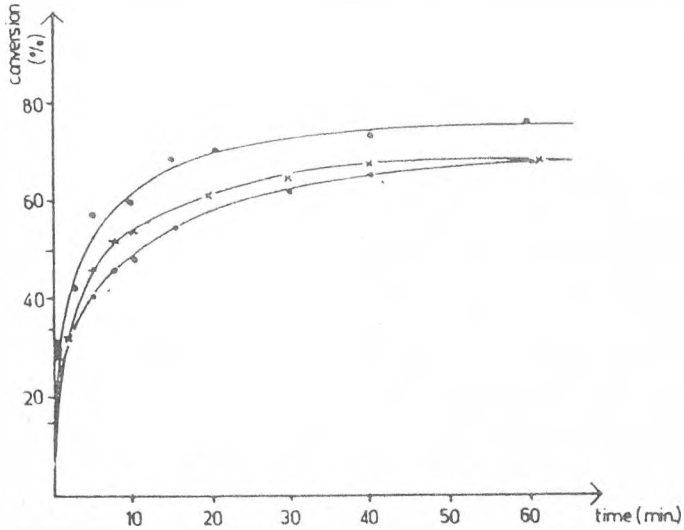

Figure 2. The conversion curves at 1:5 S/L ratio at different $PbSO_4/Na_2CO_3$ molar ratios

The doubling of the sodium carbonate concentration increases conversion, yet a further increase in concentration is not efficient.

Attempts to accomplish the reaction between the scrap and Na_2CO_3 in two steps were made in search of an increased yield. The results presented in Table 4 indicate an yield of 91% after 60 minutes at molar ratio 1:2 and S/L ratio 1:5. The reaction time in both steps was 60 minutes, because, as seen on the conversion curves, a larger period does not improve significantly the yield.

Table 4. The efficiency of lead extraction from scrap in succesive steps

Time (min)	Molar ratio $PbSO_4/Na_2CO_3$	S/L mass ratio	% Pb^{2+} in the second extraction	Total % Pb^{2+}
60	1:1	1:20	8.4	71.7
60	1:1	1:5	13.7	82.5
60	1:2	1:5	15.5	91.0

Attempts to use $(NH_4)_2CO_3$ instead of Na_2CO_3 at a $PbSO_4/Na_2CO_3$=1:2 molar ratio and a S/L ratio of 1:5 were not efficient at 20°C (9% conversion), but at 45° the conversion increased to 72%, which is close to that reached using Na_2CO_3 at 20°.

The extraction with monoethanolamine followed by reaction with Na_2CO_3 led to the dissolution of 36.8% of the initial amount of lead, while the yield obtained using diethanolamine was 56.5%. Surprisingly an increased temperature didn't induce an increased yield, as other sources indicate [2,3].

A mixture of ammonia/ammonium sulphate (4 mol sulphate/6.5 mol NH_3 aq.) containing lead in a mass ratio of 5:1 dissolves 51% of the lead. The mentioned composition is the best, and it was chosen on the basis of Guy's work on dissolution of lead compounds in ammonia/ammonium sulphate solution [4].

CONCLUSION

Experimental results show that, among the leaching agents investigated (Na_2CO_3, $(NH_4)_2CO_3$ and ammonia/ammonium sulphate solutions), the best for lead extraction from scrap is ***sodium carbonate*** in a ***molar ratio of 2:1 relative to Pb*** and with a ***1:5 S/L mass ratio***. Better results are obtained by increasing the powder surface area.

EXPERIMENTAL

The recovery experiments were carried out with the major granulometric fraction (particle size 0.4-0.5 mm) (see Table 1). 5 grams of this powder were treated for 5-60 min. (as shown in Table 3) under magnetic stirring with 5% or 15% aqueous solution of Na_2CO_3, in order to obtain different Na_2CO_3:Pb molar ratios and different solid/liquid (S/L) mass ratios. Depending on the solution pH and the reaction time, $PbCO_3$ or basic lead carbonates were formed. The precipitate was separated from the Na_2SO_4 containing solution by filtration on Buchner filter. Besides $PbSO_4$ the precipitate included other insoluble products. The SO_4^{2-} ions were washed with water to avoid the deposition of $PbSO_4$ after lead dissolution from carbonate with HNO_3, CH_3COOH or H_2SiF_6. Then the precipitate was treated with HNO_3. The quantitative separation of the supernatant (which contains Pb^{2+} ions) was accomplished by filtration on narrow pores paper. The Pb^{2+} concentration was determined gravimetrically as $PbCrO_4$ [9] and by atomic absorption spectroscopy. As the reaction between pure Na_2SO_4 and $PbCO_3$ has a low activation energy (only 15.8 kj/mol [10]) the temperature influence upon the reaction rate is negligible and therefore the work was carried out at room temperature.

Attempts were made for the extraction of lead with mono and diethanolamines, followed by reaction with Na_2CO_3, and also for dissolution of lead sulphate in ammonia/ammonium sulphate.

REFERENCES

1. C. O. Bounds, *J. Metals*, 1989, 41, 25.
2. D.A. Begun, M.F. Islam, R.K. Biswas, *Hydrometallurgy*, 1989, 22, 259.
3. D.A. Begun, M.F. Islam, R.K. Biswas, *Hydrometallurgy*, 1990, 23, 397.
4. S. Guy, C.P. Broadbent, D.J. Jackson, G.J. Lowson, *Hydrometallurgy*, 1982, 8, 251.
5. J. Laszlo, J. Mayer, I. Molnar, Hung. *Pat. H.U.* 195708, 1988.
6. Takeo Oki, Isao Iraki, *U.S. Pat.* 4.409.072, C.A. 99, 221148, 1983.
7. I. Gyulasi, I. Molnar, *Banyasz. Kohasz. Lapok, Kohaszat*, 1987, 120, 118.
8. J. Bear, R.C.A. Flann, R. Woods, *Aust J. Chem.*, 1988; 41, 1857; 1988, 41, 1875, 1988, 41, 1897.
9. C. Macarovici, "Analiză chimică cantitativă anorganică", Ed. Acad., București, 1979, p. 351.
10. Y. Gong, J.E. Dutrizac, T.T. Chem, *Hydrometallurgy*, 1992, 28, 399.

STUDIA UNIVERSITATIS BABEȘ-BOLYAI, CHEMIA, XLII, 1-2, 1997

MODELING BIOLOGICAL PROPERTIES BY SZEGED FRAGMENTAL INDICES[1]

IOSEFINA SCHIRGER[2], MIRCEA V. DIUDEA[3]

ABSTRACT. Modeling the inhibition activity of nitrogen containing aromatic structures on the growth of cultures of tetrahymena pyriformis, by using Szeged fragmental indices as molecular descriptors, is presented.

INTRODUCTION

A bioactive compound, when introduced in an organism, induces a biological response, i.e., a specific reaction of that organism. The response is function of the structure and chemical identity of that compound.

The interaction between the bioactive compound and the organism occurs, at molecular level, in the so-called biological receptors (active situses of proteic nature, located either on membranes or in the cells [1-4]. According to FISCHER (1894), the receptor is assimilated with a rigid cavity in which the bioactive compound (i.e., the effector) has to fitt (the "kee in lock" interaction).

Nowadays it is admitted that the receptors may be semi-rigid ones, in checking a mutual optimization with the effectors. The two partners of the complex effector-receptor, {E...R], loose their own minimal conformational energy to the expence of the most stable complex. This complex will generate the biological response.

Thus, the biological response is proportional to the concentration of the complex [E...R], resulting in the reaction

$$\mathbf{E + R \xleftrightarrow{K} [E...R] \xrightarrow{k} P} \tag{1}$$

The complex may either dissociate in the components (the equilibrium characterized by the constant K) or produce (with the rate constant k) the product P. The concentration of the last one vary according to relation

$$\frac{d[P]}{dt} = k[E...R] \tag{2}$$

so that the concentration of the complex can be approximated from the equilibrum state

$$[E...R] = [E][R]K = [E][R]\exp(-\Delta G / RT) \tag{3}$$

---

[1] This work is dedicated to Prof. Dr. Ioan Silberg, for his 60th aniversary and valuable contribution to the developement of the heterocyclic chemistry in Romania.

[2] Institutul de Chimie "Raluca Ripan", 3400 Cluj-Napoca, România.

[3] Facultatea de Chimie și Inginerie Chimică, Universitatea "Babeș-Bolyai", Arany Janos 11, 3400 Cluj-Napoca, România.

By substituting (3) in (2) and integrating between t = 0 and t = t*, one obtains

$$[P]^* = t^* [E]^* [R] \exp(-\Delta G / RT) \quad (4)$$

Since the concentration [E]* cannot be measured, the following relation between $[E]_0$ and [E]* is accepted

$$[E]^* = A[E]_0 \quad (5)$$

where A is a quantity dependent of the structure of effector. By substituting (5) in (4) the relation becomes

$$[P]^* = t^* kA[E]_0[R] \exp(-\Delta G / RT) \quad (6)$$

or also

$$\log(1/[E]_0) = \log(t^*/[P]^*) + \log k + \log[R] + \log A - 0.4343\Delta G / RT \quad (7)$$

Eq 7 is the expression of the biological response. If the set of bioactive compounds are congeners (i.e., they belong to one and the same clase of compounds) and if the response occurs by the same mechanism, then log(t*/[P*]), log k and log [R] are constants. They can be included in the global constant B, and in such a case. relation (7) becomes

$$-\log([E]_0) = B + \log A - 0.4343\Delta G / RT \quad (8)$$

where - log ($[E]_0$) is the quantitative biological response, log A describes the ability of the given compound to reach the biological receptor while ΔG express the affinity of the receptor for the given effector. These parameters can be correlated with physico-chemical and mathematical properties of the bioactive compounds.

QUANTITATIVE MODELS OF BIOLOGICAL ACTIVITY

Several quantitative models have been proposed; they differ in the manner of expanding the right member of eq 8.

Briefly, the HANSCH model [5-8] looks the biological response as a function of pasive transport, T (T = log A, in eq. 8), of the bioactive compound to the receptor, and of electronic , El, steric, S and hydrophobic, H, interactions of the effector with the receptor (f(El, S, H) = -ΔG in eq. 8).

$$-\log([E]_0) = T + f(El, S, H) \quad (9)$$

The passive transport can be described by a parabolic function of log P

$$T = a \log P + b(\log P)^2 + c \quad (10)$$

where P is the partition coefficient of the bioactive compound in the system octanol/water. This parameter accounts for the hydrophobic interactions between effector and receptor. Values log P may be measured experimentally or calculated by aditive models [1, 5-11].

The affinity of the receptor vs. the effector (the term f(El, S, H) in eq. 9) can be described by a HAMMETT formalism (see [1]).

The FREE-WILSON model looks the biological activity as a sun of the contributions of substituents bonded in the position j, (j = 1, 2, ...), of the common structure, within a congeneric series of bioactive compounds [12].

$$-\log([E_i]_0) = \sum_j a_{ij} X_{ij} + \mu \tag{11}$$

where a_{ij} is the contribution to the biological activity of the substituent located in position j, X_{ij} is the binary counter (taking the value 1 if there exists a substituent in oposition j and 0 otherwise) and μ is the arithmetic mean of the bioactive compounds within the set under study: μ=Med(-log([E_i]$_0$)). Since a mean value is used, the condition $\Sigma_i a_{ij} X_{ij}$=0 needs to be added. Examples can be found in [1, 8, 13-22].

In the FUJITA - BAN model, [23], the mean value in eq (11) is replaced by the activity of the unsubstituted structure (viewed as a reference). The parameter a_{ij} is now the ratio of the contribution of the substituent in j to that of the hydrogen [11, 19, 24-27].

More sophisticated models have been further proposed: MSD (Minimum Steric Difference), [28], MTD (Minimum Topological Difference), [28], SIBIS, [29], and recently COMFA, [30].

The present paper presents the modeling of a biological activity by using topological indices as the parameter X_{ij} in eq 11.

SZEGED FRAGMENTAL INDICES

Szeged property matrices are defined by the following relations [31].

$$[\mathbb{SZ}_u\mathbb{P}]_{ij} = P_{i,(i,j)} \tag{12}$$

$$P_{i,(i,j)} = m \sum_v P_v \tag{13}$$

$$P_{i,(i,j)} = \left(\prod_v X_v\right)^{1/N_{i,(i,j)}} \tag{14}$$

Entries in a Szeged property matrix are evaluated on the set of vertices v which obey the Szeged index condition ($v \in V(G)$; $D_{jv}<D_{iv}$) [32]. In fact, such a set of vertices can be viewed as a fragment (i.e., a subgraph) since a molecular graph is always a connected one.

Some special cases of the above definition deserve special attention:

(a) $P_v = 1$; $m = 1$ (classical matrix, SZ_u)

(b) $P_v = \Sigma_u A_u$; $m = 1/12$ (mass matrix, $\mathbb{SZ}_u\mathbb{A}$)

(c) X_v = group electronegativities [33] (electronegativity matrix, $\mathbb{SZ}_u\mathbb{X}$)

In case (a) $P_{i,(i,j)}$ represents the cardinality of the set of vertices v (see above). In case (b) A_u is the atomic mass and the summation runs over all atoms u, which are represented by the same vertex v. The factor m = 1/12 indicates that $P_{i,(i,j)}$ is a fragmental mass, relative to the carbon atomic mass.

In case (c) $P_{i(i,j)}$ is just the geometric mean of vertex values, X_v, of group electronegativities.

The above matrices are illustrated, for the graph G_1 (3-picoline) in Figure 1.

Indices are calculated on these matrices by the general relation

$$I_{e/p} = \sum_{e/p} [SZ_u P]_{ij} [SZ_u P]_{ji} \quad ; I = SZ;\ SZA;\ SZX \tag{15}$$

Indices calculated in the cases (b) and (c) are useful in discriminating chemical graphs which contain heteroatoms and multiple bonds.

G_1 G_2

$SZ_p = 182$; $SZ_e = 78$

$SZ_uA(G_1)$

0.000	1.250	3.500	1.250	2.333	1.250	3.500
3.500	0.000	4.667	3.500	3.500	2.333	4.667
4.667	3.500	0.000	2.333	4.667	3.500	2.333
6.917	4.667	3.500	0.000	4.667	4.667	3.500
3.500	2.333	3.500	3.500	0.000	2.333	3.500
3.500	2.333	4.667	3.500	3.500	0.000	4.667
4.667	3.500	2.333	2.333	4.667	3.500	0.000

$SZ_pA = 248.785$; $SZ_eA = 106.646$

$SZ_uA(G_2)$

0.000	1.250	3.333	1.250	2.250	1.250	3.333
3.250	0.000	4.417	3.250	3.333	2.167	4.417
4.417	3.333	0.000	2.167	4.417	3.250	2.167
6.500	4.500	3.333	0.000	4.417	4.417	3.333
3.333	2.250	3.333	3.333	0.000	2.167	3.250
3.333	2.250	4.500	3.333	3.333	0.000	4.417
4.417	3.333	2.250	2.250	4.500	3.333	0.000

$SZ_pA = 224.701$; $SZ_eA = 96.264$

$SZ_uX(G_1)$

0.000	0.958	0.964	0.958	0.965	0.958	0.964
0.962	0.000	0.963	0.962	0.964	0.962	0.963
0.962	0.962	0.000	0.962	0.963	0.962	0.962
0.964	0.963	0.964	0.000	0.963	0.963	0.964
0.962	0.962	0.962	0.962	0.000	0.962	0.962
0.962	0.962	0.963	0.962	0.964	0.000	0.963
0.962	0.962	0.962	0.962	0.963	0.962	0.000

$SZ_pE = 19.452$; $SZ_eE = 6.484$

$SZ_uX(G_2)$

0.000	0.958	1.016	0.958	1.014	0.958	1.016
1.020	0.000	1.017	1.020	1.016	1.020	1.017
1.080	1.101	0.000	1.020	1.017	1.020	1.020
1.069	1.077	1.016	0.000	1.017	1.017	1.016
1.101	1.144	1.101	1.101	0.000	1.020	1.020
1.101	1.144	1.077	1.101	1.016	0.000	1.017
1.080	1.101	1.144	1.144	1.077	1.101	0.000

$SZ_pE = 23.120$; $SZ_eE = 7.702$

Figure 1. Szeged Property Matrices; Fragmental Indices in the Graph G_1

APPLICATIONS

Szeged fragmental indices are useful in discriminating molecular graphs containing heteroatoms and multiple bonds (see Figure 1). They are also useful in modeling physico-chemical [31] and biological properties (see below).

In corelating tests, a multivariable regression equation is used [34]:

$$Y = a + \Sigma_i b_i X_i \qquad (16)$$

where a and b_i are regression coefficients, Y is the modeled property and X_i independent variable (in particular, topological indices). A satisfactory single variable regression is however a happy case. The quality of such an equation is expressed by the following statistics: r (correlation coefficient), s (standard error) and F (Fischer ratio).

A set of 24 heterocyclic molecules, [35], (Table 1), have been considered for testing the ability of Szeged fragmental indices in modeling the biological resopnse (as log BR) induced by these structures in inhibiting the growth of axenic cultures of the common feeshwater ciliate tetrahymena pyriformis strain GL-C. The biological descriptor, log BR is defined as the reciprocal of the IGC50 (i.e., the concentration - in mmol/l - which inhibites 50% the growth of tetrahymena cultures).

Correlation coefficient values ranges from 0.93 and 0.94, in single and two variable regression (Table 2). In single variable regression the best correlation coefficient, r = 0.9367, is showed by SZ_pE. The best two variable equation given by our indices is

$$\log BR = -2.056 + 0.053\, SZ_pE - 0.003\, SZ_eA$$

$$N = 24;\ r = 0.9414;\ s = 0.346;\ F = 81.75$$

Note that the superindex EATI [35] offers the following correlation: r = 0.9420; s = 0.3068. Despite the modeling of this activity both by EATI and Szeged fragmental indices is not satisfactory and not suitable in prediction, it demonstrates, however, the dependency of the biological response by the molecular structure.

Table 1. Topological indices and biological activity (log BR)

No.	Formula	SZ_p	SZ_e	SZ_pA	SZ_eA	SZ_pX	SZ_eX	log BR
1		105	54	126.389	65.000	16.859	6.740	-1.19
2	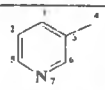	182	78	224.701	96.264	23.120	7.702	-1.02
3	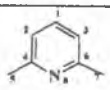	296	108	370.667	135.500	29.915	8.583	-0.81
4		105	54	129.639	66.667	18.236	7.278	-1.82
5		182	78	229.097	98.229	24.523	8.184	-1.09
6		296	106	377.194	135.431	31.930	9.105	-0.87
7	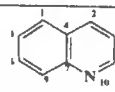	783	243	910.993	282.361	49.680	12.165	0.01

Table 1. (continued)

8		1144	308	1354.500	364.333	59.803	13.055	0.47
9		1636	386	1970.236	464.875	71.298	14.015	0.68
10		783	243	924.590	286.604	51.951	12.719	-0.30
11		1144	308	1371.028	369.167	62.058	13.565	0.02
12		1620	378	1961.139	458.729	73.364	14.452	0.25
13		3149	656	3586.694	748.333	99.422	17.522	1.40
14		3149	656	3617.528	755.500	101.900	18.002	1.40
15		105	54	129.604	66.653	18.205	7.278	-1.75
16		105	54	129.569	66.639	18.205	7.278	-1.41
17		783	243	929.771	287.965	53.030	12.930	-0.34
18		783	243	927.181	287.285	52.475	12.825	-0.29

Table 1. (continued)

19	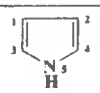	40	20	49.833	24.917	10.731	5.365	-1.11
20	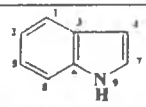	474	144	560.847	170.028	38.770	10.795	0.21
21	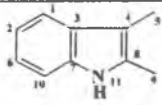	996	229	1212.750	279.264	58.113	12.686	0.84
22	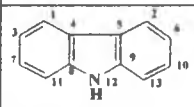	2122	420	2444.208	485.278	83.978	16.201	0.91
23		40	20	51.306	25.653	11.777	5.889	-1.71
24	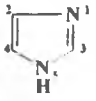	40	20	51.361	25.681	11.777	5.889	-1.00

Table 2. Statistics of regression equations: $Y = a + \Sigma_i b_i X_i$, for the set of Table 1

No.	TI	b	a	r	s	F
1	SZ_pX	0.033	- 1.830	0.9367	0.351	157.33
2	SZ_pX	0.038	- 1.655	0.9369	0.359	75.36
	SZ_eX	-0.037				
3	SZ_pX	0.038	- 1.926	0.9375	0.357	76.18
	SZ_pA	- 0.0002				
4	SZ_pX	0.038	- 1.923	0.9375	0.357	76.21
	SZ_p	- 0.0002				
5	SZ_pX	0.049	- 2.029	0.9406	0.348	80.52
	SZ_e	- 0.002				
6	SZ_pX	0.053	- 2.056	0.9414	0.346	81.75
	SZ_eA	- 0.003				

A second set of 18 aromatic structures [35] containing nitrogen both in a heterocycle and in a side chain (Table 3) and having inhibition activity on the growth of tetrahymena was modeled by the Szeged fragmental indices for the. The statistics of the regression equations are given in Table 4. For comparison, correlations given by the EATI index [35] are included. The biological activity is taken as log(IGC50).

Tabel 3. Topological indices and biological activity (log IGC50)

No.	Formula	SZ_n	Sz_v	SZ_nA	SZ_vA	SZ_nX	SZ_vX	log(IGC50)
1	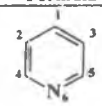	105	54	126.389	65.000	16.859	6.740	1.1853
2	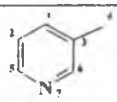	182	78	224.701	96.264	23.120	7.702	1.0175
3	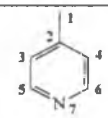	182	78	225.292	96.458	23.261	7.745	0.8921
4	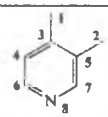	296	106	371.479	133.361	30.553	8.696	0.5051
5	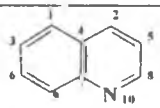	783	243	910.993	282.361	49.680	12.165	-0.0132
6	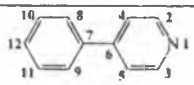	1684	360	1970.458	421.875	72.835	14.396	-0.6576
7	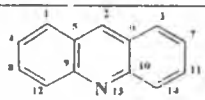	3149	656	3586.694	748.333	99.422	17.522	-1.3979
8	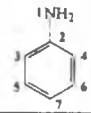	182	72	225.042	96.306	22.466	7.486	0.2201
9	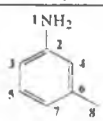	296	108	372.757	136.028	29.614	8.454	0.4133

Table 3. (continued)

10	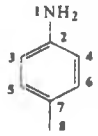	310	110	391.653	138.944	29.641	8.463	0.1271
11	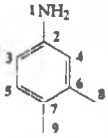	474	144	604.354	184.306	37.824	9.429	0.2878
12	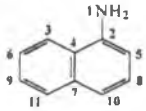	1107	300	1311.201	355.194	59.020	12.896	-0.2218
13	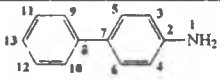	2350	450	2791.792	356.167	83.451	14.994	-0.8239
14		182	78	381.917	161.097	35.286	11.573	0.0645
15	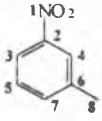	296	108	604.242	218.528	43.954	12.548	-0.3098
16	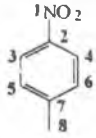	310	110	646.653	227.278	44.368	12.704	-0.2366
17	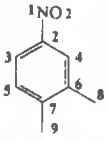	474	144	956.854	290.347	54.123	13.634	-0.6383
18	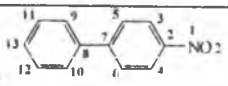	2350	450	3988.944	76.611	107.022	20.024	-1.0000

Table 4. Statistics of regression equations: $Y = a + \Sigma b_i X_i$, for the set of Table 3

No.	TI	b	a	r	s	F
1	EATI	- 0 084	1.823	0.9313	0.265	104.54
2	ln EATI	- 1.911	5.762	0.9419	0.244	125.79
3	SZ_pX	- 0.024	1.110	0.9087	0.304	75.83
4	ln SZ_pX	- 1.236	4.580	0.9424	0.243	126.94
5	SZ_pA	- 0.0005	0.508	0.8365	0.399	37.39
6	ln SZ_pA	- 0.646	4.167	0.9300	0.267	102.46
7	$1/SZ_pX$ SZ_eX	22.695 -0.099	0.486	0.9440	0.248	61.44
8	ln SZ_pX ln SZ_eX	- 0.775 - 0.801	4.776	0.9459	0.244	63.75
9	$1/SZ_eX$ SZ_p	17.223 - 0.0002	- 1.501	0.9475	0.240	65.88
10	ln SZ_pX ln SZ_p	- 1.644 0.223	4.725	0.9480	0.239	66.53
11	ln SZ_pA ln SZ_e	- 1.103 0.648	3.877	0.9463	0.243	64.31
12	ln SZ_pA ln SZ_p	- 1.289 0.606	4.345	0.9510	0.232	70.98

In single variable regression (Table 4, entries 1-6), the best correlation was found for SZ_pX (as natural logarithm - entry 4):

$$\log(IGC50) = 4.58 - 1.236 \ln SZ_pX$$
$$N = 18;\ r = 0.9424;\ s = 0.243;\ F = 126.94$$

This result surpasses the best correlation reported for the EATI index [35] (entry 2). Note the benefic action of logarithmic function applied to the Szeged-type indices (compare entries 3 and 4 and also 5 and 6).

In two variable regression, the standard error was slightly reduced (entries 9-12) in comparison to the best single variable regression. The best equation was

$$\log(IGC50) = 4.345 - 1.289 \ln SZ_pA + 0.606 \ln SZ_p$$
$$N = 18;\ r = 0.9510;\ s = 0.232;\ F = 70.98$$

Again the modeling is not satisfactory and not suitable in prediction. As above mentioned, it demonstrates the dependency of the biological response by the molecular structure.

CONCLUSIONS

The biological response induced by chemical compounds can be properly modeled by the aid of topological indices. Among these ones, the Szeged fragmental indices appears to be adequate descriptors of structures containing multiple bonds and heteroatoms. They proved to be at least as good as the famous EATI superindex.

ACKNOWLEDGEMENT

This work is supported in part by the GRANT of the National Education Ministery, No. 74/339/1997 and in part by the GRANT of the Romanian Academy of Sciences, No. 2627/1997.

REFERENCES

1. I. Moţoc, Structura moleculelor şi activitatea biologică, *Ed. Facla*, Timişoara (1980).
2. E. J. Ariens, *Med. Res. Rev.*, 1986, 6, 451.
3. E. J. Ariens *Med. Res. Rev.*, 1987, 7, 367.
4. E. J. Ariens, *Med. Res. Rev.*, 1988, 8, 309.
5. C. Hansch, T. Fujita, *J. Amer. Chem. Soc.*, 1964, 86, 1616.
6. C. Hansch, *Acc. Chem. Res.*, 1968, 8, 232.
7. C. Hansch, Drug design, Ed. E.J. Ariens, *Academic Press*, New York, 1971, 16, 271.
8. H. Kubinyi, *Struct.-Act. Relat.*, 1988, 7, 121-133.
9. R. F. Rekker, The Hydrophobic Fragmental Constant. Its derivation and Applications. A Means of Characterizing Membrane System, Elsevier, Amsterdam (1977).
10. R. F. Rekker, R. Mannhold, Calculation of Drug Lipophilicity. The Hydrophobic Fragmental Constant Approach, VCH Weinheim (1992).
11. H. Kubinyi, *J. Med. Chem.*, 1977, 20, 1991.
12. S. M. Free, Jr., J W. Wilson, *J. Med. Chem.*, 1964, 7, 395.
13. J. D. P. Graham, M.A. Karrar, *J. Med. Chem.*, 1963, 6, 103.
14. P. N. Craig, Biological Correlations - The Hansch Approach, *Ed. R.F. Gould, Advan. Chem. Series*, 1972, 114, 115.
15. W. P. Purcell, G.E. Bass, J.M. Clayton, Strategy of Drug Design: A Guide to Biological Activity, N.Y. Wiley, New-York (1973).
16. K. C. Chu, Burger's Medicinal Chemistry, *Ed. M.E. Wolff*, Wiley, New-York, 1980, 393.
17. P. N. Craig, Chem. Inf. Syst., *Ed. J.E. Ash and E. Hyde, Ellis Horwood Ltd.*, Chichester (1975) England, 259.
18. D. Maysinger, M. Birus, M. Movrin, *Acta Pharm. Jugosl.*, 1980, 30, 9.
19. B. Tinlqand, *Farmaco, Ed. Sci.*, 1975, 30, 935.
20. S. L. Galdino, I.R. Pitta, C. Luu Duc, *Farmaco Ed. Sci.*, 1986, 41, 59.
21. J. Halgas, V. Sutoris, P. Foltinova, V. Sekerka, *Chem. Zvesti*, 1983, 37, 799.

22. D. V. S. Jain, V. Gombar, *Int. J. Quantum Chem.*, 1981, 20, 419.
23. T. Fujita, T. Ban, *J. Med. Chem.*, 1971, 14, 148.
24. H. Kubinyi, O.H. Kehrhahn, *J. Med. Chem.*, 1976, 19, 578.
25. H. Kubinyi, O.H. Hehrhahn, *J. Med. Chem.*, 1976, 19, 1040.
26. J. Reiter, L. Toldv, I. Schaefer, E. Szondy, J. Borsy, I. Lukovits, *Eur. J. Med. Chem.-Chim. Tehr.*, 1980, 15, 41.
27. M. Butan, C.M. Pop, M.V. Diudea, *Studia Univ. Babeș-Bolyai*, 1995, 40, 129.
28. Z. Simon, A. Chiriac, S. Holban, MTD-Receptor Site Mapping, Preprint Univ. Timișoara, 1980. 4, 1.
29. I. Moțoc, *Quant. Struct. Act. Relat*, 1984, 3, 43.
30. R. D. Cramer, III, D.E. Patterson, J.D. Bunce, *J. Am. Chem. Soc.*, 1989, 110, 5959.
31. A. A. Kiss, I.E. Kacso, O.M. Minailiuc, M.V. Diudea, S. Nikolic, I. Gutman, *Studia Univ., Babeș-Bolyai*, 1997, 42, 000.
32. I. Gutman, *Graph Theory Notes, N.Y.*, 1994, 27, 9.
33. M. V. Diudea, I.E. Kacso, M.I. Topan, *Rev. Roumaine Chim.*, 1996, 41 141.
34. M. V. Diudea, O. Ivancuic, "Topologie Moleculară", Ed. COMPREX, Cluj, 1995.
35. M. Guo, L. Xu, C.Y. Hu, S.M. Yu, *Commun. Math. Comput. Chem.(MATCH)*, 1997, 35, 185.

STUDIA UNIVERSITATIS BABEȘ-BOLYAI, CHEMIA, XLII, 1-2, 1997

THE ATRAZINE DETERMINATION FROM HYDROALCOHOLIC PLANT EXTRACTS

SIMONA GOCAN[1], SIMONA COBZAC[1], VIORICA MUTU[1]

ABSTRACT. The present paper deals with the atrazine quantitation from plant extracts. The analysis were performed on spiked samples by two methods TLC and HPLC. The recovery was in the range 81.8-111% for TLC and 77.47-95.1% for HPLC. The limit of detection LOD from calibration curve was 25.46ng/spot for TLC and 2.87ng/20µL for HPLC.

INTRODUCTION

The herbicides can enter into the plants through their root, where they are non-specific degraded by hydrolysis and desalkilation reactions. Atrazine can be found also on the leaves when spraying methods are used [1].

In the literature many different possibilities for the extraction of atrazine from plants and extract analyses can be found. After extraction in $CHCl_3$ atrazine was extracted three times with HCl 0.1M [2]. The aqueous layer was neutralised at pH 8-7, mixed with 5 mL NaCl saturated solution and then atrazine was extracted in CH_3Cl. The atrazine was found to be present in *Salvia Off.* leaves [3]. Atrazine can be extracted with hexane after dilution of alcoholic extract with H_2O and mixed with a NaCl saturated solution [4]. The matrix composition can be simplified by SPE with two solids phases, on coal and atrazine elution with a mixture CH_2Cl_2 - CH_3OH [5]. The efluent is passed through a cationic resign where atrazine is selectively retained. For purifying Dowex 50W-X4, Amberlite XAD-2, Bio-Gel P-2 were also used [6]. Chromatographic separation and quantification were performed by GC with N-P detector [7] where LOD was 0.02ppm, and recovery 92%, GC-MS LOD 0.005ppm [8], HPLC with Lichrosorb Si (10µm) as stationary phase, a mixture of $CHCl_2$ - CH_3OH - H_2O - H_3PO_4 87% (70 : 30 : 6 : 0.1, v/v) as eluent flow rate : 0.5 - 1 mL/min and UV detection at 260 nm LOD was 0.05mg/kg [9], TLC using Kieselgel G plates, benzene - chloroforme - etil cetate (2 : 2 : 2, v/v) as eluent LOD 0.02ppm [10]. Atrazine from other matrix was also analysed [11, 12, 13, 14].

In the case of plant extracts used in homeopathy it is necessary to identify and quantify the content of triazinic herbicides. A simple method was elaborated for atrazine determination by liquid chromatography. A solvent extraction of atrazine from plants extract was chosen and then an elution system for chromatographic separation, so that the spot or peak of atrazine do not interfere with other compounds from the analysed plant extracts.

---

[1] Facultatea de Chimie și Inginerie Chimică, Universitatea "Babeș-Bolyai", 3400 Cluj-Napoca, Romania

EXPERIMENTAL

Solvents as chloroforme, toluen, methanol and acetone (Chimopar - Bucureşti), acetonitrile super purity solvent (Romil - England), Sil G F_{254} plates (Merck, Darmstadt), and atrazine (Atlas) were used for experiment. The alcoholic plants extracts of *Aesculus Hippocastanum, Avena Sativa, Calendulaa Off. and Eleuterococus* were from Plantextrakt (Rădaia - România). A methanol stock solution was prepared as 0,25mg/mL atrazine for spiked samples for TLC analysis and as 5µg/mL for the spiked samples analysed by HPLC.

For TLC analysis, 10mL plant extract was spiked with 1 mL atrazine solution (0,25mg/mL). The atrazine was extracted three times with 5 mL $CHCl_3$. The organic layers were mixed together, evaporated at 60°C and solved in 1 mL methanol. The blank sample was prepared in the same way for each plant extract. From blank and spiked samples 10µL were automatically spotted as lines (5mm long) with a Desaga AS - 30 applicator on Sil G F_{254} plates. The plates were developed with toluene - acetone (85:15, v/v) and evaluated, with a Shimadzu CS-9000 dual wavelength flying - spot scanner at 222 nm.

For HPLC analysis the same quantity of plants extract was spiked with 3mL atrazine solution as 5µg/mL. The atrazine was extracted with $CHCl_3$ three times with 5 mL. The organic phases were mixed together and evaporated at 60°C. The residuum was solved in 3 mL methanol. The HPLC analysis was perform with a Jasco equipment Jasco PU - 950 intelligent HPLC pump and Jasco UV - 975 intelligent UV-VIS detector. The chromatographic separation was perform on column (Jones Chromatography) 25cm long, with Apex ODS (5µ), with acetonitrile - water (65.35, v/v) at 0.8mL/min as eluent. Detection was perform at 222nm.

RESULTS AND DISCUSSION

The densitogram for spiked and blank samples of *Aesculus Hippo., Avena Sativa, Calendulaa Off. and Eleuterococus* extracts are shown in figures 1-4. In figure 5 is presented the calibration curve for atrazine analysed by TLC.

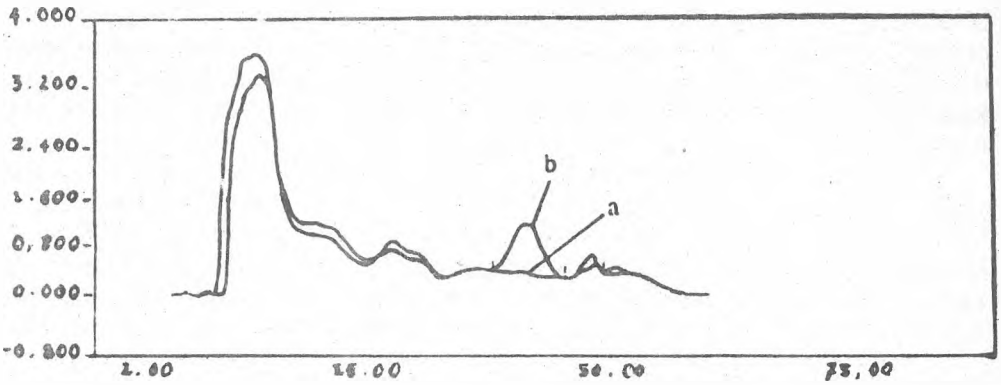

Figure 1. The chromatogram obtain from blank (a) and spiked (b) plant extract of *Aseculus Hippocastanum*

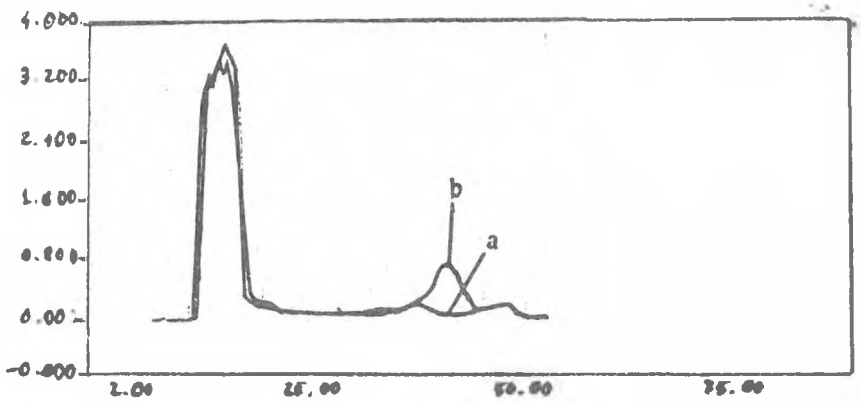

Figure 2. The chromatogram obtain from blank (a) and spiked (b) plant extract of *Avena Sativa*

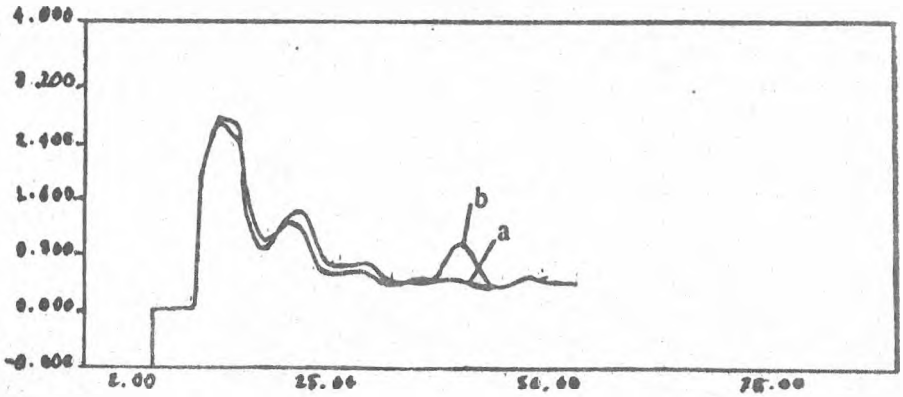

Figure 3. The chromatogram obtain from blank (a) and spiked (b) plant extract of *Calendula Off*

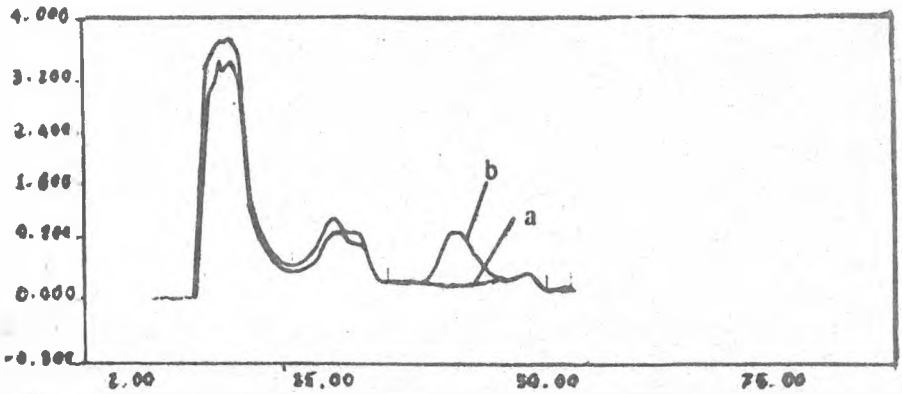

Figure 4. The chromatogram obtain from blank (a) and spiked (b) plant extract of *Eleuterococus*

The area values corresponding to the atrazine spot are given in table 1.

Table 1. The area values for atrazine from stock solution (0.25mg/mL), blank and spiked plant extracts analysed by TLC

Sample	Area	Recovery (%) *
Stock	66735	---
Aesculus Hippo. (blank)	---	---
Aesculus Hippo. (spiked)	54586	81.8
Avena Sativa (blank)	5143	---
Avena Sativa (spiked)	73962	110.8
Calendula Off. (blank)	2993	---
Calendula Off. (spiked)	65606	98.3
Eleuterococus (blank)	---	---
Eleuterococus (spiked)	60585	90.8

* The recovery value was calculated by reporting the spiked sample spot area corresponding to atrazine to spot area of the same compound from stock solution (0.25mg/mL)

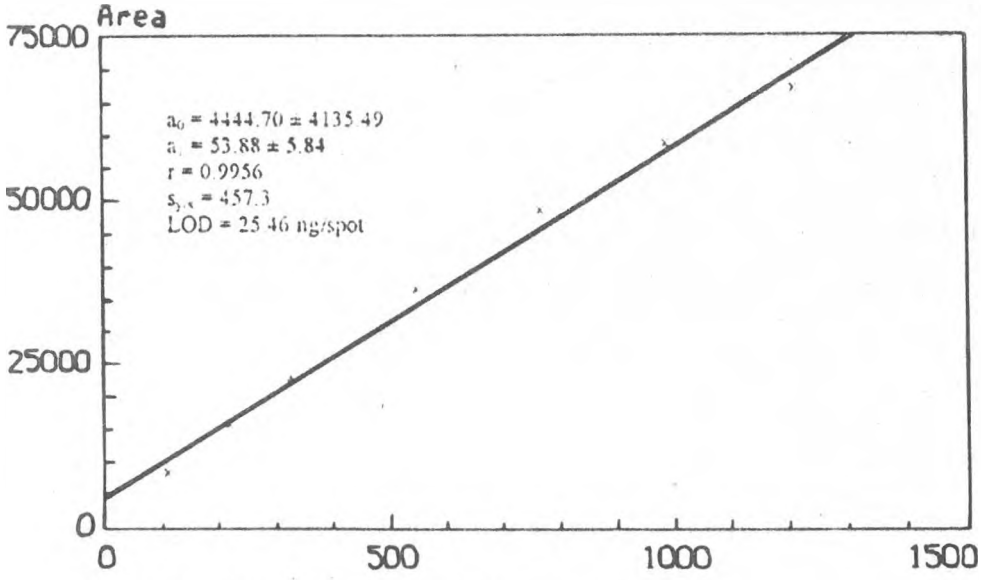

Figure 5. The calibration curve for atrazine by TLC

The R_f value obtained with the chosen sistem was 0.36. The TLC analyse for spiked samples do not assure in all cases a good separation of atrazine from plant compounds (*Avena Sativa, Calendula Off.*). A change of eluent composition (from toluene - acetone 85 : 15 to 90 : 10) do not show better separation. This fact can produce errors in identification and quantitation of atrazine.

In figures 6-9 are presented the chromatograms for plant extractes obtain by HPLC. The calibration curve for atrazine by HPLC is presented in figure 10. In table 2 are presented the areas value of atrazine from spiked plant extractes and recovery value.

Table 2. The area values for atrazine from stock solution (5µg/mL), blank and spiked plant extracts analysed by HPLC

Sample	Area	Recovery (%) *
Stock	969181	---
Aesculus Hippo. (blank)	---	---
Aesculus Hippo. (spiked)	750897	77.5
Avena Sativa (blank)	---	---
Avena Sativa (spiked)	921497	95.1
Calendula Off. (blank)	---	---
Calendula Off. (spiked)	921692	95.1.3
Eleuterococus (blank)	---	---
Eleuterococus (spiked)	921788	95.1

* The recovery value was calculated by reporting the spiked sample spot area corresponding to atrazine to spot area of the same compound from stock solution (5µg/mL)

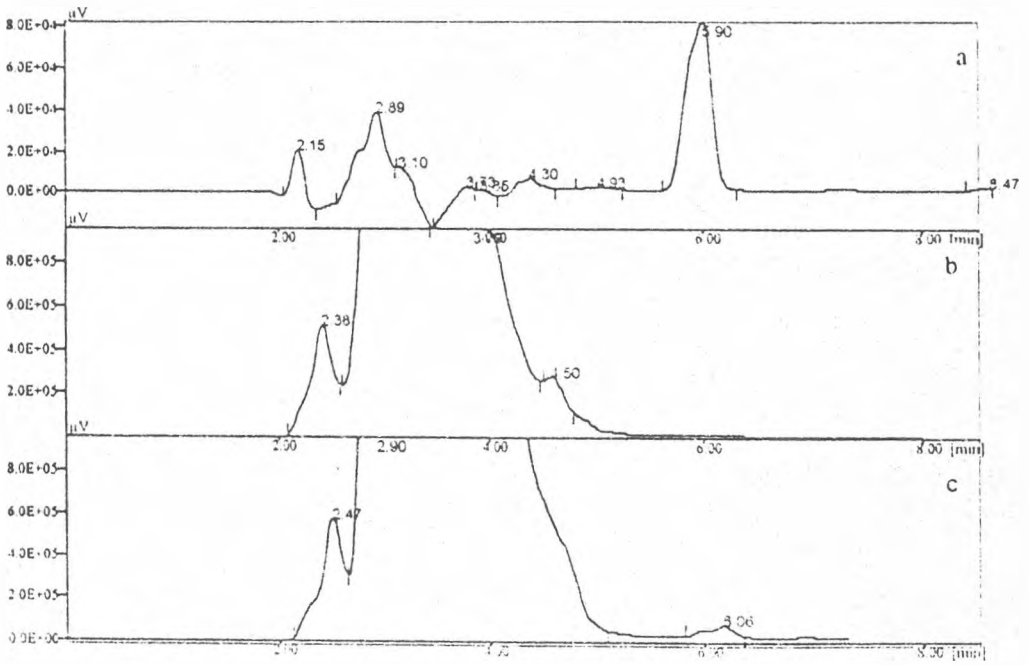

Figure 6. Typical chromatogram of a- stock solution (atrazine 5µg/mL), b- blank and c- spiked *Aesculus Hippo.* extract

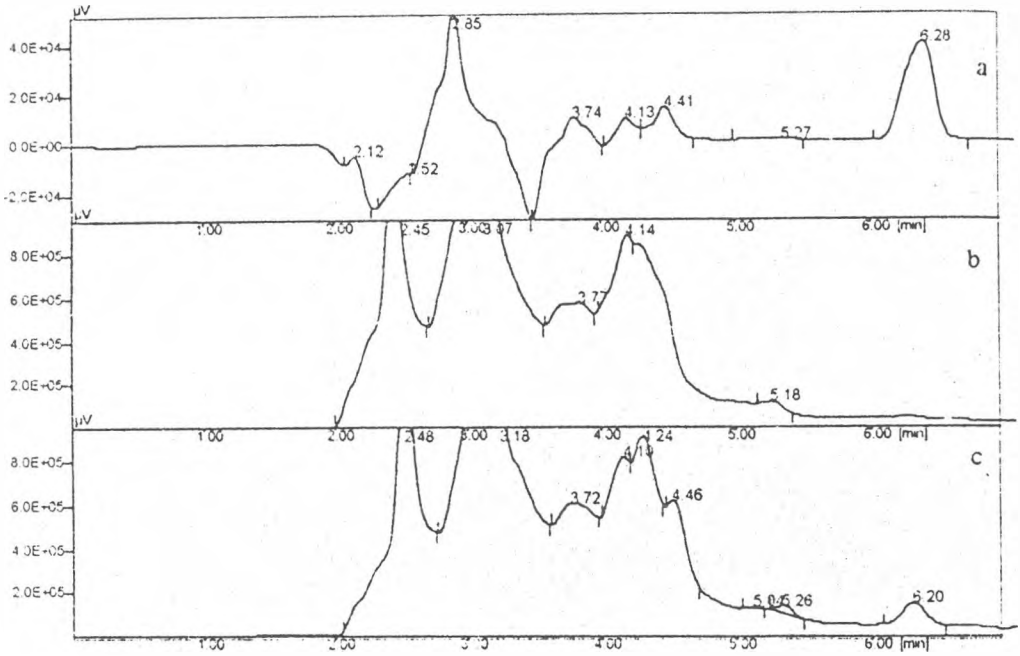

Figure 7. Typical chromatogram of a- stock solution (atrazine 5µg/mL), b- blank and c- spiked *Avena Sativa* extract

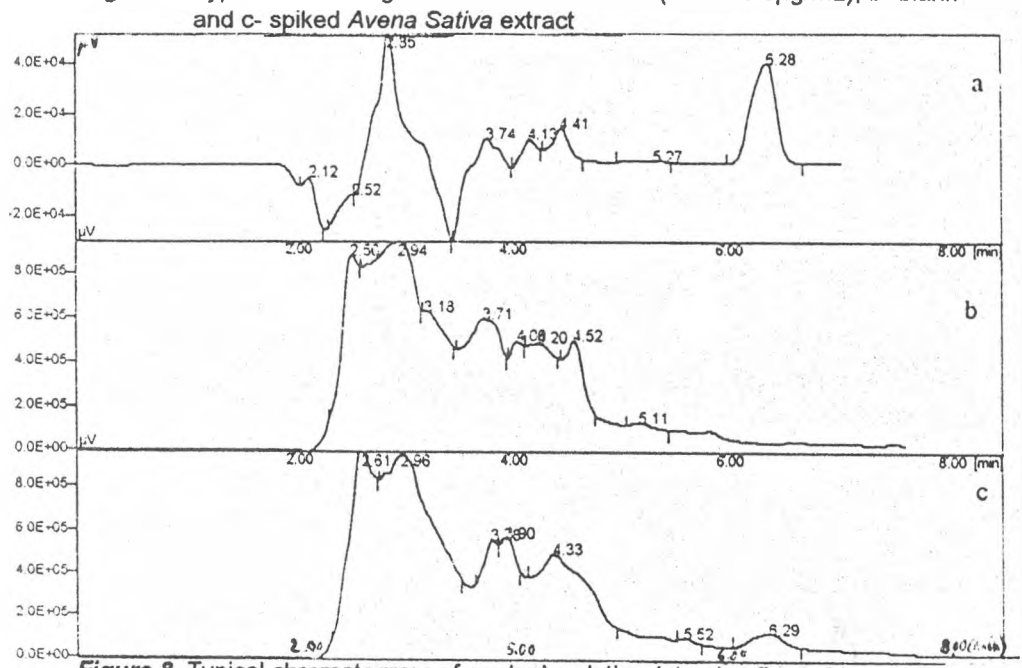

Figure 8. Typical chromatogram of a- stock solution (atrazine 5µg/mL), b- blank and c- spiked *Calendula Off.* extract

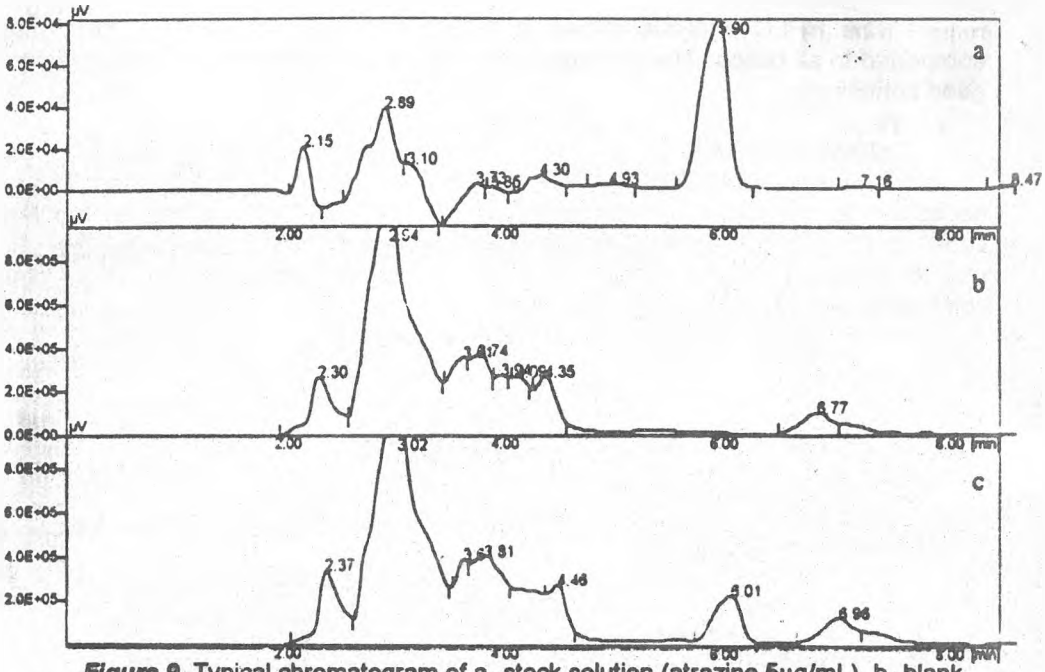

Figure 9. Typical chromatogram of a- stock solution (atrazine 5µg/mL), b- blank and c- spiked *Eleuterococus* extract

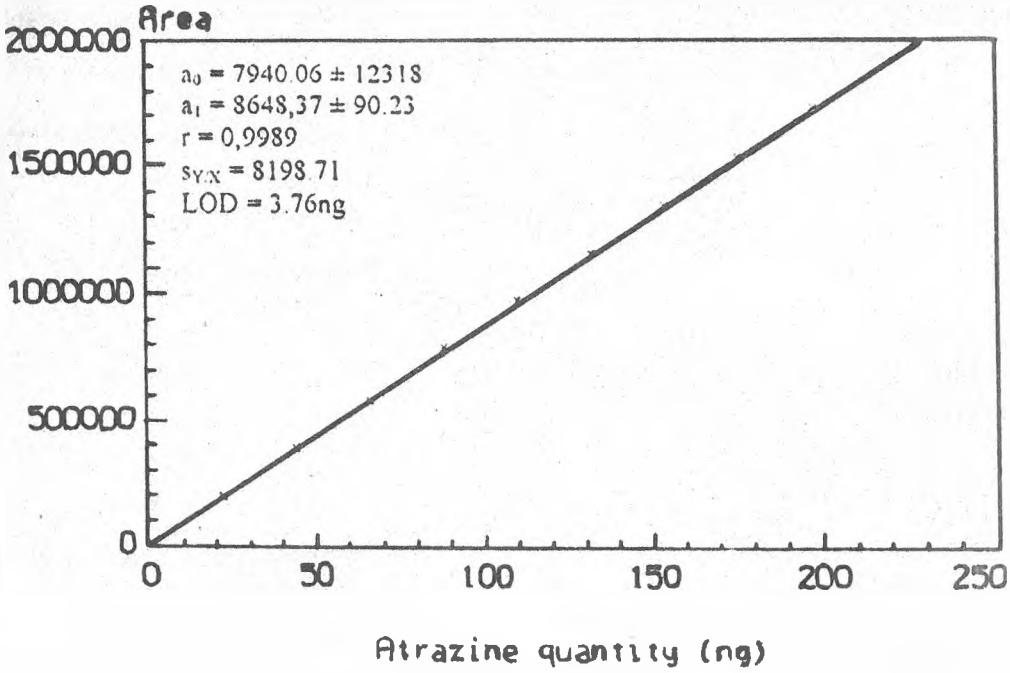

Figure 10. The calibration curve for atrazine by HPLC

The HPLC analysis shows a better separation of atrazine from plant ıund in all cases. The qualitative and quantitative analysis can be perform in ɔnditions.

CONCLUSIONS

The analysis of plant extractes, where matrix is very complex and when is sary to determine small quantity to herbicides can be perform in the best ion using HPLC on ODS as stationary phase and acetonitrile - water (65 : 35, s eluent. It can be obtain high degree of separation of atrazine from plant ɔund and the limit of detection is lower.

REFERENCES

.. Ghinea, I. Vlăduțu, M. Berca, *Efectele reziduale ale erbicidelor*, Ed. Academiei, București, 1989, 17, 43.

V. A. Popkov, S.A. Puzakov, *Farm. Zh.*, 1990, 6, 59.

B. K. Machatov, *Farm. Zh.*, 1991, 2, 84.

J. Pluta, Z. Obzewschi, *Acta Pol. Pharm.*, 1980, 37(7), 675.

M. Battista, A. Di Corcia, M. Marchetti, *Anal. Chem.*, 1989, 61(1).

K. A. Reimsteiner, W.D. Hoermann, *J. Agric. Food Chem.*, 1979, 27, 984.

D. Emmet, T. Gabrio, *Pharmazie*, 1982, 37(6), 375.

H. Haase Strey, W. Heidemann, H.A. Pussel, *Fresenius J. Anal. Chem.*, 1994, 318.

J. F. Lawrence, *J. Agric. Food. Chem.*, 1979, 27, 1236.

H. Reinfenstein, F. Pank, *Pharmazie*, 1975, 30(6), 391.

M. Berg., S.R. Muler, R.P. Schwartzenbach, *Anal. Chem.*, 1995, 67(11), 1860.

M. Kolb, B. Enhgert, Acta Hidrochim. Hidrobiol., 1996, 24(6), 277.

P. Onnerfjord, D. Barcelo, L. Gorton, G. Marko-Varga, *J. Chromatogr.*, 1996, 737, 35.

A. Junker-Buchheit, M. Witzenbacher, *J. Chromatogr*, 1996, 737, 67.

În cel de al XLII-lea an (1997) *STUDIA UNIVERSITATIS BABEȘ-BOLYAI* apare în următoarele serii:

matematică (trimestrial)
informatică (semestrial)
fizică (semestrial)
chimie (semestrial)
geologie (semestrial)
geografie (semestrial)
biologie (semestrial)
filosofie (semestrial)
sociologie (semestrial)
politică (anual)
efemeride (anual)
studii europene (semestrial)
business (semestrial)
psihologie-pedagogie (semestrial)
științe economice (semestrial)
științe juridice (semestrial)
istorie (trei apariții pe an)
filologie (trimestrial)
teologie ortodoxă (semestrial)
teologie catolică (anual)
educație fizică (anual)

In the XLII-th year of its publication (1997) *STUDIA UNIVERSITATIS BABEȘ-BOLYAI* is issued in the following series:

mathematics (quarterly)
computer science (semesterily)
physics (semesterily)
chemistry (semesterily)
geology (semesterily)
geography (semesterily)
biology (semesterily)
philosophy (semesterily)
sociology (semesterily)
politics (yearly)
ephemerides (yearly)
european studies (semesterily)
business (semesterily)
psychology - pedagogy (semesterily)
economic sciences (semesterily)
juridical sciences (semesterily)
history (three issues per year)
philology (quarterly)
orthodox theology (semesterily)
catholic theology (yearly)
physical training (yearly)

Dans sa XLII-e année (1997) *STUDIA UNIVERSITATIS BABEȘ-BOLYAI* paraît dans les séries suivantes:

mathématiques (trimestriellement)
informatiques (semestriellement)
physique (semestriellement)
chimie (semestriellement)
géologie (semestriellement)
géographie (semestriellement)
biologie (semestriellement)
philosophie (semestriellement)
sociologie (semestriellement)
politique (annuel)
ephemerides (annuel)
études européennes (semestriellement)
affaires (semestriellement)
psychologie - pédagogie (semestriellement)
études économiques (semestriellement)
études juridiques (semestriellement)
histoire (trois apparitions per année)
philologie (trimestriellement)
théologie orthodoxe (semestriellement)
théologie catholique (annuel)
éducation physique (annuel)